The development and validation of a hydrostatic pressure bioreactor for applications in bone tissue engineering

Joshua Colm Felician Aeddan Price

Thesis submitted for degree of Doctor of Philosophy

January 2017

Keele University

Abstract

Current orthopaedics treatments of bone defects often involve the use of implanted fixatives and/or autograft procedures to restore function to the afflicted area following injury. Fixatives and implants are usually temporary solutions, since they are intrinsically prone to failure. In addition to this, replacing implants involve expensive and invasive procedures that cause great hardship to patients. Whilst autografts can provide an excellent outcome in healing of the initial injury site, donor site morbidity from the autologous bone graft can lead to complications such as infection, chronic pain and an abnormal walking gait. Bone tissue engineering is a field of science aiming to address these limitations by providing *in vitro* manufactured bone to replace autografts, and also limit the use of temporary fixatives. Hydrostatic force bioreactors are currently being developed within this field to attempt improve the outcome of the tissue engineered bone by mimicking the forces typically experienced by cells in the native bone niche. Based on this principle, it is hoped that such systems will aid the translation of research in bone tissue engineering from the lab to the clinic.

This research aims to investigate and validate the use of a hydrostatic force bioreactor for improving the outcome of *in vitro* manufactured bone using a clinically relative strategy employing human mesenchymal stem cells seeded in 3D scaffolds. The research first describes a validation process to determine the initial response of cells to hydrostatic pressure in monolayer cultures. The outcome of this study indicated that mechanical responsiveness in cells can vary according to cell phenotype and the integrity of the f-actin cytoskeleton. Next it was demonstrated that hydrostatic pressure can improve the outcome of *in vitro* bone formation by MG-63 human osteoblast like cells, validating the bioreactor as a potential preconditioning platform. Following this, a model of bone

formation in hMSCs/collagen scaffolds was described, whereby a predictable rate of bone formation was determined by adjusting cellular distribution and protein concentration in collagen type-1 scaffolds.

Finally, an organotypic fracture repair model was established using explanted embryonic chick femurs to test the hypothesis that hydrostatic preconditioning of hMSC/collagen hydrogels can improve the outcome of fracture repair. The results of this study showed that bioreactor stimulation could enhance the outcome of repair using a combination of undifferentiated hMSC/collagen type-1 scaffolds, and global mechanical signalling (stimulation of entire femur constructs). It was then shown that hydrostatic preconditioning of hMSC seeded hydrogels prior to implantation did not increase the rate of *in vitro* bone formation. Following implantation of the hydrogels into the fracture repair model, it was demonstrated that highly mineralised preconditioned implants actually inhibited the fracture repair process. In addition to this, it was shown that preconditioned implants with a lower level of mineralisation allowed invasion and bone formation by native cells from the host tissue. Collectively, the results implied that the outcome of repair using this model relied on three main factors: the presence of global hydrostatic stimulation; the lineage commitment of hMSCs in collagen scaffolds at the time of implantation; and the permeability and cell invasion capacity of the implant.

Contents

List of figures

List of tables

List of abbreviations (in order of appearance)

RM – Regenerative medicine

BTE – Bone tissue engineering

UBC - Unicameral bone cyst

ABMI - Aspiration and percutaneous autogenous bone marrow injections

SSC – Skeletal stem cells

OI - Osteogenesis imperfecta

MSC - Mesenchymal stem cell

OC – Osteoclast

OB – Osteoblast

OS – Osteocyte

RANKL - Receptor activator of nuclear factor kappa-β ligand

NO – Nitric oxide

OPG - Osteoprotegerin

Runx2 - Runt-related transcription factor 2

Wnt - int/Wingless family

BMP – Bone morphogenetic protein

OCN – Osteocalcin

DMP-1 - Dentin matrix protein 1

FGF23 - Fibroblast growth factor 23

ALP - Alkaline phosphatase

PSC - pluripotent stem cells

iPSC - induced pluripotent stem cell

ESC - Embryonic stem cell

BMSC - Bone marrow derived stem cell

ADSC - Adipose derived stem cell

MLO - Mouse long bone osteocyte

MG63 - Human osteoblast-like cells

ECM -Extra cellular matrix

FDA – food and drug administration#

PLA - Poly-lactic acid

PGA - Polyglycolic acid

PCL - Polycaprolactone

PLGA - Poly(lactic-co-glycolic acid)

PGE2 - Prostaglandin E2

COX – cyclooxygenase

HP – Hydrostatic pressure

sGAG - Sulphated glycosaminoglycan

RGD - arginylglycylaspartic acid

ATP - Adenosine triphosphate

TRP - Transient receptor protein

PC – Primary cilia

IHH -Indian hedgehog pathway

OA – Osteoarthritis

YAP – Yes associated protein

TAZ – PDZ – binding motif

DMSO - Dimethyl sulfoxide

DMEM - Dulbeco’s Modified Eagle Medium

PM – Proliferation media

FBS - Fetal bovine serum

PBS - Phosphate buffered saline

UV - Ultra violet

CytoD - Cytochalasin D

CH - Chloral hydrate

DH_2O – Distilled water

BSA - Bovine serum albumin

DAPI - 4',6-diamidino-2-phenylindole

NaOH – Sodium hydroxide

Sulpho-SANPAH - sulfosuccinimidyl 6-(4'-azido-2'-nitrophenylamino)hexanoate

FI – Fluorescence intensity

CytoB - Cytochalasin B

ATPase – Adenylpyrophosphatase

PCD – Primary cilia dyskinesia

LATS - Serine/threonine-protein kinases

µCT - x-ray micro computed tomography

A/R - Alizarin red S

V/K - Von Kossa

IHC – Immunohistochemistry

Cx43 - Connexin 43

MMP - matrix metalloproteinase

IMN – Intramedullary nail

4-MUP - 4-Methylumbelliferyl phosphate

EDTA - Ethylenediaminetetraacetic acid

Acknowledgements

I would to thank my supervisor Professor Alicia El Haj, whose support has been instrumental in producing this thesis. Her guidance and advice has developed my approach to, and undertaking of scientific research and I thank her immensely for giving me the opportunity to undertake a PhD in her lab. I would also like to sincerely thank Dr James Henstock for his advice and tutoring in experimental techniques and analysis, but also for providing moral and personal support through some of the more challenging periods of my studies. To that end I would like to acknowledge my colleagues and friends at the ISTM, in particular my fellow lab members Michael Rotherham, Yanny Marliana Baba Ismail, Sandhya Moise, Hareklea Markides and Katie Bardsley. Their help and friendship, and at times shared misery! has been a great support. I also would like to acknowledge the neuroscience crowd up on top of the hill at Keele campus, in particular Sile Griffin, Alinda Fernandez and Jackie Tickle for many a good conversation at the KPA and elsewhere. I would like to acknowledge my Iraqi and Middle Eastern friends in the ISTM. It has been a privilege to work around their example of hard work and commitment, and to experience their overwhelming kindness and goodwill.

I would like to thank Dr Alan Richardson for allowing me to contribute to his research, and also Dr Paul Roach for the help and advice in developing and publishing my own research. I would like to acknowledge Professor Ying Yang for her continued support and for giving me the opportunity to share my research interests and expertise with my colleagues at the lunchtime seminar sessions, which I have very much enjoyed being a part of. I would like to extend a big thankyou to my DTC cohort at Nottingham and Loughborough. I'm grateful to have been part of the EPSRC DTC in regenerative medicine and thank the EPSRC for funding my research.

I would like to pay special tribute to my good friends and fellow DTC'ers Dr Alan Weightman, Dr Christopher Adams and Dr Rupert Wright for their sincere and down to earth advice, innumerable laughs and collaborative drunken escapades by which many a good memory has been more or less partially retained.

A heartfelt thankyou goes to my partner Kaarjel Kauslya Narayanasanalamadamaramy… or something along those lines. In you I have found a great deal of happiness and a source of aspiring commitment to better myself as an individual. A great deal of thanks goes to my family and also to my friends back in Wales for their company and support, a special mention to Brynglas, Sam, Gary Blew, Rich Howarth and his lordship Huw Price.

I acknowledge and sincerely thank Professor Damien McDonnel, his advice not only encouraged me to undertake a PhD, but his ongoing support has inspired the development my own research interests, from which I have found a great sense of enjoyment and satisfaction.

Finally I want to thank my closest friend and lifelong pal Nipper. From your very earliest days as a pup to our most recent strolls through the dimly lit backstreets of Stoke-on-Trent, you have given me the friendship and support that I could not have found in any other individual be it Hominid or Canine.

Chapter 1

General introduction

1.1. Introduction

Regenerative medicine (RM) is an emerging field in science that explores aspects of translational research in order to restore normal function to diseased or injured regions of the body. The field itself encompasses broad multidisciplinary practises that aim to address growing concerns for public health in the years to come. With an aging population and increasing trends in both childhood and adult obesity, the challenges facing orthopaedics to effectively treat patients will quickly become impracticable using current treatments (Wills 2004)(Lawrence et al. 2008). Bone tissue engineering (BTE) is a branch of RM that utilises developments in biomedical science to treat orthopaedic injuries that are incapable of self-regeneration such as massive traumatic bone loss or tumour resection (Lichte et al,. 2011). Bone tissue engineering aims to overcome limitations facing current orthopaedic practises, and in practise should incorporate clinical safety, predictability and reproducibility in the outcome of potential treatments (Shrivats et al. 2014).

Engineering bone tissue *in vitro* translates our biological understanding of *in vivo* osteogenesis and applies it to bioengineering concepts that aim to grow replacement bone tissue in the lab. Osteogenesis is defined as the process by which osteoprogenitor cells recruit, and/or differentiate into bone forming osteoblasts to mineralise the surrounding extracellular matrix (Orlando et al. 2013). Bone has remarkable capacity for self-renewal relative to other tissue types. Throughout the life of a person, the mechanical integrity of the skeleton is maintained by a constant rate of turnover known as bone homeostasis (Kalfas 2001). Adult bone healing during fracture repair recapitulates many pathways of normal foetal skeletal development such as intramembranous and endochondral ossification (Ferguson et al. 1999) . Thus, there exists very real opportunity to address a

growing health concern by translating our ever increasing understanding of biological events into useful clinical applications.

1.2. Limitations in current orthopaedic gold standards

As mentioned previously, bone has a relatively good regenerative capacity after injury and many orthopaedic injuries such as stress fractures and minor trauma heal with minimal intervention and without complication. It is the more complex and more severe injuries which require review of the gold standard, currently utilising temporary fixation, or autografts harvested directly from the patient. Both of these methods have significant limitations, particularly in addressing a larger scale clinical need. Fixation techniques employ metal and ceramic implants and are intrinsically prone to failure. Implant failure can cause severe pain to the patient and great expense and hardship in their removal and replacement (Sivakumar et al. 1995). Autologous bone grafts usually involve removal of bone from the iliac crest and have a number of associated complications such as pain, sensory disturbances, gait abnormality, or post-operative infection (Ahlmann et al. 2002). One patient follow up study found that in certain cases as much as 18% of patients experienced major complications as a result of the autograft procedure (Younger & Chapman 1989). The cumulative cost of osteoporotic fractures alone in the UK was estimated at £20.3 billion between 2000 and 2010, and is set to increase by 20% by 2020 (Burge et al. 2008). If BTE engineering can emerge as a new gold standard in orthopaedics it could have significant positive impact on both the patient and the healthcare economy through a growing RM industry.

1.3. Orthopaedic applications from bone tissue engineering

1.3.1. Pathological abnormalities

Pathological abnormalities occur due to an underlying disease state and can lead multiple complications that require surgical intervention. There are a number of pathological abnormalities that occur in bones, each of which carry different levels of risk. As an example, unicameral bone cysts (UBCS) are benign bone lesions that commonly occur in children and young adults but are not generally considered to pose a serious health risk. However, if large enough, they introduce an increased risk of pathological fracture due to mechanical instability (Weinman et al. 2013). Bone grafts are one of the current gold standards in the treatment of this affliction (Kadhim et al. 2014), however as discussed previously, these procedures arguably represent the current limitations in orthopaedic practise. Concepts that have emerged from understanding of basic biology have seen the implementation of aspiration and percutaneous autogenous bone marrow injections (ABMI) into the injury site (Delloye et al. 1998). The use of ABMI is now considered to provide an excellent alternative treatment for UBCs over autografts, with one study demonstrating an 82% success rate of healing using ABMI (Zamzam et al. 2009).

Other approaches in targeting pathological bone abnormalities include the enrichment of isolated skeletal stem cell (SSC) populations which can then be reintroduced into the body to target the injury site (Oreffo et al. 2005). It is hoped that techniques such as SSC isolation and enrichment might be effective in treating osteogenesis imperfecta (OI), a genetic disorder which results in abnormal collagen type 1 production by native osteoblasts. This disorder can lead to recurrent multiple fractures and growth abnormalities that commonly result in a shortened stature (Undale et al. 2009). Current gold standards for OI involve ongoing and intensive surgical procedures

to correct abnormalities, or treatment with bisphosphonate therapy, for which the long term clinical outcome is currently unknown (Rauch & Glorieux 2004). Allogeneic mesenchymal stromal cell (MSC) transplantations have recently shown increased efficacy in the treatment of OI in a number of studies (Horwitz et al. 2002)(Le Blanc et al. 2005)(Götherström et al. 2014), demonstrating how we can utilise concepts from BTE to address currently limited procedures to heal pathologies in bone tissue.

1.3.2. Delayed healing during fracture repair

The nature of orthopaedic treatment will depend on the type and severity of the injury or abnormality. Fractures for example are generally categorised into three types; Traumatic fracture, pathological fracture, and fracture by fatigue (Dhillon & Dhatt 2012). Traumatic fractures are caused by excessive force, which can incorporate a variety of fracture subsets, for example, compression, torsion or blunt trauma. Pathological fractures have underlying causes such as bone diseases or prolonged disuse. Finally fatigue fractures are usually a result of repetitive stress, leading to a cumulative excess in force that leads to stress fractures (Packer & Colditz 1986). An accurate understanding of the nature of injury facilitates the correct prognosis and treatment type. A compression fracture resulting from low bone density (a common injury among elderly women suffering with osteoporosis) typically would employ a form of injectable bone cement to the fracture site (Klazen et al. 2010). By contrast a non-union caused by blunt trauma in a young male patient could require fixation of an autograft to facilitate bone repair (Sen & Miclau 2007).

The general stance on using BTE for restoring function to bone that do not heal, is to exploit the correct combination of stem cell derived cell phenotypes, 3D scaffolds, and external cues that then improve vascularised bone formation after implantation (Dawson et al. 2014)(**Figure 1**). Whilst BTE has shown some success in producing large bone

volumes suitable for transplantation (Stevens et al. 2005), there remain limitations in translating BTE from *in vitro* to *in vivo,* such as the poor predictability of clinical outcomes from rodent models of vascularised bone tissue formation, into human bone defects (Stevens 2008). We must not overlook early successes demonstrating the potential of BTE in long term clinical outcomes in large bone defects (Marcacci et al. 2007). However, existing evidence implementing clinical therapies derived from BTE does not yet offer orthopaedic surgeons enough proven efficacy to take the place of autografts as the gold standard (Amini et al. 2012). For BTE to become the new gold standard, scientists must utilise the increasingly interdisciplinary field of RM to develop novel concepts that overcome the current limitations facing the field such as reproducibility and predictability, and preclinical models that adequately translate into use in humans.

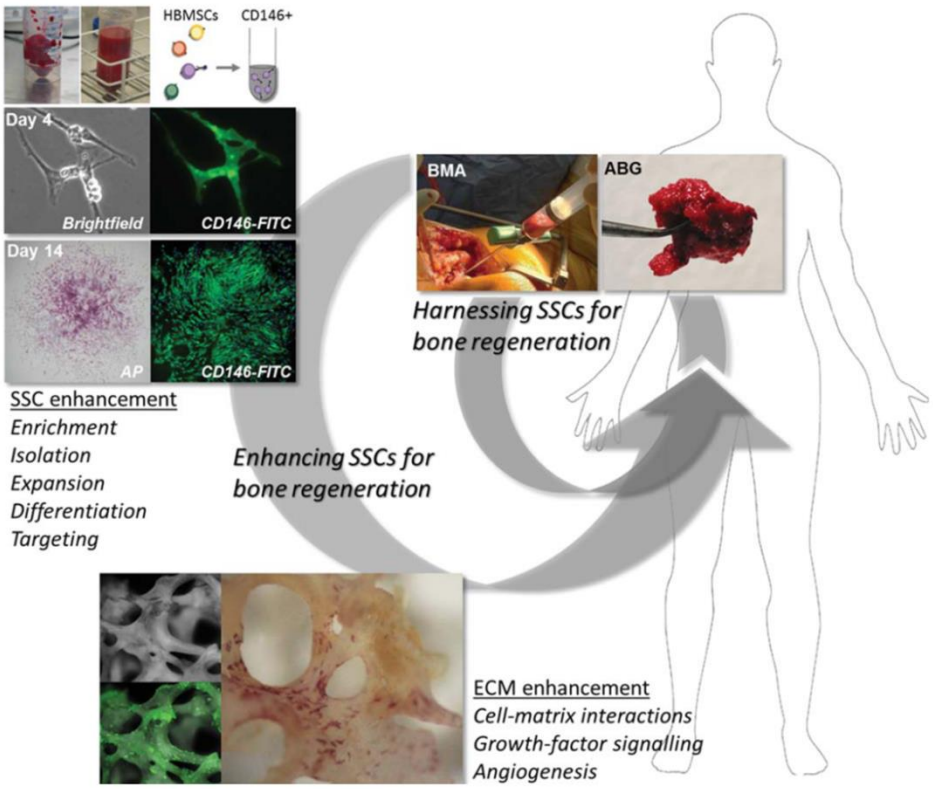

Figure 1. Concept in bone tissue engineering of stem cell isolation and differentiation on 3D scaffolds prior to implantation to promote bone regeneration. *Adapted from (Dawson et al. 2014), reprinted with permission of John Wiley and Sons [license number:3791881189997]*

1.3.3. Commercially available artificial bone substitutes 'from bench to bedside'

Orthopaedic surgeons already employ a wide range of artificial bone substitutes to treat a range of injuries such large defects, craniofacial abnormalities and spinal fusion. There are an increasing number of industry based efforts to develop and commercialising materials for orthopaedic tissue repair, such as the university spin out venture Apatech, who develop porous synthetic hydroxyapatite based bone grafts, which have shown success in a number of clinical case studies (McNamara et al. 2010) (Lerner & Liljenqvist 2013). To date, Apatech are estimated to have successfully treated over ½ million people across 30 countries and in 2012 occupied around 10% of a market worth over $500 million (source: National Centre for University and Business, *http://www.ncub.co.uk/apatech-development-synthetic-bone-grafts-2.html*). Apatech is just one example of the clinical and commercial successes of the bench to bedside strategy, and these successes continually drive research activity to find lower cost, minimally invasive and more effective ways of treating bone abnormalities. Since many artificial bone substitutes employ cell free approaches, they can avoid many regulatory issues associated with using cell based therapies. With artificial bone substitutes already so widely and successfully employed, it is then tempting to ask why so many are seeking to develop cell based strategies to treat bone abnormalities. The main drawback of using artificial bone substitutes is that they are unsuitable for treating pathological abnormalities such as OI, discussed previously. A cells unique ability to actively adapt to an *in vivo* environment can allow the treatment of OI with allogeneic an MSC transplantation (Götherström et al. 2014). Hence there are distinct limitations in the use of artificial bone substitutes which continue to inspire new approaches to treating bone abnormalities with more widely applicable techniques. A combination of the correct

cell/scaffold environment could potentially address many of the limitations which commercially available treatment options face.

1.4. Bone anatomy

1.4.1. Structure and function

Bone is a dynamic tissue that plays a role in structure, stability and protection of the body. Its functions include maintaining blood calcium levels, providing mechanical support to soft tissue and levering muscle action, supporting haematopoiesis, and housing the brain and spinal cord (Harada & Rodan 2003). Bone consists of two main types; compact or cortical bone and cancellous or spongy bone. Compact bone forms a dense cylinder around the mid diaphysis of long bones and comprises highly aligned collagen fibrils which form lamella. Within this lamella are embedded osteocytes interconnected via dendritic processes extending through channels called canaliculi. These channels act as a mass transfer system, delivering nutrients and exporting waste, and are also believed to mediate mechanical signals through interstitial fluid, allowing cells to detect and process external mechanical stimuli (Kamioka et al. 2001). Cancellous bone is present at load bearing sites toward the epiphysis of long bones and comprises porous, randomly oriented bone matrix called trabeculae. Cancellous bone has evolved to allow optimal load transfer, by pairing suitable strength and stiffness to minimal weight according to rules of mathematical design (Huiskes et al. 2000).

Cortical Bone structure

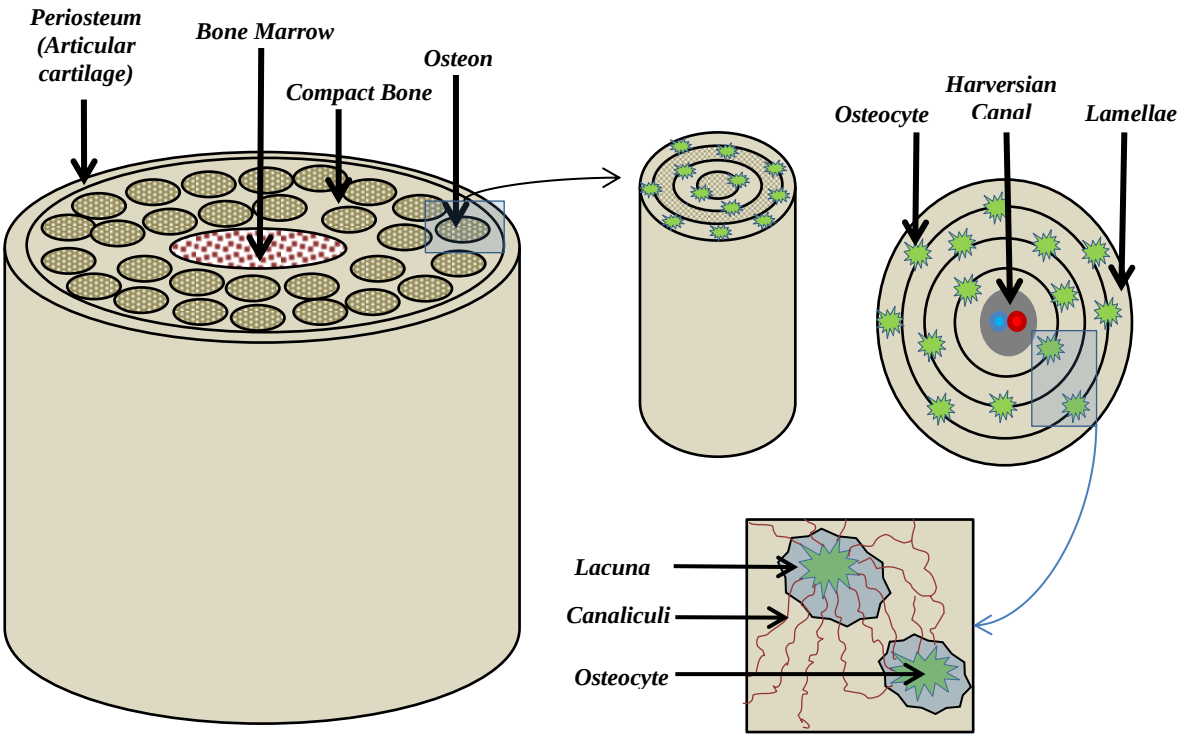

Cancellous Bone structure

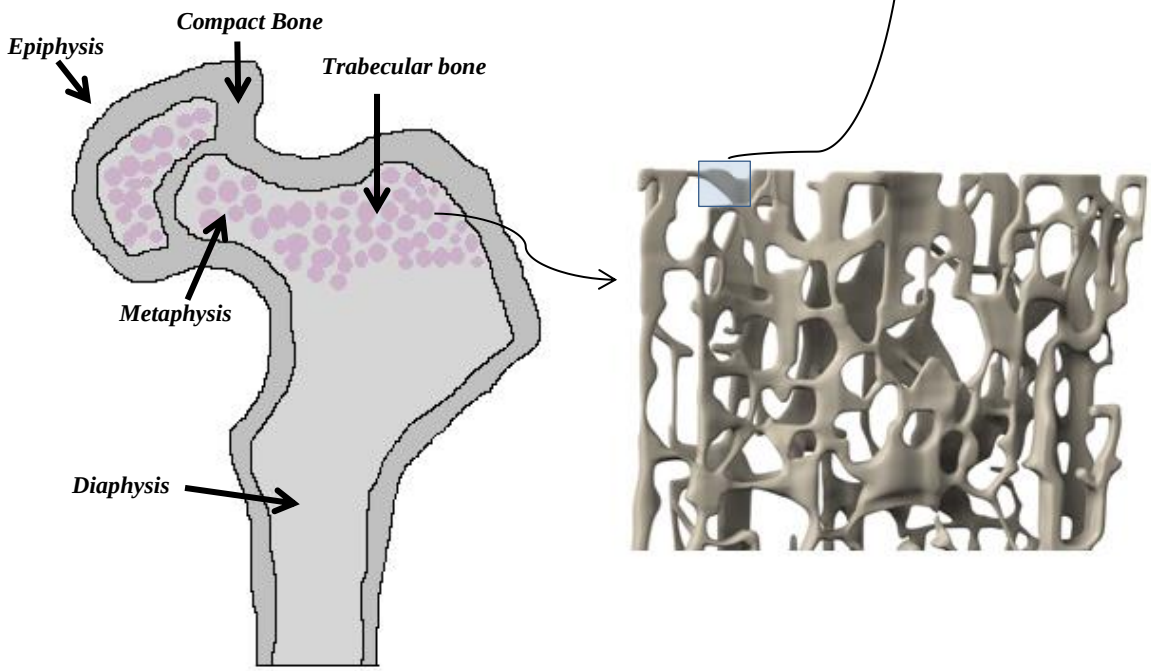

Figure 2: Schematic showing the structure of compact and cancellous bone. *Within a typical femur there is both compact and cancellous bone in different regions. Compact bone forms a dense bone collar extending the femur diaphysis consisting of mineralised collagen in a highly ordered lamella structure. Cancellous bone is present toward the femoral head or epiphysis, providing a lightweight, robust structure ideal for load bearing.*

1.4.2. Formation in vivo

Bone is carefully regulated by a constant flux of remodelling and resorption, involving a delicate balance of bone resorbing osteoclasts and bone forming osteoblasts. The mechanisms that control bone homeostasis are complex and there is a large body of literature on the many potential candidate cues for regulating bone mass. There are various ways in which bone forms and maintains itself. During embryonic development endochondral ossification **(Figure 3A)** controls the formation of most long and irregular bones. Endochondral ossification involves the formation of a cartilage like matrix that is then mineralised to form mature bone tissue (Mackie et al. 2011). Most flat bones such as the calvaria (skull) are formed via the process of intramembranous ossification **(Figure 3B)**. Intramembranous ossification occurs by first recruiting progenitor cells to the site of interest via chemotaxis. These progenitor cells then differentiate into matrix secreting osteoblasts which subsequently mineralise surrounding fibrous tissue, forming distinct mineralised nodules (Cooper et al. 2006). These nodules grow in size and interconnect with surrounding nodules to form new bone. Both intramembranous and endochondral ossification are present in embryonic development, fracture healing and adult bone homeostasis, however there is debate as to which process is more favourable for generating bone tissue *in vitro*. Evidence suggests that bone formation via these mechanisms is dictated by the cell-matrix environment and the lineage commitment of cells present within these bone forming regions (Tortelli et al. 2010).

During bone remodelling, cells will exhibit a number of different phenotypes as they progress from a dormant or ‘quiescent’ state to becoming embedded osteocytes. Osteoclasts are first recruited to deliver hydrochloric acid and proteases to degrade old bone, releasing factors contained in the matrix which encourage recruitment of osteoblasts

(Väänänen et al. 2000)(Rucci 2008). Osteoblasts then invade the site and gradually lay down mineralised matrix until the region is entirely replaced by new bone

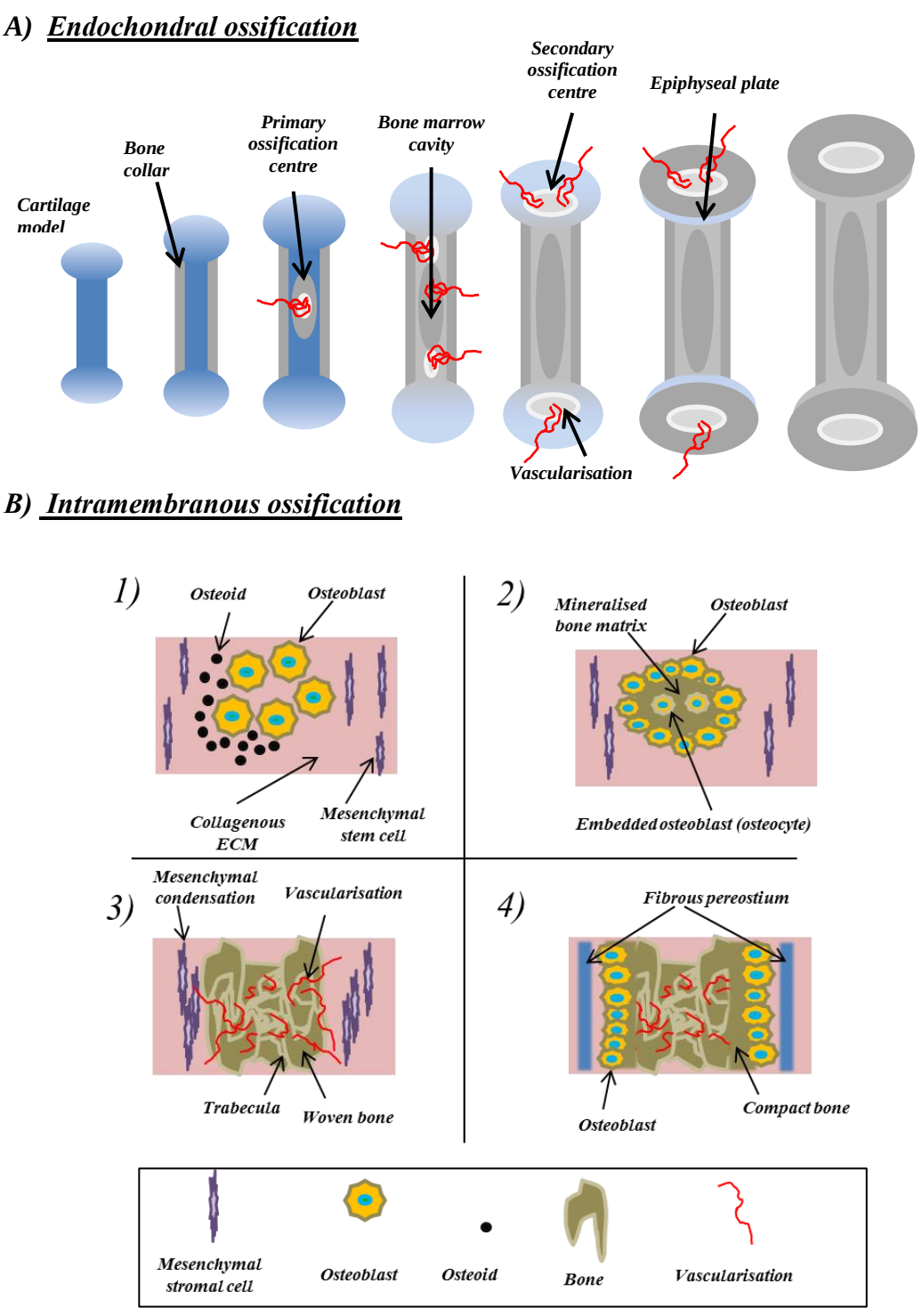

Figure 3: Picture representation of the different stages of endochondral (A) and intramembranous bone formation (B).

1.4.3. Bone homeostasis

During bone remodelling and homeostasis, native bone cells will exhibit a number of different phenotypes as they progress from a dormant or 'quiescent' state to becoming embedded osteocytes. Osteoclasts (OC) are first recruited to deliver hydrochloric acid and proteases to degrade old bone, releasing factors contained in the matrix which encourage recruitment of osteoblasts (Väänänen et al. 2000)(Rucci 2008). Osteoblasts (OB) then invade the site and either undergo apoptosis or encapsulate themselves in mineralised matrix, the latter process completing terminal differentiation into osteocytes (OS) (Manolagas 2000) **(Figure4)**.

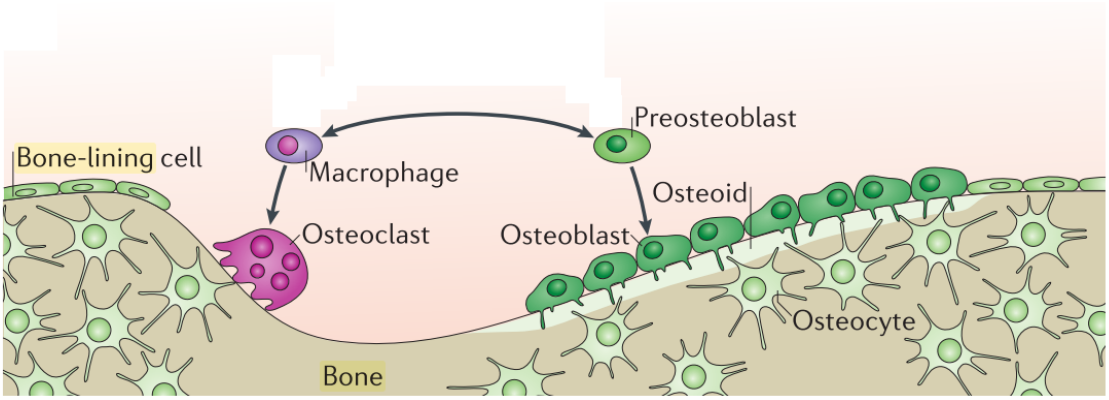

Figure 4. Cartoon depiction describing bone formation in the context of bone cell turnover *(Long 2011)* ***.*** *Reprinted with permission of Nature publishing group [license number: 3791991136324]*

The mechanisms involved in regulating native osteoblast and osteoclast populations that are required for a healthy rate of bone remodelling are currently not well defined. Osteoclasts are thought to differentiate from haematopoietic derived macrophages (Udagawa et al. 1990) via proximal signalling of receptor activator of nuclear factor kappa-β ligand (RANKL) from osteoblast lineage cells (Yasuda et al. 1998). Proximal signalling mechanisms play an important part in regulating both recruitment and cell functionality of osteoclasts. OBs have been shown to influence OC differentiation by negatively regulating

RANKL expression via paracrine signalling (Udagawa et al. 1990). Sclerostin is a soluble factor secreted by OSs and interestingly has recently been shown to regulate bone resorption by interacting with RANKL production (Wijenayaka et al. 2011)(Xiong & O'Brien 2012), highlighting a complex multiparameter system that is to date, poorly correlated. In addition to that previously discussed, an increases in nitric oxide (NO) signalling has also been shown to regulate OC differentiation *in vitro* and in the developing chick embryo (Collin-Osdoby et al. 2000). NO signalling, an early mediator of bone formation induced by mechanical loading (Fox et al. 1996), has also been shown to regulate RANKL and osteoprotegerin (OPG) in osteoprogenitor cells (Fan et al. 2004), again highlighting the broad interplay of signalling events involved in bone remodelling. OC recruitment has also shown to be sensitive to surface topography, whereby a smooth surface rather than a rough surface promoted tartrate-resistant acid phosphatase (TRAP) expression (Costa et al. 2013). Age is another important factor that influences OC, shown by a positive correlation between increased age and OC differentiation (Chung et al. 2014).

OBs are thought to derive from MSC progenitors residing in the bone marrow (Pittenger et al. 1999). MSCs differentiate into osteoblasts via transcription of Runt-related transcription factor 2 (Runx2), which when abrogated in mice results in a complete lack of ossification of the developing skeletal system (Komori et al. 1997). Runx2 is often referred to as the 'master switch' for osteogenic differentiation in MSCs and has a number of upstream effectors such as; bone morphogenetic protein (BMP) (Gori et al. 1999), the int/Wingless family (Wnt) (Ling et al. 2009) which has also been shown to interact with the BMP during osteogenic differentiation (Bain et al. 2003), and external mechanical stimuli (Sittichokechaiwut et al. 2010)(Chenyu & Rei 2012b) which again can influence the behaviour of intermediate pathways of Runx2 through Wnt (Yu et al. 2010) and BMP (Sumanasinghe et al. 2006) signalling.

Whilst the molecular mechanisms that govern the process of MSC to osteoblast differentiation are complex, the behaviour of osteoblasts is distinct from other bone cell types. Functional responses of osteoblasts *in vitro* are easily identified through the production of proteins such as; osteocalcin, non-collagenous protein secreted by osteoblasts which is thought to be involved regulating of bone metabolism (Long 2011), and alkaline phosphatase, which is thought to assist bone mineralisation by cells(E. E. Golub & Boesze-Battaglia 2007). The physical environment also plays an important role in regulating OB behaviour. For example, in contrast to OCs, OB functionality is favoured by rough surfaces. This has been shown by a number of groups to promote bone formation and osteogenic gene expression (Costa et al. 2013) (Gough et al. 2004)(Cheng et al. 2014).

As mentioned previously, when OBs become encased in mineralised matrix they are considered to have become terminally differentiated osteocytes (OS) (Chan et al. 2009). During this process there is a shift in gene expression from markers such Runx2 and osteocalcin (OCN) in bone lining osteoblasts, to markers such as E11 (Schwab et al. 1999), which is believed to play a role in the formation of dendritic processes characteristic of osteocyte formation (Bonewald 2011) (Zhang et al. 2006). OSs contribute the largest population of cells in bone tissue relative to OBs and OCs, and play an important role in regulating bone remodelling by OBs and OCs via the transport of signalling molecules such as dentin matrix protein 1 (DMP-1) and fibroblast growth factor 23 (FGF23) (Bonewald 2007). Osteocytes are interconnected via dendritic processes that span the canaliculi in bone. These canaliculi are filled with interstitial fluid, which as mentioned previously, allows mass transport to occur, and importantly for this research the transduction of fluid pressures, resulting from external mechanical stimuli, into biophysical processes that determine cell behaviour (Chen et al. 2010). Munrow and Piekaeski were the first to conclusively demonstrate that the loading of bone results in the changes in

interstitial fluid pressure in the canaliculi of bone (Munrow & Piekarski 1977). There has since been an incentive, particularly in the context of BTE, to understand the process of loading of bone and cell signalling between osteocytes, osteoblasts and osteoclasts. It is hoped that by understanding what mechanical signalling events manage bone remodelling, we can design *in vitro* growth environments that promote bone tissue constructs to be used as substitutes for autografts and/or temporary implants.

1.4.4. Protein and mineral composition of bone

The mineralised inorganic phase of bone is comprised primarily of a crystal structure of calcium hydroxyapatite (Hall & Guyton 2006), and constitutes between 60-70%of the dry weight of bone. The remaining organic phase of bone contains in the region of 10-20% water and collagen type-1, comprising about 90% of proteins constituting bone tissue (Hadjidakis & Androulakis 2006). Collagen provides an elastic, highly ordered lamellar structure that is made stiff by the presence of calcium phosphate and hydroxyapatite mineral phases on the collagen fibres themselves (Olszta et al. 2007). Bone matrix also contains a number of different non-collagenous proteins (5%) and lipids (2%) (Young 2003). Non collagenous proteins play numerous roles in the formation and regulation of bone, however their specific roles in regulating bone homeostasis is still debated. Alkaline phosphatase (ALP) is a metalloenzyme that is highly expressed in mineralised bone. Although the mechanism of action of ALP is not fully understood, it is believed to increase the local concentration of inorganic phosphates involved in bone mineralisation (Ellis E Golub & Boesze-Battaglia 2007)(Harmey et al. 2004). OCN is a non-collagenous protein secreted by OBs which, as mentioned previously, is thought to be involved in the regulation of bone metabolism (Long 2011), but has also been shown to facilitate the orientation of calcium ions within the mineralising hydroxyapatite lattice (Hoang et al. 2003). Both ALP and OCN are positively expressed by differentiating

MSCs, with expression of both ALP (Jaiswal et al. 1997) and OCN (Nakamura et al. 2009) considered representative of the early osteogenic phenotype. The process of controlled mineralisation during bone development is at present unclear. Recent evidence has suggested that the presence of collagen in a hierarchical assembly, often cited as the formation of a collagen liquid crystal phase (Giraud-Guille et al. 2003)(Giraud Guille et al. 2005)(Giraud-Guille et al. 2008), can initiate and orientate the formation of the apatite minerals that form bone(Wang et al. 2012).

1.4.5. Bone fracture healing

During normal fracture healing there are three main processes that occur; the inflammatory phase, the repair phase, and the remodelling phase (**Figure 5**). During the initial stage prior to injury a haematoma forms, followed rapidly by the inflammatory phase. The inflammatory phase involves neovascularisation and invasion of collagen secreting fibroblasts to form a vascularised soft callus. After this the reparative phase sees recruitment of osteoblasts which lay down new osteoid, forming a spongy woven bone matrix bridging the fracture. The reparative phase see's the formation of both endochondral bone, providing a soft cartilaginous template (**Figure 3C)**, and also mesenchymal condensation via intramembranous ossification, leading to the formation of a hard callus (**Figure 3D)**(Marsell & Einhorn 2011). The remodelling phase then sees a balance of OBs and OCs resorbing and relaying new bone matrix until the injury site is fully healed (Oryan et al. 2013). Multipotent stem cells are believed to be involved in the healing process, first being recruited to the injury site by different cytokines, and subsequently differentiating to form new bone in the injury site(Liu et al. 2009). The first two stages cumulatively last around 4-7 days whilst the remodelling phase can last anywhere between 6 weeks and 12 months (Tsiridis et al. 2007).

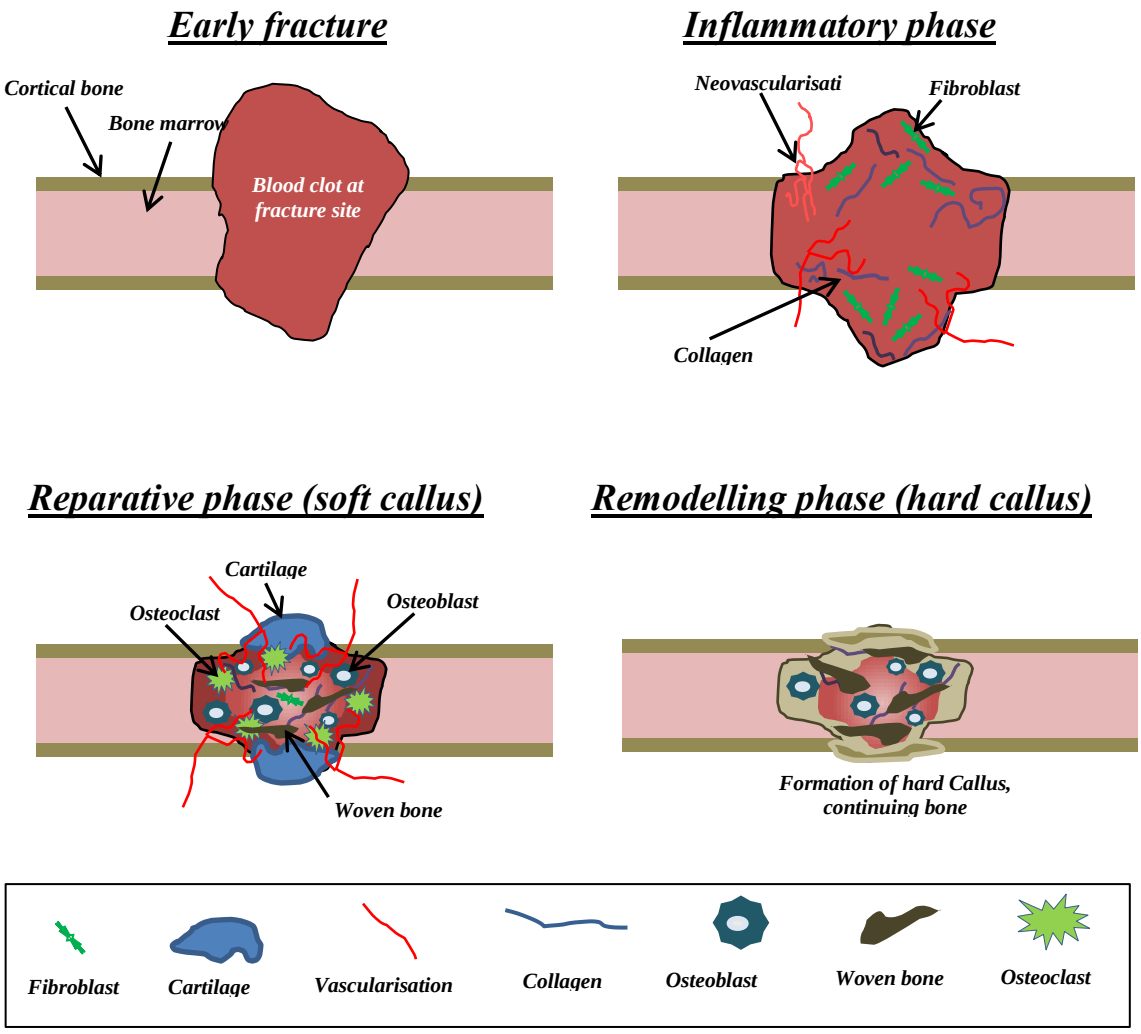

Figure 5: Cartoon depiction of the different stages of fracture healing

1.5. Tissue engineered bone

1.5.1. Primary cell sources in bone tissue engineering

In vitro research of bone formation utilises a range of established bone cell lines to probe the underlying biological phenomena that regulate both developmental bone formation as well as adult bone homeostasis. Human primary cells are most desirable since they are both clinically relevant and lack interspecies differences. There has been a large body of research in recent years investigating different cell phenotypes for engineering bone tissue. There are two main branches of stem cell that are utilised in the BTE, pluripotent stem cells (PSCs) and multipotent stem cells.

PSCs were originally extracted in the form of embryonic stem cells (ESCs) from the blastocyst stage of embryonic development (Reubinoff et al. 2000). PSCs possess the unique ability to differentiate into any cell type in the body and are often considered to be one of the clinical milestones for RM therapies. This is in part due to recent developments in the production of induced pluripotent stem cells (iPSCs), which possess the same characteristics as ESCs, but have the added advantage of originating from adult somatic cells that have undergone genetic modification to unlock their multi lineage potential (Takahashi & Yamanaka 2006). Evidence has demonstrated the potential for both ESCs and iPSCs for *in vitro* production of tissue engineered bone (Marolt et al. 2012) (de Peppo et al. 2013). Promisingly, ESC therapies have already made their way into phase I/II clinical trials. Advanced cell therapies sponsored a trial investigating the effect of ESC transplantation on patients with Stargardts's macular dystrophy, demonstrating improved ocular function after a 22 month patient follow up study with little adverse reaction to the treatment (Schwartz et al. 2015). However, there are still some major concerns for ESC and iPSC derived cell therapies that have recently come to light. There was initially hope that ESCs would overcome complications of immune rejection due to their limited

expression of histocompatable antigens (Drukker 2004). However, more recent evidence has shown that ESC derived tissue lineages express histocompatibility antigens that potentially make them unsuitable for allogeneic therapies (Nussbaum et al. 2007). Coupled with this, whilst autologous iPSCs overcome the barriers set by the immune system, current technologies lack the ability to efficiently produce iPSC derived tissue lineages without introducing the risk of malignant tumour formation (Herberts et al. 2011)(Geoghegan & Byrnes 2008).

Mesenchymal stromal cells (MSCs) are were first recognised in their current definition by a Russian scientist, who observed adherent cell populations isolated from rodent bone marrow (Friedenstein et al. 1970) that were capable of forming ectopic bone *in vivo* after transplantation (Friedenstein et al. 1966). The definition of MSCs is generally characterised by their ability to differentiate toward derivatives of the mesodermal germ layer, which contributes to the formation of tissues such as bone, cartilage, fat, and muscle. Hence, MSCs are considered multipotent stem cell derivatives with a rapid proliferation potential (Piertenella et al, 2003), making them a good choice of cell for large scale production of cells for RM therapies. They can also be isolated in adults from a number different tissues in the body such as adipose tissue (Zuk et al. 2002), dental pulp (Shi & Gronthos 2003), tendon (Salingcarnboriboon et al. 2003), umbilical cord blood (Secco et al. 2008), and synovial tissue (Secco et al. 2008). Since MSCs from bone marrow and adipose tissue can be easily isolated using low cost, minimally invasive procedures, and yield a high population of MSCs relative to other tissue sources such as umbilical cord blood (Lee et al. 2004), they have occupied much of the focus in research aiming to use MSCs in BTE.

Bone marrow derived stem cells (BMSCs) and adipose derived stem cells (ADSCs) have been shown to have somewhat ostensible similarities (Zuk et al. 2001), nonetheless they share numerous distinct positive and negative surface markers characteristic of MSCs; positive: CD29, CD44, CD90, SH2/CD105 and negative: CD11b, CD14, CD45 (Zuk et al. 2001)(Dominici et al. 2006). MSCs are shown to have potent immunomodulatory properties such as supressing the proliferation of T-cells (Klyushnenkova et al. 2005) and secretion of cytokines that can reduce inflammation at the site of injury (Guo et al. 2007). Interestingly, it has been shown that BMSCs and ADSCs also share similar immunosuppressive properties after osteogenic differentiation *in vitro,* suggesting both cell types could be suitable for allogeneic as well as autologous cell therapies (Niemeyer et al. 2007). However, there is conflicting evidence regarding the immunomodulatory properties of allogeneic MSCs, in which T-cell responses are not fully silenced, resulting in rejection of the allogeneic graft (Nauta et al. 2006).

There has been a relatively large body of research aiming to determine the efficacy of MSCs for BTE when sourced from different tissue types (Dragoo et al. 2005)(Niemeyer et al. 2010)(Niemeyer et al. 2007). An *in vivo* study by Niemeyer et al. use radiographic evaluation to compare newly formed bone in critically sized defected sheep tibia treated with ADSC and BMSC collagen sponges (Niemeyer et al. 2010). The results showed that sheep tibia treated with BMSC seeded sponges had significantly higher bone formation over both ADSC groups and unseeded controls, suggesting a more relevant use for BMSC in the clinic. However, subcutaneous fat has been found to contain up to 50-100 times as many stem cells per gram of tissue than bone marrow aspirates (Orbay et al. 2012), highlighting the need for future clarity of the true efficacy in using BMSCs over ADSCs or vice versa.

1.5.2. Established cell lines for studying in vitro bone formation

Limited availability, donor variation, and labour intensive isolation procedures are some key motives for substituting primary human cell lines for animal derived and immortalised cell lines for *in vitro* research. Consideration of the most suitable cell type for a particular experiment can maximise both output and the significance of the end result. Cell lines such as Mouse long bone osteocyte-A5 (MLO-A5) are useful in studying the transition from late OB to early OSs. This transition typically occurs when differentiating OBs encase themselves in mineralised matrix (Bonewald 2011). They are highly expressive of bone markers such as ALP and OCN (Bonewald et al. 2006), and maintain a high proliferative potential and consistent phenotype over multiple passages. Since they so readily mineralise in culture, MLO-A5s also provide a useful tool for studying mechanotransduction. MLO-A5s have been shown to undergo physiological changes during application of fluid shear in monolayer(Delaine-Smith et al. 2014)(Siller-Jackson et al. 2008), which leads to increased calcium deposition in both 2D (Delaine-Smith et al. 2014) and 3D growth environments (Sittichockechaiwut et al. 2009).

There are pros and cons of using different cell lines for different studies, reviewed extensively by Czenkanska et al (Czekanska et al. 2012). Czenkanska highlights that whilst mouse cell lines such as MLO-A5s are useful for studying bone cell behaviour, they also possess interspecies and genomic differences that introduce translational complications for BTE therapies. Coupled with this, the response of MLOA5s is not representative of less committed cell phenotypes such as stem cells or osteoprogenitors. Human osteoblast-like cells (MG-63s) provide useful insights into bone cell function. Like MLO-A5 cells they exhibit high proliferative potential and no loss of phenotype during extended culture. Unlike MLO-A5, MG-63s are thought to represent a relatively early stage of OB differentiation (Pautke et al. 2004). They have also been shown to exhibit a profile of

expression similar to primary human OBs for the mineralisation marker OCN (Czekanska et al. 2014). The response of MG-63s to mechanical loading has been widely reported, demonstrating active responses to strain (D.-Y. Lee et al. 2010), fluid flow (Su et al. 2014), and to a lesser extent hydrostatic pressure (Kubo et al. 1998)(Haskin & Athanasiou 1993). Thus MG-63s appear to represent a useful model for evaluating mechanical preconditioning tools that is cost effective and comparable to a large body of literature. Furthermore, established protocols for studying events that commonly occur in OBs exposed to mechanical loading such as increased collagen and calcium deposition (Michael Delaine-Smith et al. 2015) are readily available in the literature. Utilising these protocols could provide useful validation techniques to identify mechanotransduction events using our bioreactor system. Whilst primary human cell lines will be necessary to establish a clinical benchmark for developing BTE therapies, the range of alternative cell lines from other sources can generate valuable data that is cost effective and applicable across the scope of literature that characterise mechanical force bioreactors.

1.6. Tissue engineering scaffolds

Selecting the appropriate scaffold material to provide an optimal growth environment for *in vitro* bone formation encompasses in itself an entire field of biomaterials research in BTE. From a TE perspective, scaffolds should incorporate: an interconnected porous structure that allows cell migration; appropriate diffusion characteristics that enable efficient mass transport process; appropriate biocompatibility that supports the function of a desired cell phenotype; and suitable architecture that best promotes integration and tissue regeneration after transplantation (Liu et al. 2007). In the context of BTE, and more specifically for fracture healing, scaffolds should provide adequate mechanical stability to the fracture site, and promoting the biological activity of bone and the surrounding tissue

(Babis & Soucacos 2005) (Schatzker et al. 2005). Generally the biological potential of BTE scaffolds is characterised by three main principles: osteoconductivity, which allow both implanted and native cells to proliferate and populate the scaffold (Rupani et al. 2012); osteoinductive, to induce differentiation of osteoprogenitor cells into bone forming osteoblasts; and to provide a reservoir of replenishing stem cell progenitors to maintain bone tissues innate capacity for self-renewal (Albrektsson & Johansson 2001)(Rupani et al. 2012) (Bueno & Glowacki 2009). Another important factor influencing the implementation of scaffolds in BTE is a controlled degradation rate. In principle, this would allow native cells to replace the degrading scaffold with newly synthesised extra cellular matrix (ECM) without negatively affecting the functionality of the injury site (Babensee et al. 1998).

1.6.1. Targeted strategies in tissue engineered scaffolds

There are numerous different studies that have attempted to incorporate these principles into single scaffolds. A number of groups describe the implementation of biomimetic hydrogels with a sustained release of growth factor cocktails to facilitate fracture repair (Lienemann et al. 2012)(Smith et al. 2014a)(Smith et al. 2014b)(Gothard et al. 2014). However, limitations exist in the use of growth factor laden scaffolds due to their relatively short half-life *in vivo* and suboptimal release kinetics, leading to administration of un-physiologically high concentrations of growth factors (Stevens 2008). Administration of BMP-2 in patients receiving a posterior lumbar interbody fusion has been shown to lead to neurological impairment due to ectopic bone formation in the lumbar canal (Wong et al. 2008). Other approaches have attempted to overcome the safety concerns associated with growth factor loaded scaffolds by utilising techniques such as magnetic targeting of cell surface receptors which are thought to regulate stem cell differentiation (El Haj et al. 2012)(Henstock et al. 2014). Whilst this approach seems

promising in terms of safety versus growth factors, current research is yet to provide preclinical data and subsequent evaluation of efficacy in larger animal models that is required for clinical translation.

1.6.2. Synthetic vs natural biomaterials

The argument of whether to use synthetic versus natural biomaterials for BTE is difficult to interpret since both approaches have distinct and numerous advantages over the other. For example, synthetic biopolymers are considered to offer an advantage over natural biopolymers since they can be tailored to give a wide range of properties and more predictable kinetics (Liu et al. 2007). As such, there has been a large research space occupied by the development of synthetic biopolymers, particularly those which have already obtained FDA approval for use in humans such as poly-lactic acid (PLA), polyglycolic acid (PGA), polycaprolactone, (PCL) and poly(lactic-co-glycolic acid) (PLGA) (Ma 2004)(Liu et al. 2007)(Pitt et al. 1981). Today, synthetic polymers are commonly used in orthopaedic surgery due to their biocompatibility and ability to undergo bulk degradation at a predictable rate (Hutmacher 2000)(Rothstein et al. 2009).

Natural biomaterials possess an intrinsic advantage over synthetic biomaterials in that they are in many cases derived from the ECM of native tissue. Collagen for example is arguable the most widely used natural biomaterial in TE because it constitutes the majority of proteins found in mammals, accounting for over 1/3 of the total protein content in the body (Patino et al. 2002). In reference to BTE, collagen type 1 is extensively used as a biomaterial, both in its pure form and in composite with many other natural and synthetic materials (O'Brien 2011). Many collagen composites have already seen clinical approval for use in humans such as: collagen/glycosaminoglycan copolymers for skin regeneration (Yannas et al. 1989); mineralised collagen scaffolds for

lumbar spinal fusions (Neen et al. 2006)(Ploumis et al. 2010); collagen tricalcium phosphate composites for lumbar spinal fusions (Kraiwattanapong et al. 2005); and demineralised bone matrix in a type 1 collagen/sodium alginate carrier for alveolar cleft reconstruction (Francis et al. 2013). Interestingly, collagen alginate scaffolds have also been developed into a tuneable hydrogel composite to allow user defined initiation of human pluripotent stem cell differentiation (Dixon et al. 2014). This suggests future research using these clinically approved materials might be adapted to allow controlled differentiation and replenishing of the stem cell pool after transplantation. The use of collagen in BTE arguable represents one of the more clinically relevant strategies to translate research from the bench to the bedside; however certain aspects of its use still need addressing such as its poor mechanical properties (O'Brien 2011).

1.7. Tissue engineering models

Since RM ultimately aims to employ translatable research into medical treatments, the associated regulatory hurdles make it essential that not only are potential treatments safe, but that they demonstrate sufficient efficacy in preclinical testing. Muschler and colleagues summarise in detail the challenges facing translational research in bone tissue engineering (Muschler et al. 2010). They highlight the use of animal models to provide relative clinical efficacy, but also identify gaps in the availability of such systems based on three principles. The first discusses the need for assessment of the predictive power of such models, taking into account variation between different species and how this translates to use in humans. The second considers the need for models that mimic the wound healing process; incorporating the healing environment whilst considering mass transport conditions in different sized injuries. The third, and perhaps the most relevant from a research point of view, is the ability to measure and detect

different effects such as cell trafficking events and cell fate during bone remodelling and regeneration. Gothard et al. provide an extensive review on the current use of animal models and the associated factors one should consider in selecting appropriate models for clinical evaluation of BTE therapies (Gothard & Smith 2014). Similar to Muschler and colleagues, Gothard et al. describe in some detail the importance of identifying animal models in which the interspecies similarities in bone physiology can allow effective translation of treatments into humans. For example, pig models could be advantageous in this sense, since their anatomy and mineral bone density is not too dissimilar from humans (Aerssens et al. 1998). In contrast, rat models whilst being low cost and high throughput relative to pig models, their small size and high rate of bone turnover introduces translational problems when considering the scale up of vascularised bone constructs (Gomes & Fernandes 2011). By taking into consideration these key aspects of animal models, I can review the current basis of research on which animal models best suits a translational based evaluation of the hydrostatic force bioreactor.

1.7.1. Live animal models

The use of live animal models to evaluate potential treatments for large bone defects addresses models that incorporate the wound healing process, whilst considering mass transport complications that might arise from massive bone loss, due to for example bone tumour resections. Zhu and colleagues modelled repair of critical sized femur defects in goats, using autologous bone marrow stromal cells in natural coral scaffolds (Zhu et al. 2006). They showed a significant increase in healing of the defect versus acellular scaffolds and empty defects, and importantly that the loading bearing capacity in the injury site after 4 months was similar to the opposite side normal femurs. Studies

have also demonstrated increased healing capacity in defects using autologous based stem cell therapies in different animal species including; primate models (Boden et al. 1998)(Cook et al. 2002) canine models (Luangphakdy et al. 2013); and equine and ovine models (Niemeyer et al. 2010) among many others. Smaller animal models can overcome some of the time and cost constraints that limit the use of larger animal models. For example, preclinical evaluation of autologous cell therapies for bone defect repair has shown success in rabbits (Zhang et al. 2012), and mice (Zwingenberger et al. 2013). Interestingly clinical translation of rabbit models has been successful, with the use of Progenix™ Putty showing efficacy in rabbits (Smucker & Fredericks 2012), and now clinically approved for use in humans (Kurd et al. 2015).

1.7.2. Organotypic models of tissue regeneration

Whilst live animal models are useful from the point of view of preclinical testing, Gothard et al. correctly identify that live animal models in any form are inherently unethical (Gothard & Smith 2014). Moreover, live animal models do not represent a transition in today's research toward the 'three Rs' principle (replacement, refinement and reduction). The Animal (Scientific Procedures Act) 1986 incorporates the three R's principle into law (Hollands 1986), rightly urging scientists to approach medical based research without relying on live animal models. Coupled with this, the ability to monitor cell trafficking and cell fate (Muschlers 3rd consideration (Muschler et al. 2010)) is made complicated by the use of live animal models when compared with recent advances in organotypic tissue models.

Organotypic models of tissue regeneration have been providing researchers with a base for addressing the three R's by trying to recapitulate *in vivo* niches of both

developmental and adult systems. The use of organotypic tissue models has provided a platform to study regeneration of spinal cord lesions (Weightman et al. 2014), skin (Oh et al. 2014) and bone, using embryonic chick femurs (Smith et al. 2013)(Kanczler et al. 2012). The developing chick embryo offer a useful developmental system to study bone repair, and has received a revival in recent years due to both time and cost effectiveness, and reduced ethical concerns owing to the stage of embryonic development in which the chicks are culled. The model has proven effective in studying the developing bone niche in a vascularised environment (Gellynck et al. 2013) using the chorioallantoic membrane (CAM) assay. The isolation of chick femurs has been utilised for modelling bone formation in response to pharmacological agents (Smith et al. 2015) and to study femoral defect repair (Smith et al. 2014a)(Smith et al. 2014b). As mentioned previously, our bioreactor system has already proven effective in stimulating new bone formation in isolated chick femurs, thus the potential to use this model to study the effect of hydrostatic pressure on fracture repair could provide interesting and novel findings. Coupled with this, the use of isolated chick femurs is easily compatible with Muschlers 3rd consideration and can allow accurate tracking of cells, as well as their associated stem cell fate.

1.8. Mechano-active responses in bone cells

A mechanically active environment *in vivo* is crucial in the development and maintenance of bone tissue. The effect of increased or reduced mechanical stimulus is demonstrated by observations of an average 30% thicker cortical bone in the fore arms of elite tennis players (Jones et al. 2007), to a significant loss in bone mass in people exposed to prolonged bed rest (Rubin et al. 2001). *In vitro* studies have suggested OSs to be primary mechanosensors in bone, evidenced by the development of fragile bones and

micro fractures in mice when OS function was ablated (Tatsumi et al. 2007). Interestingly the same study showed that ablation of osteocyte function also prevented the loss of bone mass in mice after prolonged hind leg unloading, suggesting that osteocytes may orchestrate both the formation of bone by osteoblasts and the resorption of bone by OCs. As mentioned earlier in this chapter, mechanical loading of osteocytes has been shown by a number of studies to induce NO production (Fox et al. 1996)(Tjabringa et al. 2006)(McGarry et al. 2005), which has been reported to inhibit OC function (Tan et al. 2007)(van't Hof & Ralston 1997) whilst also stimulating OB function (Mancini et al. 2000). Other signalling events commonly associated with mechanical loading in bone cells include; ion channel activation (el Haj et al. 1999)(Yang et al. 2002), integrin mediated gene transcription (Plotkin et al. 2005), and mechanosensing by primary cilia (Temiyasathit et al. 2012)(Malone et al. 2007). The overall picture of how these events regulate bone remodelling *in vivo* is complex and to date not fully understood. However, a consistent agreement in the literature, first proposed by the surgeon Julius Wolf in the 19th century (Chen et al. 2010) is that mechanical loading of bone is translated into biochemical signals in cells, resulting in adaptive bone remodelling.

1.8.1. Distinguishing between different types of force

It is generally accepted that mechanical loading of bone tissue generates: high hydrostatic pressures in the interstitial fluid that fills the lacuna network (D. Zhang et al. 1998); interstitial fluid flow resulting from pressure gradients in the lacuna network of bone (Munrow & Piekarski 1977); and strains caused by physical deformation of bone ECM(Burr et al. 1996). Hydrostatic -pressure by definition is the force exerted by a fluid in a confined space. The force transduction of pressure on an object will depend on the compressibility of the object, either leading to deformational stress and strain if the object is compressible, or static pressure if the object is incompressible. Since bone is relatively

incompressible, and pressure is transduced through interstitial fluid, which is also incompressible, the transduction of force from hydrostatic pressure to cells is considered to be static and does not induce significant deformational change. By contrast, if hydrostatic pressure gradients are generated upon loading, fluid flow in the lacuna space can result fluid shear and deformational strain on osteocytes in the lacuna network, hence it is important to distinguish the effect of static vs dynamic in the context of changes in cell behaviour upon loading.

1.8.2. Influence of strain

Strain is an intrinsic consequence of mechanical loading in bone tissue. Estimates of strain in human bone during loading have suggested: peak compressive strains of -(400-600με) when walking and -(500-1000με) when running; a peak tensile strain of between 400-500με when walking and 600-700με when running; and peak shear strains of 800-1000με when walking, and 900-1600με when running (Burr et al. 1996). Chen and colleagues provide an excellent summary of the various mechanical factors that influence bone remodelling (Chen et al. 2010). Interestingly, they suggest that hydrostatic pressure and fluid flow rather than strain to be the primary stimuli for OSs, and that strains role in providing mechanical stimuli is more prominently featured in OB precursors present in the softer fibrous tissue of the periosteum, which would deform significantly during loading relative to cortical bone. A number of groups have observed enhanced proliferation in MSCs due to applied strains (Song et al. 2007)(Qi et al. 2009)(Subramony et al. 2013). The effect of strain has been implicated to be sensitive to the loading regime. As an example, Kioke et al. showed that MSC proliferation was enhanced at higher strains, whereas osteogenic differentiation was more favoured at low strains (Koike et al. 2005). Lee et al. also reported changes in response to strain in adipose derived MSCs, where strain inhibited both proliferation and cell differentiation. This might imply that

responses of MSCs from different cell niches can also affect cellular response to strain (Lee et al. 2007). The effect of strain in osteoblast phenotypes is reportedly similar to that of MSCs, with increases observed in cell proliferation (Ignatius et al. 2005) and osteogenic differentiation (Ignatius et al. 2005)(Visconti et al. 2004). It should be stated however that the Visconti also reported changes in cell behaviour according to the characteristics of the applied strain regime. It should be mentioned that Mullender et al. discuss in their paper the ambiguity associated with many *in vitro* systems for applying strain, whereby by 'true strain' is in fact not present and is in most cases accompanied by fluid flow (Mullender et al. 2004). Interestingly they demonstrate that fluid flow and not strain was responsible for prostaglandin E2 (PGE2) production in human primary bone cells, whereas both strain and fluid flow influences NO production. This demonstrates nicely how changes in the nature of the applied force can potentially change the behavioural outcome of bone cells.

1.8.3. Influence of fluid flow

As mentioned previously, fluid flow in bone occurs due to pressure gradients in the canaliculi and lacuna spaces of bone during normal loading (Munrow & Piekarski 1977). This fluid flow is sensed by osteocytes as shear force and is translated into biochemical signals that regulate bone formation. Early experiments have shown onset of NO signalling in chick osteocytes but not periosteal fibroblasts following just a few minutes exposure to fluid flow (Klein-Nulend et al. 1995). Other studies have observed similar phenomena, whereby fluid shear induces rapid onset of PGE2 production in MLO-A5 cells (Delaine-Smith et al. 2014), less committed MC3T3 preosteoblasts (McGarry et al. 2005) and more recently NO release in MSCs (Lu et al. 2015). It should be mentioned at this point that NO and prostaglandins are often used interchangeable when defining mechanotransduction in cells responding to fluid flow. This is in part due to the evidence

describing NO increasing the activity of cyclooxygenase (COX) enzymes (Salvemini et al. 1993), which act as a precursor to the synthesis of prostaglandins (Mollace et al. 2005). After the onset of NO or PGE2 release, another widely reported phenomena that occurs are after mechanical stimulation with fluid flow is stress fibre formation in the actin cytoskeleton (Chen et al. 2000) (McGarry et al. 2005)(Gardinier et al. 2009). Interestingly, the study by Gardinier et al. directly compared the effect of fluid shear and cyclic hydrostatic pressure in osteoblasts, concluding that whilst similarities occurred in the levels of COX2 expression, the effects on cytoskeletal remodelling were distinct to each stimulus. A recent study suggested that cytoskeletal tensioning is a necessary requirement for osteogenic differentiation via Runx2 transcription in murine mesenchymal stromal cells exposed to fluid flow (Arnsdorf et al. 2009). It may be that changes in cytoskeletal dynamics during mechanical loading contributes to the changes in cellular behaviour.

Our current understanding of fluid flow and its effects on bone cells extends from the very earliest responses to flow as discussed above, to its prolonged effect on the osteogenic differentiation of stem cells and their ability to produce new bone. There is a large body of research studying the effect of flow perfusion systems that aim to improve the outcome of tissue engineered bone. Unlike strain, application of fluid flow *in vitro* possesses the ability to provide a combinatorial stimulus in the form of mechanical signalling, and improving the homogeneity of tissue maturation through enhanced nutrient diffusion. This effect has been demonstrated by a number of groups in: synthetic biomaterial scaffolds (Porta et al. 2015); natural biomaterial scaffolds (Antebi et al. 2013); and also trabecular bone explants (Grayson et al. 2008). Other groups have also utilised a combination of fluid flow and compression (Hoffmann et al. 2015)(Bouet et al. 2015), with earlier reports suggesting that the combination of both compression and fluid

flow is a more effective stimulus than fluid flow or compression alone (Bolgen et al. 2008).

1.8.4. Influence of Hydrostatic Pressure

The use of hydrostatic pressure (HP) as a therapeutic tool was first recognised by Lipello and co-workers in 1985 when they observed increased metabolic activity in articular cartilage segments when exposed to low hydrostatic pressure (Lipello et al. 1985). The majority of studies using hydrostatic pressure that have been performed over the last 15 years regarding hydrostatic preconditioning in cell seeded scaffolds have focussed on functional improvements to cartilage tissue *(***Table1***).* The functional aspects of cartilage are considerable different to bone. For example, hydrostatic pressures have been estimated at as high as 18MPa in cartilage tissue present in the hip joint (Afoke et al. 1987), nearly an order of magnitude higher that pressure estimated in the interstitial fluid of bone (D Zhang et al. 1998). In addition to this, whereas the main constituent protein in bone is collagen type I, cartilage consists primarily of collagen type II (Sophia Fox et al. 2009). Despite these functional differences it would not unreasonable to postulate that mechanisms of mechantransduction that occur in bone and cartilage are related, particularly when we consider the transition from cartilage to bone during the process of endochondral ossification. The effectiveness of HP for stimulating *in vitro* bone formation (**Table 2)** clinically relevant cell types such as hMSCs is not currently well defined. Many groups have adopted fluid shear as the primary mechanical stimulus for tissue engineered bone, however there have been some interesting findings in the last 10 years regarding hydrostatically stimulated bone formation (**Table 2)**.

Study	Methods	Results
(Angele et al. 2003)	• *hMSC aggregates* • *Cyclic HP, 1Hz, 0.55 – 5MPa, 3h/day for 7 days,* • *14-28 day culture, chondrogenic media*	*HP resulted in larger constructs and histological staining indicated a greater matrix/cell ratio. Stimulated groups showed statistically significant increases in proteoglycan and collagen content at day 14 and day 28.*
(Miyanishi et al, 2006)	• *hMSC's pellet cultures* • *Cyclic HP, 1Hz, 0.1-10MPa 4h/day* • *14 day culture in chondrogenic media*	*HP in the presence of growth factors increased chondrogenic gene expression up to 3.3 fold by day 14. Extracellular matrix deposition of type II collagen and aggrecan increased in cell pellets.*
(Meyer et al, 2011)	• *hMSCs multiple donors seeded in agarose gel scaffold,* • *Cyclic (10MPa) 1Hz, 1hr/day) and continuous HP(10MPa)* • *42days culture, chondrogenic media*	*HP increased collagen and GAG accumulation by day 42, resulting in an increased dynamic modulus compared to FS controls. Effect variable between donors. Static pressure had no effect on either matrix accumulation or construct mechanical properties for both donors*
(Jeong et al. 2012)	• *hMSC/chondrocyte co-culture seeded in Alginate gels* • *Continuous HP, 0.02- 0.2MPa 2min HP, 15min rest, 2h/day, 7 days* • *20 day culture, proliferation media.*	*HP resulted in higher proliferation of MSCs Gene expression of Collagen type II, SOX9, and aggrecan in MSCs under intermittent HP was comparable with that in unstimulated MSCs in chondrogenic media.*
(Steward et al. 2012)	• *hMSC's seeded in either agarose or fibrin gels* • *10MPa 4hr/day CHP, 1Hz,* • *3 week culture, in chondrogenic media*	*Agarose gels better supported tissue maturation. Significant increase in secretion of sGAGs present only in fibrin gels exposed to HP. HP decreased ALP activity in both agarose and fibrin.*
(Correia et al. 2012)	• *hASC seeded gellan gum hydrogels* • *Cyclic(0.1-1Hz, 3hr/day) and Sustained(3hr/day) HP 0.4-5MPa* • *3 week culture, chondrogenic media.*	*Cyclic HP resulted in enhanced chondrogenic differentiation and matrix deposition at physiological loading (5MPa), indicated by increased gene expression of aggrecan, collagen type II, and sox-9.*

Table 1: Key articles published in recent years concerning the effect of HP on cartilage tissue engineering

Study	Methods	Results
(Chenyu & Rei 2012a)	• *hMSC seeded hydroxyapatite scaffold.* • *Cyclic HP 0.5Hz, 0 – 500kPa, no rest period.* • *3week culture, osteogenic media*	*HP resulted in cells distributed evenly throughout the scaffolds. HP groups expressed higher levels of osteocalcin, osteopontin, osteonectin and collagen type 1 versus controls after three weeks.*
(Kim et al. 2007)	• *hMSC seeded polymeric scaffolds* • *200kPa for 1min under combined with fluid shear, 14mins rest. Controls receive fluid shear only* • *21 days culture in osteogenic media*	*Enhanced expression of osteocalcin in HP treated groups over 21 days. Effect of HP was supressed by addition of U0126-MAP kinase inhibitor.*
(Maxson & Burg 2012)	• *hMSCs seeded in 2% agarose constructs.* • *2.5hrs perfusion followed by 30 mins Cyclic HP, 300 kPa, 0.5Hz, 4hrs stimulation/day* • *21 day culture in both osteogenic and chondrogenic conditioned media (CM)*	*Increase in osteogenic differentiation in HP treated cells cultured in chondrogenic conditioned media. Increased chondrogenic differentiation in HP treated cells cultured in osteogenic conditioned media.*
(Henstock et al. 2013)	• *Ex vivo culture chick foetal femurs* • *0-280kPa, 1 hr, 0.001-1hz.* • *14 days culture in either basal or osteogenic media*	*Increased bone formation and bone density in HP treated femurs - linearly dependant of cycling frequency. Increases in bone formation only observed in osteogenic but not proliferation media.*
(Zhao et al. 2015)	• *hMSC monolayer cultures* • *30-300kPa 1hour static pressure* • *2 week culture in osteogenic media*	*Increased expression of collagen type1 and osteocalcin in HP treated cells after 1 week but not after 2 weeks. Increased F-actin stress fibre formation immediately after pressure.*
(Reinwald et al. 2015)	• *Chick skeletal cells seeded in collagen hydrogels* • *280kPa, 1hr, 1Hz, 5days/week* • *2 weak culture in osteogenic media*	*Increased matrix mineralisation and density after 14 days in HP treated groups. mathematical modelling indicated increased stress and fluid shear at hydrogel boundary caused peripheral mineralisation of the hydrogels*

Table 2: Key articles published in recent years concerning the effect of HP on bone tissue engineering

If we adopt a comprehensive view of evidence encompassing studies performed on both cartilage and bone, it becomes clear that the therapeutic effects of HP on tissue regeneration are broadly similar. Cyclic but not static pressure appears effective in upregulating chondrogenic (Correia et al. 2012)(Meyer et al. 2011) and osteogenic (Henstock et al. 2013) gene expression, which is followed by enhanced tissue maturation. It appears too that HP alone improves homogeneity of tissue engineered cartilage (Huang et al. 2010) and bone (Chenyu & Rei 2012b). It is interesting to note that some studies utilise a combination of HP and fluid flow (Maxson & Burg 2012) (Kim et al. 2007) based on evidence demonstrating increased homogeneity in engineered bone tissue (Grayson et al. 2008). Whilst there is a broad agreement in the literature on the effect of HP as a therapeutics stimulus, the effect of HP appears to highly sensitive to the cell matrix environment. Steward et al. reported a reduction in HP induced sulphated glycosaminoglycan (sGAG) in hMSC cartilage constructs when changing the ECM environment from fibrin to agarose (Steward et al. 2012). Steward went on to show that HP induced changes in agarose cartilage constructs depended on construct stiffness as well as the presence of arginylglycylaspartic acid RGD binding sites (Steward et al. 2013). The effect of substrate stiffness on stem cells has been shown to have a significant effect on the lineage commitment of undifferentiated hMSCs (Engler et al. 2006). Based on this, it would be interesting to study the effect of substrate stiffness and HP, which has not yet been investigated in hMSC undergoing osteogenesis.

1.9. Mediators of mechantransduction

1.9.1. Ion channels

Ion channels were first shown to mediate mechanotransduction in Escherichia Coli in 1985 by Sachs et al. (Sachs 1985). There is a large body of literature documenting the role of ion channels in mediating cellular function in response to mechanical stimuli. Ion channels are macromolecular pores in the cell membrane which function to stabilise membrane potentials by allowing the flow of ions across the cell membrane (**Figure 6**). When the cell membrane undergoes conformational change, fluctuations in intra/extracellular ion potentials are believed to trigger signal cascades, resulting in transcription of genes specific to the applied stimulus (Hille 1984). Ion channels are referred to as gated if they can be opened or closed, and stimuli for such gating events can be electrical, chemical or mechanical (Garcia 2004). During these gating events, different ions pass in and out of the cell such as potassium (K^+), sodium (Na^+) and calcium (Ca^+) (Sackin 1995), which in turn will have specific actions on cell behaviour. For example, in osteocyte MLO-Y4 is has been shown that three distinct forms of K^+ currents are active across the cell membrane during stimulation with different pharmacological agents (Gu et al. 2001), and that these characteristics lead to distinct functions in OSs versus more osteoblastic phenotypes (Rawlinson et al. 1996). Subsequent events following ion channel activation such as NO and PGE2 production (Rawlinson et al. 1996) can be induced via application of external mechanical loading. NO and PGE2 are widely reported to be produced by bone cells in response to mechanical loading (McGarry et al. 2005)(Reher et al. 2002)(Siller-Jackson et al. 2008), suggesting ion channels might mediate these signalling events during mechanical loading.

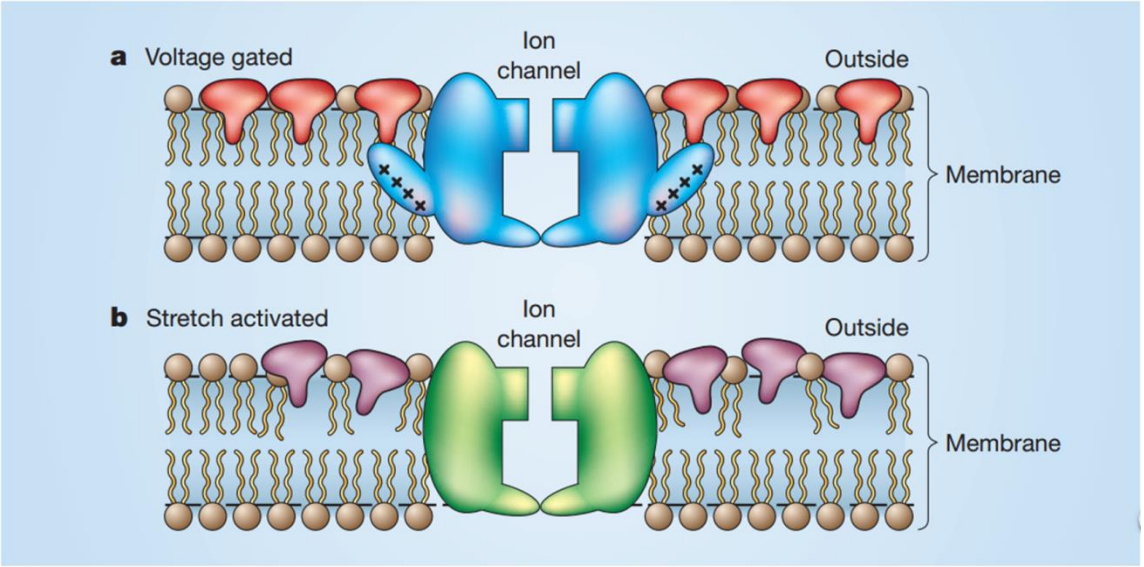

Figure 6: Picture representation of ion channels found on the cell membrane. A) *Voltage gated ion channels.* ***B)*** *Stretch activated ion channels* (Garcia 2004) *reprinted with permission of Nature publishing group [license number: 3794280056729]*

Studies investigating ion channel activation under hydrostatic pressure are relatively limited. Ulb et al. used patch clamping techniques to observe increased membrane potential in opossum kidney cells under hydrostatic pressure (Ubl et al. 1988). HP was also found to stimulate adenosine triphosphate (ATP) release in rat bladder urethral cells, which was subsequently completely diminished after inhibiting stretch activated channels along with transient receptor protein (TRP) channels and epithelial sodium channels (Olsen et al. 2011). In bone cells, patch clamping has been used to investigate the effect of applied pressure in osteoblast osteosarcoma G292, which showed locally applied membrane pressures of 0-50kPa resulted in increased membrane potential (Davidson et al. 1990), a phenomena observed in osteocytes after exposure to prostaglandin E2 (Chow, 1984) . Klein-Nulend et al observed increased PGE2 production in both osteoblasts and osteocytes exposed to 15kPa, 0.3hz HP (Klein-Nulend, 1995), implying a relationship between membrane potential, PGE2 and HP that could be mediated through ion channel activation. Surprisingly, whilst the influence of HP on NO release has been reported in

the eye (Liu & Neufeld 2001) and in the renal system (Majid et al. 2001), the effect of HP on NO production in bone remains poorly characterised.

1.9.2. Primary cilia

Primary cilia (PC) are cell membrane protrusions into the extra cellular space comprised of an axoneme of nine doublet microtubules encapsulated by a continuous membrane that is incorporated into the cell's plasma membrane. The microtubules are linked to the cytoskeleton via a subset of cytoplasmic microtubules at the base of the doublet microtubule structure (Anderson et al. 2008). PC have been well described in a number different cell types including osteocytes, osteoblasts (Whitfield 2008) and hMSCs (Shao et al. 2012). They act as both chemical and mechanosensors, relaying signals for a variety of cellular functions in most tissues in the body (Christensen, 2007). Genetically engineered mice with a knockout of Kif3a, an osteocyte specific protein required for PC formation, show reduced bone forming ability in response to mechanical loading (Temiyasathit et al. 2012). More recent *in vivo* evidence has also shown that Kif3a deletion in mice results in poor integration of implants with native bone, suggesting that PC also play a role in osseo-integration of implants in an orthopaedic setting (Leucht et al. 2013). Hence PC are considered an essential organelle both in regular maintenance of bone and its response to external mechanical stimuli.

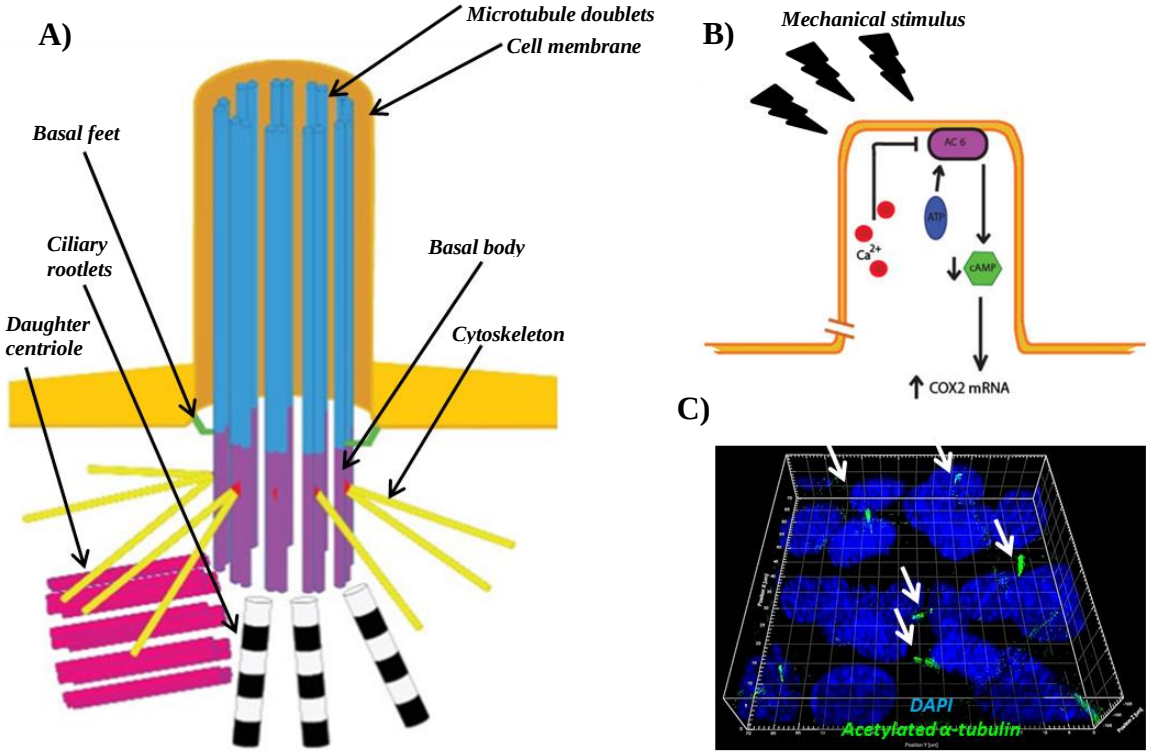

Figure 7: Structure and function of primary cilia in osteocytes. ***A)*** *Primary cilia structure.* ***B)*** *Proposed mechanism of primary cilia mediated mechanotransduction in osteocytes. Adapted from* (K. L. Lee et al. 2010). *Reprinted with permission of Springer Link [license numbers: 3794800269031, 3794800388861].* ***C)*** *Immunofluorescent staining visualising primary cilia (green) in MLO-A5 osteocytes using acetylated alpha tubulin antibody.*

As discussed in previous sections, mechanical stimuli *in vivo* results in local deformation in bone matrix leading to pressure gradients and fluid flow in the canaliculi, hence PC could likely to experience a number of different forces. In the context of defining PC response to the different 'types' of force as defined previously, it is interesting highlight that the present body of literature suggests that deviatoric forces such as fluid shear are mainly responsible for PC mediated mechanotransduction in bone cells. Indeed there is strong body of evidence reporting how deformation of PC by fluid shear increases osteogenic gene expression (Malone et al. 2007), calcium deposition by osteoblasts (Delaine-Smith et al. 2014). Interestingly whilst pressure sensing has been reported by primary cilia in the eye (Luo et al. 2014), there appears no evidence to

suggest hydrostatic pressure sensing by PC in bone. This may in part be down to trying to rationalise a mechanism by which static pressure could induce deviatoric stress on PC that could be translated to biochemical signals in the cell. One could speculate that if bone cells contain a source of compressible material, application of external hydrostatic pressures could generate internal fluid flows in the cell which results in transport of biomolecules through the PC, creating internal, as opposed to external fluid shear caused by extracellular fluid flow.

However, current evidence indicates that physical deformation of PC results an influx of Ca^{+} through stretch activated ion channels residing on the ciliary axoneme (**Figure 7B)**. This has been demonstrated in renal epithelial cells (Liu et al. 2005) and also osteoblasts and osteocytes (Xiao et al. 2006). A recent study also directly observed Ca^{+} signalling through osteocyte PC using fluorescence energy resonance transfer (FRET) biosensors (Lee et al. 2015). However there is conflicting evidence regarding the actual significance of Ca^{+} influxes and mechanosensation in bone cells (Malone et al. 2007), and very recently in a number of different cell types isolated from transgenic mice expressing a Ca^{+} flux sensitive PC reporter construct (Delling et al. 2016). It appears then that the role of PC in mediating bone mechanotransduction is diverse, complex and to date, poorly understood. This does however present exciting opportunities to test novel hypotheses using the mechanical force bioreactors, yielding valuable information on the nature of PC mediated mechanotransduction in bone.

1.9.3. Integrin receptors

Integrin receptors are described as trans-membrane protein structures consisting of heterodimers made up from α and β subunits (Rubin et al. 2006). Integrins tether a cell to the surrounding ECM and are involved in regulating a number of physiological phenomena including embryonic development (Yang et al. 1993)(Stephens et al. 1995), tumour progression (Reynolds et al. 2009), programmed cell death (Cardó-Vila et al. 2003), bone resorption by osteoclasts (Teitelbaum 2000) and mechanical sensing of the ECM (García & García 2014). In stem cells, it now widely accepted that the mechanical environment of the ECM has a strong influence on stem cell behaviour (F. M. Watt; T. S. Huck 2013). As such, there has been a recent revival in research studying integrins and their downstream effectors. Engler et al. arguable provides the most comprehensive evidence yet demonstrating the effect of mechanical sensing on stem cell behaviour. They were able to show that hMSC grown on soft substrates differentiated into neurons, medium stiffness promoted myogenic differentiation, and hard substrates promoted osteogenic differentiation (Engler et al. 2006). Integrin's transmit information about the local microenvironment through focal adhesions attached to the actin cytoskeleton (Nemir & West 2010). The interaction of integrins with the ECM determines the effect that ECM can have on cell behaviour. In the context of osteoblast function, it has been shown that RGD binding sites promote integrin mediated activation of focal adhesions, which in turn initiated increased matrix mineralisation in partially denatured collagen relative to intact collagen ECM (Taubenberger et al. 2010). This highlights how small changes in the ECM environment can have pronounced effects on tissue development due to the specificity of integrin mediated cell responses.

The role of specific integrins in mediating certain cell responses such as differentiation in stem cells is currently not well defined. However there are a number of

common downstream events that occur as a result of the interaction of integrins with focal adhesions. In the latter case of substrate stiffness these include; actin stress fibre formation (Discher et al. 2005), increased cell spreading and adhesion (Yeung et al. 2005) and nuclear translocation of transcriptional proteins that regulate stem cell differentiation (Dupont et al. 2011). In the case of the latter Dupont et al. demonstrated that the yes-associated protein (YAP) not only regulates stem cell differentiation but also by inducing expression of YAP, showed that it acts to override physical constraints such as ECM stiffness that dictate cell behaviour.

Since integrins act as the initial sensory mechanism of the cell to the ECM, it seems reasonable to postulate that external forces like hydrostatic pressure might further enhance integrin mediated changes in cell behaviour, similar to those observed when changing substrate stiffness. This hypothesis seems reasonable when we consider that integrin's are able to translate the stiffness of the surrounding ECM into stiffening of the cell itself (Tee et al. 2011)(F. M. Watt; T. S. Huck 2013) (**Figure 8**). Coupled with this, it has been shown that both fluid flow and hydrostatic pressure increase cell stiffness in MC3T3 osteoblasts (Gardinier et al. 2009).

Consideration of integrin mediated responses in cells provokes re-assessment of experimental design parameters when attempting to define the effectiveness of hydrostatic pressure for *in vitro* preconditioning of bone. The varied range of effects in cells exposed to HP reported in the literature are could due to changes in design between experiments, which based on current evidence, would have a profound effect on integrin mediated mechanotransduction. In light of this, evidence describing integrin mediated mechanotransduction provides us with a robust set of comparisons through which we can delineate the possible underlying mechanisms. Moreover, there is to date no evidence

detailing the mechanisms described above on different stiffness substrates in the context of stem cells and hydrostatic pressure.

For the purpose of characterising mechanoactive responses in our bioreactor, the literature provides a platform for developing rapid, high throughput screening of events in cells responding to hydrostatic loading. Understanding such mechanisms could contribute to a deeper understanding of the interplay between mechanical stimuli, the cell microenvironment and their combined effect on *in vitro* bone formation.

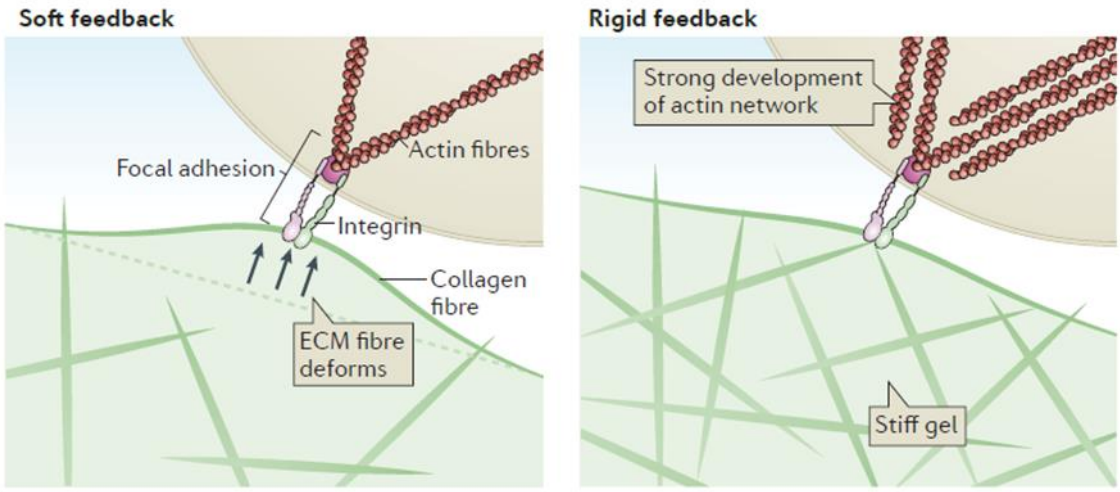

Figure 8: Cartoon representation of effect of ECM stiffness on cell sensing of the surrounding microenvironment. *In softer microenvironment* ***(A)*** *(low concentration collagen hydrogel) cell traction forces through integrin receptors deform the ECM microenvironment. In stiffer microenvironments* ***(B)*** *(higher concentration collagen hydrogel) cell traction forces are instead directed through the actin cytoskeleton and hence change the subsequent behaviour of the cell such through events such as cell stiffening (Tee et al. 2011). Figure adapted from (F. M. Watt; T. S. Huck 2013). Reprinted with permission of Nature publishing group [licence number: 3795980655788]*

1.10. Hydrostatic force bioreactors for bone tissue engineering

The development of hydrostatic force bioreactors may provide a translatable platform to transfer knowledge of *in vitro* tissue engineering concepts to applicable clinical procedures. An evidence based understanding of what chemical/mechanical conditions are best suited to generate bone tissue *in vitro* should be combined with the appropriate bioreactor design that appropriately addresses both clinical and manufacturing requirements. A key element of bioreactor design utilises the appropriate mechanical stimuli, as well as a move towards an automated platform to allow a reduction in batch to batch variability. A clinically translatable bioreactor system should ideally be scalable from a manufacturing point of view. This requires the design to enable simultaneous culture of multiple constructs without affecting individual construct maturation. The study by Maxson and Burg (**detailed in Table 2**) utilises a bioreactor design that incorporates both fluid flow and HP as stimuli, allowing a combination of forces to be simultaneously applied whilst also replenishing media, thus eliminating human intervention during culture. Whilst this is a promising approach to design clinical translatable bioreactors, the system only allows for stimulation of a single construct at a time (Orr & Burg 2008). This is a disadvantage on two fronts: The first disadvantage from a manufacturing perspective is scalability, and from a research point of view, the lack of sample numbers required to generate statically relevant data from a single experiment. The second disadvantage is the complexity of the system. The use of multiple valves within a peristaltic pump configuration required for fluid flow, introduced air bubbles in the bioreactor chamber and interfered with HP treatment. This was overcome through design adjustment; however it highlights potential complications that can arise from using combinatorial stimuli in such systems.

Another similar system using media perfusion in combination with HP have addressed the issue of scalability, to allow multiple constructs (Chenyu & Rei 2012b). However, experiments designed to delineate fluid shear and pressure were not carried out, making it difficult to separate the effect of HP versus fluid flow in stimulating bone formation. (Meyer et al. 2011) utilised a bag configuration submerged in a pressurised water tight vessel. Whilst this has the advantage of being in a sense 'truly hydrostatic', the engineering itself would be problematic in addressing waste accumulation in the sealed bags over prolonged culture. These systems provide intuitive and practical approaches for applying physiological stimuli in the context of design specification, and their use in tissue engineering constructs provides important preclinical validation data, as well as allowing process improvement for future designs. However from a translational point of view, we seek to acquire a system that incorporates simplicity, experimental efficacy and scalability, thus improving the outcome for these systems in reaching the clinic.

1.10.1. Keele/TGT hydrostatic bioreactor

The bioreactor described in this thesis was manufactured by Tissue Growth Technologies, US in collaboration with Keele University, UK with the intention of evaluating standardized, commercially available systems for use in engineering clinically applicable tissue engineered bone constructs (**Figure 5)**. The system consists of a sealable pressure chamber, housing a standard size tissue culture plate (6 to 384wells), which is connected to a compressor via a hose. Both compressor and chamber can be placed inside a cell culture incubator. The magnitude, frequency, waveform and duration of mechanical loading may be set using an in house software platform (Growthworks, TGT). Previous

research has demonstrates that the system yields a degree of efficacy over static culture in the developing chick femur, whereby HP resulted in increased bone collar volume in femurs cultured in Osteogenic media (Henstock et al. 2013).

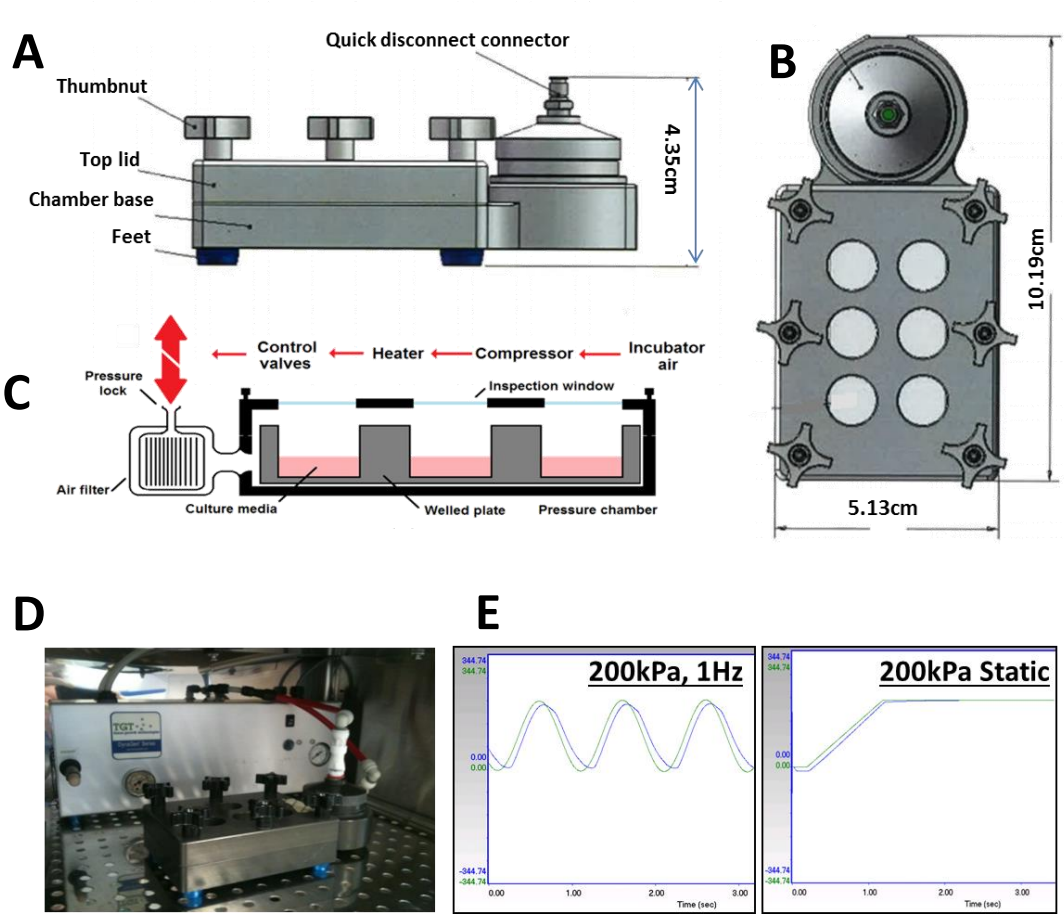

Figure 9: Schematic and pictorial representation of the Keele-TGT hydrostatic bioreactor. A&B) *the dimensions of the compression chamber are such that they can be housed in a standard cell culture incubator. The thumbnuts seal the top lid to the chamber whilst the quick disconnect connector provides a pressure lock to maintain pressure during operation.* ***C)*** *The chamber itself houses a standard cell culture plate, which during operation is subjected to hydrostatic force due to compression of gas/air interface residing above the culture media. Cells and/or constructs then sense this force as it is transduced through the culture medium. Compression is provided by a stimulator box housed in the incubator* ***(D)*** *which is linked to an external rotary oil compressor. The growth works software is capable of generating both static and cyclic waveforms, with magnitudes between 0-333kPa and frequency from 0-2Hz.*

1.11. Aims and objectives of the project

The aim of this thesis is to evaluate the Keele/TGT bioreactor as a preconditioning tool for bone repair. I have discussed in some detail in the preceding sections of this introduction, the various structural and functional aspects of bone and its comprising cells and proteins. I then explored different aspects of bone tissue engineering and the use of appropriate animal models to investigate the mechanisms of fracture repair. Through this I sought to identify the advantages and disadvantages of using different experimental approaches and animal models which are required to generate research based evidence for potential therapies to address the limitations facing current orthopaedic gold standards.

I then aimed to identify the mechanisms and responses of mechanical loading that are commonly used to evaluate the effectiveness of bioreactors for bone tissue engineering, and how the different design parameters make these systems suitable for translatable therapies. To that end, the structure of my thesis is separated into three experimental chapters which aim to define a strategy for evaluating the Keele/TGT bioreactor as a tool for preconditioning cell seeded scaffolds to be used as bone implants.

1.11.1. Chapter 1 - Monolayer characterisation

This chapter aims to utilise the current knowledge of literature with regard to cell responses to hydrostatic loading; identifying events that occur due to bioreactor stimulations which are considered common responses in cells, such as actin remodelling and nitric oxide release. Additionally I aim to understand how different magnitudes and frequencies of loading affect these responses. Next, I will identify novel aspects of mechanotransduction through the activation of YAP. I explore how different aspects of cell physiology and cell phenotype (stem cell or osteoblast) regulate this signalling pathway. Finally I aim to investigate whether tailoring the ECM environment to promote

YAP expression worked synergistically with hydrostatic stimulation to enhance osteogenic differentiation in adult stem cells.

1.11.2. Chapter 2 - Translation from 2D to 3D, optimisation and scale up

This chapter looks at validating the bioreactor as a hydrostatic preconditioning tool for *in vitro* bone tissue formation. I explore the differences in response to hydrostatic pressure in osteoblast MG-63s in 2D monolayers and 3D collagen hydrogels, to underline how the ECM environment changes cellular response to external mechanical stimuli. I then aimed to define a set of conditions in which static *in vitro* culture of hMSC collagen hydrogels best promotes bone formation. In doing so I will look at changes in the ECM environment such as collagen content, and understand if the spatial distribution of cells can produces quantifiable changes in bone formation during *in vitro* culture. This will ultimately provide an internal benchmark of static culture (no bioreactor treatment) by which we can compare changes due to daily loading with hydrostatic pressure.

1.11.3. Chapter 3 - Developing an ex vivo fracture repair model for preclinical testing

This chapter aims to develop an organotypic tissue model to study fracture repair using isolated embryonic chick femurs. I first detail construction of the model and then investigate the effect of stem cell seeded scaffolds to heal induced femoral defects. By comparing the effect of freshly seeded stem cell/collagen scaffolds in femurs subjected to hydrostatic pressure, with static cultured femurs using hydrostatically preconditioned stem cell/collagen scaffolds, I hope to determine if preconditioning of stem cell seeded scaffolds is sufficient to enhance repair in an organotypic fracture repair model. In developing this model, I aim to characterise a high throughput system for preclinical

evaluation that adheres to the 3 R's principle but also recapitulates *in vivo* bone formation *in vitro.*

Since each chapter incorporates within itself a fairly distinct set of analyses and protocols, the materials and methods shall precede the results section for each chapter. I believe this will allow the conceptual flow of results easier to follow compared with a self-contained materials and methods chapter, in which reference in then made to within each of the following chapters.

Chapter 2

Monolayer characterisation

2.1. Introduction

As discussed in the previous chapter, the response of cells to mechanical stimuli will vary according to cell type, extracellular matrix environment, the nature of mechanical stimulation applied and the time over which cells experience this stimulus. The downstream effects on cell behaviour appear to share common responses to mechanical stimuli which include: induction of gene expression (Ignatius et al. 2005); matrix synthesis (Sittichokechaiwut et al. 2010); changes in proliferation (Yan et al. 2012); and in stem cells, differentiation toward lineages specific to the nature of stimulus applied (Chenyu & Rei 2012)(Xu et al. 2015).

OSs are widely considered to be the primary mechanosensory cells that control bone resorption and remodelling (Klein-Nulend et al. 2013). They have been shown to respond to both fluid shear and compressive loading by multiply transduction processes. One of these is increased production of NO, which is thought to inhibit bone resorption by preventing osteoclast activity(Wimalawansa 2010). Application of cyclic pressure in OBs also induces stress fibre formation in the actin cytoskeleton and is accompanied by increased cell stiffness (Gardinier et al. 2009).

The Hippo signalling cascade, which involves intracellular transport of YAP/PDZ-binding motif (TAZ) proteins is emerging as an important regulator of cell differentiation due to changes in the mechanical environment of the ECM (Dupont et al. 2011). A recent study of YAP/TAZ co-activation in OBs demonstrated that fluid flow increased nuclear accumulation of YAP/TAZ, and was required for increased mechanosensing via downregulation of the Sost gene (Kaneko et al. 2014), which itself is upregulated in response to prolonged unloading of bone (Lin et al. 2009). By contrast, phosphorylation and subsequent nuclear accumulation of YAP has been shown repress Runx2 transcription (Zaidi et al. 2004), and thus inhibits Runx2 mediated osteogenesis in MSCs

(Sen et al. 2015). Another recent study showed that cyclic stretch induces actin tensioning, which was required for nuclear accumulation of YAP (Driscoll et al. 2015).. The current body of literature seems to indicate a complex, but nonetheless prominent role of YAP/TAZ in mechano-sensing, suggesting that YAP/TAZ signalling is sensitive to both cell phenotype and the nature of stimulus applied (strain, fluid flow etc). To date there have been no reports studying the effect of hydrostatic pressure on this signalling pathway. Based on the existing evidence, it is reasonable to suggest that hydrostatic pressure might be involved regulating this pathway in both MSCs and more committed OBs phenotypes.

Understanding the initial mechanosensory events that occur using the Keele/TGT hydrostatic bioreactor will give valuable knowledge in appropriately implementing the device for osteogenic preconditioning. For example, static compressive regimes using the Keele/TGT bioreactor have been shown to have little additive effect on bone formation in the developing chick femur. By contrast, a positive correlation was present between bone formation and cycling frequency (Henstock et al. 2013), however the earlier signalling mechanisms that lead to enhanced bone formation have not been investigated.

The software interface of the bioreactor described in section 1 allows for a series of defined magnitudes and frequencies to be applied to cells. I hypothesise that applying hydrostatic pressure to cells using the bioreactor will stimulate NO production and I aim to investigate the effect of change in the loading regime on this process. I also hypothesise that initial mechanosensory events such as actin remodelling and YAP signalling might take place as a result of hydrostatic loading. By testing this hypothesis in two different cell types (undifferentiated MSCs and MLO-A5 late stage OBs), I can

determine if these signalling mechanisms vary between cells at different stages of osteogenic differentiation.

Objectives

i) **Quantify nitric oxide release in MLO-A5 cells in response to pressure.** To determine the effect of static versus oscillatory loading on anabolic signalling and define changes in cell responses due to the frequency and magnitude of loading.

ii) **Investigate the role of the NO production and the f actin cytoskeleton in cells exposed to hydrostatic loading.** To determine the role of cellular actin in translating hydrostatic pressure to cell signal events.

iii) **Investigate changes in YAP expression during hydrostatic loading.** To study changes in YAP expression during hydrostatic loading and determine the role of actin cytoskeleton in regulating this pathway.

iv) **Preconditioning of hMSC on different stiffness substrates during 10 days culture in osteogenic media.** To determine the effect of hydrostatic loading on osteogenic differentiation of hMSCs and to study the importance of the extracellular matrix environment on translating external hydrostatic pressure.

2.2. Materials and methods

2.2.1. Cell culture

For each experiment hMSCs and MLO-A5 cells were culture under identical conditions unless otherwise stated. hMSCs from a human bone marrow aspirate were purchased from Lonza and isolated via plastic adherence and subsequently characterised for the relative CD markers (See **Appendix Ch1**). MLO-A5 cells were kindly donated by Professor Linda Bonewald of the University of Missouri, Kansas. Each cell type was stored in liquid nitrogen experiments in 10% Dimethyl sulfoxide (DMSO)(Sigma) in fetal bovine serum (BSA)(Biosera) until ready for use. Prior to experiments, cells were thawed by adding 0.5ml pre warmed (37^0C) Dulbeco's Modified Eagle Medium (DMEM) (Lonza) to the frozen cell suspension for 1 minute. The suspension was then transferred to 10mls pre warmed DMEM and centrifuged at 800rpm for 5mins. Cells were washed once in 10mls DMEM, centrifuged and transferred to tissue culture plastic at a seeding density of 6500 cells/cm^2. Cells were expanded in proliferation media (PM) consisting of DMEM (1ng/ml glucose, w/o L-Glutamine) containing 10% fetal bovine serum (FBS), 2% penicillin-streptomycin (Lonza), 1% Non-essential amino acids (Sigma) and 1% L-Glutamine (Lonza). During *in vitro* expansion, cells were passaged at approximately 90% confluency. Passages were performed by washing cells once in phosphate buffered saline (PBS) (Lonza) followed by 5-7mins incubation at 37^0C in 1x Trypsin (Lonza). The enzymatic reaction was quenched in PM and cells were centrifuged at 800rpm for 5 minutes. Cells were then seeded in T75 flasks (Sarstedt) at the same density as before at 6500/cm^2.

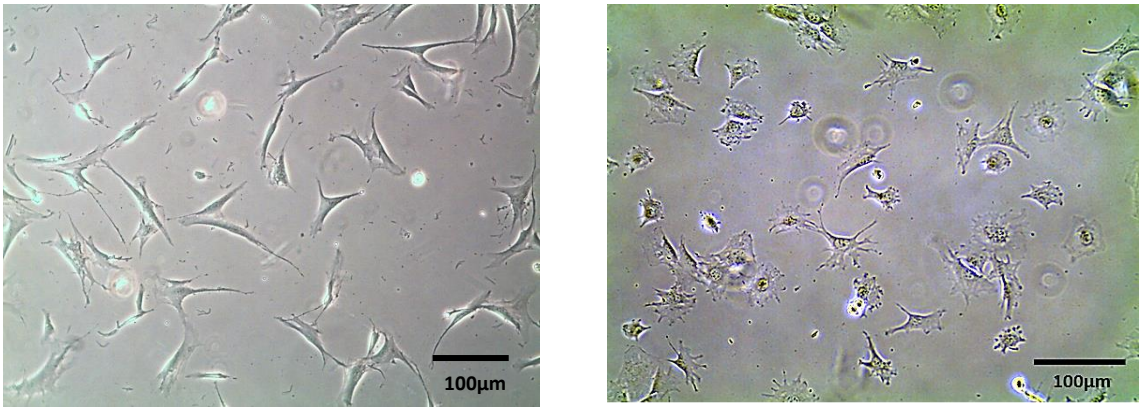

Figure 1. Left) *hMSC precursors characterised using surface markers: positive CD173, CD90, CD105; and negative CD 14, CD34, CD45, CD19, HLA – DR (See* ***appendix ch1). Right)*** *MLO-A5 late stage OBs.*

2.2.2. Cell seeding prior to experiments

For experiments using the hydrostatic bioreactor, glass coverslips (Fisher Scientific) were placed into either 6 or 24 well tissue culture plates and subjected to 15 minutes ultra violet (UV) sterilisation using a Bio-Rad gene linker UV chamber. Coverslips were coated for 1 hr at room temperature in 0.2mg/ml type-1 rat tail collagen (Corning) made from an (8-11) mg/ml stock solution. After incubation, the collagen solution was aspirated and wells were washed once in PBS prior to seeding. Unless otherwise stated in the results section, cells were seeded at approximately 80% confluencey (15,000/cm^2 for hMSC, and 100,000/cm^2 for MLO-A5 cells). Cells were seeded 24 hours prior to each experiment.

2.2.3. Inhibition of f-actin

Disruption of actin microfilaments was achieved by treatment with Cytochalasin D (CytoD) (Sigma), a myotoxin that serves as a potent inhibitor of actin polymerisation. Cells were incubated for 60 minutes at 37^0C in PM supplemented with 10μM CytoD. After incubation, cells were washed twice in PBS.

2.2.4. Fixation

All cells were fixed in 10% neutrally buffered formalin (Fisher Scientific). For NO studies, well plates were removed from the bioreactor immediately after stimulation and the media was collected and stored at -20^0C. The remaining cells were immersed in fixative for 15 minutes at room temperature followed by 2 washes in PBS. Samples were stored in PBS with 1% pen-strep, 1% amphotericin B (Lonza) at 4^0C until immunofluorescent staining was performed.

2.2.5. Nitric oxide quantification

Nitric oxide rapidly undergoes spontaneous oxidation into stable nitrite compounds under physiological conditions (Ignarro & Buga 1987). The detection of stable nitrites present in the media was quantified using a Griess assay (Life technologies). 150μl of media per sample was mixed with 150μl of Griess reagent (10μl N-(1-naphthyl)ethylenediamine dihydrochloride, 10μl sulfanilic acid, 130μl distilled water (DH_2O)) and incubated in the dark at room temperature for 30 minutes. Absorbance was measured at 548nm on a Bio-synergy 2 plate reader. Results were normalised to absorbance reading for fresh media and standardised against known quantities of nitrite containing solution.

2.2.6. Immunocytochemistry

Monolayer cultures were permeabalised in 0.01% triton-X 100 (Sigma) for 15 minutes at room temperature, followed by 2 washes in PBS- 0.1% Tween (Sigma). Cells were then blocked in 1% bovine serum albumin (BSA) (Fisher Scientific) for 1 hr at room temperature followed by two washes in PBS-0.1% Tween. Primary antibody incubations [, anti-human YAP mouse monoclonal (Santa Cruz Bio), anti-human osteocalcin mouse monoclonal (R&D systems), anti-human Runx2 goat monoclonal (R&D systems)] diluted to 2µg/ml in 0.1% BSA in PBS-0.1% -tween were performed overnight at 4^{o}C. Following primary antibody incubations, the cells were washed twice for 5 minutes each on a shaker in PBS-0.1% Tween. Cells were then incubated in respective Alexafloura 488 or 555 secondary's (2µg/ml, 0.1% BSA, 0.1% Tween-20 in PBS) (Abcam) for 1hr at room temperature in the dark followed by 2 washes in PBS-0.1% tween. Counterstaining was performed with 4',6-diamidino-2-phenylindole (DAPI) (Sigma) for 30 minutes in the dark to s cell nuclei. F-actin staining was performed using Cytopainter 555 phalloidin (Abcam) for 1 hr at room temperature in the dark. Cells on coverslips were mounted onto microscope slides using Vector shield mounting medium (Vector Laboratories).

2.2.7. Polyacrylamide gel fabrication

Polyacrylamide gel substrates with different stiffness's were fabricated according to methods published by Tse and Engler (Tse & Engler 2010). 13mm thick glass coverslips were placed on a hotplate at 70^{0}C to allow evaporation of 250µl of 0.1M sodium hydroxide (NaOH)/coverslip (Fisher Scientific), until an even coating was present.

Acrylamide (40%	**Bis-acrylamide**	**DH_2O (ml)**	**Predicted stiffness**
1.25mls	0.15mls	8.6mls	1±0.31kPa
2.5mls	0.5mls	7mls	10+0.79 kPa
2mls	2.4mls	5.6mls	40.4±2.39 kPa

Table 1. Ratios of acrylamide to bis-acrylamide for substrates with different predictied stiffness's. *(adapted from (Tse & Engler 2010)).*

Coverslips were then placed in a fume hood and coated with 200µl (3-Aminopropyl)triethoxysilane (Sigma) for 5 minutes, followed by 30 seconds washing under running DH_2O. Coverslips were transferred to square petri dishes and immersed in 0.5% glutaraldehyde (Sigma) in PBS for 30 minutes. The solution was then removed and coverslips were left to dry overnight in a fume hood. Chloro-silinated glass slides were prepared by coating slides in 100µl dichlorodimethylsilane (Sigma) for 5 minutes in a fume hood. Slides were rinsed three times for 30 secs each in DH_2O. Acrylamide/ Bis-acrylamide (Sigma) ratios were prepared accordingly, yielding solutions equating to different stiffness substrates (**Table 1**).

Polyacrylamide solutions were degassed in vacuum desiccator for 15 minutes to exhaust dissolved oxygen. Solutions were then mixed with 1/100 10% (wv) ammonium persulfate (Sigma) by volume and 1/1000 N,N,N′,N′-Tetramethylethylenediamine (Sigma) by volume. 25µl solutions were then pipetted onto chloro-silinated slides with the amino coated coverslips placed face down on top, allowing the solution to coat the coverslips evenly. The solutions were left to polymerise for 30minutes before removing polyacrylamide coated coverslips from the cholo-silinated slides. The coated coverslips

were transferred to well plates and washed twice in PBS. Well plates were then sterilised overnight under UV light in a biological safety cabinet.

2.2.8. Polyacrylamide surface functionalisation

Substrates were functionalised according to methods described in (Tse & Engler 2010). sulfosuccinimidyl 6-(4'-azido-2'-nitrophenylamino)hexanoate (Sulpho-SANPAH) (Thermo-Fisher), a protein cross-linker that covalently binds ECM proteins to the acrylamide surface, was used to enable cell attachment to the different stiffness in 40µl DMSO at 50mg/ml. Aliquots were flash frozen in liquid nitrogen and stored at -80^0C until use. For surface functionalisation, sulpho- SANPAH solutions were diluted to 0.2mg/ml in DH_2O and added to wells to immerse the coverslips. Coverslips were then placed under 365nm UV light source in a Bio rad GenX UV chamber for 10 minutes. Coverslips were then rinsed twice in 50 mM HEPES before adding 0.2mg/ml rat tail collagen. After overnight incubation at 37^0C, the collagen solution was aspirated and the coverslips were washed once in PBS and once in PM before cell seeding.

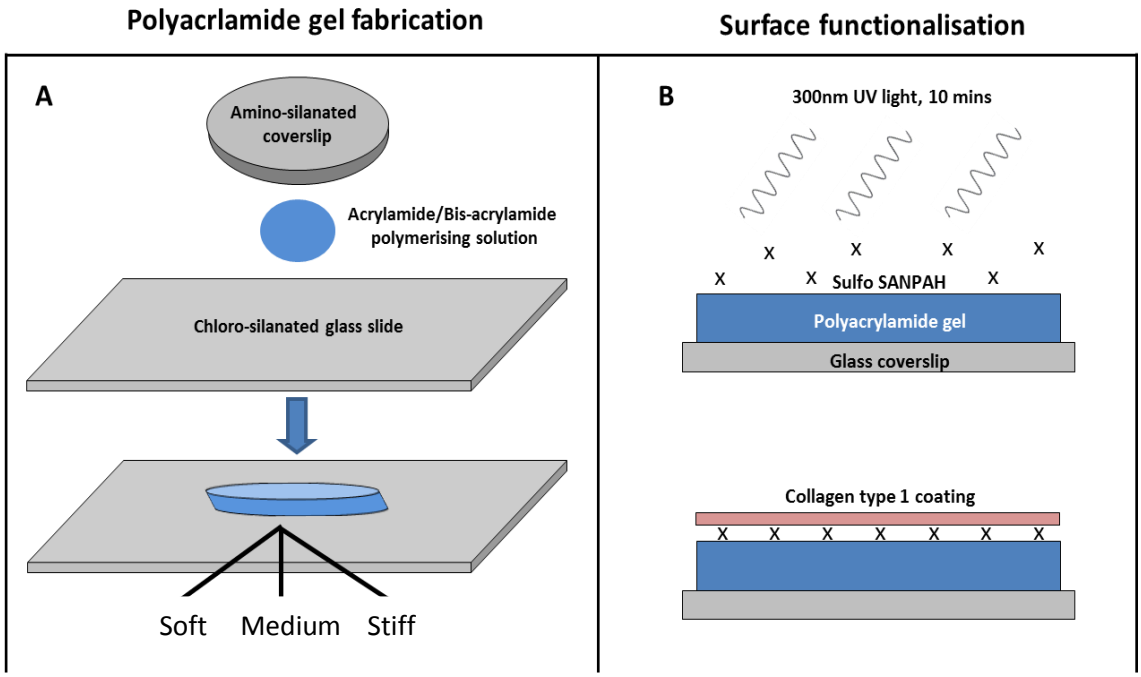

Figure 2. Preparation of polyacrylamide substrates with different stiffness's. *A) Fabrication process of substrates with different stiffness. B) Functionalisation of substrates and attachment of ECM coating.*

Frequency	Magnitude	Cell type	Analysis
0, 1, 2Hz	200kPa	MLO-A5	NO release, ICC
1Hz	0, 50, 200, 280kPa	MLOA5	NO release, ICC
1Hz	280kPa	hMSC	NO release, ICC
1Hz	280kPa	hMSC	Preconditioning

Table 2. Magnitude and frequency of hydrostatic loading used for experiments.

2.2.9. Hydrostatic regime

The pressure regimes used in experiments were selected with the aim of observing changes in cell response due to magnitude and frequency during loading (**see Table2**). Experiments studying nitric oxide production, actin remodelling and (**Section 2.3.1)** were performed using PM, which was changed immediately before stimulation. This allowed the results in both pressure treated and static controls (no pressure) to be normalised to fresh media as a negative control. For osteogenic preconditioning experiments (**Section 2.3.2)**, PM was supplemented with 150µg/ml L-ascorbic acid (Sigma), 10^{-8}M dexamethasone (Sigma) and 2mM sodium β-glycerophosphate (Sigma). Cells cultured in osteogenic media received media changes every 2 days before bioreactor stimulation. A small amount of evaporation was present in wells closest to the nozzle side of the bioreactor, which was accounted for by seeding cells in central wells of the plates and/or replacing equal volumes of media lost with DH_2O after stimulation was complete. The

remainder of the time cells were kept under static standard cell culture conditions in a cell culture incubator at 37^0C with 5%CO_2.

2.2.10. Confocal imaging

Imaging was performed using an Olympus U-TBI 90 laser scanning confocal microscope, employing three channel fluorescence microscopy. Image acquisition was performed using Fluoview10 software and image analysis was performed using Fiji/ImageJ Win64 open access software (http://fiji.sc/Fiji).

2.2.11. Quantification of fluorescence intensity

Images were acquired under identical offset and gain settings for each separate experiment undertaken. Analysis of fluorescence intensity in ImageJ was used to quantify the mean fluorescence per unit area in each cell to assess changes in the ratio of nuclear to cytoplasmic retention of YAP (**Figure 3**). The raw intensity values for nuclear fluorescence were subtracted from the total cell fluorescence and the values normalised to their respective areas to give a fluorescence intensity/ unit area. By dividing the nuclear/cytoplasmic intensity using this method for each experimental group, the relative change in nuclear to cytoplasmic intensity could be estimated.

2.2.12. Sudan black B staining

hMSCs on different stiffness substrates were incubated in 1% w/v Sudan black B in 70% ethanol (EOH) for 10 minutes. Cell were then washed 3 times for 5 minutes each on a shaker in PBS before imaging using an EVOS® FL Colour Imaging System.

2.2.13. Alkaline phosphatase activity

Alkaline phosphatase detection was employed using a Naphthol AS-BI phosphate based kit (Millipore) to assess the rate of osteogenic differentiation in hMSCs seeded on

different stiffness substrates. Fixed cells were rinsed in TBST buffer (20mM Tris-HCl, 0.15M NaCl, 0.05% Tween-20) and incubated in staining solution for 30 minutes away - from the light. Cells were rinsed once in TBST and imaged using an EVOS® FL Colour Imaging System.

2.2.14. Statistical analysis

Data was plotted and analysed in Microsoft Excel. All data point represents mean values ± standard error of the mean. Statistical significance was determined either by using a two tailed Students t-test with $p<0.05$ denoted statistical significance. When specified, statistical analyses by a two analysis of variance was performed in Origin pro 9.0, with $p<0.05$ denoted statistical significance.

A. Random field of view

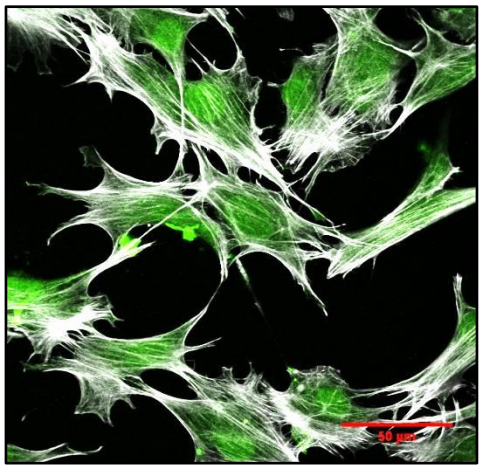

B. Quantify total cell fluorescence

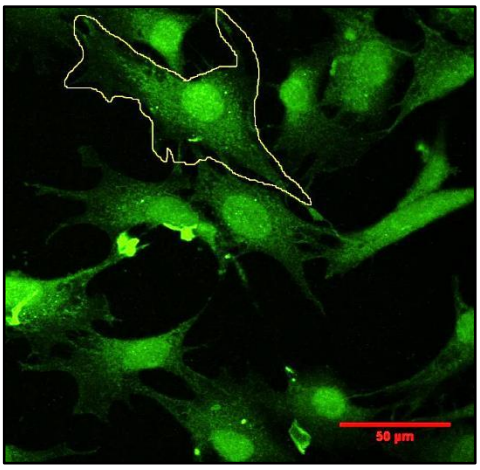

C. Highlight nuclear area

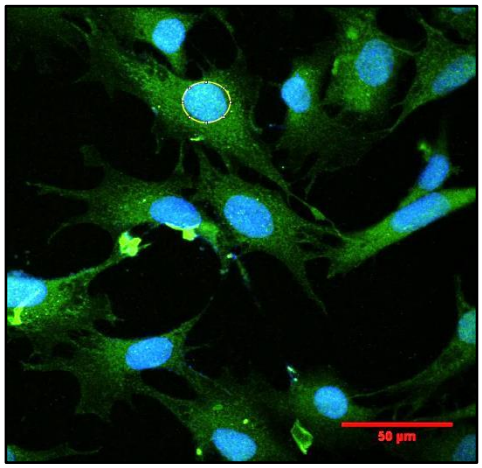

D. Quantify nuclear fluorescence

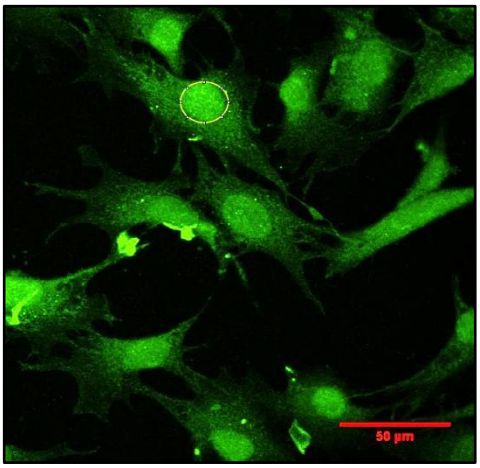

Calculation $\boldsymbol{Normalised\ nuclear\ intensity,\ I_{nuc} = FI_{nuc}/A_{nuc}}$

$$\boldsymbol{Normalised\ cytoplasmic\ intensity,\ I_{cyt} = (FI_{cell} - FI_{nuc})/(A_{cell} - A_{nuc})}$$

$$\boldsymbol{Nuclear\ localisation = \frac{I_{nuc}}{I_{cyt}} = \frac{FI_{nuc}}{A_{nuc}} * \frac{(A_{cell} - A_{nuc})}{(FI_{cell} - FI_{nuc})}}$$

Units $\boldsymbol{FI = flourescence\ intensity(sum\ of\ greyscale\ pixel\ intensities)}$

$$\boldsymbol{A = area\ (\mu m^2)}$$

Figure 3. Quantifying the nuclear to cytoplasmic ratio of fluorescence intensity (FI) in ImageJ. *For each field of view(**A**), the nuclear FI (**D**) was subtracted from the total cell FI (**B**) and expressed as FI/unit area. Dividing the nuclear by cytoplasmic intensity yielded a ratio of nuclear translocation for each cell. n>40 cells*

2.3. Results

2.3.1. Mechanotransduction in MLO-A5 late OBs and MSC precursors

2.3.1.1. Effect of pressure on actin remodelling and nitric oxide production in MLO-A5 cells

Cyclic pressure (**Figure 4C, D&E)** induced f-actin remodelling from randomly ordered actin filaments in statically controls and statically compressed MLO-A5s **(Figure 4A&B)**, to tensioned parallel stress fibres. Fluorescent quantification of F-actin (**Figure 4F**) showed a significant increase in actin fluorescence in all cyclic pressure regimes, but not in the static compression regime. F-actin remodelling correlated with an increase in NO production in pressure treated cells. Application of cyclic but not static pressure caused a significant increase in NO release over a 1 hr period. The rate of NO production (**Figure 4G**) was regulated by both the frequency and magnitude of loading and increased 3.7 fold vs static controls using a 200kPa 2Hz regime ($P < 0.001$); 2 fold using a 200kPa 1Hz regime ($P < 0.05$); and 1.4 fold at a 50kPa 1 Hz regime ($P=0.3$).

.

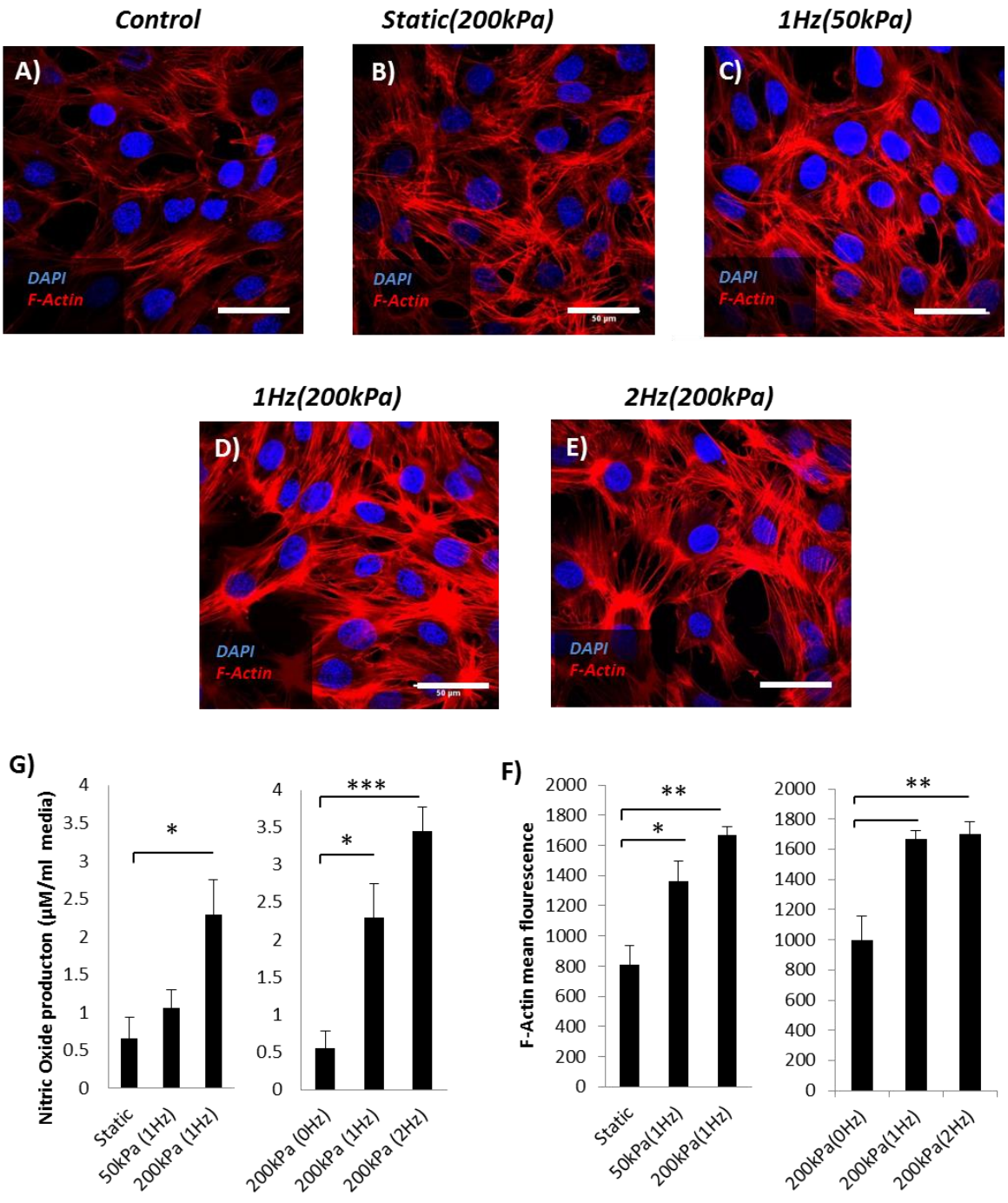

Figure 4. Regulation of actin remodelling and nitric oxide release by hydrostatic pressure in MLO-A5 late stage OBs. *(**A-E**) F-actin staining in cells exposed to different pressure regimes after 60minutes, n=6.* ***F)*** *Nitric oxide production in cells after 60 minutes* ***G)*** *Image quantification of f-actin fluorescence intensity, n=3. Scale bars = 50µm. Error bars = standard error of the mean. **** P<0.001. **P<0.01. *P<0.05.*

2.3.1.2. Role of F-actin integrity during pressure mediated NO production

To determine if pressure induced NO production required and intact cytoskeleton, MLOA5s were cultured in PM supplemented with 10μM cytoD for 1 hr before stimulation. The cells initially adopted a rounded morphology in response to the treatment which persisted during hydrostatic stimulation, but recovered after 24hrs, regaining morphology comparable with untreated cells. Consistent with observations made in **Section 2.3.1.1**, untreated MLO-A5s underwent f-actin reorganisation towards parallel stress fibres **(Figure 5C)**. CytoD treated MLO-A5s **(Figure 5 B&D)** had a noticeable disrupted cytoskeleton, forming detached aggregates of actin filaments in the cell cytoplasm. Fluorescent quantification of f-actin **(Figure 5F)** showed a significant reduction in f-actin fluorescence in cells treated with cytoD. No changes were observed in actin organisation between pressure treated and static cultures after incubation in cytoD. NO production **(Figure 5G)** was significantly higher than untreated controls in cells treated with cytoD, and was comparable with levels released by pressure treated cells. A combination of cytoD and pressure induced NO produciton to similar levels observed due to cytoD treatment alone, and pressure alone.

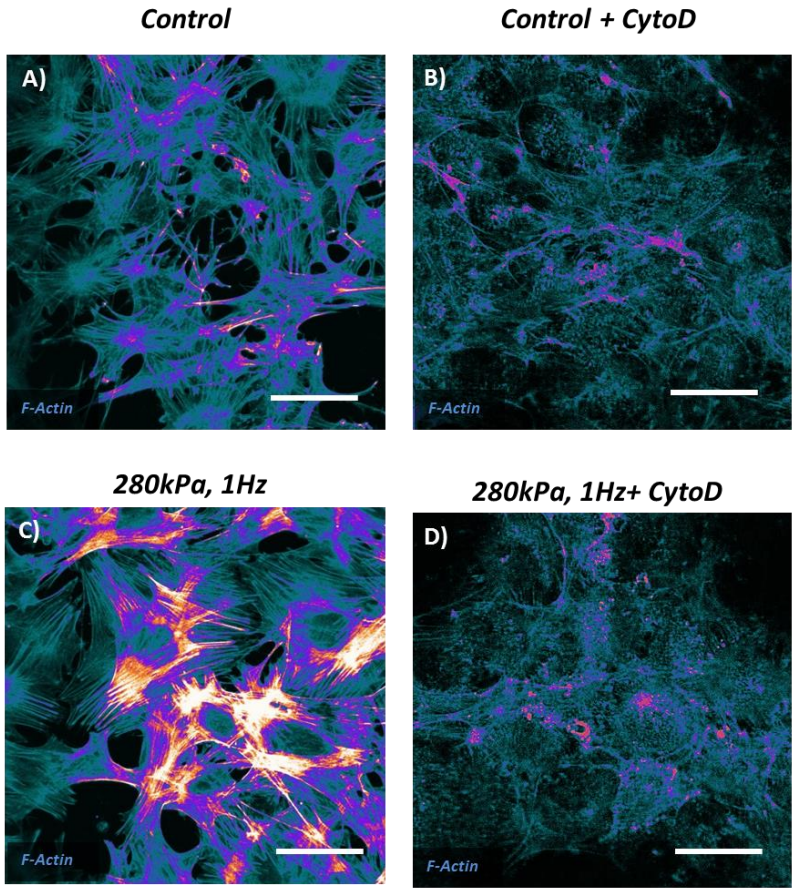

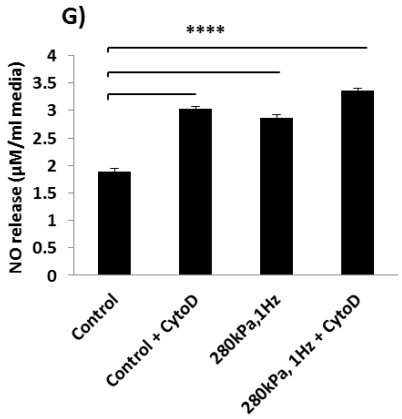

2-way Anova

	DF	Sum of Squares	Mean Square	F Value	P Value
Treatment	1	8.06045	8.06045	24.95374	9.79039E-6
Pressure	1	5.14015	5.14015	15.913	2.47175E-4
Interaction	1	1.26199	1.26199	3.90689	0.05438
Model	3	14.46258	4.82086	14.92454	7.67439E-7
Error	44	14.21269	0.32302	--	--
Corrected Total	47	28.67527	--	--	--

At the 0.05 level, the population means of **Treatment** are **significantly** different.
At the 0.05 level, the population means of **Pressure** are **significantly** different.
At the 0.05 level, the interaction between **Treatment** and **Pressure** is **not significant**.

Figure 5. Role of cytoskeletal integrity in pressure mediated nitric oxide release. ***(A-D)*** *Contrast filtered images of F-actin staining in MLOA5 cells with and without 10µM cytoD incubation prior to loading.* ***F)*** *Image quantification of fluorescence intensity prior to loading, n=3.* ***G)*** *Nitric oxide production in cells after 60 minutes, n=12. Scale bars (top) = 50µm. Error bars = standard error of the mean. *** P<0.001.*

2.3.1.3. Regulation of nuclear to cytoplasmic expression of YAP in MLO-A5 late stage OBs and hMSC precursors

The study of nuclear YAP localisation in cells responding to pressure aimed to establish the interaction of this pathway with hydrostatic pressure and actin stess fibre formation. Cyclic pressure was applied to MLOA5 cells and hMSCs to investigate changes in YAP expression using the same stimulation regime as before (280kPA, 1Hz, 60 mins), to study changes in the retention of YAP in the cytoplasm and the nucleus.

Actin remodelling in pressure treated MLOA5 **(Figure8Aii)** was accompanied by a significant increase in the nuclear accumulation of YAP versus static controls **(Figure8B).** Quantification of fluorescent intensity **(Figure8C)** indicated an increase in the accumulation of both nuclear and cytoplasmic YAP in stimulated MLO-A5s vs static controls, with a significant increase in fluorescence intensity in the nucleus of pressure treated cells versus controls.

Consistent with previous observations, pressure treated hMSC **(Figure8Dii)** did not undergo remodelling of F-actin toward parallel stress fibres. The nuclear accumulation of YAP was slightly higher in stimulated cells vs static controls (**(Figure8E**), however the levels of nuclear vs cytoplasmic YAP were comparable is between control and pressure treated cells **(Figure8F).** In contrast to MLO-A5s, pressure treated hMSCs had lower levels of YAP expression in both the nucleus and cytoplasm compared with controls. The increase in nuclear/cytoplasmic YAP was attributed to a small but significant decrease in the retention of cytoplasmic YAP in pressure treated cells.

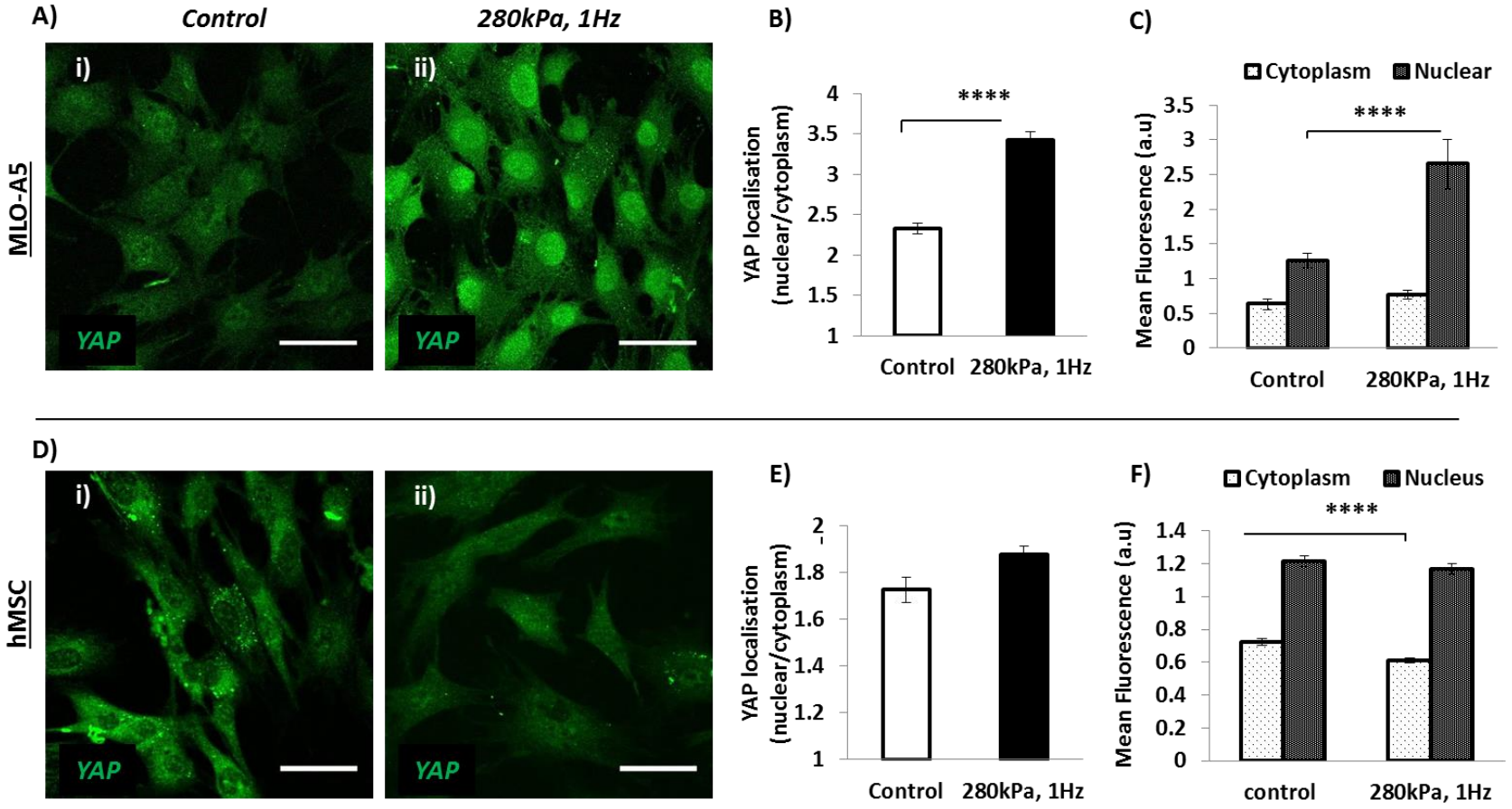

Figure 6. Regulation of nuclear to cytoplasmic YAP in MLOA5 cells and hMSCs. A)*YAP expression in MLOA5 in static culture (i) and after 60 minutes CHP (ii). (**B&E**) Corresponding fluorescence intensity of nuclear and cytoplasmic YAP. **(C&F)** Corresponding ratio of nuclear and cytoplasmic YAP, n>40. **D)** YAP expression in hMSCs in static culture (i) and after 60 minutes CHP (ii). Scale bars = 50µm. Error bars = standard error of the mean. **** P<0.0001. * P<0.05.*

2.3.1.4. F-Actin integrity regulates nuclear to cytoplasmic expression of YAP

The disruption of the actin cytoskeleton using cytoD was employed to investigate changes in YAP expression in MLO-A5s and hMSCs in both static and pressure treated cells **(Figure9)**. Consistent with previous observations, the application of cytoD disrupted pressure mediated actin remodelling and intiated sequestration of YAP from the nucleus into the cytoplasm. Application of pressure **(Figure9C, D, G, H)** did not result in any observable differences in YAP expression in either MLO-A5 or hMSC.

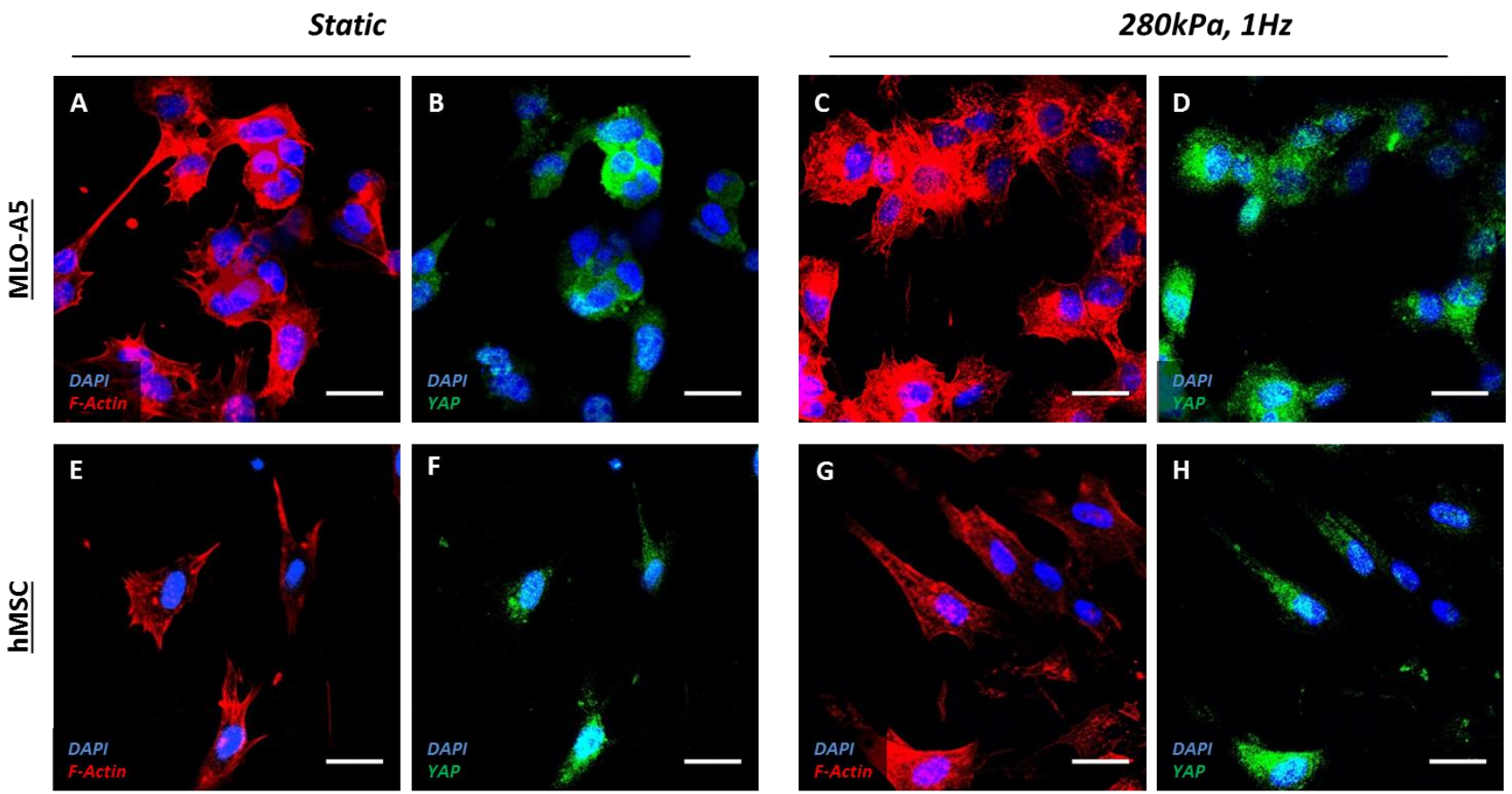

Figure 7. F- Actin integrity regulates nuclear to cytoplasmic expression of YAP. (A-D) *Immunofluorescent staining showing F-actin (**A,C,E&G**) and YAP expression(**B, D, F&H**) in MLOA5 cells (**A-D**) and hMSCs (**E-H**) treated with cytochalasin D. Scale bars = 35µm.*

2.3.2. Effect of substrate stiffness and cyclic pressure on hMSC differentiation during 10 days culture in osteogenic media

Up to this point, my experiments have identified a broad range of changes in cell behaviour during stimulation with hydrostatic pressure, confirming that the bioreactor can induce mechano-active responses in cells that are commonly observed in the literature. I now aimed to test of the hypothesis that the bioreactor can accelerate osteogenic differentiation in hMSC monolayer after 10 days in culture. Dupont et al. demonstrated that alterations in the differentiation potential of hMSCs are related to factors such as actin stress fibre formation and nuclear localisation of YAP when cells are cultured on different substrate stiffness's (Dupont et al. 2011). Coupled with my findings thus far that show changes in the behaviour of YAP due to pressure, my hypothesis is that by generating an ECM environment that favours osteogenic differentiation in MSCs, hydrostatic pressure will act synergistically with this environment to enhance differentiation when compared with unstimulated controls. Since nuclear YAP expression is more prevalent on stiffer substrates, observing the shift in YAP localisation is a useful method to validate the change in stiffness of the polyacrylamide substrates. Additionally, I can then also study changes in YAP expression as a result of hydrostatic pressure in MSCs cultured on different stiffness substrates.

2.3.2.1. Effect of substrate stiffness on cell area and YAP expression in hMSCs

hMSCs seeded on polyacrylamide gels of different stiffnesses (7500cells/cm^2) had a distinct cell morphology 24hrs after seeding. Cells seeded on soft substrates had a spindle like morphology (**Figure11 A**), attributed to a decrease in cell spreading. Increasing the stiffness **(Figure11 B&C**) of the substrates significantly increased cell spreading and consequently cell area (**Figure11 D**). The increase in cell area correlated with an increase in actin stress fibre formation and a significant increase in the nuclear accumulation of YAP on stiffer substrates (**Figure11E**).

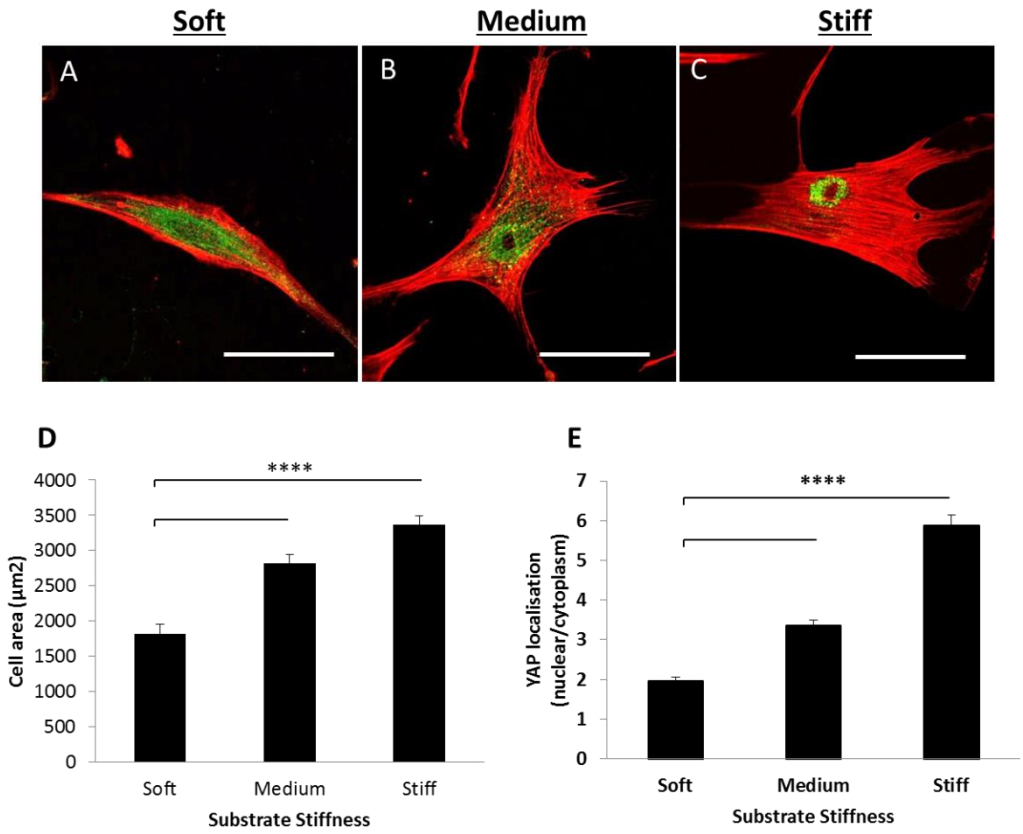

Figure 8. Substrates stiffness regulates cell spreading and nuclear accumulation of YAP in hMSCs seeded on polyacrylamide substrates. (A-C)*Immunofluorescent staining showing F-actin and YAP expression in hMSCs seeded on different stiffness substrates.* ***C)*** *Cell area on different stiffness substrates, n>40.* ***D)*** *Ratio of nuclear to cytoplasmic YAP in hMSCs seeded on different stiffness substrates, n>40. Scale bars = 50µm. ****P<0.0001 determined by one way analysis of variance.*

2.3.2.2. Effect of cyclic hydrostatic pressure on YAP expression in hMSC seeded on different stiffness substrates

Cells seeded on different substrates stiffness's were exposed to cyclic pressure to investigate changes in YAP expression during hydrostatic loading. The regulation of nuclear to cytoplasmic YAP in response to loading was dependant on the stiffness of underlying substrate, with soft substrates (**Figure 13 Ai**) inhibiting both nuclear and cytoplasmic YAP expression after loading, and stiffer substrates, **Figure 13 Aii&iii**) increasing the expression of both nuclear an cytoplasmic YAP during loading. Nuclear to cytoplasmic retention of YAP (**Figure 13D**) showed no statistically significant differences between static and pressure treated cells with respect to substrate stiffness. Analysis by a two way anova revealed there was no significant difference in nuclear YAP intensity in response to hydrostatic pressure or a change in substrate stiffness. However there was a significant interaction between pressure and stiffness with respect to nuclear YAP intensity, which can be seen by a reduction in nuclear YAP intensity in response to pressure on soft substrated, and an increase in nuclear YAP intensity on stiffer substrates in response to pressure. By contrast, analysis by two way anova on cytoplasmic YAP intensity showed that whilst the effect of pressure alone was not significant, there was a significant difference in cytoplasmic YAP intensity due to substrate stiffness. The interaction between pressure and stiffness with respect to cytoplasmic YAP was also significant. Overall these results suggest that the change in nuclear YAP localisation was determined primarily by substrate stiffness and not hydrostatic pressure. Furthermore, the two way anova's suggest that this effect was primarily due to a reduction in cytoplasmic as YAP intensity as substrate stiffness increases.

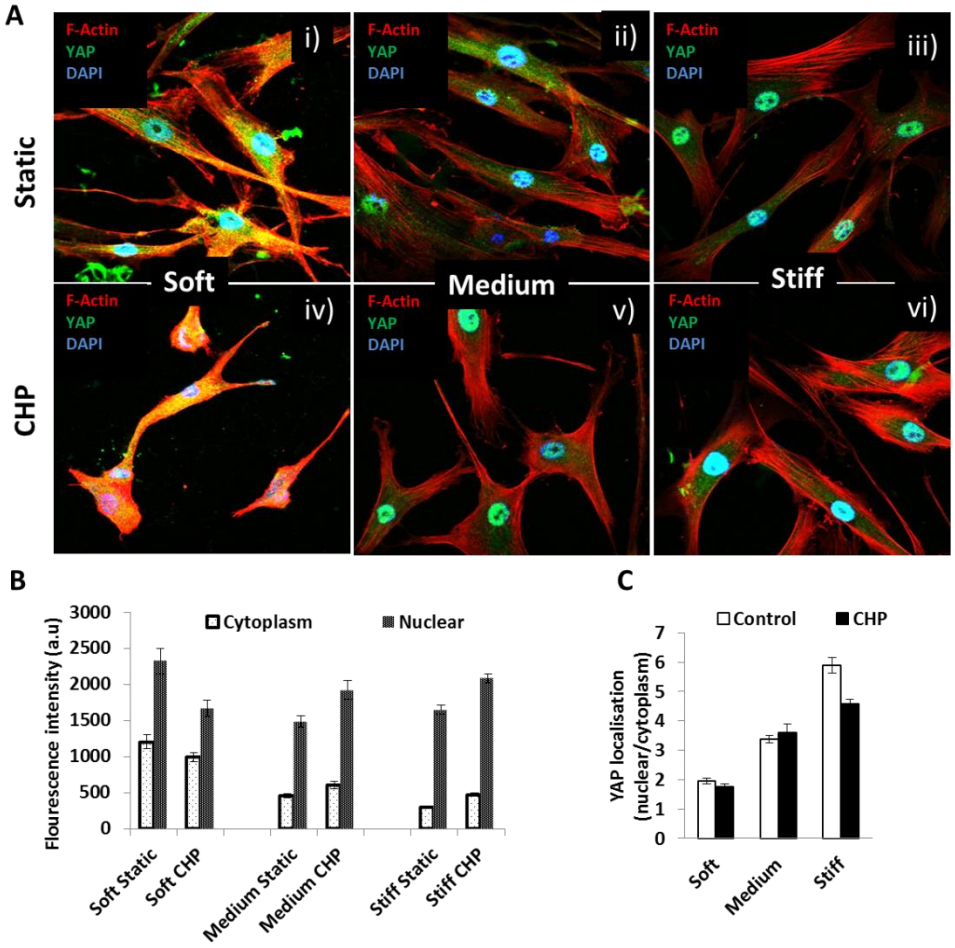

Two way anova - cytoplasmic YAP

	DF	Sum of Squares	Mean Square	F Value	P Value
Stiffness	2	1.61652E7	8.0826E6	112.64276	0
Pressure	1	172903.80228	172903.80228	2.40966	0.12193
Interaction	2	1.04331E6	521655.21771	7.27002	8.63963E-4
Model	5	1.87686E7	3.75372E6	52.31349	0
Error	235	1.68623E7	71754.29382	--	--
Corrected Total	240	3.56308E7	--	--	--

At the 0.05 level, the population means of **Stiffness** are **significantly** different.
At the 0.05 level, the population means of **Pressure** are **not significantly** different.
At the 0.05 level, the interaction between **Stiffness** and **Pressure** is **significant**.

Two way anova - nuclear YAP

	DF	Sum of Squares	Mean Square	F Value	P Value
Stiffness	2	1.83771E6	918856.81552	2.43969	0.08939
Pressure	1	897714.79928	897714.79928	2.38356	0.12396
Interaction	2	8.68521E6	4.3426E6	11.53021	1.6719E-5
Model	5	1.45796E7	2.91592E6	7.74217	9.24074E-7
Error	235	8.85077E7	376628.37888	--	--
Corrected Total	240	1.03087E8	--	--	--

At the 0.05 level, the population means of **Stiffness** are **not significantly** different.
At the 0.05 level, the population means of **Pressure** are **not significantly** different.
At the 0.05 level, the interaction between **Stiffness** and **Pressure** is **significant**.

Figure 9. Pressure mediated YAP expression in hMSC after 60 minutes is dependent on substrate stiffness. Ai-vi) *Immunofluorescent staining showing F-actin and YAP expression in hMSCs seeded on different stiffness substrates.* ***B)*** *Fluorescence intensity of nuclear and cytoplasmic YAP in hMSCs seeded on different stiffness substrates, n>40.* ***C)*** *Ratio of nuclear to cytoplasmic YAP in hMSCs seeded on different stiffness substrates, n<40. Scale bars = 50μm. Error bars = standard error of the mean.*

2.3.2.3. hMSC morphology after 10 days culture in osteogenic media

Cells proliferated during the 10 day culture period in all experimental groups but developed different morphologies depending on the stiffness of the underlying substrates. Soft substrates progressed from spindle shaped morphology (**Figures 11&12)**, to rounded island morphology (**Figure 13A)**. Stiffer substrates (**Figure 13B-D)** retained spread morphology with actin stress fibres becoming more prominent as stiffness increased. In contrast to day 1, where YAP was localised in the nucleus, by day 10 YAP was almost exclusively found in the cytoplasm.

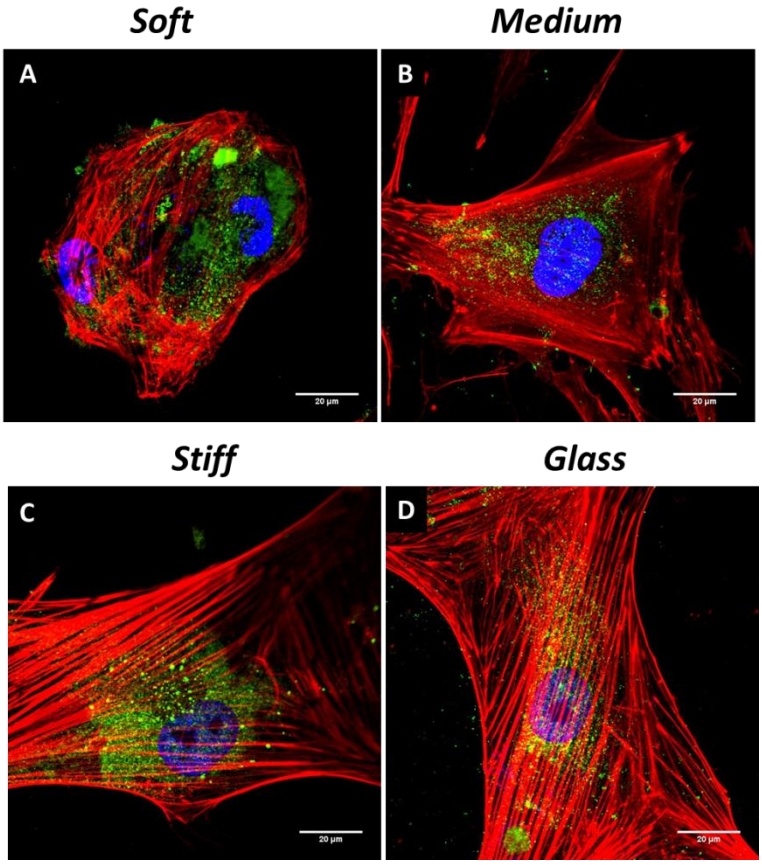

Figure 10: Substrate stiffness mediates cell spreading and cytoskeletal stress fibre formation after 10 days culture in osteogenic media. *Scale bars = 50µm*

2.3.2.4. Assessment of osteogenic differentiation in hMSCs after 10 days in culture

Osteogenic differentiation after 10 days was assessed by immunocytochemistry to detect Runx2 (discussed in **Section 1.4.3**), an transcription factor involved in osteogenic differentiation of MSCs and OCN (discussed in **Section 1.4.4**) a non-collagenous protein present that is thought plays parts in regulating bone formation. Immuno-fluorescent detection of OCN and Runx2 showed positive expression of both markers in all experimental groups (**Figure 14 A-H)**. Runx2 expression was upregulated as substrate stiffness increased (**Figure 14 A-D, E-H)**. Osteocalcin was also upregulated on stiffer substrates, with a higher number of osteocalcin rich nodules present in stiff and glass substrates vs sot and medium substrates. No clear differences in expression were noted between static (**Figure 14, A-D**) vs pressure treated (**Figure 14, E-H)** cells. The localisation of red fluorescence (Runx2) to the nucleus signified a specificity of activity in cells that represented binding of transcriptional Runx2 to DNA, initiating osteogenic differentiation. The presence of OCN in the cell cytoplasm and ECM suggested cells actively secreting the protein as a result of undergoing osteogenic differentiation. The co-localisation of green and red fluorescent (appearing yellow) on soft substrates (**Figure 14 A&E)** indicated a false positive signal generated by auto-fluorescent material present in the cells.

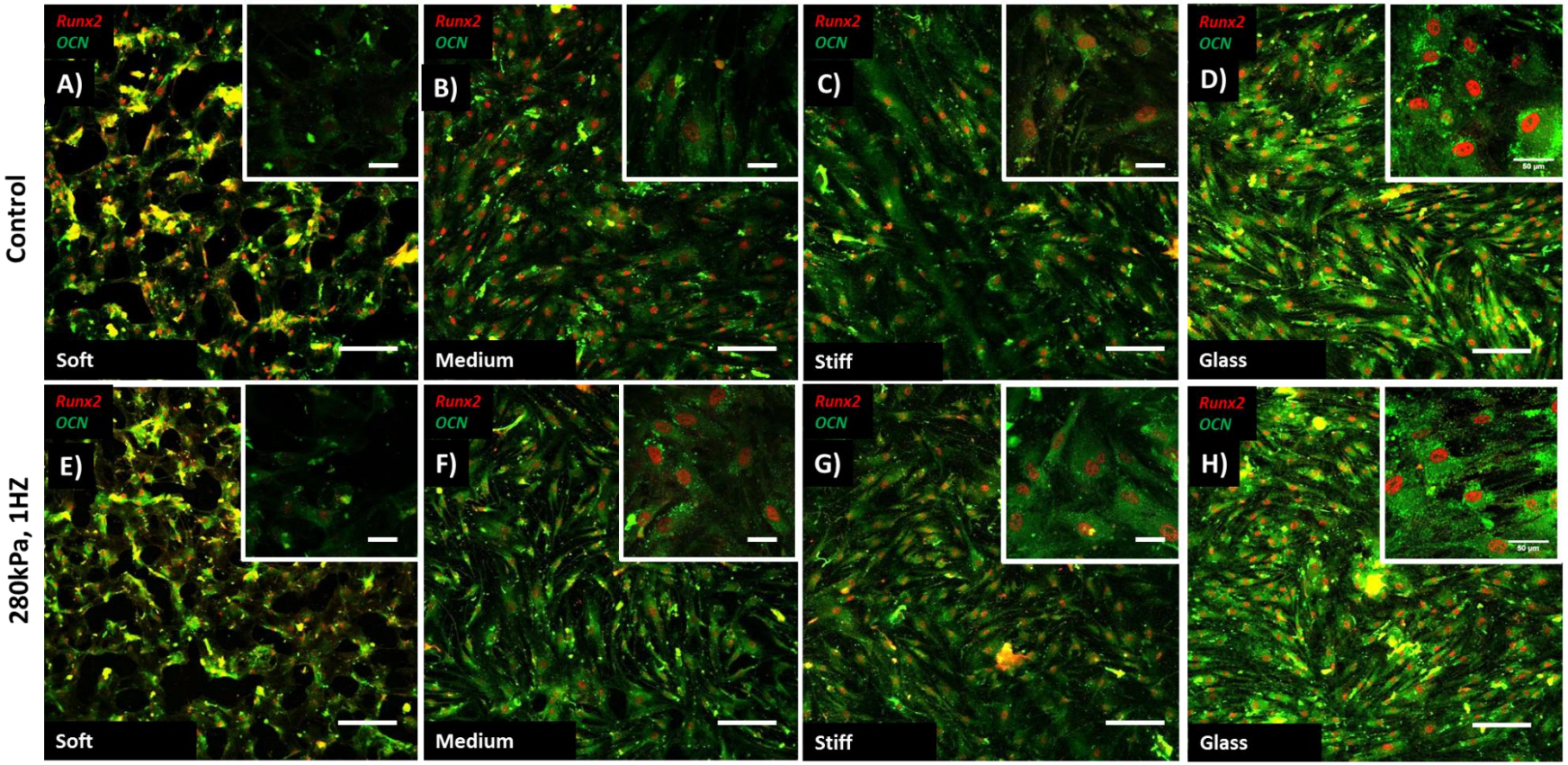

Figure 11. Immuno fluorescent staining for Runx2 (red) and osteocalcin (green) in hMSCs cultured on different stiffness substrates after 10 days culture in osteogenic media. *Scale bars = 200μm and 50μm inset*

2.3.2.5. Assessment of lipofuscin formation in hMSC cultured on different stiffness substrates

On softer substrates, whilst the presence Runx2 and OCN was detected (**Figure 14 A&E)**, the intensely stained co-localisation of green (OCN) and red (Runx2) fluorescence and indicated a false positive signal due the presence of auto fluorescent material in the cells. One potential explanation for this false positive signal was the formation of lipofuscins in cells cultured on softer substrates. Lipofuscins consist of auto fluorescent lysosomal storage bodies that accumulate in different tissues during cell senescence (Katz & Robison 2002). Sudan black B staining is commonly used to quench auto-fluorescence in tissue sections and has also been shown to be specific to lipofuscin formation in senescent cells (Georgakopoulou et al. 2013). Based on this, Sudan black B staining was employed to assess the presence of lipofuscins in cells to determine if the fluorescent signal in softsubstrates was due to the formation of auto-fluorescence lipofuscins. After staining the different stiffness substrates with Sudan black B, brightfield microscopy was used to assess the extent of lipofuscin formation (**Figure 15**). soft (**Figure 15A&E**) substrates had noticeable more nodular black deposits in the cellular cytoplasm compared with stiffer substrates (**Figure 15 B,C,D&G**), indicating that cells grown on the softest substrates experienced extensive lipofuscin formation after 10 days in culture, which was likely the cause of false positive ICC signal on soft subrates

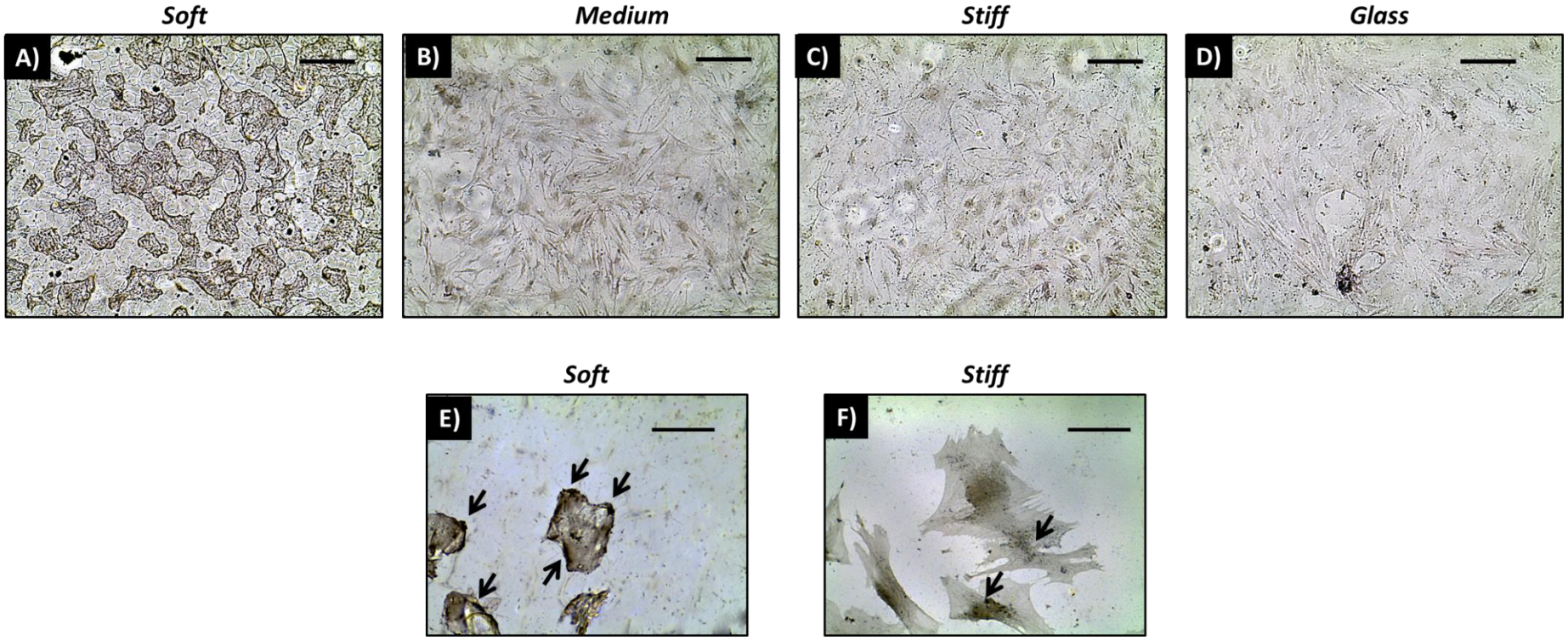

Figure 12. Soft substrates promote lipofuscin formation in hMSC after 10 days culture in OM. *Sudan black B staining of hMSC seeded on different stiffness substrates after 10 days in ostegenic media.* ***(A-D)*** *Scale bars = 100µm.* ***E&F)*** *Scale bars = 50µm.*

2.3.2.6. Alkaline phosphatase activity

. ALP staining was used to assess osteogenic differentiation in MSCs seeded on different stiffness substrates. Bright field imaging of MSCs at day 10 following ALP staining demonstrated an increase in ALP positive cells as substrate stiffness increased **(Figure 16, red)**. Softer substrates (**Figure 16 A, E, B&F**) had little to no positive detection of ALP, whilst stiffer substrates (**Figure 16 C,D,G&H**) had ALP positive cells, particular in nodular areas that correlated with increased OCN expression in **Figure 15**. Glass substrates showed the highest number of ALP positive cells, however neither static nor pressure treated cells showed a noticeable difference in ALP positive cells. This result suggests that pressure treatment did not enhance the osteogenic differentiation of hMSCs during the 10 day culture period.

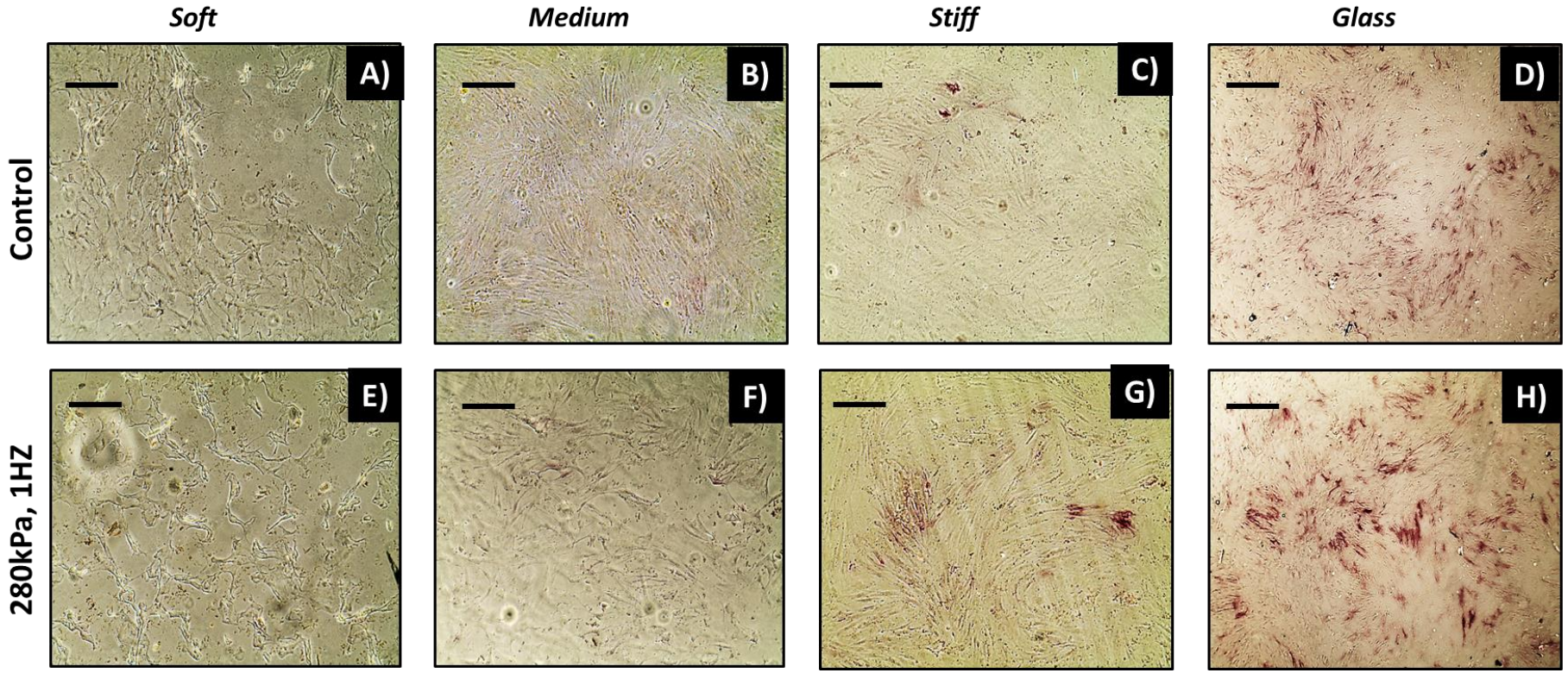

Figure 13. ALP staining (red) in hMSCs after 10 days culture in OM. *Scale bars = 200μm.*

2.4. Discussion

2.4.1. Nitric oxide and actin remodelling

Application cyclic pressure increased NO production in MLO-A5 late stage OBs, and was accompanied by remodelling of the f-actin cytoskeleton. Pressure induced nitric oxide production was dependant on both the magnitude and frequency of loading, with higher magnitudes and frequencies increasing NO production. By contrast, static compression did not alter NO production when compared with unstimulated controls. This suggests that cyclic loading regimes are required to induce cellular responses to hydrostatic pressure. Magnitude and frequency dependant NO production has been reported in MC3T3 OBs in response to fluid flow(Mullender et al. 2006). Additionally the same study also found whilst fluid flow increased PGE2 production, this was not dependant on magnitude and cycling frequency. It would be interesting in future to test PGE2 production under the regimes described in **Section 2.3.1.1** to determine if PGE2 is sensitive to different magnitudes and frequencies if hydrostatic pressure. This might highlight an important distinction in the response of cells to fluid flow and hydrostatic pressure.

Pressure mediated NO production did not require an intact cytoskeleton, suggesting that the factors influencing f-actin stress fibre formation and NO production act independently from each other. The increase in NO production in cytoD treated cells in unstimulated controls suggests that while actin integrity itself not does mediate NO production in response to hydrostatic pressure, the underlying biochemistry that influences actin organisation and NO production is related. Cytochalasins are fungal metabolites that permeate the cell membrane and inhibit actin polymerisation, membrane ruffling and cell stiffness (Yahara et al. 1982). There are many different types of cytochalasin compounds, and each can induce

distinct responses in cells. For example cytoD has been shown to have a much stronger effect on increasing adenylpyrophosphatase (ATPase) activity in cells than cytochalasin B (cytoB) (Brenner & Korn 1980), which is also commonly used to disrupt actin polymerisation. McGarry et al. studied changes in flow induced NO production in MC3T3 OBs using cytoB (McGarry et al. 2005). In contrasts to the results in **Section 2.3.1.2** which used cytoD, McGarry and colleagues observed a reduction in flow induced NO in cells pre-treated with cytoB. The same study also shows that in MLO-Y4 OSs (a later stage phenotype of MLO-A5s (Kato et al. 2001)), cytoB treatment did not affect flow induced NO production, but instead inhibited flow induced PGE2 production, implying that the regulation of these mechanisms is unique to different cell types. Studying changes in NO in combination with different cytochalasin compounds could facilitate a deeper understand of the underlying biochemical changes in cells that determine their response to hydrostatic pressure. It is possible that we might observe changes in the regulation pressure induced NO production using different cytochalasin compounds. Furthermore, since different cytochalasins can alter cellular ATPase activity, we might also further elucidate the relationship between ATP and hydrostatic pressure, of which the former has previously been reportedto be involved in pressure mediated actin stress fibre formation in OBs (Gardinier et al. 2009).

The current body of literature suggests the effects of mechanical loading in the form of flow, pressure, or strain, can have broadly similar effects on cell behaviour in the context of actin reorganisation and NO production. However, there is a vast body of literature attempting to define the mechanisms that underpin these cellular processes, making it difficult to interpret precursor events that lead to these changes. One possible explanation for why NO production and stress fibre formation in **section 2.3.1.1** appeared to coincide with each other, and then later in **section 2.3.1.2** why NO production was stimulated in the absence of an intact cytoskeleton, could be through pressure mediated release of

intracellular calcium stores. This mechanism has been shown to modulate the organisation of f-actin in OSs during cyclic pressure stimulation (Liu et al. 2010), and also in OBs responding to fluid flow (Chen et al. 2000). Interestingly, Malone et al. have also reported increased levels of intracellular calcium in OBs exposed to cytoD (Malone et al. 2007). Since the experiments described in this chapter show an increase in NO production in response to both pressure and cytoD treatment, it could be that NO production by cyclic pressure is associated with the release of intracellular Ca^{+} stores, which might also be responsible for actin stress fibre formation. However, whilst NO has been shown to correlate with calcium signalling in OSs during fluid flow (Huo et al. 2008), this relationship is not clearly defined. Initial calcium peaks have been shown in OSs to occur much earlier than the onset of NO production (Lu et al. 2012), and it has been suggested that NO instead might influence the induction of external influxes of Ca^{+} to replenish intracellular stores(Li et al. 2003). Further work studying the effect of calcium signalling in cells during bioreactor stimulation, such as blocking specific Ca^{+} ion channels or depleting intracellular calcium stores prior to loading could improve our understanding of pressure mediated changes in cell behaviour.

2.4.2. YAP expression in hMSCs and MLO-A5s in response to pressure

The results indicated that in MLO-A5s hydrostatic pressure initiates translocation of YAP to the nucleus via a mechanism associated with f-actin stress fibre formation. In contrast to MLO-A5s, nuclear accumulation of YAP did not occur in MSCs. whilst the reason for this was unclear, it is possible that this was due to the lack of actin stress fibre formation in MSCs during hydrostatic stimulation. This was further supported by the expulsion of YAP into the cytoplasm during cytoskeletal disruption with CytoD in **Section 2.3.1.3**. This result might reflect a potential mechanosensory shift between MSC precursors and mature skeletal cells.

The correlation between f-actin stress fibre formation and nuclear translocation of YAP in MLO-A5s indicated that the behaviour of YAP transport in OBs in response to hydrostatic pressure is different from MSCs. Whilst there is still some uncertainty as to how YAP/TAZ signalling regulates cell behaviour, it has been shown to be important in regulating bone formation both *in vitro* and *in vivo*(Tang et al. 2013). Whilst much of the work on YAP expression has focussed on MSC differentiation, it is surprising that there appears to be no literature on the activity of this pathway in late stage OBs. When we consider that a nuclear translocation of YAP has been shown to depend on f actin stress fibre formation, which is widely reported in OBs undergoing mechanical loading, it seems reasonable to suggest that YAP may play an important role in the transition of OBs to mineralised OSs. One potential mechanism by which pressure induced actin stress fibre formation could induce nuclear YAP accumulation is via the Serine/threonine-protein kinases (LATS). It has been shown that LATS1/2 mediated phosphorylation triggers the localisation of YAP in the cytoplasm(Dong et al. 2007)(Zhao et al. 2007). Interestingly LATS phosphorylation has recently been linked with f-actin stress fibre formation, a mechanism in which actin stress fibres bind angiomotins targeted by LATS kinases for phosphorylation, leading to localisation of YAP into the cytoplasm (Dai et al. 2013) (Mana-Capelli et al. 2014). This might explain why nuclear YAP accumulation correlated with actin stress fibre formation in MLO-A5s. A detailed examination of LATS expression during hydrostatic loading could identify changes in phosphorylation events that lead to increased nuclear YAP in OSs but not MSC. A tempting hypothesis would be to test if gradual shifts in the activation of this pathway occur during hydrostatic stimulation as MSCs transition from stromal cells to later stage OBs. **Figure 18** summarises the cellular events that were observed following application with cyclic pressure. Identifying these initial events inferred that cells interpreted external hydrostatic pressure

from the bioreactor, and translated these pressures into biochemical signals; confirming that mechanotransduction was taking place in cells dung bioreactor stimulation.

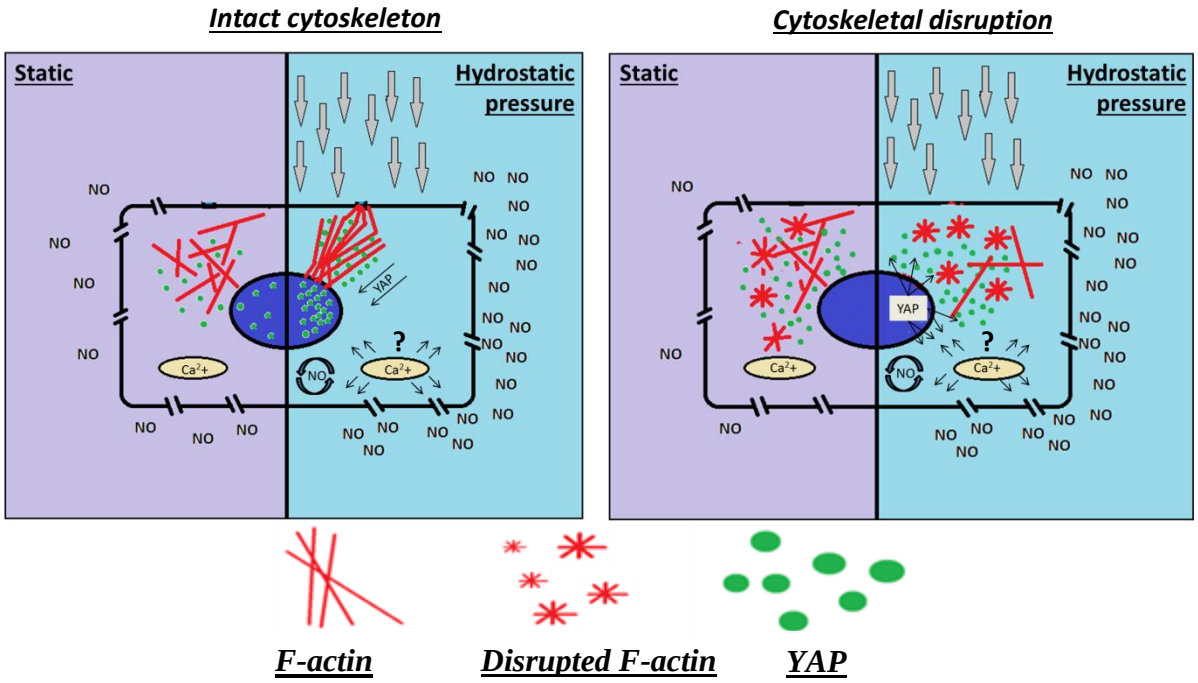

Figure 14. Summary of findings of mechanotransduction in MLO-A5s exposed to hydrostatic pressure. *Upon application of hydrostatic pressure, cytoskeletal tensioning leads to accumulation of YAP in the nucleus.. Hydrostatic pressure also induces NO release, a process that does not require an intact cytoskeleton. Existing evidence infers hydrostatically induced NO production might be related to the rapid release of intracellular calcium stores during loading.*

2.4.3. Hydrostatic preconditioning of hMSCs monolayers

The final section of this chapter aimed to investigate if the mechanisms discussed above were key determinants of osteogenic differentiation in hMSC. Analysis of osteogenic markers Runx2, OCN and ALP showed that stiffer substrates promoted osteogenic differentiation and that this correlated with the initial cell area, nuclear YAP localisation, and f actin stress fibre formation. Whilst hydrostatic pressure altered the expression of YAP on the different stiffness substrates, there did not appear a consistent pattern in the behaviour of YAP expression due to substrate stiffness and pressure. Coupled with this, daily application of pressure over 10 days did not appear to enhance MSC differentiation. This suggests that in contrast my initial hypothesis, while stiff substrates promote nuclear accumulation of YAP and enhance osteogenesis relative to softer substrates, the synergistic effect of pressure did not improve the differentiation potential when compared with unstimulated controls.

The induction of osteogenic differentiation using soluble factors such as dexamethasone and β-glycerol phosphate is a well-established technique. There is a large body of literature exploring gene expression profiles at different stages of osteogenesis(Stein et al. 2004), and the specific expression profiles of key markers is still debated. The typical timeframe for differentiation of hMSC's in osteogenic media is around 14 days, with expression of transcriptional runx2 between days 5 and 14 (Birmingham et al. 2012). During this time there is also thought to be a peak expression in ALP (Aubin 2001) before the onset of matrix production in the form of OCN, collagen and calcium deposition (Hoemann et al. 2009). The experiments described in **Section 2.3.2** showed hMSCs expressed ALP, runx2 and OCN, which is consistent with the literature describing early marker expression profiles during osteogenic differentiation of MSCs. It may be that a longer time in culture might have elucidated a response due to hydrostatic pressure that was not observed during the 10 day culture period. Additionally, a more thorough characterisation of cell behaviour such as

changes in proliferation, metabolite assays, or analysis of gene expression by qPCR might have identified mechanoactive responses that are as of yet undetermined. Whilst age related shifts in the response to mechanical loading have been identified in MSCs (Tan et al. 2015), the idea that the mechano-sensitivity might change as MSCs develop into more osteoblastic phenotypes has not yet been explored. Indeed the ability of OSs to sense certain mechanical stimuli has been shown to be fairly unique, by which it's characteristic dendritic processes more effectively translate locally applied mechanical stimuli than the main cell body(Adachi et al. 2009).

Aside from potential changes in the mechano-sensitivity in MSCs, it could be that the regime chosen for the experiments in **Section 2.3.2** did not reflect physiological pressures MSCs experience as they undergo the initial transition into pre-osteoblasts. A recent study measuring pressure and shear stress in the trabecular compartment of whole porcine femurs during whole bone loading estimated pressure gradients of between 0.013-0.46kPa, shear stresses between 1.67-24.55Pa and compressive strains around 100-150με (Metzger et al. 2015). It's reasonable to suggest that the fluid flow or strain more positively influence the early stages of MSC differentiation towards pre-OBs, and hydrostatic pressures regimes such as the one used in **Section 2.3.2** could more accurately reflect physiological loading in the later stages of OB differentiation. Likewise this maybe why MLO-A5s behave differently to MSCs in response to pressure with respect to actin reorganisation and YAP expression.

2.4.4. 2D vs 3D growth environments

The study of 2D monolayers systems has long been debated with respect to designing growth environments that accurately recapitulate the *in vivo* cell niche. Coupled with this 2D systems complicate many aspects of clinical translation due to problems with limited scalability and reproducibility (Serra et al. 2012). Chondrocytes have been shown to switch from a rounded morphology in 3D to a fibroblast morphology in 2D, which was shown to alter the rate ECM production between the two systems (Lawrence & Madihally 2008). It has also been suggested that changes between 2D fibroblast cultures and fibroblasts cultured in 3D collagen hydrogels exhibit differences in cell-cell signalling, cytoskeletal regulation and integrin mediated cell matrix interactions (Rhee 2009). It's likely that by providing a more appropriate 3D growth environment for MSCs could enhancee bone forming in response to hydrostatic pressure. We must not however overlook the seminal contributions to the understanding of bone mechano-biology that have been made through investigating 2D environments under dynamic loading. *In vitro* monolayer studies of early mechanotransduction events can offer a high throughput screening method that is cost effective, and can deliver useful preclinical evaluation of the efficacy of hydrostatic pressure bioreactors over static cell culture.

2.5. Conclusion

In this chapter, I observed active mechanotransduction in cells during hydrostatic loading using the bioreactor system. I have identified changes in cell behaviour associated with different magnitudes and frequencies of loading, determining that cyclic and not static loading is required to initiate mechanotransduction in the form of NO production and actin stress fibre formation.. Finally, I employed the bioreactor to attempt to enhance osteogenic differentiation in hMSCs cultured on different stiffness substrates; however my results

suggested that bioreactor stimulation did not improve the outcome of differentiation compared with a static culture environment. The next chapter aims investigate the difference in response of 2D and 3D growth environments in OBs, and to optimise a growth environment that reflects a clinically relevant bone graft using hMSCs.

Chapter 3

Translation from 2D to 3D:

Optimising in vitro bone formation

in cell seeded hydrogels

3.1. Introduction

In the previous chapter I demonstrated that daily treatment with hydrostatic pressure did not enhance osteogenic differentiation in hMSC monolayers after 10 days in culture. I discussed that a longer culture period may have resulted in a greater response to hydrostatic pressure, due to the developing OB phenotype potentially being more responsive to pressure than MSC precursors. In this chapter I will use a human MG63 bone cell line, considered to represent an intermediate stage of differentiation (Pautke et al. 2004)(Czekanska et al. 2014), as a reference cell line to determine if bioreactor stimulation can increase the rate of *in vitro* bone formation. MG63s (discussed **Section 1.5.2**) share many of the same phenotypic traits as primary human OBs, and also represent a heterogeneous cell population that is well characterised by the literature. Additionally, I aim to study changes in cell behaviour due the transition from 2D monolayers to a 3D environment, which more accurately represents the *in vivo* niche of bone tissue. I hypothesise that a transition between 2D and 3D culture environments will alter the MG63s response to hydrostatic pressure. A number of studies report a disparity in mechanically active responses of cells between 2D and 3D environments (Cukierman & Bassi 2010) (Tibbitt & Anseth 2009) (Polacheck et al. 2014). Thus, insight into such translational mechanisms could help bridge the gap in the understanding of how heterogeneous cell populations respond to hydrostatic pressure between 2D and 3D growth environments. Additionally, defining a loading regime that positively influences bone formation in cell seeded constructs will be important in evaluating the efficacy the bioreactor when compared with a static culture environment.

3.1.1. *Recapitulating in vivo niches in vitro*

Recapitulation of *in vivo* niches to generate tissue equivalents *in vitro* may lead to a significant step forward in advancing treatments for orthopaedic medicine(Ingber & Levin 2007). As discussed in **Section 1.4.4 & 1.6.2**, collagen type 1 represents the most substantial organic component of mammalian tissue, accounting for 20-30% of the body's total protein content (Harkness 1961). Due to its excellent bio-compatibility and the ease at which its properties can for fine-tuned for different applications, collagen remains one of the most promising candidate biomaterials for tissue regeneration. Collagen's regenerative capacity has been demonstrated in a number of different *in vitro* models, including neural tissue (Weightman et al. 2014), tendon (Lomas et al. 2013), muscle(Micol et al. 2011) cartilage(Hui et al. 2008) and bone (Schneider et al. 2010). Due to the collagen's unique chemistry, it can be readily manipulated to serve as a drug delivery vehicle (Aishwarya 2008), and has proven safety and efficacy as a bone substitute in humans when used in combination with osteo-inductive growth factors(Geiger 2003). Existing evidence demonstrates the usefulness of collagen scaffolds to translate 2D cell culture toward a cell microenvironment that more closely mimics physiological niches. Coupled with this, experiments using 3D collagen hydrogels can facilitate a deeper understanding of how environmental factors such as the ECM, affect a cells ability to translate hydrostatic pressure into biochemical responses.

3.1.2. *Defining measurable outputs for quantifying mechanically stimulated bone formation*

Utilising the appropriate forms of analysis to assess changes in the osteogenic differentiation of cells seems a somewhat trivial statement; however, characterising the level of complexity in *in vivo* tissues requires extensive analysis, and the increasingly interdisciplinary nature of BTE has introduced a vast database of analytical techniques that aim to quantify *in vitro* tissue development. It is important then to review and implement techniques that more adequately represent the aims of my hypothesis, that is, a daily cyclic pressure regime can accelerate bone formation in cell seeded 3D hydrogels. Computer aided imaging modalities such as x-ray micro computed tomography (μCT), represent a growing advance in analytical techniques which can accurately probe changes in the physical and mechanical environment of 3D cell seeded constructs(Baas et al. 2010). The first publications relevant to orthopaedic research, detailed in the late 1980's, used μCT to describe the structural mechanics of trabecular bone architecture (Feldkamp et al. 1989). The contribution of μCT since has made an astounding impact on the understanding of bone development, allowing the researcher to quantify temporal changes in the structure and density of different tissues with micrometre resolution. The sensitivity of μCT, coupled with its non-destructive imaging capabilities, makes it an excellent tool for live monitoring structural changes in pre-cultured cell seeded scaffolds.

3.1.3. *Optimising the ECM environment*

Given the extent in which collagen is used in biomedical research, surprisingly little has been done to standardise methods in which scientists can stimulate *in vitro* tissue growth. Previous studies have demonstrated that the collagen content, controlled by adjusting the relative concentration during hydrogel fabrication, is a critical determinant of subsequent tissue development. Changes in collagen concentration have been

correlated with altered gel contraction in MSCs, as well as with changes in cell mediated matrix remodelling during tenogenic differentiation (Awad et al. 2000). Interestingly, despite the evidence describing a strong correlation between cell seeding density and collagen hydrogel concentration on *in vitro* cartilage formation by hMSCs (Hui et al. 2008), studies are yet to characterise the effect of these experimental parameters on *in vitro* osteogenesis in hMSCs. Furthermore, there is currently a poor understanding of how spatial changes dictate temporal osteogenic maturation of MSC seeded collagen hydrogels. The manufacturing requirements for a viable regenerative medicine therapy require not only adequate characterisation of cell sources and expansion techniques(Want & Nienow 2012) but also a rigorous demonstration of clinical relevance through process improvement and optimisation (Williams & Sebastine 2005). I therefore aim in this chapter to assess the extent of *in vitro* bone formation in hMSC seeded collagen gels with different gel concentrations and cell seeding densities. In doing so, I can define an optimal set of initial conditions to generate 3D bone constructs. Since the beneficial effect of preconditioning in the bioreactor is at present not clear, I must first define an appropriate set of conditions in which I can reliable manufacture hMSC/collagen scaffolds that represent clinically relevant bone substitutes. By generating an internal gold standard of static culture in hMSC/collagen hydrogels, the process of assessing the outcome of experiments implementing hydrostatic preconditioning could become much simpler.

Objectives

i) **Study the effect of hydrostatic preconditioning on MG63 osteoblasts in 2D monolayers.** To determine if hydrostatic preconditioning accelerates bone formation in differentiating MG63's. I aim to test the hypothesis that changes in cytoskeletal remodelling at the point of loading (reported in **Section 2.3.1)** reflects the cells ability to increase bone formation due to hydrostatic preconditioning.

ii) **Assess changes in the behaviour of MG63 osteoblasts in 2D monolayers and 3D collagen hydrogels.** To determine if a 3D environment enhances the ability of cells to translate hydrostatic pressure into bone forming responses. This will also serve to determine if the loading regime (280kPa, 1Hz, 60 minutes) is effective for preconditioning 3D bone constructs.

iii) **Define an internal 'gold standard' of bone tissue development in hMSC/collagen hydrogels after 4 weeks in static culture.** To understand how changes in cell seeding density and collagen concentration affects bone formation in hMSCs after 4 weeks static culture, based on typical timeframes in which *in vitro* ostegenesis is performed using a trilineage differentiation assay hMSCs(Glueck et al. 2015). In doing so I aim to generate a reliable comparison for assessing the additional benefit of hydrostatic preconditioning.

3.2. Materials and Methods

3.2.1. *MG63 experiments*

3.2.1.1. *Cell culture*

MG63's stably transfected with an OCN luciferase reporter (Feichtinger et al. 2011) were kindly donated by Dr Deniz Oeztuerk of the Ludwig Boltzmann Institute for Experimental and Clinical Traumatology, Austria. Cells were thawed from liquid nitrogen at room temperature, washed once in 10mls DMEM, centrifuged at 800rmp for 5 minutes and transferred to tissue culture plastic at a seeding density 6500cells/$cm^{2.}$ Cells were maintained in PM for 2 passages prior to each experiment undertaken. For monolayer experiments, cells were seeded at a density of $2x10^4$cells/well in 24 well plates. For 3D hydrogel experiments, MG63s suspended in PM were mixed with appropriate volumes of type-1 rat tail collagen, made from a stock solutions of (8-11) mg/ml (Corning). Hydrogels were seeded with 10^5cells in 300µl volumes of 2mg/ml collagen, and kept in culture for 24 hours until stably contracted. After contraction, gels were transferred to 6 well trans-well inserts (Corning).

For the duration of the experiments: 7 days for monolayer studies; and 14 days for 3D collagen hydrogels; MG63s were maintained in osteogenic media (described in **Section 2.1.9**). For end point analysis, samples were fixed in 10% neutrally buffered formalin for 15 minutes at room temperature for monolayer samples, and for 1hr at room temperature for collagen hydrogels. Samples were washed twice in PBS and stored in PBS with 1% pen-strep, 1% amphotericin B at 4^0C until subsequent analysis was performed.

3.2.1.2. *Hydrostatic regime*

For each experiment undertaken, samples received one hour per day in the hydrostatic bioreactor. Cultures were kept in osteogenic media with media changes every 2 days before stimulation. Evaporation in wells closest to the nozzle side of the bioreactor was accounted for as described in **Section 2.1.9**. The remainder of the time constructs were kept under static standard cell culture conditions in a cell culture incubator at 37^0C with 5%CO_2. The pressure regimes applied were a) 0 – 280 kPa at 1 Hz for 60 minutes and b) no pressure as a control.

3.2.1.3. *Osteocalcin activity*

The expression of OCN in MG63s was quantified by taking media samples each day before hydrostatic stimulation. A PierceTM Gaussia Luciferase Flash assay kit (Thermo Scientific, UK) was used to quantify secreted luciferase protein in the culture media. An auto injection protocol was employed on a bio synergy 2 plate reader. 50µl of flash assay solution was injected into each well containing with 50µl of sample and mixed for 2 seconds. A 10 second reaction time preceded the luminescence reading for each sample. Pressure treated samples were normalised to static controls to give a value representing a fold change in OCN activity.

3.2.1.4. *Lysate preparation*

Monolayer cultures were lysed using a luciferase cell lysis buffer (Thermo Scientific, UK). The media was removed and cells were washed once in PBS. 250µl of 1x lysis buffer was added to each well and the plate was then placed on a shaker for 5 minutes. The lysate was transferred to an Eppendorf tube and a further 250µl of fresh lysis buffer was added to the wells to gather any remaining lysate. Samples were stored at -20^{o}C until ready for use. MG63/collagen hydrogels were washed in PBS for 15 mins and digested

in 2mg/ml collagenase from clostridium histolyticum (Sigma) for 30 minutes. Samples were then spun down at 10K rpm for fifteen minutes, the supernatant was removed and the remaining pellet washed in PBS and centrifuged twice, and re-suspended in 500µl of 1x luciferase cell lysis buffer.

3.2.1.5. *DNA quantification*

Total DNA was measured using a Quant-iT PicoGreen assay (Thermo Scientific, UK). Briefly, 25ul of cell lysate was incubated in 1x PicoGreen working solution for 5 mins at room temp, covered from light. Fluorescence was measure at 480/520nm excitation/emission spectrum and normalised to fluorescence values of known standards of DNA.

3.2.1.6. *Total Protein*

Total protein in cell lysates was quantified using a Pierce^{TM} BCA protein assay kit (Thermo Scientific, UK). 25ul samples of lysate were mixed in 200ul of the kits working solution and incubated for 30 mins at 37^{o}C. Samples were allowed to cool to room temperature before measuring absorbance at 562nm on a Biosynergy 2 plate reader. Readings were normalised against known standards of BSA diluted in DH_2O and further normalised to the DNA content of the respective samples.

3.2.1.7. *Collagen detection*

Collagen production in MG63 monolayers was quantified using the collagen stain Sirius red (Direct red 80, Sigma UK). 100ul of the cell lysate was added to a 1.5ml micro centrifuge tube and 0.5ml 1% *w/v* Sirius red S in dH_20 added. The solution was incubated at room temperature for 20 minutes and centrifuged at 10,000 rpm for 15 minutes to form a pellet. The supernatant was decanted and repeat washes were performed until supernatant became a clear solution. The pellet was resuspended in 100ul 1M NaOH to

remove the bound dye. Absorbance measurements of the pellets were measured at 540nm using a biosynergy 2 plate reader and the values were normalised to DNA content of the respect samples.

3.2.1.8. *Calcium detection*

Calcium production in MG63 monolayers after 7 days was quantified using an alizarin red S (A/R) based cetylpyridinium chloride extraction method (Gregory et al. 2004). Fixed cells were stained for 30 minutes at room temperature in 1% filtered A/R. Repeated washing in PBS and centrifugation was carried out until unbound dye was not visible in the rinsing solution of PBS. 0.5mls of 10% cetylpyridinium chloride (Sigma) in DH_2O was then added to each well and incubated overnight at room temperature to extract the bound dye from the samples. The cetylpyridinium chloride de-staining solution was then removed from each well and absorbance measurements were performed at 562nm using a Biosynergy 2 plate reader. Absorbance measurements were normalised to the DNA content of the respective samples.

3.2.2. *X-ray micro tomography*

Analysis of volume and density in cell-seeded hydrogels was by X-ray micro tomography (μCT) using a Scanco μCT40 (beam energy: 55 kVp, beam intensity: 145 μA, 200 ms integration time, spatial resolution: 10 μm). Mineralisation of the hydrogels was assessed by calculating the volume fraction of material at different density thresholds. The different density thresholds are computed by averaging the linear attenuation coefficient for each voxel within a given hydrogel and normalising this value to the attenuation coefficient for water, thus obtaining the relative density in CT units. Samples were analysed at two density thresholds (50/1000, 80/1000) firstly to determine

the total size (volume) and average density of each construct following bioreactor stimulation, and then at higher threshold to calculate the percentage change in percentage volume over time in the mineralising phase.

3.2.3. *Histological staining and imaging of 3D hydrogels*

Histological analysis of hydrogel sections was achieved by embedding whole gels in paraffin wax using an automated vacuum tissue processor (Kedee). 10µm sections were cut using a microtome, after which sections were transferred to a preheated water bath (40^0C) and mounted onto polylysine coated microscope slides (Thermo Fisher). Sections were deparaffinised in 2 xylene washes for 5 minutes each and rehydrated in serial ethanol dilutions (100%, 90% 70% 50% and DH_2O) for 3 minutes each. Mineralisation was quantified using either A/R or Von Kossa (V/K) staining to confirm the presence of calcium phosphate deposits. Sections were incubated in either 1% A/R or 5% silver nitrate in dH_2O for 30 minutes at room temperature. Sections were then washed under running tap water for 2 minutes and for V/K staining, exposed to UV irradiation for 15 minutes in a Bio rad GenX UV chamber. Cell nuclei and cytoplasm were stained using Harris Haematoxylin solution and eosin for 30 secs each followed by 30 secs emersion in scots tap water (10g $MgSO_4$, 1.75g $NaHCO_3$ in 500mls PBS). Sections were mounted in DPX mounting medium and Imaged using an EVOS® FL Colour Imaging System.

3.2.4. *hMSC experiments*

3.2.4.1. *Cell culture*

Frozen vials of hMSCs were seeded into T75 flasks as detailed previously (**Section 2.5.1**). hMSCs were expanded in PM (described in **Section 2.2.1**) until passage 5, before encapsulation in collagen. Collagen hydrogels of concentration (0.5-5mg/ml) were fabricated by diluting cells suspended in PM with appropriate volumes of stock concentration (8-11) mg/ml type-1 rat tail collagen. 300µl solutions were pipetted into non-adherent round bottom 96 well plates and left to contract for 24 hrs. Collagen hydrogels (1mg/ml) were also fabricated with different cell seeding densities ($0.1x10^5$-$3x10^5$cells/hydrogel). After 24hrs, hMSC/collagen hydrogels were transferred to 6 well trans-well culture inserts. Hydrogels were maintained in osteogenic media under static culture conditions (37^oC with 5%CO_2) for 28 days, with media changes every 3-4 days. After 28 days, hydrogels were washed twice in PBS and fixed in neutrally buffered formalin for 1 hr at room temperature, followed by two 15 minute washes in PBS. Samples were stored in PBS with 1% pen-strep, 1% amphotericin B at 4^0C until subsequent analysis was performed.

3.2.4.2. *ImageJ analysis*

ImageJ was used to quantify the average number of cells per/mm^2 to assess the change in cellular distribution between the different experimental groups. 10 µm paraffin embedded sections were deparaffinised and stained with haematoxylin and eosin (described in **Section 3.2.3**). The number of cells within a given area was counted on three separate gel sections using a cell counter plugin in ImageJ, with the corresponding area calibrated to measure in mm^2. The final values were normalised to cells/mm^2,

allowing for direct comparison of cellular distribution between different gel concentrations and seeding densities.

3.2.4.3. *Immunohistochemistry*

Immunohistochemistry (IHC) stating for OCN and Connexin 43 (Cx43) was performed on hMSC/collagen hydrogels after 28days culture. Fixed hydrogels were paraffin embedded, sectioned, deparaffinised and rehydrated as described in **Section 3.2.3**. 10 μm tissue sections were then permeabalised in 0.01% triton-X 100 (Sigma) for 15 minutes, followed by 2 washes in PBS. Antigen retrieval was performed by immersing sections in 20μg/ml pre-warmed proteinase k solution (Sigma) for 15mins at 37^{o}C. Sections were then blocked in 1% BSA (Fisher Scientific) for 1 hr at room temperature before overnight incubation at 4^{o}C in primary antibody solutions: anti-human OCN mouse monoclonal (R&D systems); and anti-human Cx43 mouse monoclonal (Santa Cruz Bio); diluted to 2μg/ml in 0.1% BSA in PBS with tween (0.1%). Secondary antibody staining was performed using an ABC immune-peroxidase method (Santa Cruz bio), following the manufacturer's instructions. Secondary only antibody staining of tissue sections were used as controls.

3.2.5. *Statistical analysis*

Data was plotted and analysed in Microsoft Excel. All data point represents mean values ± standard error of the mean. Statistical significance in MG63 experiments was determined in Microsoft Excel using a two tailed students T-Test. For hMSC/collagen hydrogels, statistical analysis was performed in Origin 9.0, employing linear fitting and iterative, non-linear fitting to determine relationships between size, density and mineralisation between experimental groups.

3.3. Results

3.3.1. *2D cell culture*

3.3.1.1. *Assessment of proliferation and OCN activity*

To assess the initial mechano-response in MG63s at Day 1, cells were fixed and stained with phalloidin immediately after loading to assess changes in the f actin cytoskeleton between control and stimulated groups (**Figure 1A)**. Similar to MLO-A5s described in **Section 2.3.1**, bioreactor stimulation induced f-actin stress fibre in MG63 monolayers. For studies looking at the temporal effects of pressure in MG63s, cells were maintained in static culture for 7 days and compared with MG63s receiving daily bioreactor stimulation. In both static and pressure treated groups, cells became confluent after 3-4 days (**Figure 1D**). Cell number remained constant for the remainder of the experiment with a slight decrease in cell number by day 7. After 7 days pressure treated groups had slightly higher numbers of MG63s but this was not statistically significant. Live dead staining (**Figure 1C**) was employed after 7 days to assess cell viability. Daily treatment with pressure enhanced cell viability, indicated by an increase in dead cells (red) in statically cultured groups receiving pressure.

Osteocalcin activity (**Figure 1E**) was normalised to represent a fold increase over static controls to account for the cumulative increase of secreted protein in between media changes, which were performed every 2 days. A second static control (**Figure 1E grey dashed line)** was used to demonstrate negligible plate to plate variability in OCN activity in static controls. Osteocalcin was activated transiently by pressure, with peak activity by day 3 (P=0.15). Activity returned to comparable levels with static controls by day 5 and remained comparable with static controls for the remainder of the experiment (day 7).

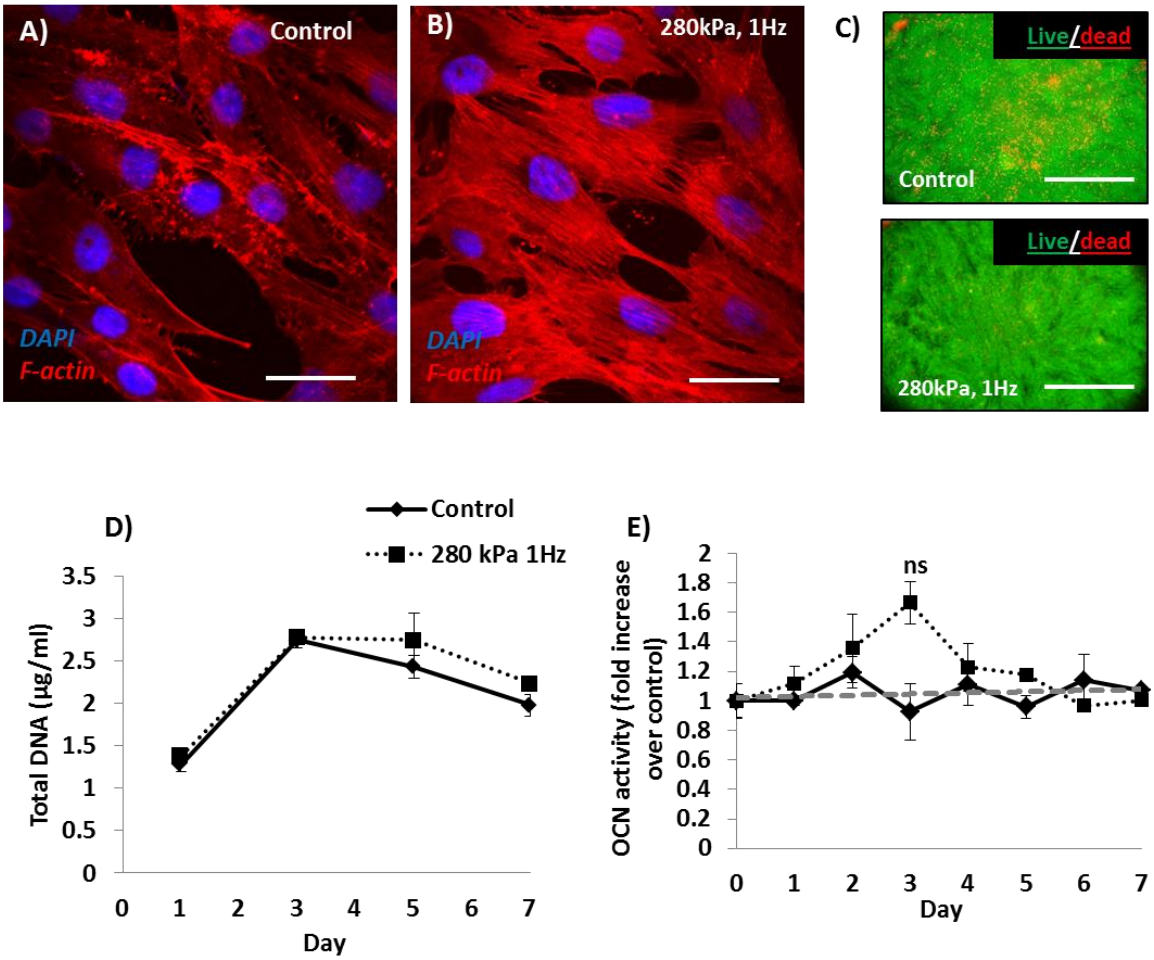

Figure 1. Evaluation of response of MG63 pre osteoblasts to hydrostatic pressure over a 7 day culture in osteogenic media. *(**A&B**) F-actin staining in cells exposed to pressure regimes after 60minutes. **C)** Live dead staining at day 7. **D)** Total DNA in MG63 monolayers over 7 days in culture, n=3. **E)** Osteocalcin activity in MG63 monolayers over 7 days in culture, n=6. Scale bars (**A&B**) = 50µm. Scale bars (**C**) = 500µm. Error bars = standard error of the mean.* ^{ns} *P>0.05*

3.3.1.2. *Assessment of extra cellular matrix production*

The rate of total protein synthesis (**Figure 2A**) over the 7 day period increased by 50% in cells treated with pressure, and was significantly higher at day 5 and day 7. Histological staining (**Figure 2B**) of the wells was performed at day seven to assess for changes in the presence of collagen and calcium between the two experimental groups. Pressure treated plates had stronger visible staining in the centre of the wells for both collagen and calcium when compared with static controls. Quantification of collagen production was performed in cell lysates to assess for changes due to pressure (**Figure 2C**). The results indicated an increase in collagen production in pressure treated cells as early as day 3, which continued to increase until day 7, however the measured increase at day 7 was not statically different from static controls ($p=0.11$). Quantification of alizarin red staining reflected the observational increases in calcium, with a significant increase in calcium production in pressure treated cells compared with static controls (**Figure 2D**).

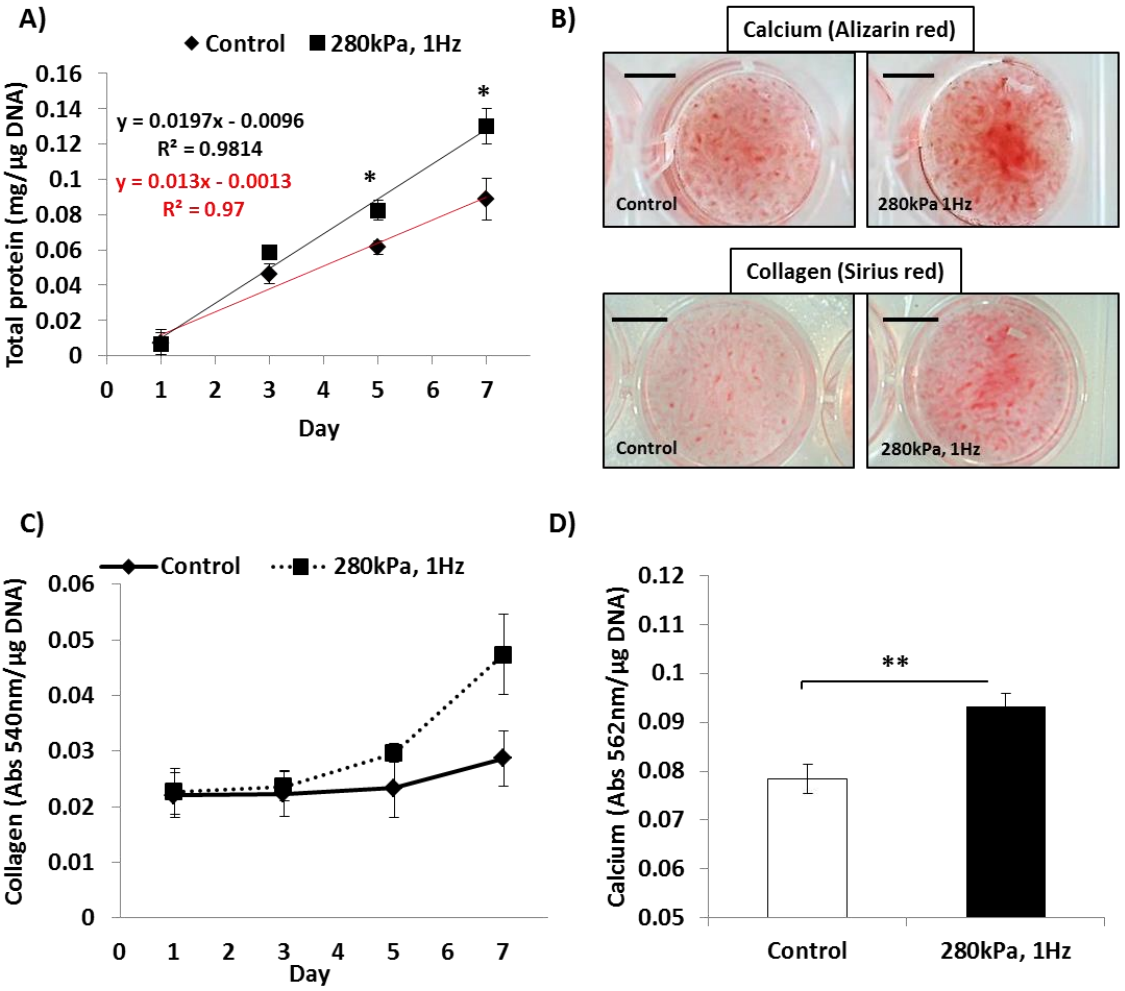

Figure 2. Collagen and calcium production in MG63s after 7 days in vitro culture. ***A)*** *Total protein in MG63 monolayers over 7 days in culture, n=3.* ***B)*** *Histological staining for calcium (top) and collagen (bottom) production in MG63 after 7 days in culture.* ***C)*** *collagen production in MG63 monolayers over 7 days in culture, n=3.* ***E)*** *Calcium production after 7 days in culture, n=3. Scale bars = 500µm. Error bars = standard error of the mean. **P<0.01 *P<0.05*

3.3.2. *3D Hydrogels*

3.3.2.1. *Assessment of proliferation and OCN activity*

Cells contracted the surrounding collagen matrix after fabrication and were stable enough to transfer to trans-well inserts after 24 hours. DNA quantification (**Figure 3A)** showed a significant reduction ($P<0.0001$) in cell number between day 1 and day 3. Since day 1 samples were lysed before hydrogels contracted, this suggested not all cells were able to attach to the surrounding collagen as the hydrogels underwent contraction. Cell numbers did not change significantly during the experiment, with a small reduction in cell number observed between day 10 and day 14. Daily bioreactor stimulation had no effect on cell proliferation.

OCN activity in stimulated hydrogels (**Figure 3B**) was significantly higher at days 3, 4, 6 and 7 of the experiment. The trend signified a transient expression profile, in which pressure increased osteocalcin activity by two fold between day 1 and day 3, and subsequently returned to control levels by day 5. A second peak in activity was observed by day 7 and day 8 with a 3 fold increase in activity compared to controls. Activity returned to comparable levels by day 10 and remained within close range of static controls for the remainder of the experiment.

Whole mount imaging of the hydrogels after 14 days (**Figure 3C**) demonstrated pressure treated hydrogels were smaller in size, implying MG63s contracted the hydrogels more when hydrostatically stimulated. Live dead staining at day 14 (**Figure 3D**) showed MG63s remained viable during the experiment, with some areas of cell death evident around the hydrogel periphery in both stimulated and statically cultured hydrogels.

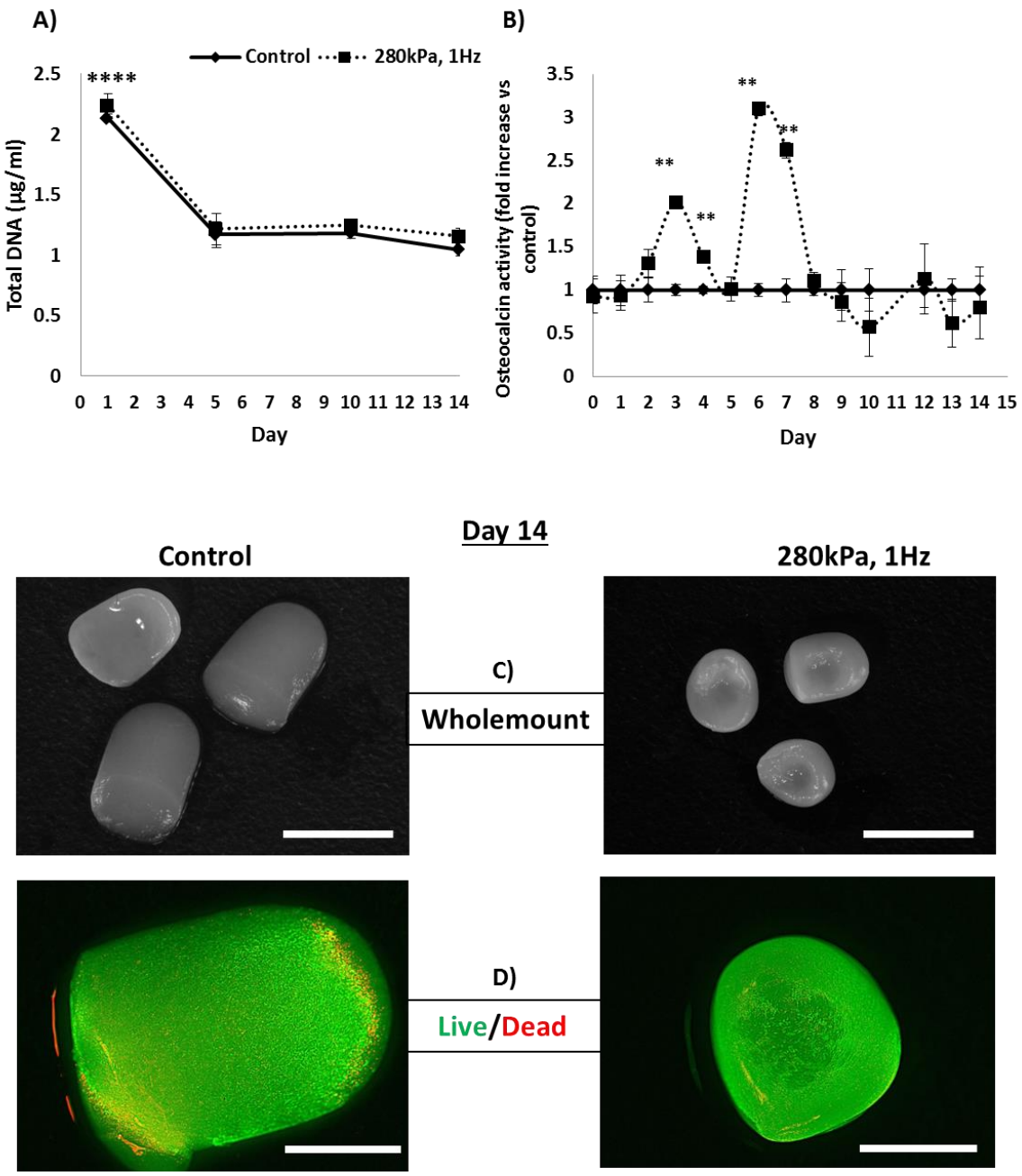

Figure 3. Evaluation of response of MG63/collagen hydrogels s to hydrostatic pressure over a 14 day culture in OM. A) *Total DNA in MG63 collagen hydrogels over 14 days in culture, n=3.* ***B)*** *Osteocalcin activity in MG63 monolayers over 14 days in culture, n=6.* ***C)*** *Brightfield images of MG63/collagen hydrogels after 14 days.* ***D)*** *Live dead staining of MG63/collagen hydrogels after 14 days. Scale bars (**C**) = 5mm. Scale bars (**D**) = 2mm. Error bars = standard error of the mean. **P<0.01. *P<0.05*

3.3.2.2. *Assessment of MG63/collagen hydrogel mineralization*

μCT was employed to assess for changes in hydrogel volume and mineralisation at different time points during the experiment (**Figure 3A-C**). Hydrogel volume (**Figure 3A**) during the initial contraction phase decreased from 300mm^3 to 17.38.±1.1mm^3. In both static and pressure treated hydrogels, the rate of change in volume over 14 days was comparable, with pressure treated hydrogels exhibiting a longer period of contraction than static controls. After 14 days, hydrogels treated with pressure were 28% smaller than static controls and 37% more mineralised (**Figure 3A**). Stimulated hydrogels began mineralising sooner than static controls becoming significantly more mineralised at day 5 and day 10 (**Figure 3B**). Hydrogels treated with pressure were significantly more dense at day 14 compared with static controls (**Figure 3C**). μCT reconstructions of the mineralised volume and revealed a noticeable larger volume of more dense tissue in stimulated hydrogels (**Figure 3D**).

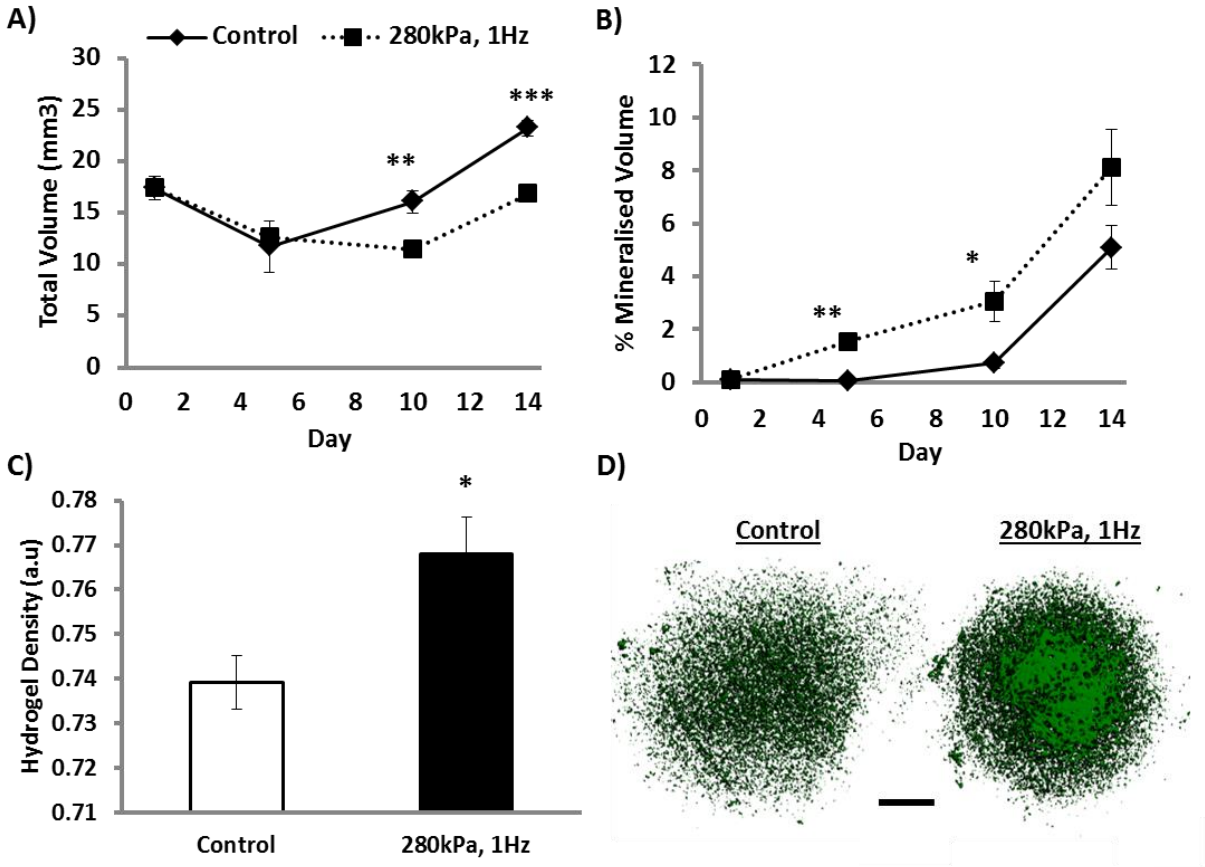

Figure 4. Assessment of hydrogel mineralisation in MG63/collagen hydrogels over 14 days in culture. A) *Change in volume of MG63/collagen hydrogels during 14 days in culture.* ***B)*** *Change in percentage mineralised volume of MG63 hydrogels over 14 days in culture.* ***C)*** *MG63/collagen hydrogel density at day 14. µCT image reconstruction of mineralised volume in MG63 collagen hydrogels at day 14. Scale bars (**D**) = 1mm. Error bars = standard error of the mean. ***P<0.001 **P<0.01 *P<0.05*

3.3.2.3. *Histological assessment of bone formation in hydrogels after 14 days in vitro culture*

Histological analysis was employed to detect calcium deposition in MG63 seeded hydrogels to assess the extent of bone mineral formation after 14 days in culture. V/K staining visualised regions of calcium deposition (black). Calcium deposition was localised to regions occupied by cells and supported the µCT data and further showing that daily bioreactor stimulation increased bone formation and hydrogel mineralisation. Stimulated hydrogels (**Figure 5D,E&F**) had more positive V/K staining than static controls and contained cells with dendritic processes extending into the ECM (**Figure 5E**). Cells in statically cultured hydrogels were also locally mineralised within the collagen ECM but did not show evidence of mineralised dendritic processes extending into the ECM (**Figure 5A, B&C**).

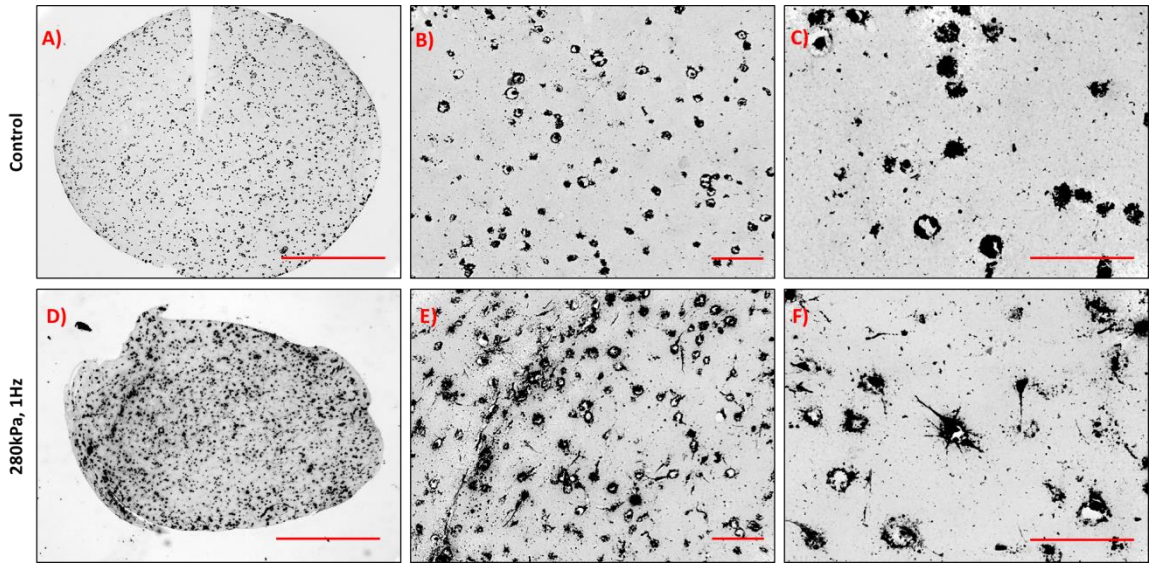

Figure 5. 10µm histology sections of MG63/collagen hydrogels at day 14. *Sections stained with Von Kossa (black) to detect bone formation. Scale bars (**A&D**) = 1mm. (**B&E**) = 200µm. (**C&F**) = 100µm*

3.3.3. *Optimising osteogenic differentiation in hMSC seeded collagen hydrogels*

The next part of this chapter aimed to optimise the osteogenic differentiation of hMSC encapsulated in collagen during a 28 day *in vitro* culture period. In doing so I wanted to define an 'internal gold standard' with which I could compare the effect of hydrostatic preconditioning during this time. By comparing endpoint analysis through µCT and histology, I can determine if µCT readouts accurately reflect the maturity of the comprising tissue.

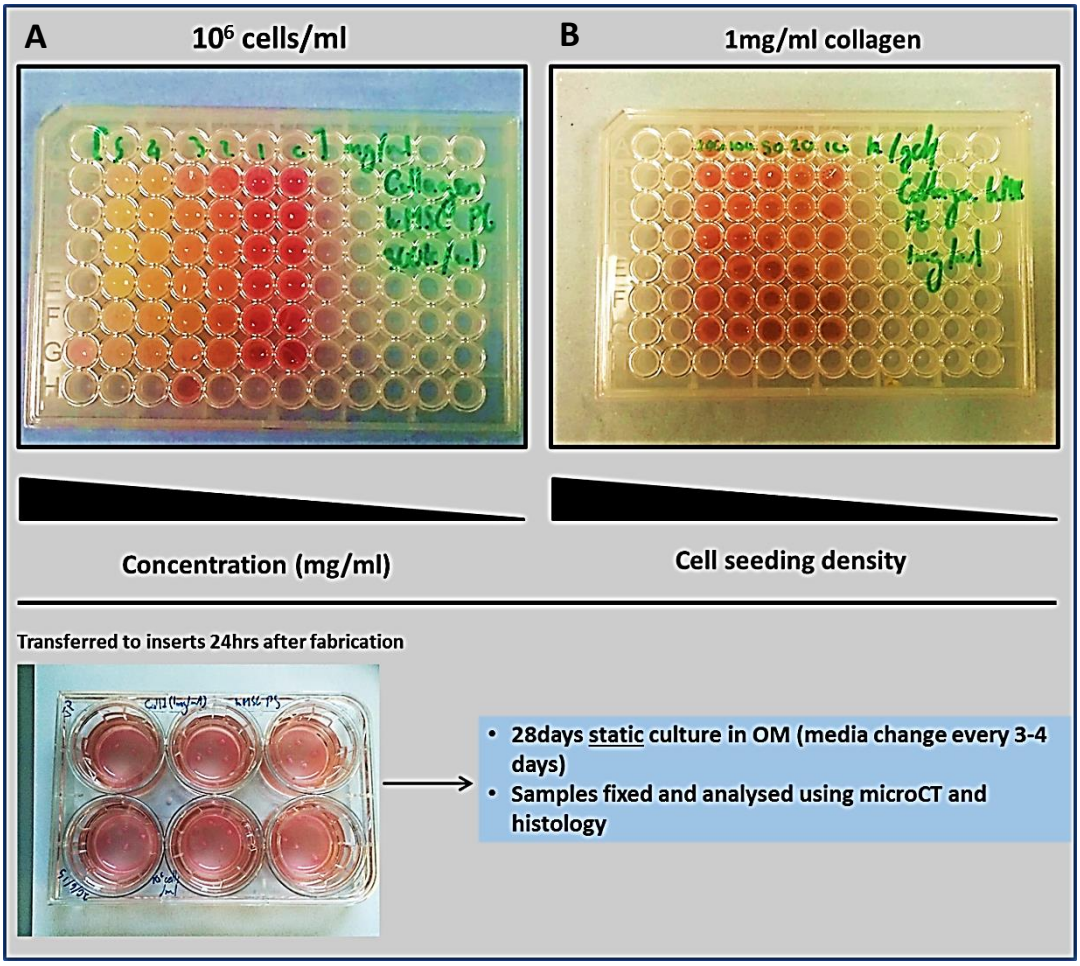

Figure 6. Assessing the effect of collagen concentration and cell seeding density on osteogenic preconditioning of hMSC collagen hydrogels. *10^6cells/ml ($3x10^5$/hydrogel) were seeded with different collagen concentration (**A**, 0.5-5mg/ml). 1mg/ml collagen hydrogels were seeded with different numbers of cells (**B**, $1x10^4$- $3x10^5$cells/hydrogel). Hydrogels were cultured for 4 weeks under static conditions in osteogenic media before fixation and endpoint analysis.*

3.3.3.1. *Hydrogel contraction and viability*

Contraction of the hydrogels was observed as soon as 1 hour after fabrication. Live dead staining 3 hrs after fabrication showed that cell viability is not adversely affected during fabrication or self-assembly of the hydrogels (**Figure 7A&B**). Lower concentration gels with a high cell seeding density (**Figure 7B)** contracted more rapidly than high concentration or low seeding density (**Figure 7A)**. All gels were stable in size after 24 hours and with a small further reduction in volume observed after 28days. Higher concentration hydrogels initially assumed a hemisphere like morphology due to shape of the round bottom well in which the gels were set. After the 28day culture period, the hydrogels had adopted a relatively homogeneous spherical shape. After 28 days in culture, live dead staining was repeated in 0.5mg/ml & 5mg/ml hydrogels to assess if the hydrogels size and/or culture regime negatively affected the viability of encapsulated cells (**Figure 7 A&B inset)**. Both low and high collagen concentrations demonstrated little adverse effect on cell viability after 28 days in culture.

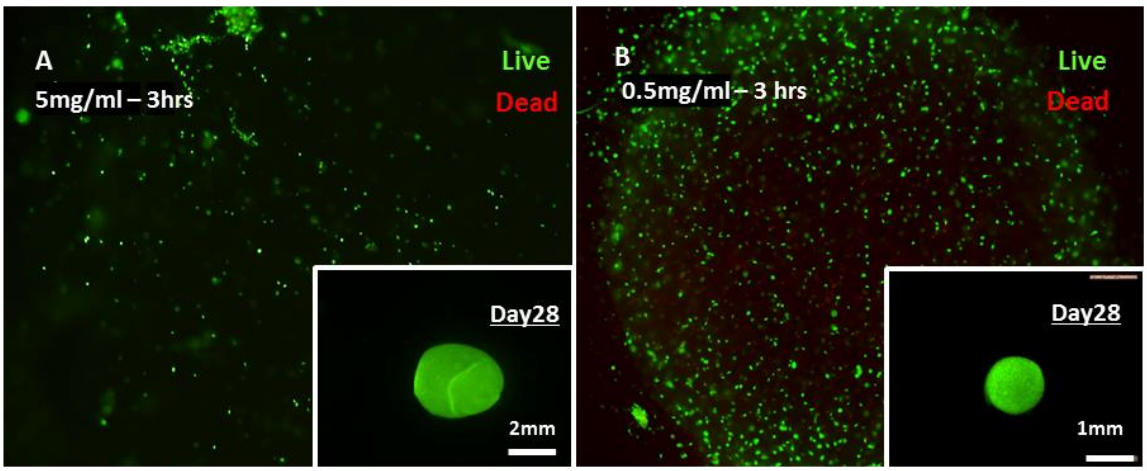

Figure 7: hMSC remained viable during gel fabrication used and remained viable over 28days in culture.

3.3.3.2. *Change in volume after 28 days culture*

The volume of the hydrogels after 28days decreased linearly when the collagen concentration was lowered (**Figure 8A&C, R^2=0.99)**. The linear decrease in volume equated to 19.21±0.23mm^3/mg of collagen, (**R^2=0.99)**. Changes in volume due to the cell seeding density (**Figure 8B&D)** could be described by a cubic fitting function (**R^2=0.52)**, however this correlation was relatively low compared to changes in collagen concentration. Despite this, the relationship allowed the calculation of critical point values for cell seeding density, defined by the roots of the derivative of the cubic function (**Figure 8D, x_1=0.69x10^5, x_2=2.12x10^5)**. These critical points represented threshold cell seeding densities that defined both: contractile equilibrium, past which higher cell numbers do not further decrease contracted volume (**x_1)**; and the threshold cell number (**x_2)** needed to overcome contractile equilibrium. Quantitation and comparison of changes in hydrogel volume demonstrated a much higher dependence of contractility on initial collagen concentration as opposed to cell seeding density. In addition, whilst both parameters provide a seemingly good rate of predictability, the correlation between collagen concentration and volume was much stronger than the correlation between cell seeding density and volume.

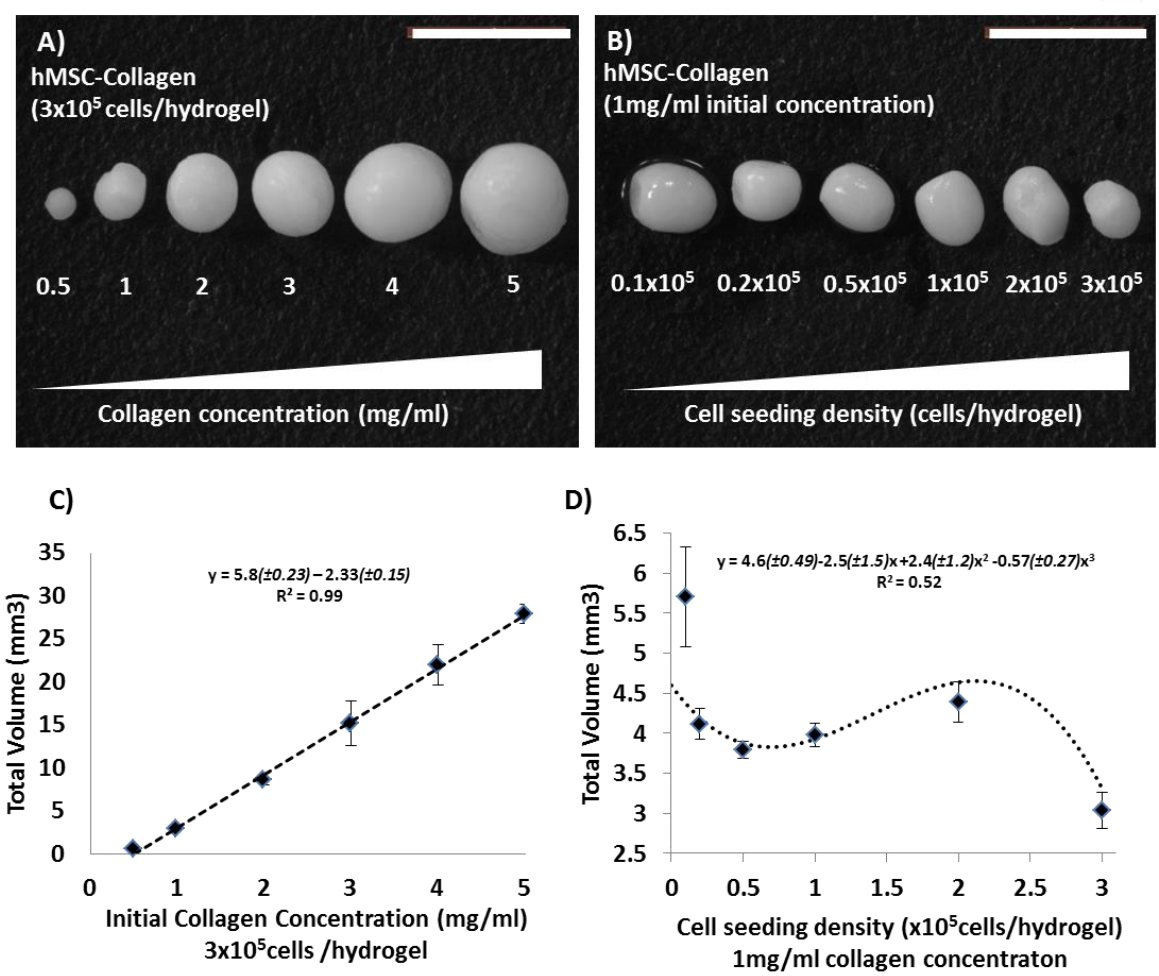

Figure 8. Volume of hMSC collagen hydrogels after 28 days in vitro culture depends on initial collagen concentration and cell seeding density. *Whole mount imaging hMSC/collagen hydrogels after 28 days in culture in osteogenic media when changing collagen concentration (**A**) and cell seeding density (**B**). Change in volume of hMSC/collagen hydrogels at 28days in hMSC/collagen hydrogels when changing collagen concentration (**C**) and cell seeding density (**D**), n=6. Scale bars = 5mm. Error bars = standard error of the mean.*

3.3.3.3. *Change in hydrogel mineralisation after 28 days in culture*

Image reconstruction of the hydrogels (**Figure 9 A&B)** showed the change in mineralised volume due to concentration (**Figure 9A, i-vi)**, and cell seeding density (**Figure 9B, i-vi)**. 1 and 0.5mg/ml concentration gels (**Figure 9A, v&vi)** showed more heavily mineralised regions (indicated by solid grey regions) compared to higher concentration gels. Mineralising regions were also more noticeable in hydrogels with higher seeding densities, with mineralised nodules visible on peripheral regions of hydrogels seeded with $2x10^5$ and $3x10^5$ MSCs (**Figure 9B(v&vi))**.

The rate of decrease in the percentage mineralisation of the hydrogels (**Figure 9C)** with respect to an increase in concentration was could be related by an inverse power relationship. Hydrogel mineralisation was inversely proportional to (collagen concentration) $^{2/3}$ **(R^2=0.94)**. If we consider as mentioned previously that the regulation of volume is linearly dependant on concentration, then the above relationship infers a significant dependence of hydrogel mineralisation on the cell to volume ratio of the constructs.

Increasing the initial cell seeding density whilst maintaining the same collagen concentration (**Figure 9D)** increased hydrogel mineralisation. The observed change in mineralisation due to cell seeding density followed the same relationship as the changes in volume, with a stronger correlation present using a cubic fitted function (**R^2=0.98).** It should be mentioned that whilst care must be taken when attempting to correlate data sets with higher order polynomial functions as a predictive tool. The use of cubic correlations to describe changes in volume and mineralisation in this experiment supports the inference that the µCT readouts appear to be a reflection of the population density of hMSCs in the contracted hydrogels.

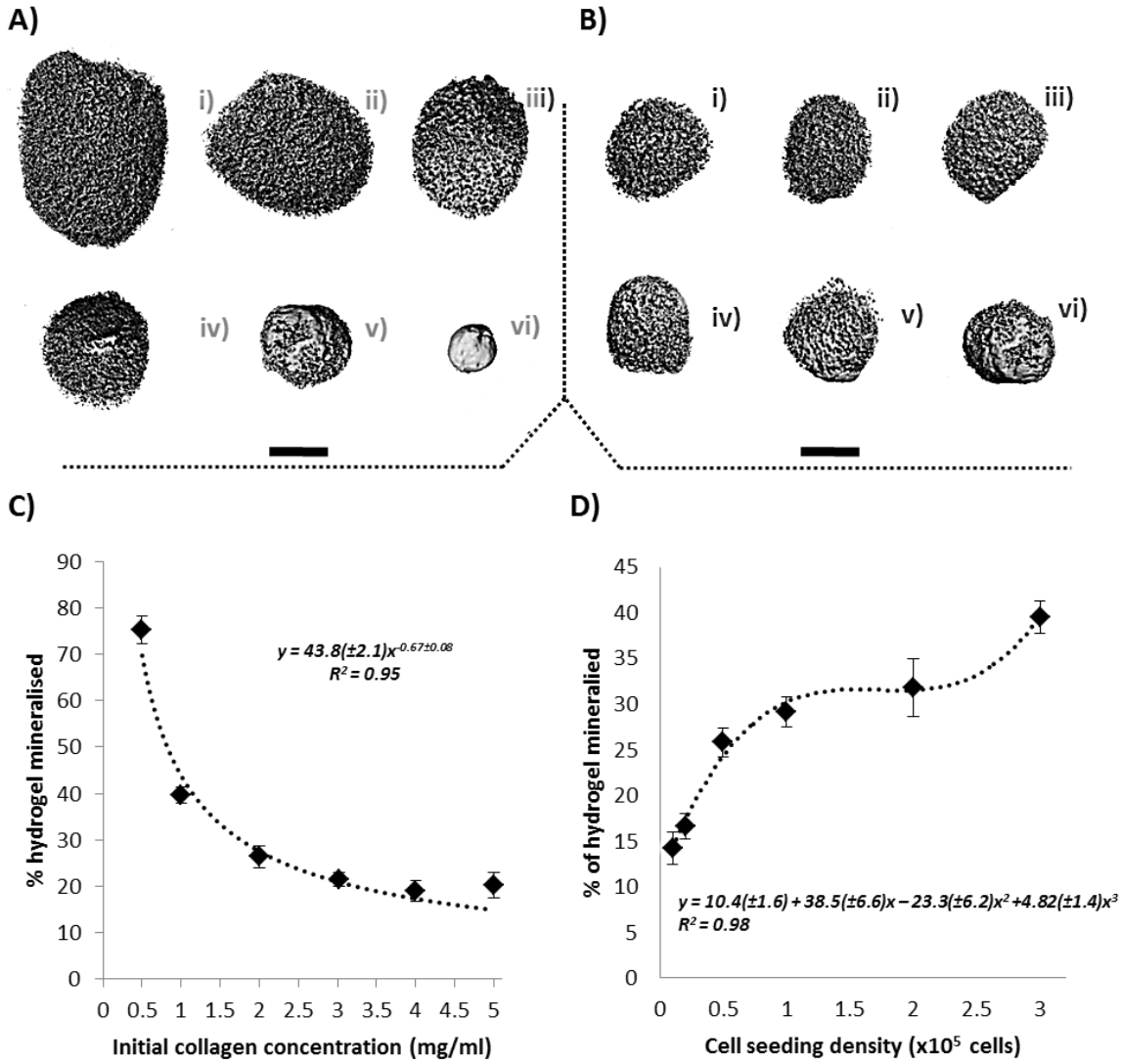

Figure 9. Hydrogel mineralisation is regulated by collagen concentration and cell seeding density. *µCT image reconstruction of mineralised volume in hMSC/collagen hydrogels at day 28 showing changes in concentration from high (**A,** 5mg/ml, i) to low (**A,** 0.5mg/ml, vi) and when changing the cell seeding density from low (**B**, $0.1x10^5$, i) to high (**B,** $3x10^5$, vi). **C)** Quantification of mineralisation with repsectthe collagen concentration. **D)** Quantification of mineralisation with repsectthe collagen concentration with respect to cell seeding density. n=6. Scale bars= 1mm. Error bars = standard error of the mean.*

3.3.3.4. *Change in hydrogel density*

Hydrogel density after 28days (**Figure 10**) was dependant on both collagen concentration (**Figure 10A**) and cell number (**Figure 10B**). The rate of change in density due to concentration was related to the rate of change in mineralisation (**Figure 10C**). The rate of change in density due to cell number was also related to the rate of change in mineralisation ((**Figure 10D**). Consequently, plotting density vs hydrogel mineralisation demonstrated that hydrogel density was linearly proportional to hydrogel mineralisation (**Figure 10C&D R^2= 0.94, 0.99**). µCT imaging was employed to visualise the local density through cross sections of the hydrogels (**Figure10 E&F**). The colour heat map depicts soft tissue in blue progressing through to green and finally red, representing densely mineralised tissue. The difference in size made it difficult to make comparisons between high and low concentration hydrogels. To overcome this, µCT reconstructions were scaled accordingly (see inset scale bars). 0.5mg/ml collagen gels showed the presence of densely mineralised tissue throughout the hydrogel whereas higher concentration gels were considerable less dense. Reconstructions of hydrogel with different cell numbers showed to a lesser extent an increase in dense material in hydrogels with high cell seeding densities ($3x10^5$cells) vs hydrogels with low cell seeding densities ($0.1x10^5$cells).

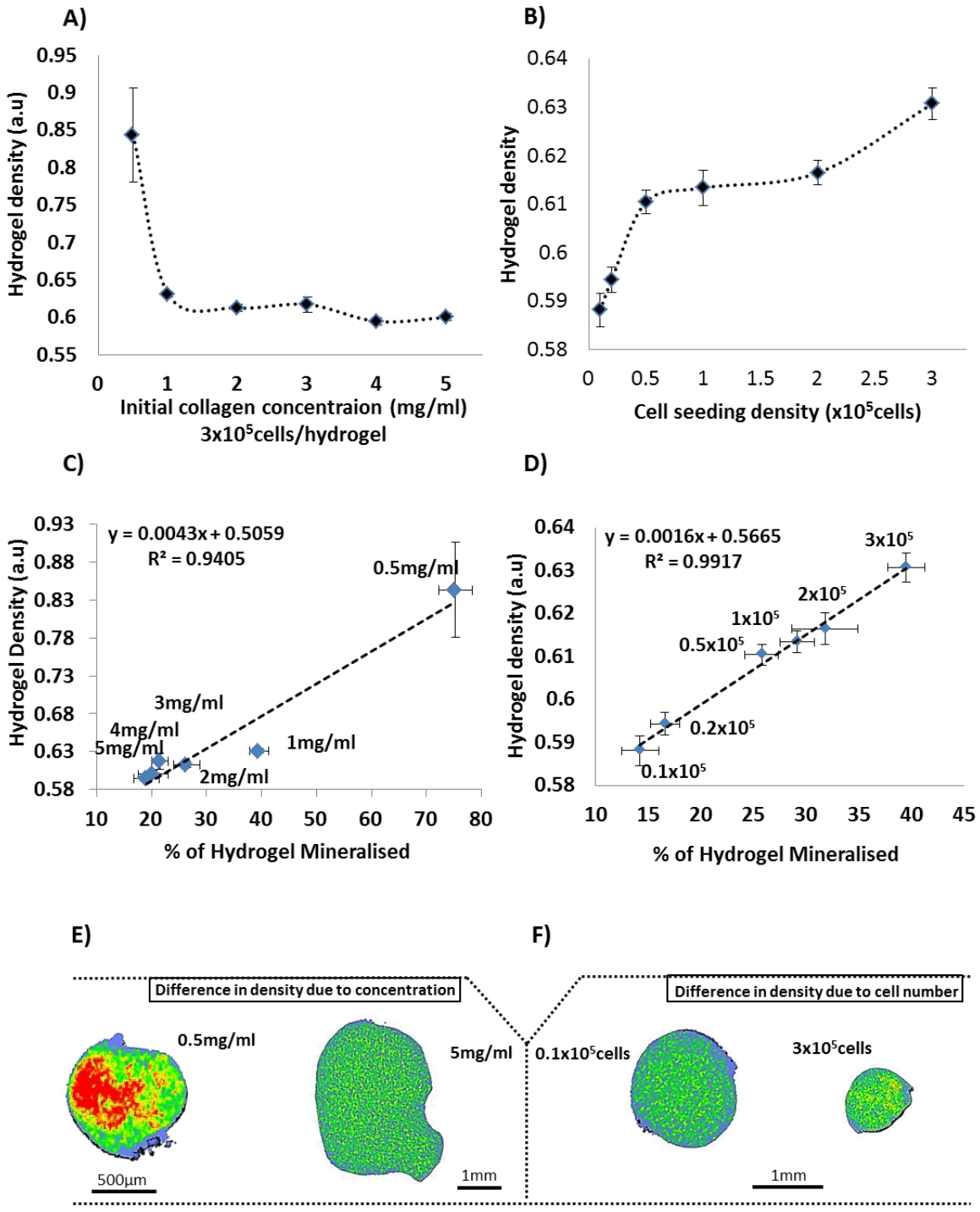

Figure 10: Collagen concentration and cell seeding density regulate hydrogel density. *hMSC/collagen hydrogel density at day 28 plotted against changes in collagen concentration A)* ***and*** *against changes in cell seeding density* ***B),*** *n=6.* ***C&D)*** *corresponding density plotted against percentage mineralisation of hydrogels at day 28, n=6.* ***E)*** *µCT image reconstruction of density distribution (red – blue = high density – low density) in hMSC/collagen hydrogels with different collagen concentrations (****E****) and different cell seeding densities. error bars represent standard error of the mean.*

3.3.3.5. *Histological evaluation of mineralisation in hydrogels with different collagen concentrations*

Haematoxylin and eosin staining (**Figure 11A**) was used to visualise encapsulated hMSCs in hydrogels with different collagen concentrations. In higher concentration gels where the volume was also higher, hMSCs were more sparsely distributed than lower concentration gels. Alizarin red (A/R) staining (**Figure 11B**) was used to visualise calcium deposition and Von Koss (V/K) (**Figure 11C**) staining to relate V/K localisation to A/R localisation. Used together they serve as a convenient and accurate method of assessing matrix mineralisation. Positive V/K and A/R staining was observed in point regions that represented encapsulated cells, implying that hMSCs became encapsulated in mineralised matrix after 28days. As the collagen concentration was lowered and cells became more closely packed. There appeared a point shift in matrix mineralisation between 2mg/ml and 1mg/ml hydrogels. Above concentrations of 1 mg/ml, mineralised hMSCs appeared homogeneously distributed within the hydrogel. In 1 mg/ml hydrogels, mineralised hMSCs were heterogeneously clustered, and in 0.5mg/ml hydrogels hMSCs appeared heavily throughout. ImageJ analysis was used to quantify the number of cells/mm^2 for each group (**Figure 11D, R^2=0.98**). The number of cells/mm^2 decreased as concentration was increased. The average distribution of cells per unit area was linearly proportional to the change in mineralisation (**Figure 11E R^2=0.97)**.

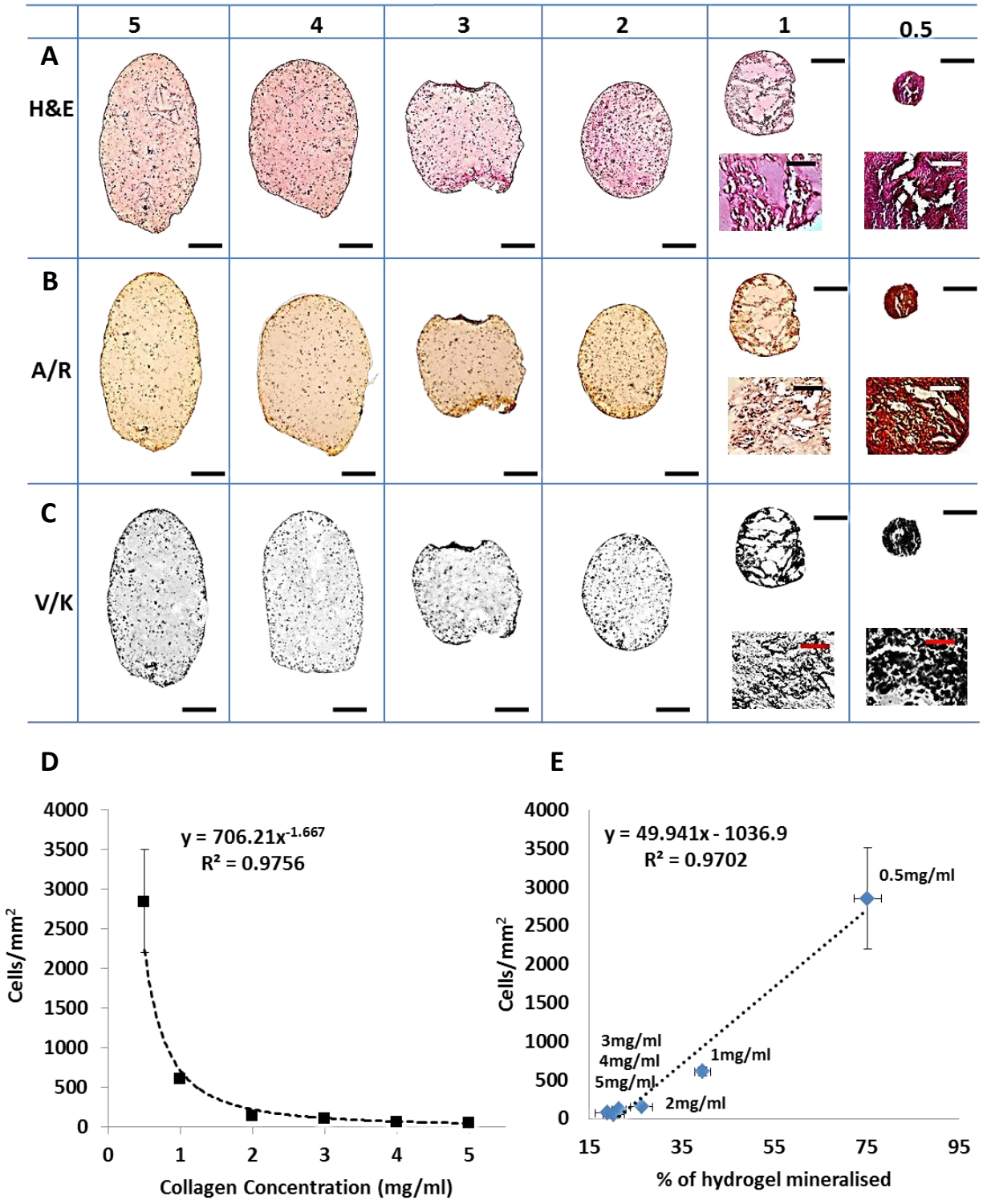

Figure 11. : Histological evaluation of matrix mineralisation and cellular distribution of hMSC in collagen hydrogels with different collagen concentraitons over 28 days in vitro culture. *10µm Parrafin embedded sections were stained with haomatoxylin and eosin* ***(A),*** *Alizarin red* ***(B)*** *and von kossa* ***(C). D)*** *Average cell distribution plotted against collagen concentraton, n=3.* ***E)*** *Average cell distribution plotted against percetage of hydrogel mineralised, n=3. Scale bars =500µm and 20µm (inset). Error bars represent standard error of the mean.*

3.3.3.6. *Histological evaluating of hydrogel mineralisation due to changes in cell seeding density*

Haematoxylin and eosin staining (**Figure 12A**) visualised encapsulated hMSCs in hydrogels with different cell seeding densities. Increasing the cell seeding density produced hydrogels after 28 days with a higher cell overall cell density. A/R (**Figure 12B**) and V/K staining (**Figure 12C**) showed point like matrix mineralisation representing mineralised cells similar to that observed previously when changing collagen concentration. The increase in cell seeding density was proportional to an increase in cells/mm^2 (**Figure 12D, R^2=0.93**) in histological sections, and was also proportional to hydrogel mineralisation (**Figure 12E, R^2=0.78**).

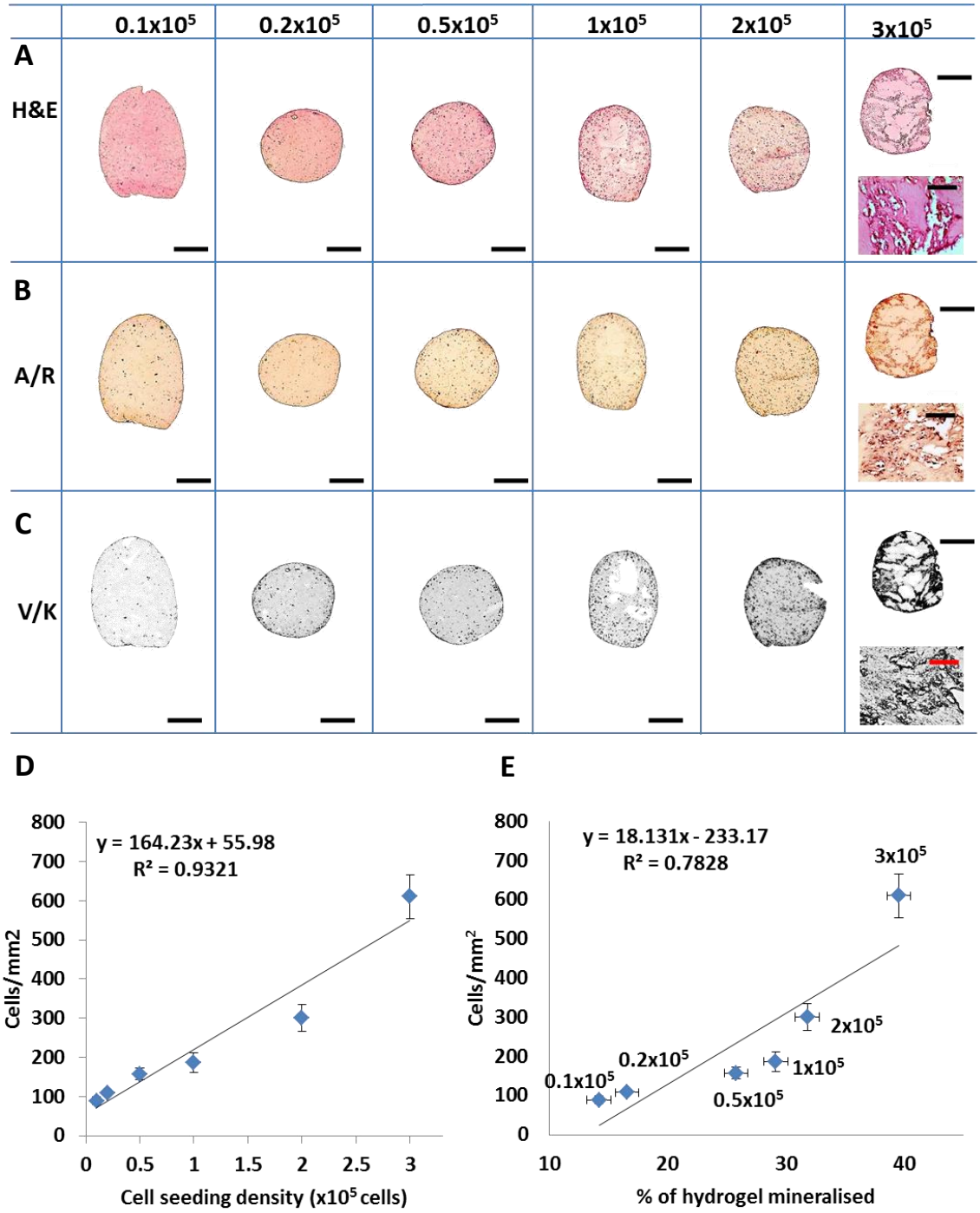

Figure 12. Histological evaluation of matrix mineralisation and cellular distribution of hMSC in collagen hydrogels with different cell seeding densities over 28 days in vitro culture. *10µm Parrafin embedded sections were stained with haomatoxylin and eosin* ***(A),*** *Alizarin red* ***(B)*** *and von kossa* ***(C). D)*** *Average cell distribution plotted against cell seeding density, n=3.* ***E)*** *Average cell distribution plotted against percetage of hydrogel mineralised, n=3. Scale bars =500µm and 20µm (inset). Error bars represent standard error of the mean.*

3.3.3.7. *Immunohistochemistry*

IHC was performed on 10μm tissue sections in hydrogels with a high number of cells/mm^2 vs hydrogels with a low number of cells/mm^2 (**Figure 13**). 1mg/ml collagen gels seeded with 3x10^5 (**Figure 13A**) and 0.1x10^5 (**Figure 13B**) hMSCs were chosen to allow comparison of two different cell densities, with the same collagen concentration. Higher concentration hydrogels (2-5mg/ml) were considered analogous to a lower cell seeding density (0.1-2x10^{5}cells) due to the similar values obtained for the hydrogel mineralisation, density and number of cells/mm^2. IHC was used to detect the presence of osteocalcin (**Figure 13Ai&Bi**) as a quality measure for matrix mineralisation, and connexin 43(**Figure 13Aii&Bii**) to determine the extent of cellular interconnectivity. Secondary only antibody staining was used as a control (**Figure 13Aiii&Biii**). Osteocalcin was abundant in 1mg/ml hydrogels seeded with 3x10^5 cells, and was specific to regions which stained positive for A/R and V/K, suggesting mineralised areas of the hydrogels gels became enriched with bone matrix proteins secreted by encapsulated cells. The presence of connexin 43 was also confined to heavily mineralised regions, suggesting that closely packed differentiating hMSC form an interconnected cellular network of connexin channels. By contrast, hydrogels with sparsely distributed cells had positive staining limited to single cells or small clusters of cells which had become mineralised. Secondary only staining showed little to no positive staining, indicating that IHC labelling was specific to the targeted antibodies.

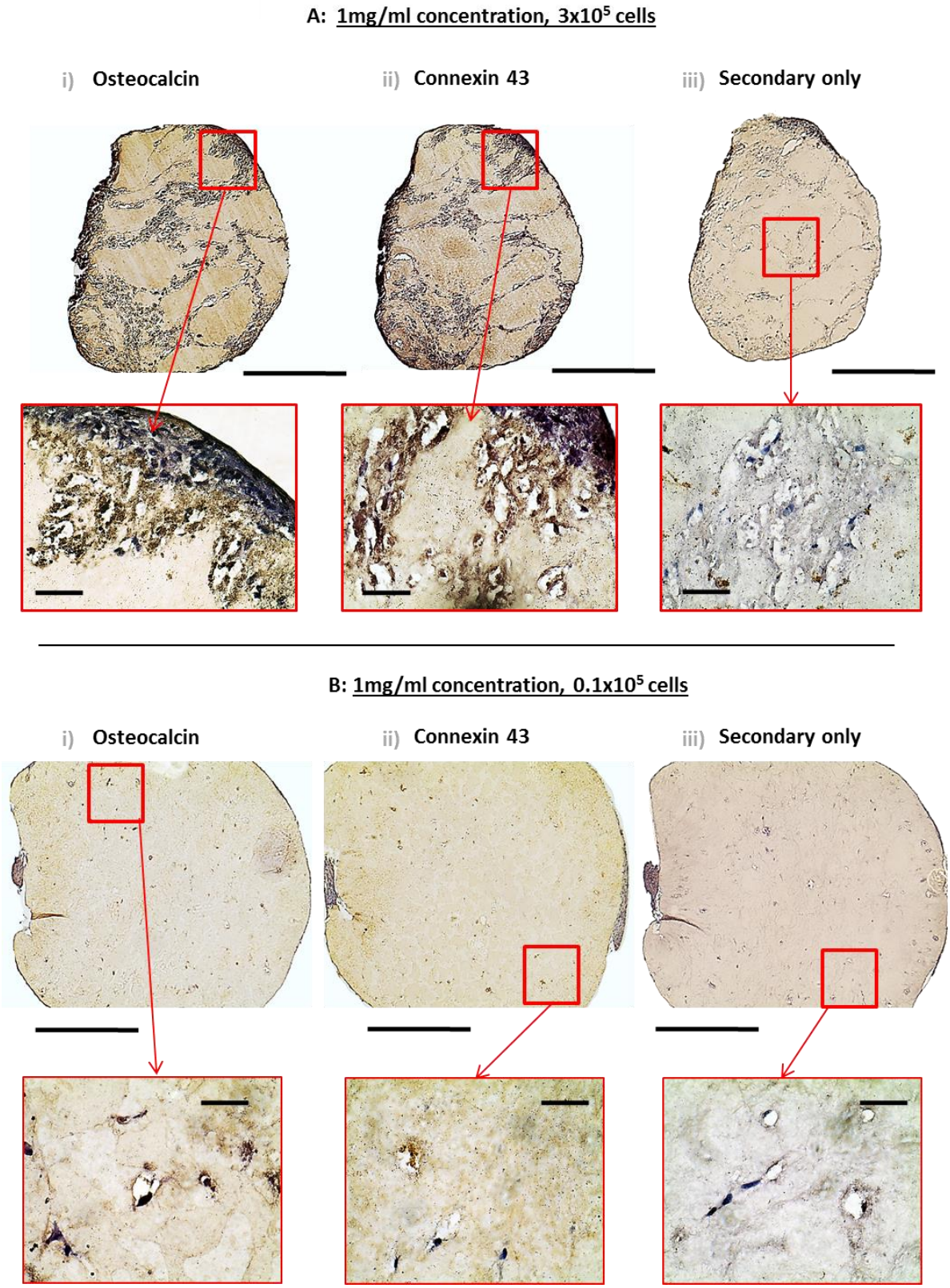

Figure 13. ***IHC staining of tissue sections from hMSC/collagen hydrogels at day 28. A)*** *Osteocalcin* ***(i)****, connexin43* ***(ii)*** *and secondary only controls* ***(iii)*** *of 1mgl/ml collagen hydrogels seeded with 3x10^5 cells.* ***B)*** *Osteocalcin* ***(i)****, connexin43* ***(ii)*** *and secondary only controls* ***(iii)*** *of 1mgl/ml collagen hydrogels seeded with 0.1x10^5 cells. Scale bars =500µm and 20µm (highlighted areas)*

3.4. Discussion

3.4.1. *Chapter overview*

The results described in this chapter evaluated the performance of the bioreactor as a preconditioning tool for 3D cell seeded constructs. I initially investigated the effect of a 1hr daily loading regime (280kPa, 1Hz CHP) on two separate growth environments of osteocalcin reporter MG63s. The first part studied the effect of pressure on cells in monolayer; the second studied the effect of pressure in a 3D environment in collagen hydrogels. Daily application of pressure increased osteocalcin expression and accelerated mineralisation in both systems. 3D collagen hydrogels intrinsically provided a more optimal growth environment for bone formation than monolayers despite the fact both environments exhibiting similar responses to pressure. After 14 days in culture, daily treatment using the bioreactor produced hydrogels that were 28% smaller and 37% more mineralised. μCT, coupled with histology demonstrated increased bone formation in hydrostatically stimulated hydrogels. This confirmed my hypothesis that the loading regime defined in chapter 1 is sufficient to accelerate bone formation in 3D cell seeded constructs.

The second part of this chapter looked to optimise culture conditions to generate tissue engineered bone constructs over a 28 day *in vitro* culture period using hMSC seeded collagen hydrogels. The study described the rate of change of in vitro osteogenic differentiation of hMSC/collagen hydrogels due to changes in collagen concentration and cell seeding density during hydrogel fabrication. Osteogenic maturation of the hydrogels was dependant on both the collagen concentration and cell seeding density, with low collagen concentration – high cell density hydrogels yielding the highest rate of bone tissue formation. Increasing the collagen concentration increased hydrogel volume whilst

increasing the seeding density decreased hydrogel volume. Increases in hydrogel volume saw corresponding decreases in hydrogel mineralisation and density. Both tissue density and mineralised volume were linearly proportional to the number of cells/mm^2 within the hydrogels, which strongly suggested the distribution of hMSC in the hydrogels was an important regulator of hydrogel mineralisation. Quantitative assessment of hydrogel mineralisation and density using μCT served as a good indicator of tissue development, and was supported by IHC, whereby the presence of highly mineralised matrix after 28 days correlated with the detection of OCN and Cx43 expression. This study enabled me to define a reliable set of measurable outputs for preconditioning hMSC/collagen hydrogels. The data can now serve as a reference point for comparing the effect of preconditioning regimes using the hydrostatic bioreactor.

3.4.2. *2D culture of MG63*

MG63s are widely used as a model to study osteoblast function; however the effect of hydrostatic pressure on MG63 response has been understudied in recent years. Existing evidence does detail some interesting observations that support the results described in **Section 3.3.1**. Haskin and Athanasiou reported a heat shock like response with cytoskeletal disruption preceding changes in gene expression following 20 minutes hydrostatic pressure at 4MPa(Haskin & Athanasiou 1993). Heat shock like responses in MG63s undergoing hydrostatic loading were similarly observed by Kaarniranta et al. using a static pressure regime of 30MPa for 12 hours(Kaarniranta et al. 2000). The Based on the current body of literature, this heat shock response has only been observed when using static compression, and has also been shown to increase production of Interleukin 8(Kubo et al. 1998), a pro-inflammatory cytokine associated with destructive bone metabolism(Neidel et al. 1995). By contrast, cytoskeletal remodelling at the point of loading in this study demonstrated increased and not decreased bone formation due to

application of hydrostatic pressure. There is evidence showing applying cyclic vs static pressure in MG63s, alters the expression of matrix metalloproteinases (MMP's) and collagen type 1 expression (Tasevski & Sorbetti 2005). Coupled with the fact that the previously documented literature use pressures that are orders of magnitude higher than used in this study, it is likely that the bone forming response in MG63s are be sensitive to both cycling frequency and the magnitude of pressure.

The results in **Section 3.4.2** show that applying cyclic pressure in MG63 monolayers initially induces cytoskeletal remodelling, which is followed by a transient increase in osteocalcin expression, resulting in increased production of collagen type 1 and calcium. These findings support the hypothesis that was not confirmed in the previous chapter in MLO-A5s, that an increase in responsiveness to hydrostatic pressure might be represented by the ability of cells to undergo actin reorganisation at the point of loading.

The proliferation of MG63s was unaffected by bioreactor stimulation, though the cell viability seemed slightly improved when compared with static controls using a live dead assay. It is well documented that osteoblasts and osteoprogenitors proliferate in response to fluid flow and strain(Scott et al. 2008) (Lee et al. 2010). Evidence describing alterations in cell proliferation due to pressure is conflicting, with some studies suggesting increased proliferation (Zhao et al. 2015) and others decreased proliferation (Chenyu & Rei 2012). One study looking at the effect of hydrostatic pressures on proliferation of cells within bone tumours found changes in proliferation associated with pressure magnitude and cell type(DiResta et al. 2005), suggesting that proliferative responses using the Keele/TGT bioreactor might change when using different cell types. Overall, the results in **Section 3.3.2** were able to confirm my hypothesis that the loading

regime defined in the previous chapter is sufficient to accelerate bone formation when compared with statically cultured cells.

3.4.3. *Translation from 2D monolayers to 3D hydrogels*

In 2D and 3D growth environments, pressure upregulated osteocalcin activity, which was followed by increased matrix mineralisation when compared with static controls. The presence of a 3D collagenous matrix naturally provides a more suitable cell niche for sustained *in vitro* tissue development. Whilst I did not directly compare OCN activity between 2D and 3D environments, others have reported enhanced OCN activity in MG63s in 3D collagen hydrogels compared with 2D monolayers (Parreno et al. 2008). The same study also showed that treatment cytoD inhibited gel contraction and osteogenic gene expression. Parreno et al. also demonstrated that the contraction kinetics of MG63s in collagen hydrogels mediates bone formation through regulation of cytoskeletal integrity(Parreno & Hart 2009). It is reasonable to postulate that theobserved increase in contraction in pressure treated hydrogels was mediated by changes in cytoskeletal dynamics of encapsulated MG63s during loading. This hypothesis seems tempting when we consider the changes in cytoskeletal architecture in stimulated monolayers, however further investigation of cytoskeletal remodelling in 3D hydrogels would be needed to confirm this hypothesis.

An interesting finding was the transient activation of OCN in hydrogels over the 14 day culture period. Transient activity of osteocalcin could indicate that a daily stimulation regime may not be necessary to accelerate bone formation *in vitro*. The transient activation of OCN has been shown in MCT3T OBs, using a similar OCN luciferase reporter, reporting a peak expression in OCN at day 10 (Quarles et al. 1997). Quarles et al. also showed an increase in OCN in Ros12/2.8 OBs after 14 days exposure

to vitamin D, demonstrating how these reporter cell lines are useful for assessing the osteogenic activity to different treatments. It is likely that bioreactor stimulation in the MG63 reporters in **Section 3.3.2** accelerated the transition of committed osteoprogenitors to mature OBs, a process which has been shown to involve a late stage transient peak in OCN expression (Liu et al. 2003).

A potentially useful application of the transient activation profile would be to test if shorter periods of time in the bioreactor (1-3 days/week) yield the same level of bone formation as the 7days/week regime used in **Section 3.3.2**. Existing evidence has shown that short term mechanical loading can induce osteogenic differentiation to levels comparable to dexamethasone treatment (Sittichokechaiwut et al. 2010). Moreover, periodic stimulation followed by static resting phases of 3 or more days has also demonstrated accelerated matrix mineralisation in OB seeded scaffolds over 20 days in culture (Sittichockechaiwut et al. 2009). Based on this, implementing the bioreactor using periodic stimulation regimes may yield important information on how to optimise efficient preconditioning profiles that minimise labour costs and human intervention.

3.4.4. *Preconditioned hMSC collagen hydrogels*

3.4.4.1. *Hydrogel contraction*

The contraction kinetics of collagen have been well characterised over the years, with the general consensus agreeing on three main events that mediate the contraction process: The lag phase, followed by linear rapid contraction, preceding a slow contraction phase(Nishiyama & Tominaga 1988). Nishiyama and colleagues directly related the time spent in these phases to the quiescent nature of the cellular actin network, with the initial lag phase dictated by the elongation of actin with the surrounding ECM. Chen et al studied the changes in the time spent within each of these phases during fibroblast

mediated collagen contraction. They found they could reduce the time spent in the earlier two phases by lowering the concentration, or increasing the cell density (Chen et al. 2007). The results in **Section 3.3.3** might reflect changes in the time spent in the lag phase at different concentrations and cell seeding densities. It is reasonable to suggest that in lower concentration, cell dense collagen hydrogels, less time is spent in the initial contraction phases, allowing longer exposure of contractile quiescent cells to osteogenic supplements in the media.

3.4.4.2. *Cellular distribution*

Collectively, the results in **Section 3.3.3** strongly suggest that the overriding factor influencing the formation of *in vitro* bone tissue in the hMSC/collagen hydrogel system was the average distance between each cell within a given area. This can be seen if we plot distribution vs mineralisation for both seeding and concentration on the same graph (**Figure 14)**. This is consistent with previous findings demonstrating the effect of seeding density on enhancing tissue maturation (Holy et al. 2000)(Lode et al. 2008). Control of the cellular distribution was mediated by adjusting either the concentration, or the cell seeding density. Previous reports have shown that changes in collagen concentration influence the contraction kinetics more than equivalent changes in cell seeding density (Nirmalanandhan et al. 2006), explaining why stronger correlations were present in groups with different collagen concentration as opposed to different cell seeding densities. It would be interesting in future to measure the volume change in higher concentration gels seeded with different cell seeding densities to compare any correlation with that observed in **Section 3.3.3.2**. Since the change in volume of hydrogels was more heavily influenced by collagen concentration, it is likely that at higher collagen concentrations, higher cell seeding densities would be required to establish a similar cubic correlation as reported **Section 3.3.3.2.** Future characterisation of such processes

will be important from a manufacturing point of view, since increasing the size and cell density of the hydrogels could foreseeable alter the tissue density and hydraulic permeability (altering nutrient diffusion), which in collagen has been shown to have a significant effect on osteogenic differentiation of encapsulated MSC (Serpooshan et al. 2010).

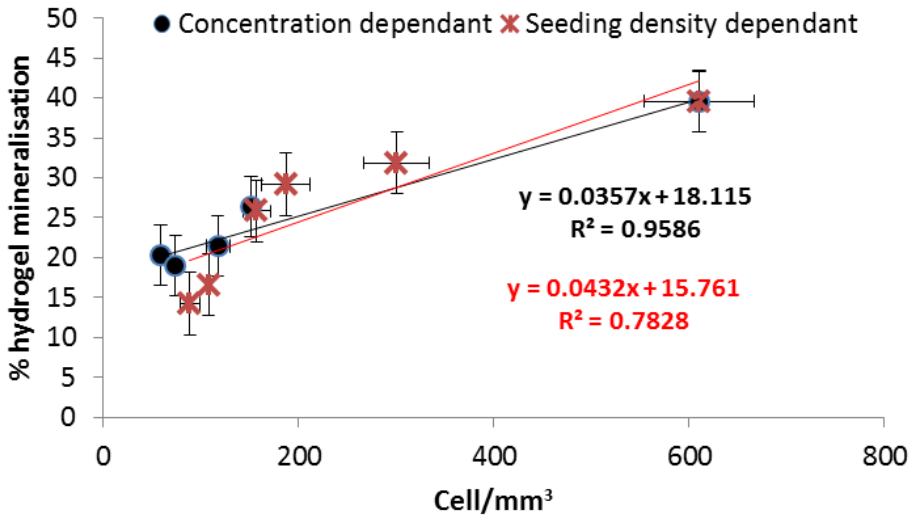

Figure 14: comparison of cell distribution vs hydrogel mineralisation for variable hydrogel concentration (black), and variable cell seeding density (red). *Error bars represent standard error of the mean, y-axis n=6, x-axis n=3.*

3.4.4.3. *Non-invasive 'scoring' of tissue maturation*

What separates the findings in **Section 3.3.3** from other similar systems in the literature studying collagen contraction is the predictive power of tissue maturation, whereby the trends in volume, density and mineralisation correlated with histological evaluation of tissue composition. Using µCT to identify hydrogels with different tissue densities, I were able to infer that in dense tissue regions, cells produced highly interconnected, osteocalcin rich matrix. By comparing histological evaluation of calcium deposition via A/R and V/K staining with ICC, I determined that only highly interconnected cells became embedded in osteocalcin rich, mineralised bone matrix. Further to this positive staining of OCN and Cx43 indicates that the hMSC/collagen

system is capable of generating tissue architecture and composition similar to that of bone tissue *in vivo*. As discussed in **Section 1.4.4.** OCN is a non-collagenous protein found in bone that served a number of functions including regulation of bone metabolism (Long 2011) and orientation of crystal lattice structure in hydroxyapatite (Hoang et al. 2003). Cx43 is a one of a family of connexin proteins which form gap junctions between neighbouring cells, and is the most common type of connexin found in bone tissue(Plotkin & Bellido 2013). Cx43 is believed to play an important role in mechanotransduction, whereby mechanical loading has been shown to open connexin hemichannels(Batra et al. 2012), which in turn allows the transport of signalling molecules between cells (Siller-Jackson et al. 2008). Deletion of Cx43 in mice has been shown to promote osteocyte apoptosis and bone resorption(Bivi et al. 2012), thus connexins are considered important in maintaining regular function in bone tissue. The abundant formation of such channels in lower concentration/high seeding density hydrogels suggests that cell distribution during *in vitro* bone formation is important for the formation of these proteins. It could indicate that such systems might respond more positively to hydrostatic pressure in future experiments due to biochemical responses to hydrostatic pressure being more effectively distributed between cells through Cx43 hemichannels.

3.4.4.4. *Scaling up tissue engineered bone grafts*

The correlation between collagen concentration and hydrogel mineralisation via a relatively simple inverse power relationship implies an interesting and useful application of the results of this study. By considering the relative change in cell distribution as concentration increases, it is possible to define parameters for hydrogel fabrication that could allow the size of the constructs to be scaled up without changing the resultant tissue properties.

As an example, if I use the results obtained for the cellular distribution within a 10µm section of tissue in **Section 3.3.3.5**, I can estimate the total cell population in the different concentration collagen hydrogels after 28 days. In doing so we find that the total cell number in the hydrogels is roughly the same irrespective of the initial concentration used. This first further supports my previous statement that the µCT readouts were a reflection of the population density of hMSCs. Second, I can now in theory use this information to estimate the total cells/hydrogel required to generate constructs of different sizes, but with the same resultant tissue properties. This could allow constructs to be tailored to account for different size defects, whilst maintaining a level of predictable tissue formation. The scale up model presented in **Figure 15** uses the cell distribution measured in the lowest concentration hydrogels gels (0.5mg/ml) seeded with the highest number of cells ($3x10^5$cells), since this yielded the highest measured level of mineralisation. The estimated cell number required at larger volumes would in theory generate constructs that reflect the density and mineralisation of 0.5mg/ml hydrogels seeded with $3x10^5$ cells.

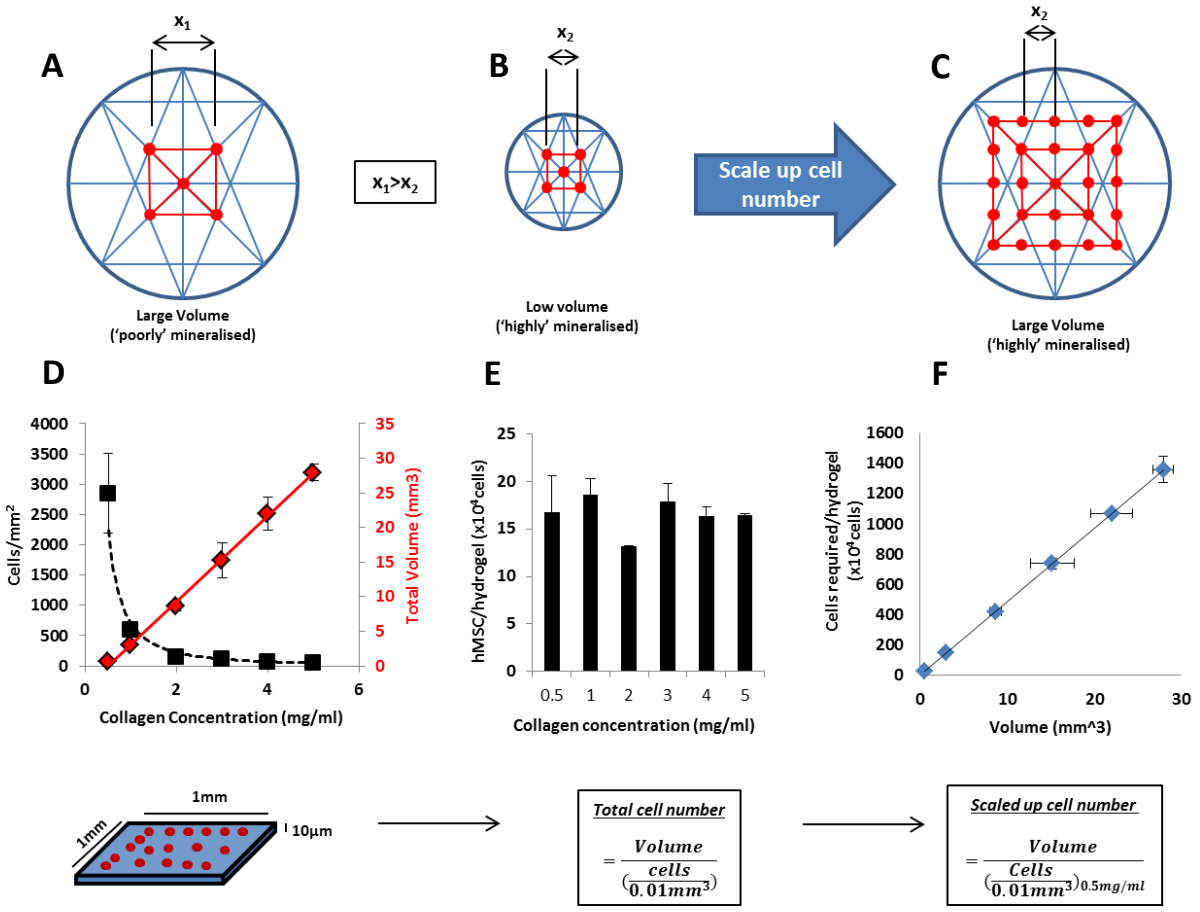

Figure 15: Proposed scale-up of preconditioned hMSC collagen bone grafts with comparable levels of hydrogel mineralisation. *My results inferred that hydrogel density and mineralisation was a reflection of the population density of encapsulated cells (**A&B**), Red dots represent cells). I propose that we can scale up the size of the constructs without affecting the endpoint density and mineralisation of the hydrogels (**C**), by estimating the number of cells required in larger volumes to achieve a population density that reflects smaller, more mineralised hydrogels. Using data obtained via image analysis to count the number of cells/mm^2 in a 10µm section of tissue (**D**, black data set), we can take the hydrogel volume (**D**, red data set) at different concentrations to show that the total cell number after 28days culture is roughly the same irrespective of initial collagen concentration (**E**). Based on this, we can then estimate the total cell numbers required to generate constructs of increasing size with the same level of mineralisation (**F**). Estimated cell numbers (**F**) are based on the cellular distribution measured in 0.5mg/ml hydrogels seeded with 3x10^5 cells. Error bars in E&F represent propagation of error from µCT and image analysis.*

Another potential approach for scaling up the size of the constructs could be to consider the change in the concentration of the hydrogels after contraction. We can this time roughly estimate the final collagen concentrations in the hydrogels after 28days using the equation $V_iC_i=V_fC_f$ with an initial seeding volume (300µl. This gives us a hypothetical final concentration in mg/ml for each starting concentration ranging between 0.5-5mg/ml (**Figure 16)**. Interestingly the change in estimated final concentration followed the same trend as for the hydrogel mineralisation and hydrogel density. By consequence, this implies that the mineralisation and density may also be linearly proportional to the collagen concentration in the hydrogel system. Plastically compressed collagen, a process which experimentally induces rapid expulsion of fluid has been developed extensively in recent years as a potential tissue equivalent. The theory is that that high collagen concentrations more accurateley mimic the physiological niche of *in vivo* tissues (Brown 2013). It has also recently been shown to enhance osteoconductivity of collagen in Saos-2 osteoblast cells (Liu et al. 2016). Based on this my results might also reflect a case where the lower collagen concentrationon before cell mediated contraction represents a more osteoconductive niche due to a higher final collagen density after 28 days in culture

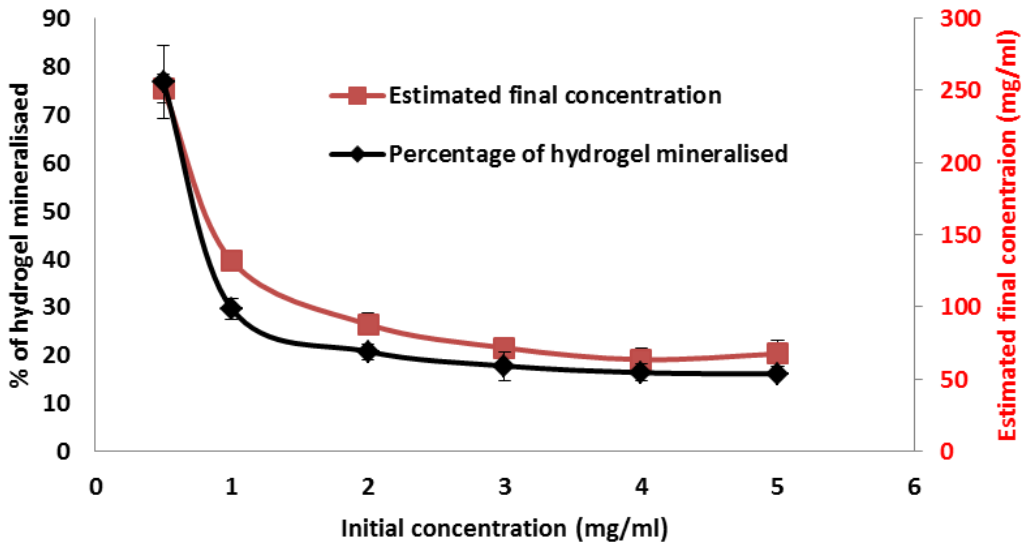

Figure 16: Comparison of estimated collagen concentration and hydrogel mineralisation in hMSC collagen hydrogels after 28days culture in osteogenic media

Of course it must be stated that the inherent nature of biological variability, coupled with the complications that might arise from of using such high cell numbers in small volumes highlights the need for further work to validate this scale up method. However, it nonetheless presents a potential useful application of μCT for process control and scale up of tissue engineered constructs that has not been previously reported.

3.4.5. *Targets for clinical translation*

A clinical relevant RM therapy will require tissue engineering protocols that incorporate minimal human intervention and reduction of time and labour costs. The use of hydrostatically preconditioned scaffolds for BTE has the potential to provide a scalable manufacturing platform that could address these requirements, as well as providing minimally invasive procedures to treat large bone defects. The success of these concepts will be underpinned by the performance and quality control assessment of newly developed methods for *in vitro* osteogenesis. Generally, scaffolds design concepts should consider; scaffold porosity and interconnectivity; surface properties that are optimized for cell attachment, migration, proliferation and differentiation; and a controllable rate of

tissue growth and maturation (Park et al. 2007). Basic parameters such as cell seeding density and hydrogel protein concentration provide the researcher with a good starting point to deliver the quality control outputs that will be required for developing new manufacturing protocols. Further to this, characterisation of quality control parameters in biomaterials (such as collagen) that are already approved by regulatory authorities for use in humans, will inevitable reduce the time taken for these procedures to reach the clinic (Woodruff et al. 2012).

3.5. Conclusion

In conclusion, this chapter demonstrated that the conditioning regime defined in previous chapter was suitable for preconditioning cell seeded scaffolds. I used MG63 OBs to show as a reference cell line to increase bone tissue formation in collagen hydrogels using daily treatment with hydrostatic pressure. I then developed and optimised an *in vitro* protocol for generating clinically applicable bone grafts using hMSC collagen hydrogels. In doing so I found that μCT analysis presented a method of evaluating bone tissue development that is non-destructive, and accurately reflected the tissue composition of native bone. By using μCT analysis in combination with histology, I was also able to propose a method for scaling up the size of tissue engineered bone grafts without compromising the maturation of the comprising tissue. The next chapter will aim to develop an *ex vivo* fracture repair model using embryonic chick femurs to test the hypothesis that hMSC seeded collagen hydrogels in combination with bioreactor stimulation can enhance the repair of a femoral defect.

Chapter 4

Developing an ex vivo fracture repair model for preclinical testing

4.1. Introduction

4.1.1. Modelling fracture repair

The previous two experimental chapters showed that the hydrostatic bioreactor induces a variety of physiological changes in cells from the point of loading to changes in tissue maturation after a prolonged culture period in both 2D and 3D growth environments. The previous chapter also describes how the cell seeding density and collagen concentration in static cultured hMSC/collagen hydrogels dictates the density and mineralisation of the developing tissue over a 4 week preconditioning period. By defining a predictable rate of bone formation in preconditioned hydrogels I can now test the effect hydrostatic preconditioning in the hydrogels to determine if the bioreactor has an additive effect on bone tissue formation. As discussed in chapter 1, the use of animal models to study the fracture repair presents a preclinical testbed to validate the effectiveness of potential treatments, as well as making sure these treatments ultimately are safe for use in humans. The concept of preconditioning tissue engineered bone constructs prior to implantation has been explored by a number of groups in the last 10 years. Interestingly, it has been frequently reported that an *in vitro* pre-culture period may not in fact be beneficial to the outcome of healing after implantation. Byers at el. showed that a 21 day preconditioned bone marrow stromal cells seeded in PCL implants showed a low rate of bone formation, comparable to that of empty defects, after implantation into rat cranial defects (Byers et al. 2006). However in the same study, this effect was rescued, yielding an improved outcome of healing by inducing over expression of Runx2 during the pre-culture period, demonstrating that by providing the appropriate cues during the pre-culture period, the outcome of healing using preconditioned implants can in some instances be improved. Lyons et al. have also suggested that extended preconditioning of MSC seeded implants may actually inhibit bone formation when compared with cell free

implants (Lyons et al. 2010), concluding that peripheral mineralisation of the preconditioned implants inhibits macrophage led remodelling after implantation. By contrast to the studies described above, MSC seeded silk implants preconditioned for 5 weeks in spinner flasks prior to implantation were shown an increase in bone formation compared with undifferentiated MSCs and acellular implants(Meinel et al. 2005). Based on existing evidence, whilst the benefit of static *in vitro* pre-culture in cell seeded constructs prior to implantation is not well defined, by actively encouraging the maturation of the implant using exogenous cues, the outcome of healing after implantation could potential be enhanced.

4.1.2. Organotypic chick femur cultures

By exploring Muschlers and colleague's considerations for addressing the challenges facing translational research in BTE (discussed in **Section 1.7**), the use of isolated embryonic chick femurs was highlighted as an appropriate tissue source to model fracture repair. Recently there has been a resurgence of interest in the study of ex vivo embryonic chick organ cultures due to their relative low cost, ease of expansion and isolation, and limited ethical concerns (Kanczler et al. 2012)(Roberts et al. 2012)(Smith et al. 2013). A small body of literature has been documented over that last 25 years investigating *ex vivo* chick organ cultures and fracture repair (Takahashi et al. 1991, Lidor et al. 1987, Grant et al. 1987), however these studies aimed principally to determine the underlying mechanisms of fracture repair and not methods in which it can be enhanced. The development of reproducible, low cost and ethically sound fracture repair models has the potential to provide a pre-clinical test bed for a variety of different orthopaedic procedures. As mentioned in **Section 1.7.2**, a defect model in isolated chick femurs has been explored by Smith and colleagues (Smith et al. 2014a) (Smith et al. 2014b). This two part study used an ECM/ alginate hydrogels loaded with PLGA micro

particles releasing different growth factors to enhance repair of the defect. Whilst the study demonstrated some success in encouraging new bone formation in the defect site, the integration of the implant with the native femurs appeared to be hindered by mineralised capping of the femurs at the implants/femur interface (**Figure 1**).

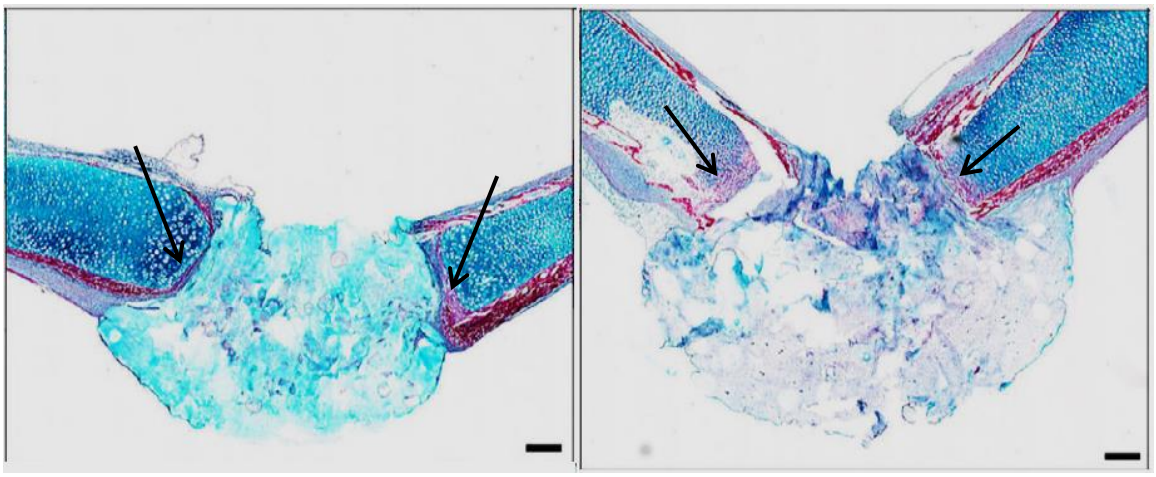

Figure 1. Histological sections of organotypic chick femur defect model developed by Smith et al. (2014) *10 µm sections stained for cartilage (blue) and new bone (red), showing mineralised capping of the femurs at the femur/implant interface (black arrows). Scale bars = 200µm Figure adapted from (Smith et al. 2014b). Reprinted with permission of ELSVIER publishing group, [licence number: 3811420008926].*

Delayed healing in a human femoral fracture that has not received treatment soon after injury is referred to as a neglected non-union (Tall et al. 2014). Non unions are thought to arise from inadequate fixation and/or immobilisation of the fracture site following trauma. Many complications arise from this type of fracture such as; hypertrophic callus formation, where a vascularised callus is formed but union is not achieved, leaving an absence of mechanical stability (Said et al. 2013); atrophic non unions, in which bone healing capacity is depleted, forming a sclerotic and usually avascular environment between the long bone ends (Reed et al. 2003); or the formation of a pseudo arthritic joint, in which capping of the medullary cavities at each end of the fracture, results in the formation of synovial fluid within a cartilaginous pseudo capsule bridging the capped femur ends(Johnston & Birch 2008).

To overcome problems that might occur from inadequate fixation in my organotypic model, we can look to current orthopaedic practises that employ the use of intramedullary nails (IMNs). IMNs are common place in orthopaedic surgery and involve insertion of a metal rod through the medullary cavity of long bones. IMNs provide support and contact guidance to heal unstable fractures(Brumback et al. 1988). IMNs are also used in distraction osteogenesis, a procedure employed to gradually separate bone segments to allow growth of new bone in the defect site(Richards et al. 1998).

4.1.3. Design concept

By applying the concepts from current orthopaedic practises employing IMNs, the issue of femur capping reported by Smith could be resolved, but also IMNs could provide structural stability in the fracture repair model. Since the previous chapter defined metrics in which I can control the size of the implants, I can also choose the appropriate metrics (cell number and collagen concentration) to compliment the size of the fracture site in the chick femurs.

A key element to the success of the model will be the appropriate material used for the IMN. The IMN must be small enough to fit through the medullary cavity of isolated chick femurs, whilst strong enough to support the construct during culture. The IMN must also be biocompatible to prevent cell death due to interaction with the material, and be suitable for sustaining the developing osteogenic phenotype without introducing artefacts due to, for example material degradation. Borosilicate glass is commonly used to make microscope slides, glassware and microinjection needles. It is being increasingly used as a scaffold in BTE due its excellent biocompatibility, controllable degradation rate and its ability to be doped with different tissue promoting growth factors (Rahaman et al. 2011). The typical diameter of isolated chick femurs after

extraction at 11days is around 0.5-1mm thick; suggesting the diameter of the IMN should be in the range of 0.1-0.5mm thick. It is possible to construct rods of such thickness by anchoring glass capillary tubes either side of a heated coil element which is normally used to fabricate microinjection needles. This could allow the manufacture of IMNs suitable for fixation in isolated chick femurs.

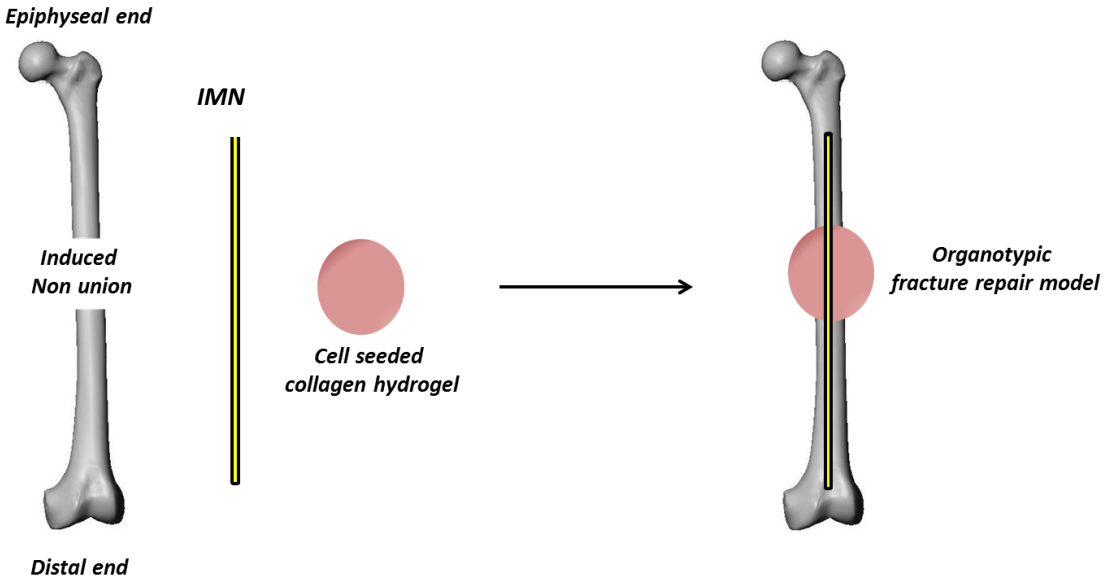

Figure 2: Design concept for organotypic fracture repair model using isolated embryonic chick femurs. The isolated femurs are sectioned down the mid-section of the diaphysial shaft and separated to model a non-union fracture. The intramedullary rod is inserted through the marrow space, with the cell seeded implant filling the defect. The purpose of the rod is to prevent femur capping, as well as provide structural support to the finished construct during *in vitro* culture.

4.1.4. Assessment of hydrostatic preconditioned implants in an organotypic non-union fracture repair model

To determine if the bioreactor is effective in preconditioning implants to enhancefracture repair, we must consider the appropriate experimental design that can test this hypothesis. Since the bioreactor has already been shown to enhance bone growth in isolated femurs (Henstock et al. 2013), it seems rational to test the fracture model first under the same dynamic loading regime. By using undifferentiated hMSC/collagen implants in a dynamic environment, I can evaluate how pressure influences the maturation of the construct. This could represent a treatment in which stem cell seeded implants receive no preconditioning, but are subject to mechanical stimuli that would be naturally present in the fracture site due to movement. Then, by comparing preconditioned implants in static femurs, I can distinguish if hydrostatic precondiitoning of collagen hydrogels prior to implantation is sufficient to encourage fracture repair. If this hypothesis is validated, it provides promising preclinical data for use of the bioreactor system to treat bone defects in humans.

Objectives

i) **To construct and establish an organotypic femur defect model using isolated embryonic chick femurs.** To determine the feasibility constructing a fracture repair model in chick femurs using a borosilicate glass needle as an intramedullary nail. I aim to generate structurally stable constructs that can be easily maintained in culture by using glass capillary tubes as IMNs to provide contact guidance for cells, and prevent to femur capping.

ii) **To evaluate the effect of hydrostatic loading on fracture repair in the model using undifferentiated hMSC collagen hydrogels.** To determine if the model accurately represents an *in vitro* fracture repair process. By implementing the design metrics for hMSC/collagen hydrogels from the previous chapter I aim to use the collagen gel system as an implant to encourage new bone formation in the defect using hydrostatic loading.

iii) **To determine if hydrostatic preconditioning of hMSC/collagen hydrogels prior to implantation is effective in enhancing fracture repair in statically cultured femur defects**. To assess the effectiveness of the bioreactor for hydrostatic preconditioning of hMSC/collagen implants. By comparing the effect of dynamic loading in undifferentiated hMSC/collagen hydrogels vs preconditioned implants, I aim to test the hypothesis that the bioreactor provides a clinical translation platform for enhancing bone formation

.

4.2. Materials and Methods

4.2.1. Embryonic chick femur isolation

Intact femurs were removed from freshly killed Dekalb white chick foetuses com (Henry Stewart & Co) after 11 days incubation in an Ova-Easy ADVANCE incubator from Brinsea (UK). Residual muscle and connective tissue was removed and femurs were washed in DMEM before being transferred to porous poly carbonate membrane inserts (Corning) in 6-well cell culture plates (**Figure 3**).

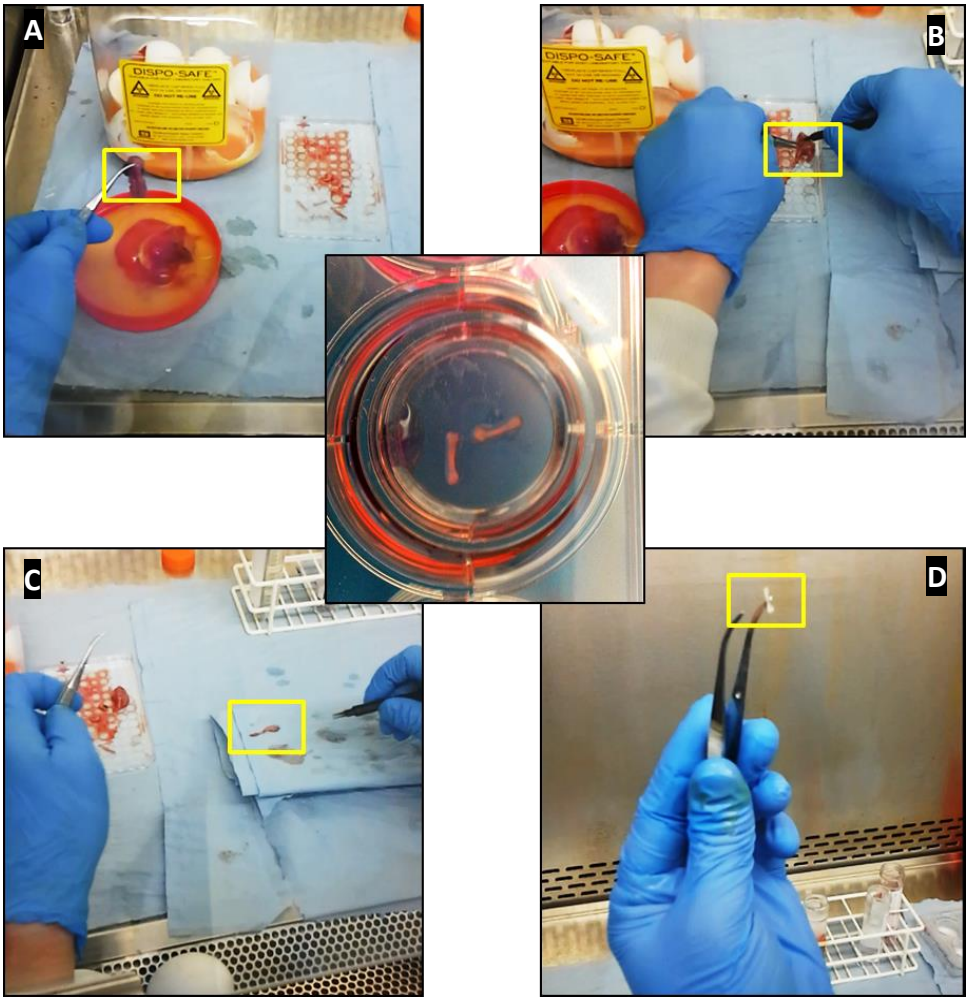

Figure 3: Isolation of femurs from day 11 chick foetuses. *All extractions were performed in a biological safety cabinet to ensure sterility. The chick foetus and yolk sac were tipped into a small dish (**A**), after which the foetus was quickly culled by separating the torso from the head. The two legs were then carefully dissected from the torso (**B**) which was then discarded. The legs were rolled on sterile paper towels to remove connective muscle and cartilage tissue (**C**) and the femurs were carefully separated from the acetabulum (Hip) and lower connecting tibia. The intact femurs (**D**) were then placed in a 6 well Trans well insert (Centre) and cultured in serum free media supplemented with 2% pen-strep and 1% L-glutamine until defect fabrication was performed.*

Isolated femurs were maintained in serum free PM (described in **Section 2.1.1**) for 24 hrs prior to defect fabrication.

4.2.2. Collagen hydrogel fabrication

Frozen vials of hMSCs were seeded into T75 flasks as detailed previously (**Section 2.1.1**). Cell populations were expanded to passage 3 in PM (described in **Section 2.1.1**)) before being incorporated into collagen hydrogels (as described in **Section 3.2.4.1**). Hydrogels were kept in culture for 24 hours to allow for gel contraction. Hydrogels were seeded with $3x10^5$cells in 1mg/ml collagen solutions. Based on findings presented in **Section 3.3.3.2**, these parameters would yield hydrogel volumes of between 2- 3mm^3. Acellular hydrogels were fabricated by neutralising 1ml of ice cold 9.22mg/ml type-1 rat tail collagen (Corning) with 23µl 1M NaOH solution, and pipetting 10µl beads into round bottom 96 well plates using a Finntip™ Stepper Pipette (Thermo Scientific, UK) to ensure equal volumes were dispensed. Acellular hydrogels were incubated at 37^{o}C for 24hrs prior to the experiments and washed for 15mins in PM prior to use in defects to remove residual NaOH from the gels.

4.2.3. Fluorescent tracking of hMSC/ collagen implants

PKH26 cell tracker (Sigma) was used to label populations of hMSCs prior to seeding in collagen hydrogels. The dye solution was formulated according to the manufacturer's guidelines. hMSCs were then suspended in dye solution and incubated for 10 minutes at 37^{o}C before the reaction was quenched in PM. Cells were then spun down and suspended in media before incorporation into collagen hydrogels.

4.2.4. Femur defect fabrication

The IMNs were produced using a coiled heating element designed to produce glass syringe needles (Narishige Scientific). The heated element stretched out glass capillary tubes (Sutter instruments, UK) into thin needles ~ 60-100µm in width (**Figure 4A)**. Construction of organotypic non-union defects was performed by first slicing the mid diaphysial section of the femurs using a sterile scalpel blade (**Figure 4B)**. Collagen implants were then threaded onto the borosilicate glass IMN, making sure the IMN was inserted through the central region of the implant (**Figure 4C)**. One of the femur halves was then threaded onto the needle such that bone collar just made contact with the collagen implant (**Figure 4D)**. The thicker capillary tube was then carefully removed from the thinner rod by breaking the glass at an appropriate length with tweezers. The remaining femur half was then threaded onto the opposing side of the IMN, again making sure the bone collar just made contact with the collagen implant (**Figure 4E&F)**. The finished constructs were transferred to 6 well trans-well inserts and cultured in PM (described previously) for 24 hrs prior to the experiment (**Figure 4G)**.

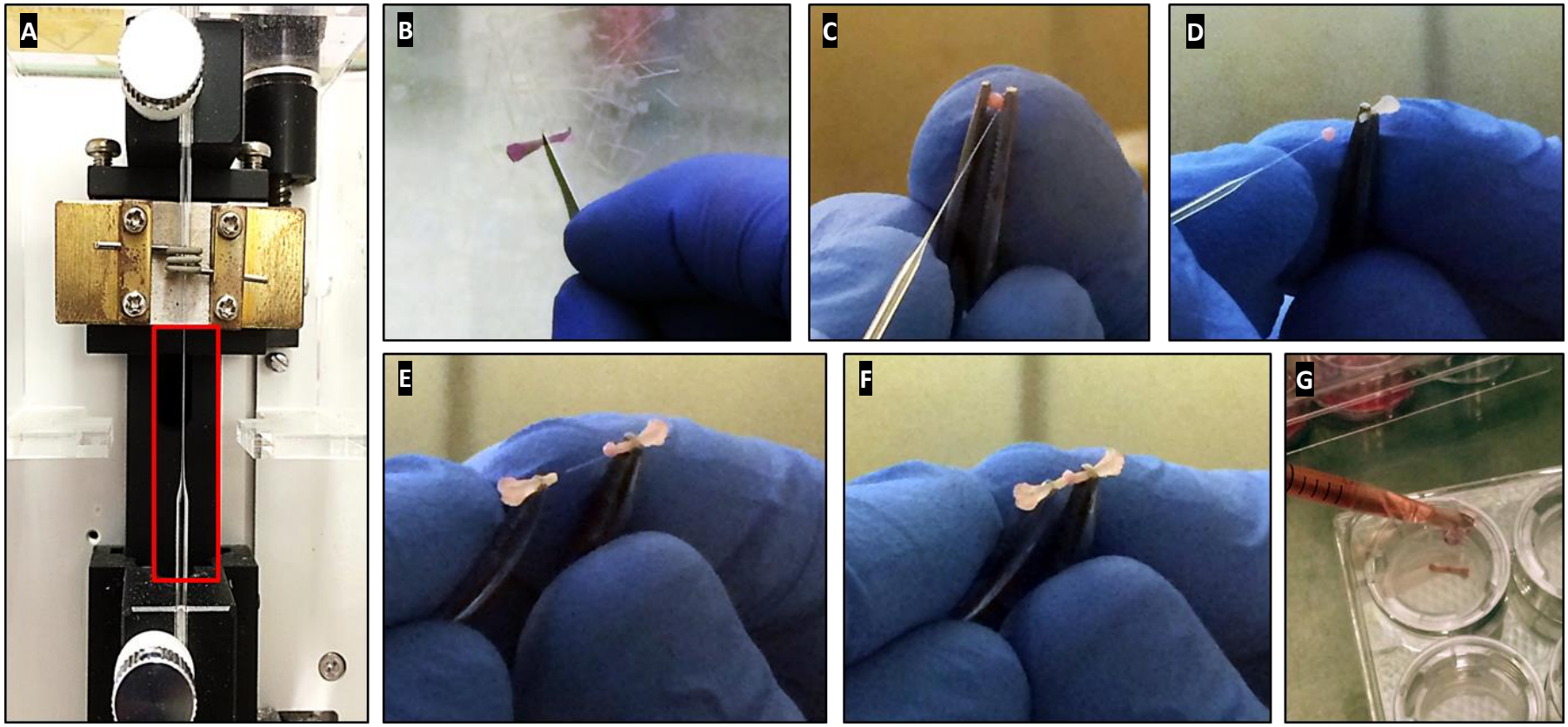

Figure 4. Fabrication of organotypic non-union defects in isolated embryonic chick femurs. *Intramedullary rods were made by anchoring borosilicate glass capillary needles between a heated coil element used to make microinjection needles (A). Isolated femurs were cut with a scalpel blade through the mid diapyhsial section of the femur (B). Collagen implants were were skewed onto the glass rod (C) with one femur end then threaded onto the rod to make contact with the implant (C). Thicker end of the capillary tube was carefully removed and the remaining femur half was threaded onto the glass rod until just making contact with the implant (E&F). Constucts were then transferred to 6 well Trans well inserts and maintined in basal culture media supplemented with 10% FBS for 24hrs prior to experiments*

4.2.5. Hydrostatic regime in undifferentiated hMSC/collagen implant femur constructs

Femur constructs were cultured for a period of 14 days with one hour per day 5 days/week in the hydrostatic bioreactor using a 280kPa, 1Hz regime. Constructs were cultured in OM (described in **Section 2.1.9**) with daily media changes before stimulation. The remainder of the time constructs were kept under standard cell culture conditions in a cell culture incubator at 37^0C with 5%CO_2.

4.2.6. Hydrostatic regime for preconditioned implant/femur constructs

hMSC seeded collagen hydrogels ($3x10^5$cells in 1mg/ml collagen hydrogels) were cultured for a period of 28 days prior to implantation in the femur constructs. Hydrogels were cultured in fresh OM and received bioreactor stimulation on given days for one hour. The remainder of the time hydrogels were kept under static standard cell culture conditions in a cell culture incubator at 37^0C with 5%CO_2. The pressure regimes applied were **a)** 0 – 279 kPa at 1 Hz, **1day/week** and **b)** 0 – 279 kPa at 1 Hz, **3days/week**, **c)** 0 – 279 kPa at 1 Hz, **5days/week** and **d)** Static control. After 28 days preconditioning, (to remain consistent with findings in **Chapter 3**) hydrogels were implanted into the femur defects and the constructs were cultured under static conditions in OM for 14 days.

4.2.7. X-ray micro tomography

Changes in the mineralised volume and density of the defect regions were analysed using a Scanco μCT40 (beam energy: 55 kVp, beam intensity: 145 μA, 200 ms integration time, spatial resolution: 10 μm) as described in **Section 3.3.2**. The defect region was highlighted in the software and analysed at the two density thresholds (50/1000, 80/1000) as before to determine the percentage mineralisation of the defect site. Bone morphometric analysis of the defect regions was analysed at a density

threshold of 50/1000 to determine the change in trabecular number, trabecular thickness and connective density of the tissue within the defects.

4.2.8. ALP Activity

ALP activity was assessed during culture by collecting media samples 24hrs post stimulation at day 7, day 10 and day 14 days of the culture period. Media samples were run in triplicate for each construct and activity was detected enzymatically using 4-Methylumbelliferyl phosphate (4-MUP) Liquid Substrate System (Sigma). 50 µl media samples were mixed in the same volume of substrate and incubated at room temperature for 30 mins. The reaction was stopped using 0.5M Ethylenediaminetetraacetic acid (EDTA) solution (Sigma). Fluorescence readings were measured at 360/440nm using a Biotech synergy 2 plate reader. Results were normalised against fluorescence readings from fresh OM.

4.2.9. Histological staining and imaging

After 14 days in culture, constructs were fixed in 10% neutrally buffered formalin for 2 hours at room temperature. The constructs were then washed three times for 5 minutes each in PBS. Constructs were then embedded in paraffin wax using an automated vacuum tissue processor (Kedee). 10µm sections were cut using a microtome and the sections were then mounted and processed according to methods described in **Section 3.2.3**. Mineralisation was quantified using the V/K method (described in **Section 3.2.3**). Sections were then counter stained using Harris Haematoxylin solution and Eosin (as described in **Section 3.2.3**). Sections were then mounted in DPX mounting medium and Imaged using an EVOS® FL Colour Imaging System.

4.2.10. Statistical analysis

Results were plotted and analysed in Microsoft Excel. All data point represents mean values ± standard error of the mean. Statistical significance for undifferentiated hMSC and acellular constructs was performed in Origin 9.0, employing a two way ANOVA between cellular/acellular and hydrostatic stimulation groups. Statistical significance for preconditioned implant experiments was determined in Microsoft Excel using a two tailed students T-Test.

4.3. Results

4.3.1. Construct stability

As stated in **Section 4.1.4**. The constructs were kept in culture for 24 hrs prior to each experiment undertaken, during which time native chick periosteal cells rapidly migrated around the defect site **(Figure 5)**. In acellular defects **(Figure 5A)** chick cells migrated into central regions of the implant as well as forming an encapsulating periosteum, which was easily observed due to the transparency of the implant. Periosteal chick cells encapsulated hMSC seeded implants; however the extent of migration of chick cells inside the implants themselves was unclear (**Figure 5B)**. In both acellular and hMSC groups, the formation of the chick periosteum around the defect site was important for maintaining construct stability throughout the culture period.

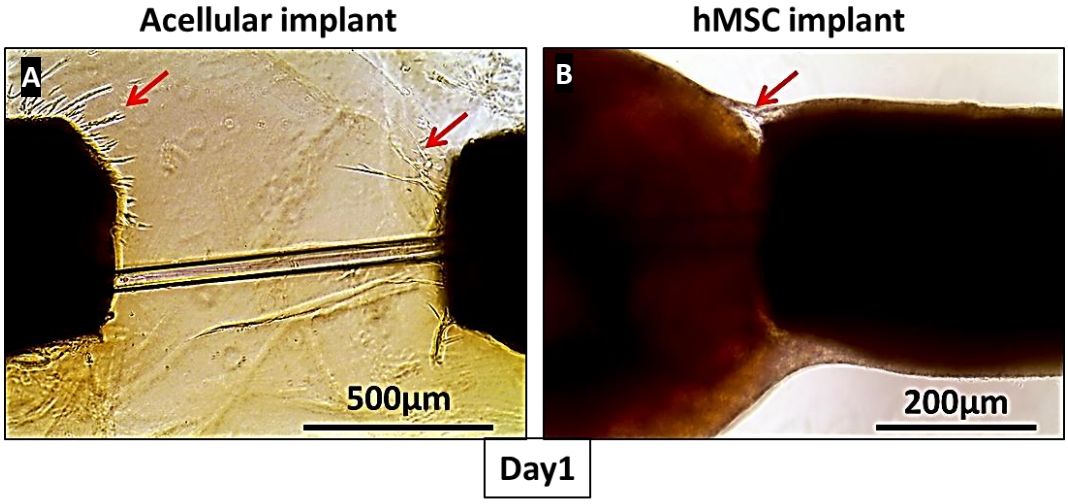

Figure 5. Migration of native chick cells into the defect site at day 1. *Arrows inset represent regions of chick cell migration*

4.3.2. Construct maturation

During the 14 day culture period, the defect site underwent a considerable amount of remodelling. There was some initial concern in using collagen as a implant material, for acellular implants, due to collagens readiness to undergo cell mediated contraction. In spite of this concern, after 14 days in culture the implants integrated well with femur ends and showed little sign of cell mediated contraction that might inhibit the healing process (**Figure 6A-D)**. PHK26 cell tracker was used to visualise the implanted hMSC during the experiments **(Figure 6C)**. After 14 days hMSCs were observed migrating along the chick periosteum (**Figure 6E,** red cell tracker) inside the mineralising bone collar and also through the medullary cavity **(Figure 6F)**. This highlighted benefit of using an IMN to prevent femur capping and to allow integration of the implanted hMSC with the native femur tissue. Empty defects **(Figure 6D)** sites supported by the IMN bridging the fracture site were used as negative controls for repair. Chick cells were observed migrating along the extending IMN, however very little tissue formation occurred after 14 days, representing a scenario of complete non-union in the organotypic model.

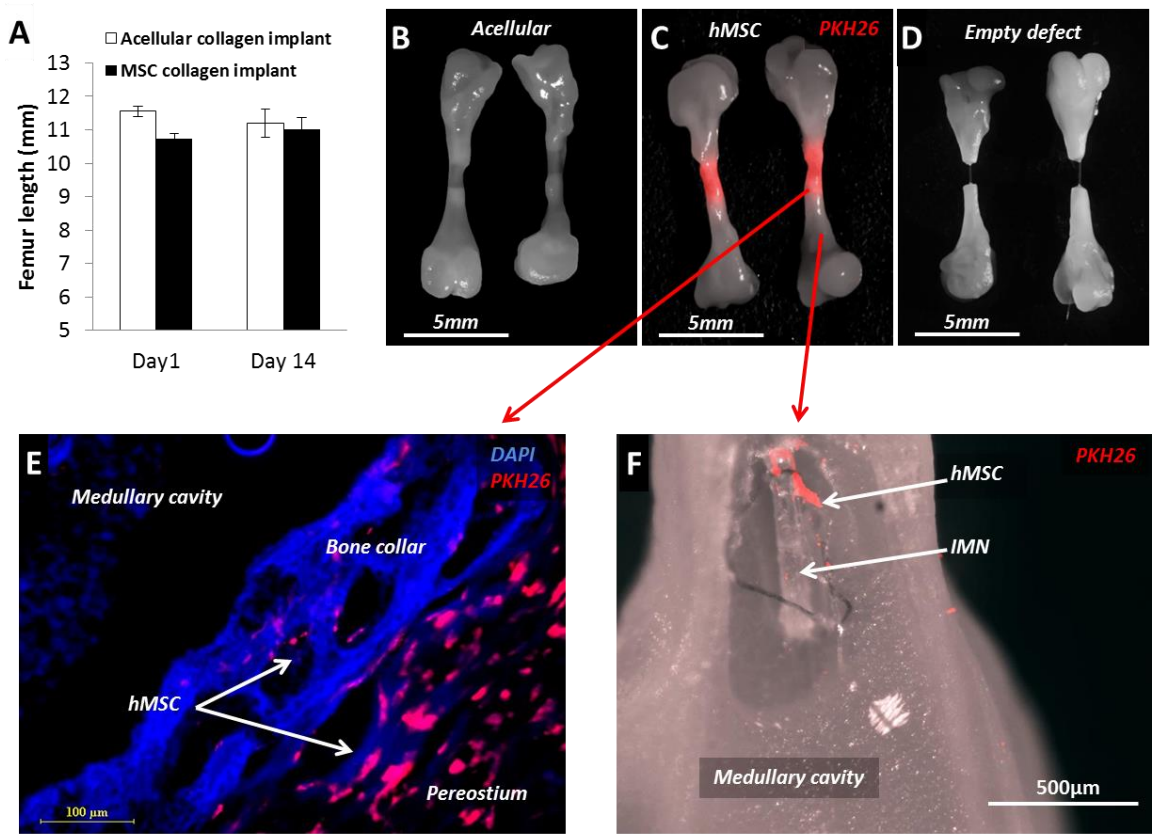

Figure 6: Maturation of organotypic chick femur fracture model after 14 days in culture. ***A)*** *Femur construct length at day1 and day 14 days.* ***B)*** *Acellular collagen implant constructs at day 14.* ***C)*** *hMSC/collagen implant constructs at day 14.* ***D)*** *Acellular collagen implant constructs at day 14.* ***E)****Migration of hMSCs (red) into femur constructs along the periosteal bone collar and into the medullary cavity (****F****).*

4.3.3. Effect of daily hydrostatic loading on construct viability

To evaluate the effect of daily hydrostatic pressure on the viability of the organotypic model, femurs constructs containing either hMSC/collagen implants or acellular implants were cultured for 14 days, with and without daily bioreactor stimulation. After 14 days, a dual fluorescence live dead assay was performed on whole constructs to assess cell viability (**Figure 7**). In all experimental groups the femur constructs remained viable for the 14 day culture period, indicated by strong positive green fluorescence in the whole mount images (**Figure 7 A, D, G&J**). Some cell death was present in all groups, indicated by the detection of red fluorescent cells (**Figure 7B,**

E, H&K). No differences were observed in viability between control and hydrostatic treated constructs in both acellular collagen implant groups (**Figure 7 A, B, C, D, E&F**), and hMSC/collagen implant groups (**Figure 7 G, H, I, J, K&L**). The localisation of dead cells in acellular implant groups was different from hMSC implant groups. In acellular groups, dead cells were present almost exclusively along the femur periosteum and not at the femur implant interface. By contrast in hMSC implant groups, dead cells were not present around the periosteum but instead localised around the implant/femur interface.

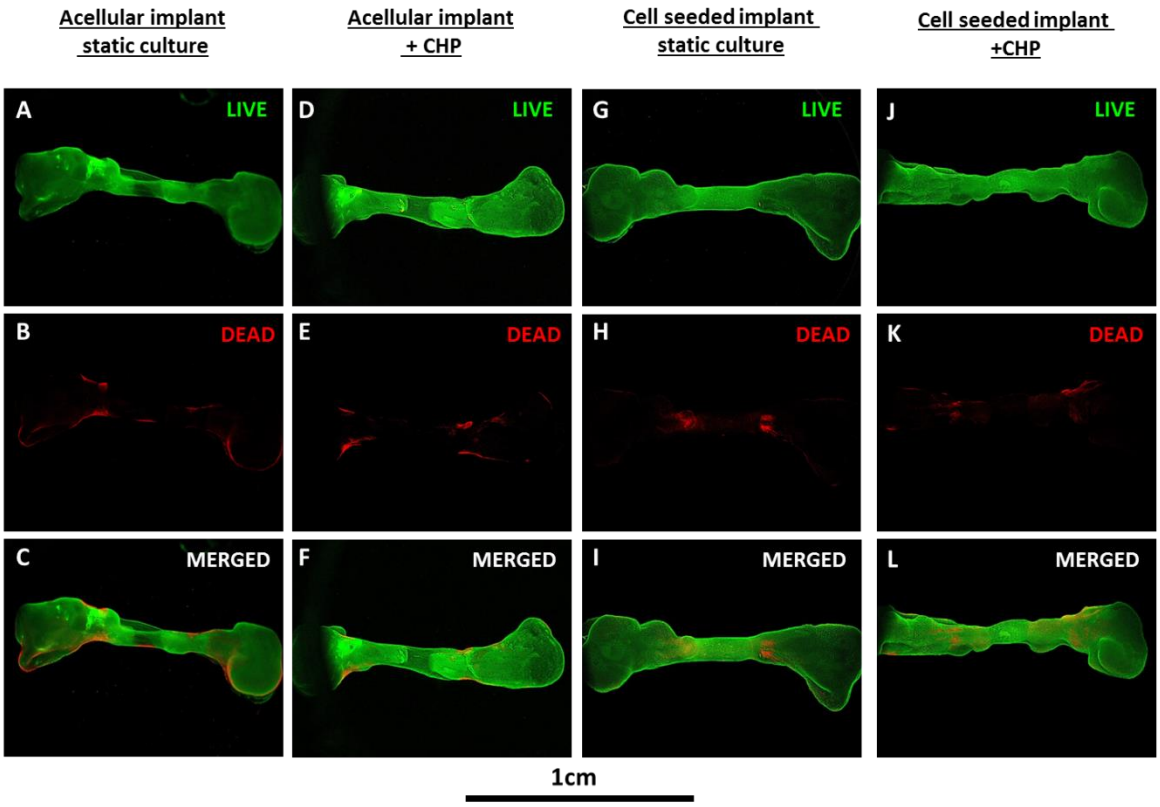

Figure 7. Whole mount live/dead staining in femur constructs after 14 days in culture. *Live cells are shown in green and dead cells are shown in red.*

4.3.4. ALP activity

Media was collected from cultures throughout the experiment to monitor the ALP activity of the constructs (**Figure 8**). ALP activity was significantly higher in hMSC seeded constructs at days 7, 10 and 14 ($p<0.05$) in stimulated vs static cultured constructs. ALP activity was significantly higher at day 7 and day 10, but not at day 14, in stimulated acellular constructs versus static acellular constructs. ALP activity in stimulated acellular constructs decreased between day 7 and 14 days and was comparable with static/acellular constructs by the end of the experiment. By contrast, activity in hMSC seeded constructs in both static and stimulated groups remained high relative to acellular constructs throughout the experiment.

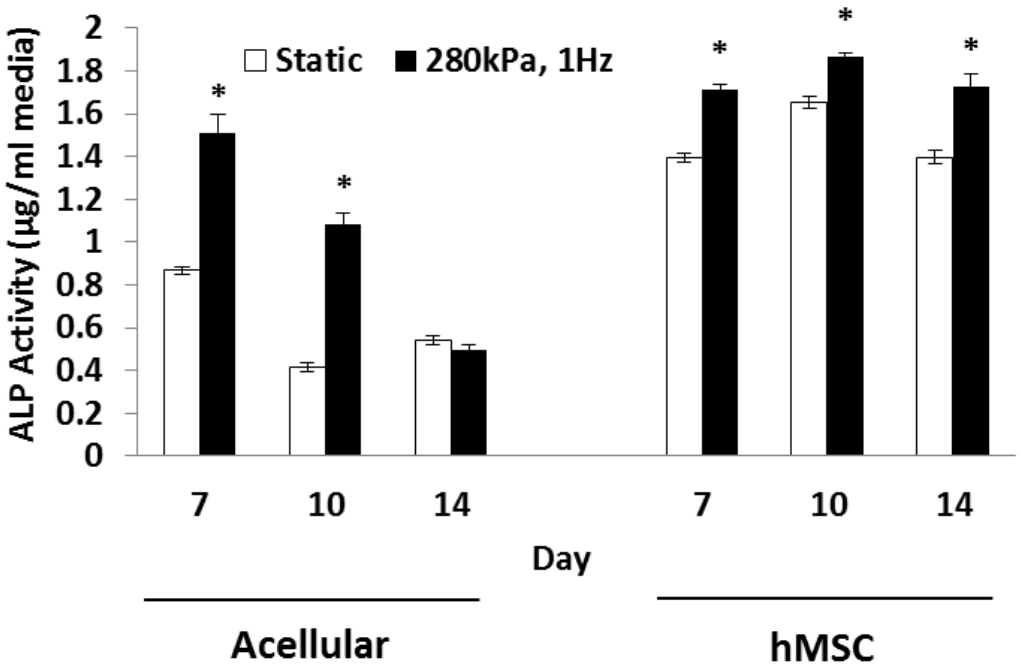

Figure 8. Alkaline phosphatase activity in femur constructs during in vitro culture with and without hMSCs present in the implants. *Error bars represent standard error of the mean, n=4. * P<0.05*

4.3.5. Defect mineralisation

μCT was employed following fixation of the constructs after 14 days in culture to assess the extent of new bone formation within the defect site. As discussed in the previous chapter, by combining μCT analysis with histological evaluation for bone mineral deposition, we obtain strong inference as to the amount of new bone formation in the implants. Whole mount imaging (**Figure 9A**) after 14 days demonstrated significant remodelling of the initial defect site. Native chick cells migrated along the periphery of the femur diaphysis, bridging and encapsulating the defect with a periosteal collar. hydrostatically stimulated constructs also appeared to have visible thicker cortices in the extending diaphysis (**Figure9A, ii&iv**) compared with unstimulated femurs (**Figure9A, i&iii**).

Analysis by μCT of the percentage volume of mineralised tissue within the defect site (**Figure9B)** showed that both acellular and hMSC seeded defects had a higher percentage of mineralised volume when hydrostatically stimulated. Stimulated acellular defects had a 1.79 fold increase in mineralisation compared with static acellular defects ($p=0.26$), whilst stimulated hMSC defects were significantly more mineralised with a 2.31 fold increase in mineralisation over static hMSC defects. The increase in percentage volume in the defect region correlated with μCT reconstructions (**Figure9C)**, which revealed large areas of dense tissue in stimulated hMSC defects (**Figure9C(iv)**). By comparing μCT imaging and histological sections stained with von kossa (black) and eosin (pink) (**Figure9D)** we could confirm that calcium deposition (black) was localised to regions dense tissue regions (red) in μCT reconstructions. Analysis of the data set using a two way Anova (**Figure9E**) indicated that whilst the presence of the hMSC/collagen implants in response to stimulation did not significantly affect

mineralisation (p=0.13), the application of hydrostatic pressure did (p=0.004). There was no significant interaction between the two parameters (p=0.33).

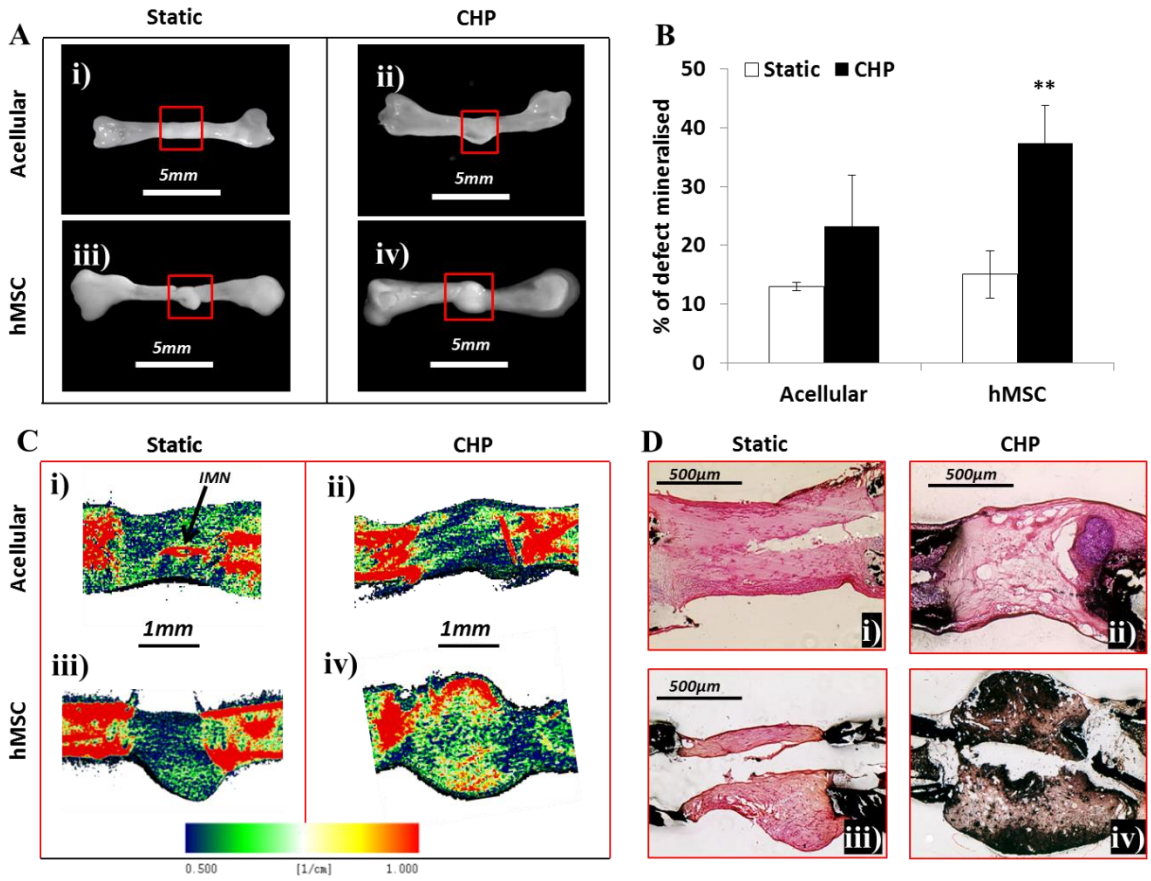

	DF	Sum of Squares	Mean Square	F Value	P Value
Cells	1	253.83055	253.83055	2.61099	0.13209
Stimulation	1	1200.97903	1200.97903	12.3537	0.00426
Interaction	1	98.66815	98.66815	1.01494	0.33361
Model	3	1553.47774	517.82591	5.32654	0.0145
Error	12	1166.59385	97.21615	--	--
Corrected Total	15	2720.07159	--	--	--

At the 0.05 level, the population means of **Cells** are **not significantly** different.
At the 0.05 level, the population means of **Stimulation** are **significantly** different.
At the 0.05 level, the interaction between **Cells** and **Stimulation** is **not significant**.

Figure 9: µCT analysis of chick femur constructs after 14 days. (Ai-iv)*Whole mount imaging showing remodelling of the defect by the chick cells after 14 days.* ***(B)****Analysis by µCT showing an increase in defect mineralisation (indicated by red inset in* ***A****) in femur constructs at day 14.* ***(C)*** *Image reconstructions of the density distribution in defect sections.* ***(D)*** *Histological sections showing von kossa (black) and eosin (pink) staining non mineralised tissue.* ***(E)*** *Results for two a way Anova to determine the interaction between hMSC seeded collagen implants and bioreactor stimulation on defect mineralisation. Error bars are standard error of the mean, n=4. * P<0.05*

4.3.6. Cell morphology and trabecular analysis

Fluorescent imaging of the actin cytoskeleton in hMSC seeded implants (A&B) showed a change in cell morphology between static and stimulated groups. Cells in static implants (**Figure 10A**) possessed an undistinguished morphology, typical of the developing hMSC phenotype in collagen. Cells in mineralised regions of stimulated defects (**Figure 10B**) possessed morphology typical of embedded osteocytes, with long dendritic processes protruding into the extra cellular matrix. High magnification imaging of histological sections (**Figure 10C&D**) showed marked differences in the ECM structure between static and stimulated implants. Mineralised regions in stimulated defects (**Figure 10D**) exhibited porous trabecular architecture, whereas the static defects (**Figure 10C**) had tissue fibrous gel structure. Quantification of trabecular morphometry using μCT (**Figure 10E,F&G**) showed a significant increase in trabecular number (**Figure 10**E, $p<0.05$), trabecular thickness (**Figure 10F**, $p<0.01$) and connective density (**Figure 10G**, $p<0.05$) in hMSC seeded defects vs stimulated acellular and static controls. Stimulation alone was sufficient to increase trabecular thickness in acellular defects vs static controls (**Figure 10F**, $p<0.01$). Results of a two way Anova performed on the data sets in (**Figure 10E, F&G**) revealed that the presence of cells was responsible for the significant increase in trabecular number in hMSC/collagen implants. The effect of stimulation on trabecular thickness and connective density of trabeculae was significant irrespective of the presence of hMSCs. In all three data sets the interaction between cells and stimulation was not significant ($P>0.05$).

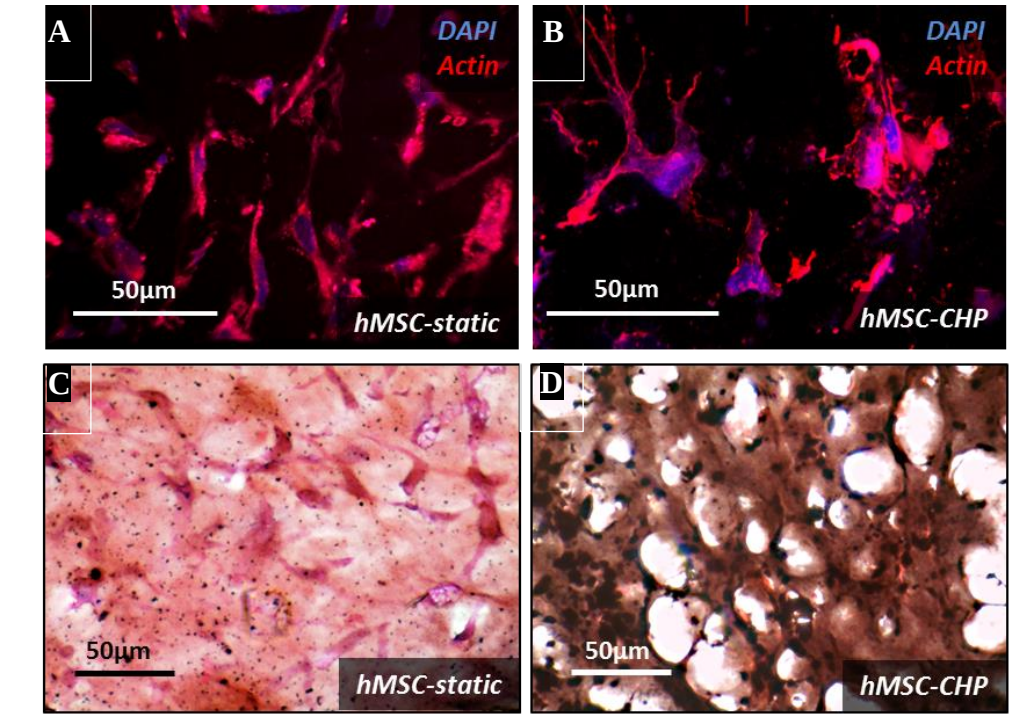

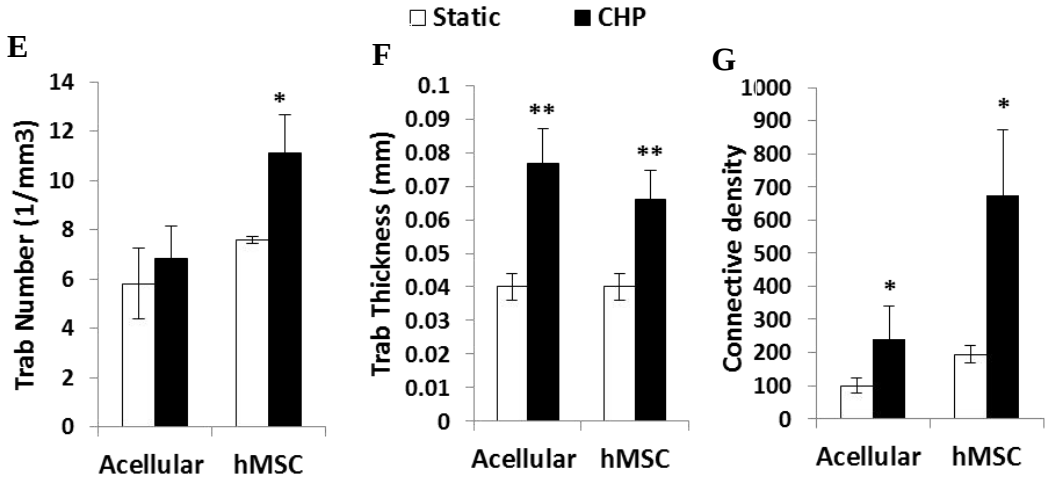

H

Trabecular thickness

Overall ANOVA

	DF	Sum of Squares	Mean Square	F Value	P Value
Cells	1	1.0016E-4	1.0016E-4	0.51595	0.48755
Stimulation	1	0.00365	0.00365	18.82259	0.00118
Interaction	1	1.0016E-4	1.0016E-4	0.51595	0.48755
Model	3	0.00371	0.00124	6.36676	0.00924
Error	11	0.00214	1.94129E-4	--	--
Corrected Total	14	0.00584	--	--	--

At the 0.05 level, the population means of **Cells** are **not significantly** different.
At the 0.05 level, the population means of **Stimulation** are **significantly** different.
At the 0.05 level, the interaction between **Cells** and **Stimulation** is **not significant**.

Connective density

Overall ANOVA

	DF	Sum of Squares	Mean Square	F Value	P Value
cells	1	257935.65613	257935.65613	5.16648	0.04408
STIMULATION	1	359640.99274	359640.99274	7.20365	0.02126
Interaction	1	107721.72074	107721.72074	2.15768	0.16987
Model	3	781704.35233	260568.11744	5.21921	0.01748
Error	11	549172.88297	49924.80754	--	--
Corrected Total	14	1.33088E6	--	--	--

At the 0.05 level, the population means of **cells** are **significantly** different.
At the 0.05 level, the population means of **STIMULATION** are **significantly** different.
At the 0.05 level, the interaction between **cells** and **STIMULATION** is **not significant**.

Trabecular number

	DF	Sum of Squares	Mean Square	F Value	P Value
Cells	1	34.0387	34.0387	5.59837	0.03741
Stimulation	1	19.21514	19.21514	3.16033	0.10307
Interaction	1	5.89685	5.89685	0.96986	0.34588
Model	3	62.99316	20.99772	3.45351	0.055
Error	11	66.88117	6.08011	--	--
Corrected Total	14	129.87433	--	--	--

At the 0.05 level, the population means of **Cells** are **significantly** different.
At the 0.05 level, the population means of **Stimulation** are **not significantly** different.
At the 0.05 level, the interaction between **Cells** and **Stimulation** is **not significant**.

Figure 10: Cellular morphology and trabecular analysis in femur constructs after 14 days. A&B) *Fluorescent imaging of the actin cytoskeleton in static* ***(A)*** *and stimulated* ***(B)*** *implants.* ***C&D)*** *High magnification imaging of histological sections* ***(C&D)*** *stained with V/K and H&E showing marked differences in the ECM mineralisation and trabecular architecture between static and stimulated implants. Heavily mineralised regions in stimulated defects* ***(D)*** *had porous trabecular architecture, whereas the static defects* ***(C)*** *had a fibrous tissue structure. (****E, F&G****) Quantification of trabecular morphometry using µCT.* ***EH)*** *Results for two way anova for figures* ***E****,* ***F&G,*** *demonstrating a significant effect of cyclic pressure on trabecular architecture. Error bars represent standard error of the mean, n=4. ** P<0.01, * P<0.05*

4.3.7. 4 week preconditioning of hMSC seeded collagen hydrogels

4 weeks daily application of CHP was applied to hMSC collagen hydrogels ($3x10^5$cells/hydrogel, 1mg/ml collagen concentration) to evaluate if preconditioning the hydrogels prior to implantation could enhance fracture repair in the femur defect model. Hydrogels were stimulated with CHP for periods of 1, 3 and 5 days/ week, to determine if the time spent in the bioreactor could be reduced without jeopardising bone formation, by reducing time and labour demands, a further realisation of clinical efficacy for these bioreactor systems might be obtained. The hydrogels were preconditioned using the same regime as for o undifferentiated hMSC seeded defects, and after 4 weeks were analysed by µCT and histology to compare tissue composition before implantation.

µCT analysis of the hydrogels after 4 weeks showed a significantly larger volume in hydrogels preconditioned for 5 days/week compared with statically cultured hydrogels (**Figure 11 A**, $p<0.01$). The hydrogel mineralisation and density (**Figure 11 B&C**) was within the range predicted by the optimisation data described in

chapter 3, however preconditioning with CHP did not increase hydrogel mineralisation or density when compared with statically cultured hydrogels. µCT reconstructions of the hydrogels (**Figure 11 D**) demonstrated extensive mineralisation of the gels after 4 weeks, and also showed point mineralisation in cross-sectional density profiles (**Figure 11E**) due the presence of differentiated hMSCs. 10µm tissue sections stained positive for mineralised bone, as indicated by von kossa and alizarin red staining (**Figure 11 F&G**). No differences in calcium deposition were observed between hydrostatically preconditioned and statically cultured hydrogels.

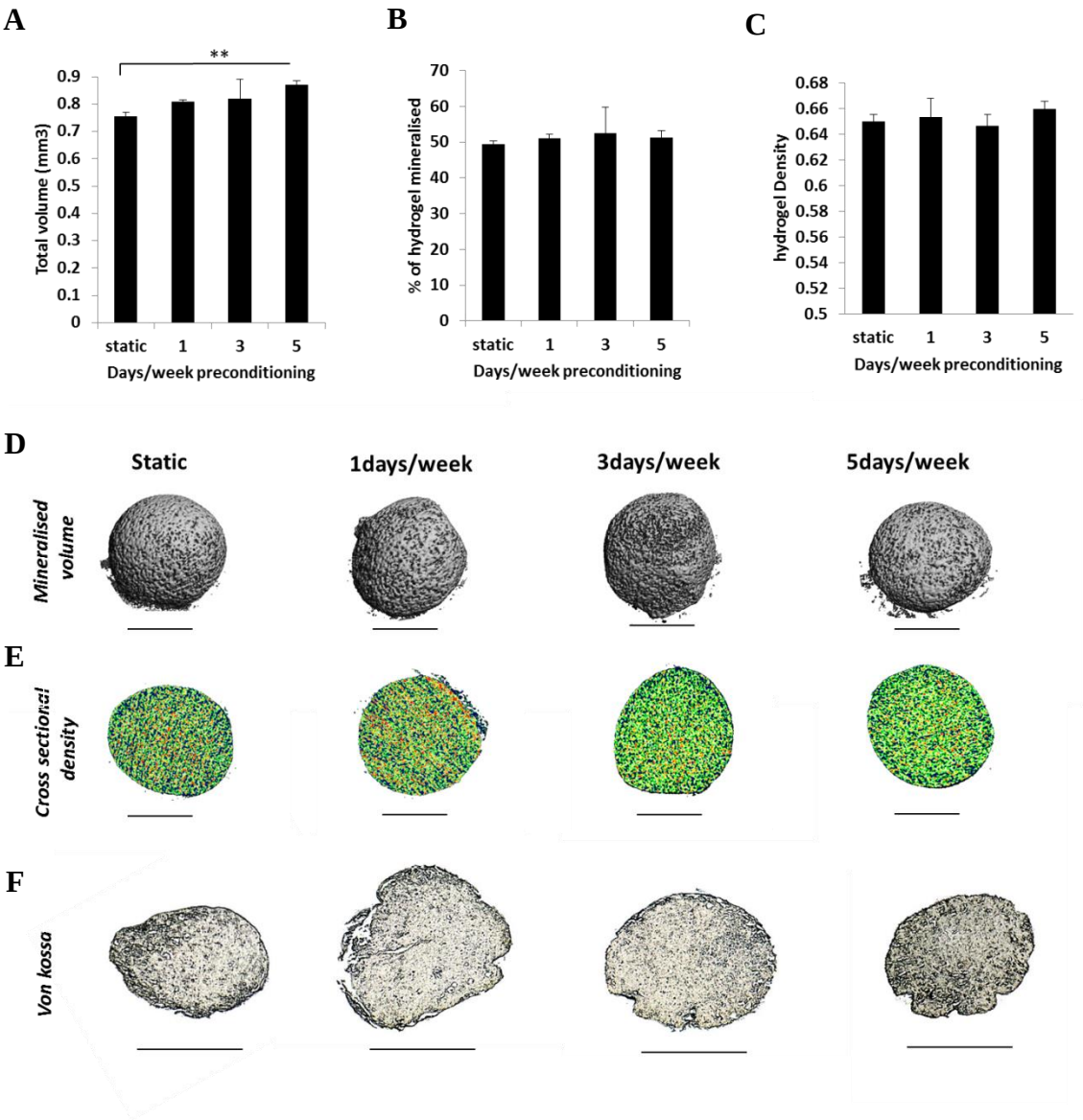

Figure 11. hMSC/collagen hydrogels preconditioned for 4 weeks prior to implantation into femur constructs. (A-C) *µCT data after 4 weeks showing total hydrogel volume (**A**) percentage mineralisation (**B**) and hydrogel density (**C**). (**D&E**) Image reconstruction of hydrogels showing mineralised volume (**D**) and crossectional density **(E)** of the hydrogels after 4 weeks. **(F)** 10µm sections of formation by von kossa to assess bone formation in the hydrogels after 4 weeks. Sections correspond to cross-sectional density reconstructions. error bars represent standard error of the mean, n=3. Scale bars = 500µm*

4.3.8. 2 week culture of embryonic chick femur constructs using hydrostatically preconditioned hydrogels

Following preconditioning, the hydrogels were implanted into chick femur defects and cultured for 2 weeks in osteogenic media to determine if hydrostatically preconditioning of hydrogels prior to implantation was sufficient to accelerate the fracture repair process. Consistent with previous findings, the native chick cells formed an encapsulating periosteum around hMSC/collagen implant after 2 weeks in culture. Live dead staining (**Figure 12**) was performed on whole femurs to assess changes in femur and hydrogel viability and indicated no loss in viability in either the femurs or the hMSC implants. Dead chick cells formed a thin periphery on the outer periosteum in all experimental groups and no changes in viability were observed between statically cultured and hydrostatically preconditioned implants.

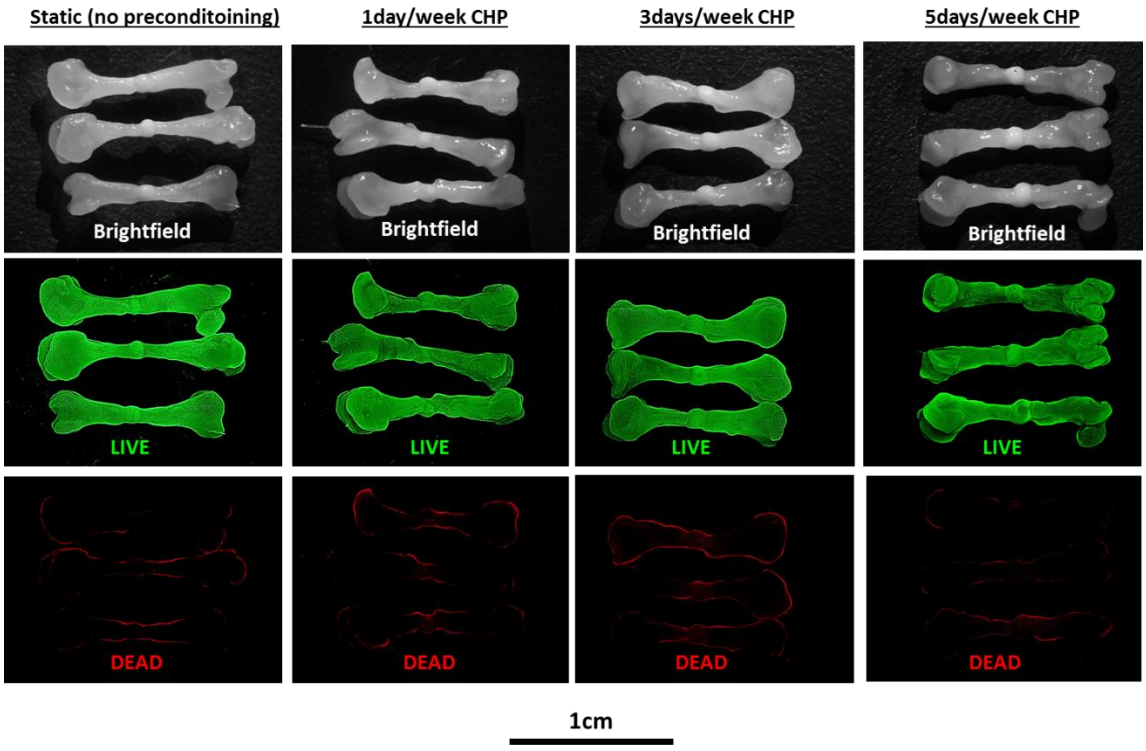

Figure 12. Bright field imaging and live dead staining of whole femurs constructs at day 14 in culture.

4.3.9. Assessment of defect mineralisation 2 weeks post implantation

The femur constructs were then analysed by µCT to quantify the volume of mineralised tissue in the collagen implants. The results were plotted against µCT data of the hMSC/collagen hydrogels prior to implantation to assess the rate of change in mineralisation. Surprisingly, after 14 days in culture, all experimental groups underwent a significant decrease in mineralisation of the hMSC/collagen implants (**Figure 13A).** The mineralisation of the implants in the femur constructs was comparable between experimental groups, with approximately a 4 fold decrease in hydrogel mineralisation after 2 weeks. Hydrogel density was also significantly lower in all post implantation hydrogels (**Figure 13B)** and did not change significantly between static and

hydrostatically preconditioned groups. µCT density reconstructions (**Figure 13C**) of the defect regions correlated with histological analysis of 10µm tissue sections (**Figure 13D)**, showing a reduction in the amount of positive Von Kossa staining in the implants when compared with hMSC/collagen hydrogels prior to implantation.

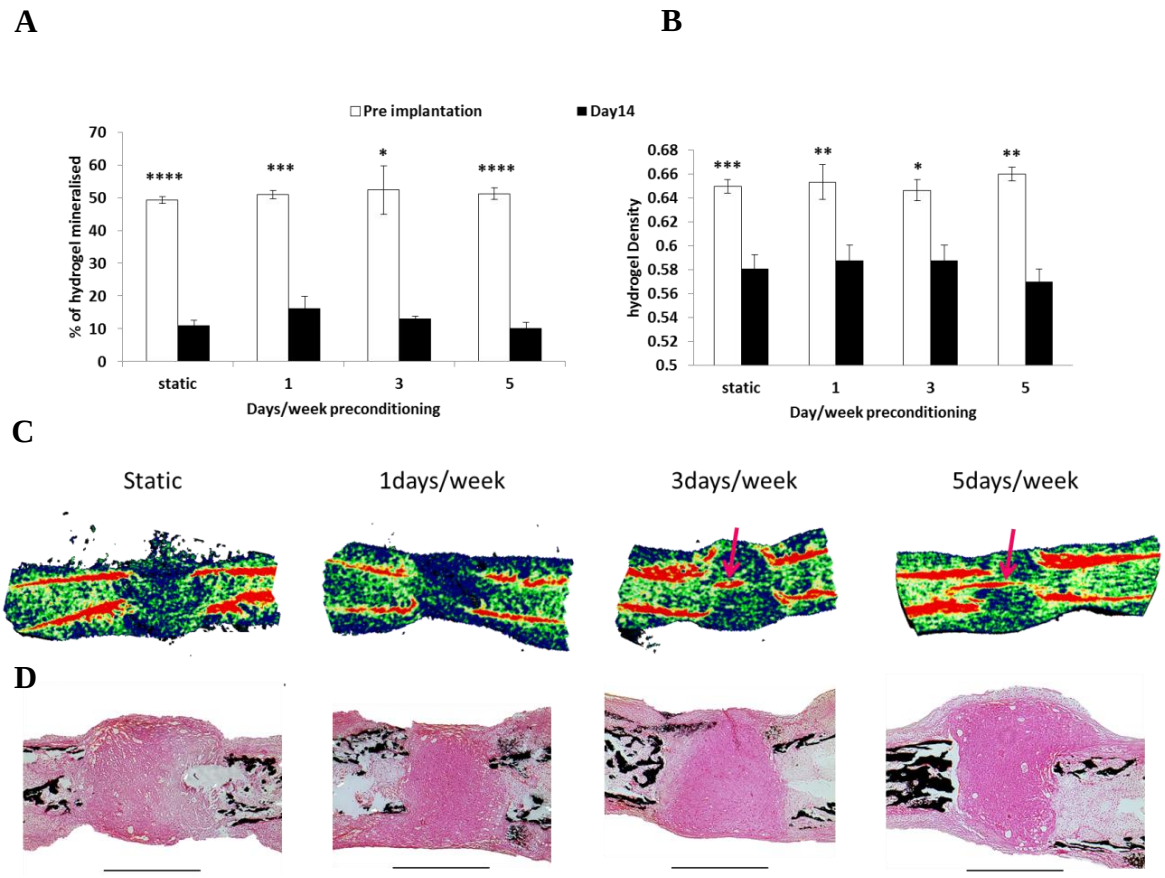

Figure 13. Comparison of implant mineralization by µCT and histology before implantation and after 2 weeks culture in chick femur defects. A) *Percentage mineralisation and density* ***B)*** *of hMSC/collagen hydrogels before and after implantation into chick femur defects.* ***C)*** *µCT density heat map image reconstructions of the defect site after 2 weeks in culture, pink arrows (inset) represent IMN.* ***D)*** *10µm tissue sections of the defect site after 2 weeks stained with von kossa (black) for bone formation and countered stained eosin (pink) to represent non mineralised tissue. Error bars represent standard error of the mean. n=4. Scale bars (bottom) = 500µm ****P<0.0001, ***P<0.001, **P<0.01, * P<0.05*

4.4. Additional observations

After establishing in **Section 3.3.2** that the precondition regime was sufficient to increase the rate of bone formation in MG63 collagen hydrogels, the pre-conditioned hydrogel experiment was performed prior to optimisation of the seeding parameters in **Section 3.3.3.** The results of this experiment whilst not optimal in terms of the model design provided an interesting contrast to the results described in **Sections 4.3.7, 4.3.8 and 4.3.9**. The seeding parameters for this experiment were set at 100,000 hMSCs per 1mg/ml collagen hydrogel, and the hydrostatic pressure regime was identical to the preconditioning regimes described previously, which stimulated hMSC/collagen hydrogels for different numbers of days of the week using a 280kPa, 1hz regime for 1 hour per day. The key difference between the experiments was the stock concentration of collagen and the protocol used to fabricate the hydrogels.

The use of collagen hydrogels as a growth environment for cells is a widely established technique and generally follows a common set of protocol. Much of the literature, and indeed many manufacturer's recommendations describe a stock concentration (typically 3-5mg/ml) diluted to a working concentration in a cell suspension in 10xDMEM and PBS, after which the solution is neutralised with 1M NaOH. The protocol described in this thesis, differed in that cell suspensions in regular DMEM supplemented with 10% FBS were diluted to a working concentration from a higher stock concentration of collagen (9.81mg/ml) without the addition of NAOH. The protocol allowed cell mediated self-assemble of the collagen hydrogels, which was typically complete 24hrs after fabrication. The addition of NaOH reported in the literature is to neutralise the acidic environment present in collagen/acetic acid solutions of lower stock concentrations (3-5mg/ml), which induces polymerisation of the hydrogel.

By using a higher starting concentration of collagen (8-11mg/ml), the relative volume of acetic acid-media was such that neutralisation with NaOH was not required.

The initial studies for preconditioned hMSC/collagen hydrogels utilised the standard protocol from the literature, which requires neutralising the cell/collagen solution in 10xDMEM (made from a stock of 3.61mg/ml) with 1M NAaOH (23ul/ml working solution). Comparing the results from these experiments showed that the NaOH/ low stock fabrication, and the self-assembly/high stock fabrication methods yielded very different endpoint results (**Figure 14)**, which in turn had an effect on the outcome of hydrogel mineralisation after implantation into the chick femurs.

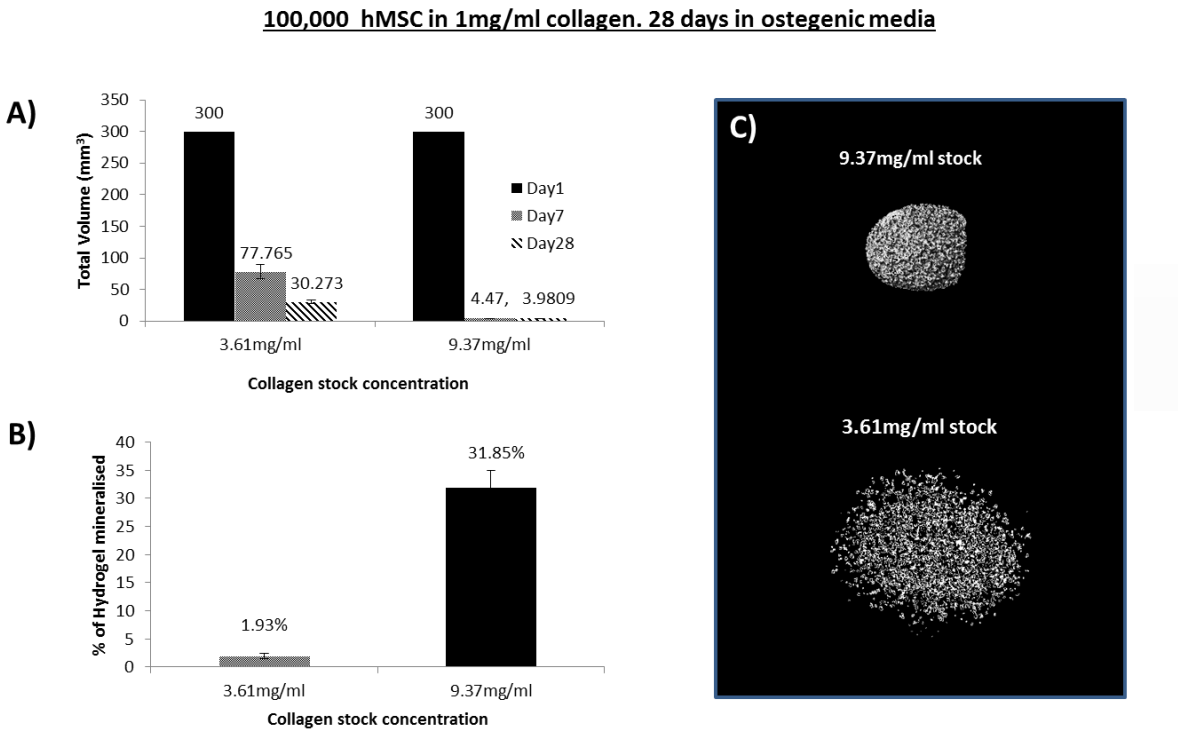

Figure 14. ***Effect of fabrication method on contraction and mineralisation of hMSC/collagen hydrogels after 28 days in OM. A)****Total volume at day 1,7 and 28.* ***B)*** *Percentage mineralisation after 28days.* ***C)*** *µCT image reconstruction after 28days in using self-assemble fabrication from high stock concentraitons (8-11mg/ml) (top) and NAOH neutralisation in low stock collagen hydrogel fabrication (3-5mg/ml) (bottom)*

4.4.1. 4 week preconditioning of hMSC seeded collagen hydrogels fabricated using low stock concentration collagen

Live dead staining of the hydrogels (**Figure 15A**) demonstrated that cells remained viable for the 4 week preconditioning period in all experimental groups. Analysis by µCT visualised the mineralised volume (**Figure 15B**) of the different preconditioned hydrogels. Quantitative analysis was performed to determine the change in volume over the 4 week preconditioning period (**Figure 15C**), the total hydrogel volume at 28days (**Figure 15D**) and the percentage mineralisation of the hydrogels at 28 days (**Figure 15E**).

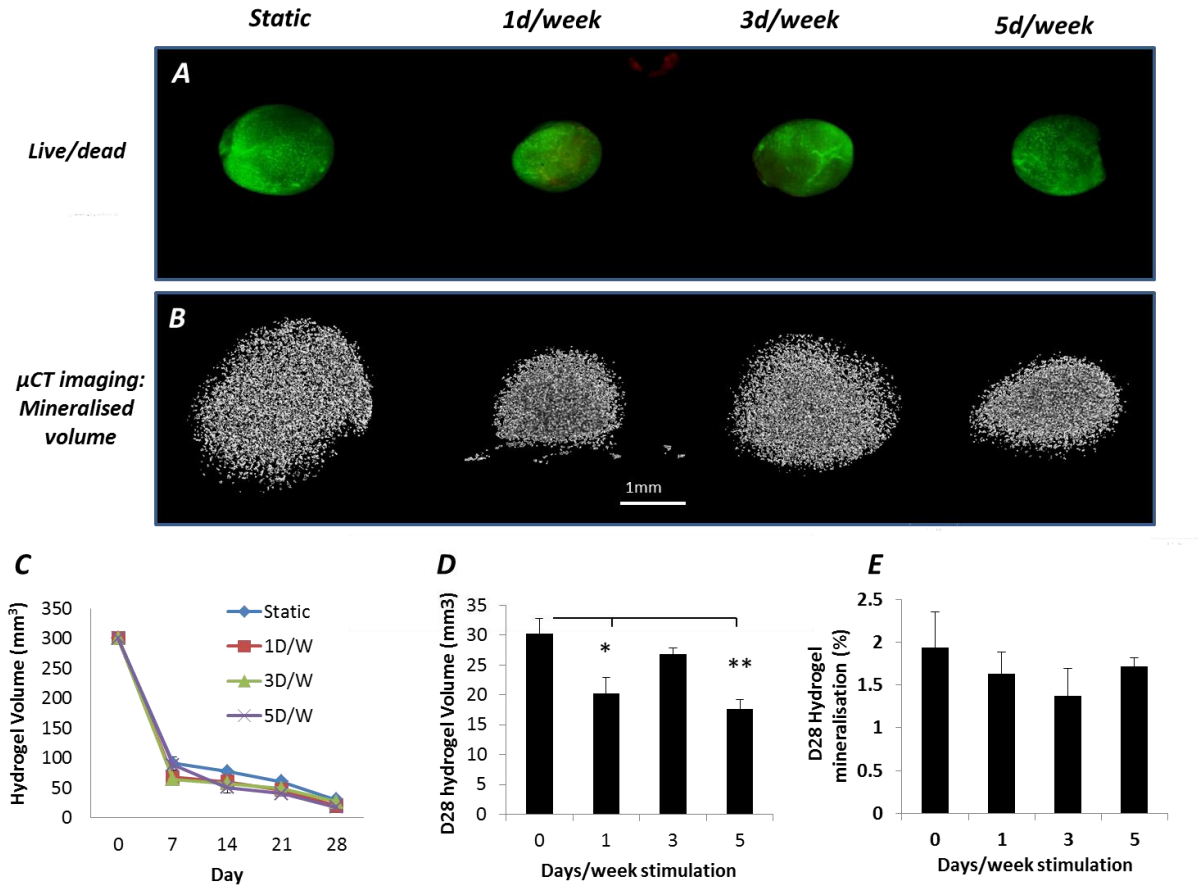

Figure 15: ***hMSC/collagen hydrogels fabricated from low stock concentration, preconditioned for 4 weeks prior to implantation. A)*** *Live dead staining at day 28 in hydrogels preconditioned for different numbers of days per week.* ***B)*** *µCT images showing mineralised volume of the hydrogels at day 28.* ***C,D&E)*** *µCT data showing the volume of hydrogels over the 4 week preconditioning period (**C**), hydrogel volume at Day 28 (**D**) and hydrogel mineralisation at day 28 (**E**). **P<0.01, * P<0.05*

Hydrogels contracted significantly during the first 7 days in culture, and there on continued to contract gradually to about 5-10% of their original volume. Compared with statically cultured hydrogels, preconditioning for either 1 or 5 days per week had a significantly effect on cell mediated contraction and resulted in lower volume hydrogels. Interestingly hydrogels preconditioned for 3 days per week did not contract significantly more than statically cultured hydrogels. The mineralisation of the hydrogels after 4 weeks was between 1-2% of their total volume and did not vary significantly between experimental groups. Compared with statically preconditioned hydrogels described in **Section 3.3.3.3**, hydrogels fabricated using a low stock concentration showed a 15-20 fold reduction in percentage mineralisation.

4.4.1. 2 week culture of embryonic chick femur constructs using hydrostatically preconditioned hydrogels fabricated from low stock concentration collagen

Following the 4 week preconditioning period, the hMSC/collagen hydrogels were implanted into the femur defects and cultured for a further 2 weeks as described in **Section 4.2.6**. After the two week culture period, the femur constructs were fixed and analysed by μCT to assess the changes in implant mineralisation. Whole mount imaging of the constructs (**Figure 16A)** showed the implants large size relative to the implants described in **Section 4.3.8.** Contraction of the hydrogels in all experimental groups continued after implantation into the femur defects. Static hydrogels, and hydrogels preconditioned for 1day/week contracted a further 40% of their pre implantation volume, whilst hydrogels preconditioned for 3&5days/week contracted a further 50% their pre implantation volume (**Figure 16D**).

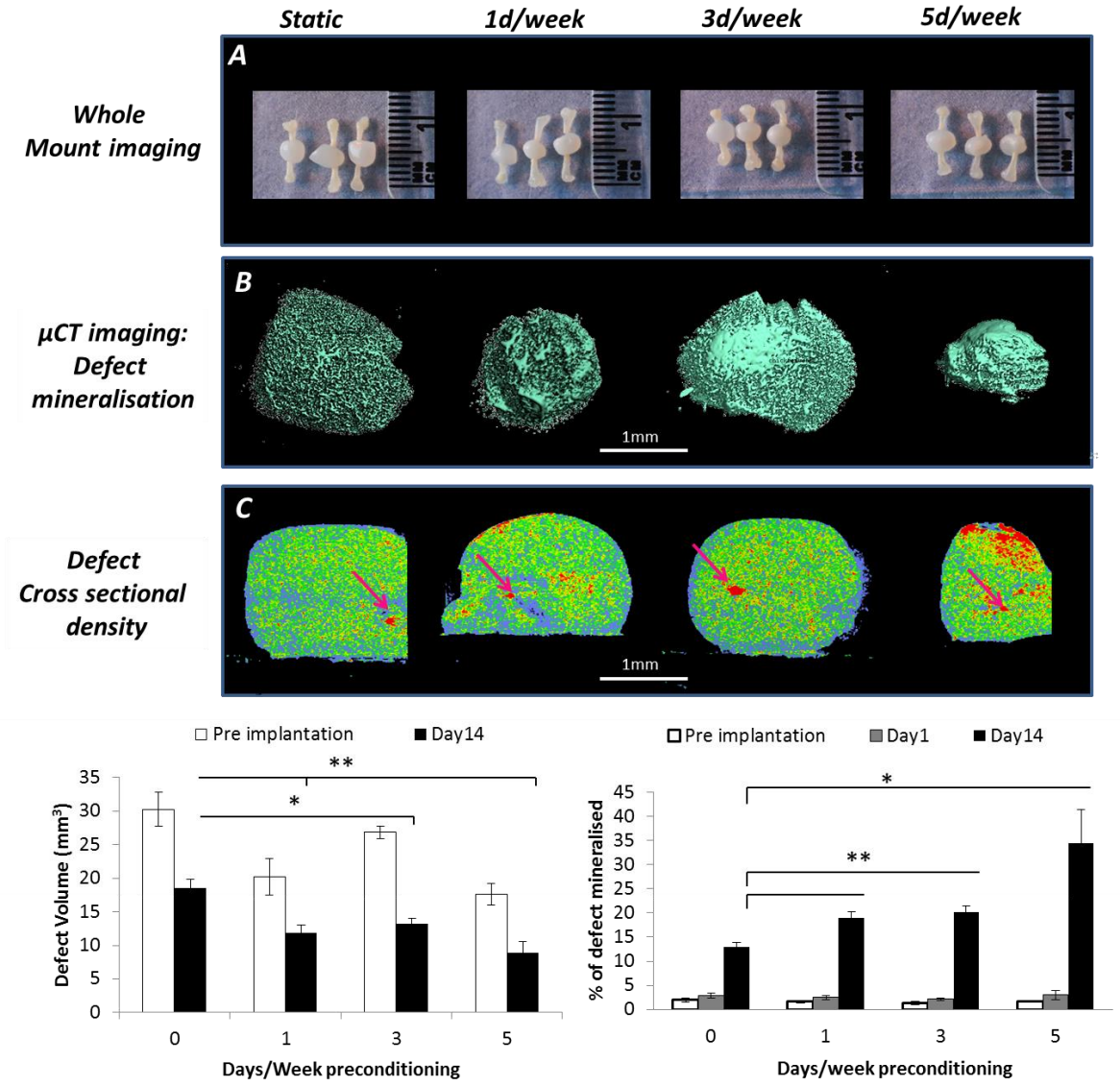

Figure 16: Comparison of implant mineralization by µCT and histology before implantation and after 2 weeks culture in chick femur defects. A) *Wholemount imaging of constructs after 2 weeks in culture.* ***B)*** *µCT images showing mineralised volume of the defect region after 2 weeks in culture.****C)*** *µCT images showing cross sectional density of the defect after 2 weeks in culture. (****D****) Comparison of defect volume for preimplantation hydrogels, and after two weeks culture in femur defects. (****D****) Defect mineralisation before implantation, at 1 day and 14 days culture in femur defects* ***(E)****.Error bars represent standard error of the mean. n=5. **P<0.01, * P<0.05.*

After two weeks culture, analysis of the defect region by µCT showed mineralisation on peripheral regions of implants that received hydrostatic preconditioning. Mineralisation was particularly prominent on the peripheral regions of

defects receiving a 5 day/week treatment compared with 1&3days/week, or statically preconditioned hydrogels. Cross sectional density sections of the implants (**Figure 16C**) showed peripheral mineralisation in implants preconditioned for 1&5days/week, with mineralisation most prominent in 5days/week groups. Quantification of the percentage defect mineralisation (**Figure 16E**) showed a significant increase in defect mineralisation after 14 days in implants preconditioned for 1, 3 and 5 days/week versus statically preconditioned implants. Preconditioning the hydrogels for 5 days/week yielded the highest level of mineralisation, with an average 34.4% of the defect mineralised. 3&1 days/week preconditioning resulted in 20.2% & 19% of the defects mineralised, whilst static preconditioning resulted in an average 13% of the defect mineralised.

4.5. Discussion

4.5.1. Chapter overview

In this chapter I aimed to evaluate the hydrostatic bioreactor as a tool for hydrostatically preconditioning hMSC/collagen hydrogels to be used as bone grafts for fracture repair. By hydrostatically stimulating the hydrogels for a different number of days each week, I hypothesised that we could enhance the amount of new bone formed after implantation into a chick femur defect. The first part of the chapter sought to establish and characterise an organotypic fracture repair model. The model consisted of induced fracture in embryonic chick femurs, grafted with hMSC seeded collagen hydrogels, and utilised a borosilicate glass capillary needle to represent internal fixation using an IMN.

Initially I found that the presence of the IMN provided good structural stability to the constructs, allowing ease of fabrication whilst also guiding chick periosteal growth

which bridged the defect during culture. I also observed rapid migration of native chick cells into acellular collagen implants as soon as 24 hrs after defect fabrication, which continued for the 2 week culture period and formed a dense periosteum bridging the defects in both acellular and hMSC seeded implant groups. Migration of hMSCs during culture was monitored using a fluorescent cell tracker and demonstrated integration of hMSCs with the chick bone collar, along the chick periosteum, and into the medullary cavity. I then employed live/dead fluorescent staining to demonstrate the constructs remained viable for the 2 week culture period.

By studying the effect of pressure on the femur constructs using undifferentiated hMSCs in collagen, I found that daily bioreactor stimulation in combination with hMSCs in the implants, increased bone formation in the defects when compared with statically cultured or hydrostatically stimulated constructs without hMSCs. I then used a fluorescent cell tracker to show that cells embedded within the porous trabecular ECM of stimulated implants assumed a more osteocytic morphology compared with cells in the less mineralised statically cultured implants. These initial results first demonstrated that the organotypic femur constructs could recapitulate certain aspects of fracture in the context of bridging of the fracture site, and increased bone formation under experimental conditions. Second, they provided a useful comparison for then assessing the extent of new bone formation in hydrogels receiving hydrostatic preconditioning prior to implantation in the femur constructs.

I then proceeded to hydrostatically precondition hydrogels for 4 weeks prior to implantation into the femur defects. hMSC/collagen hydrogels were stimulated for 1,3 and 5 days/ week with statically cultured gels used as a control. After 4 weeks, analysis by μCT showed that whilst the hydrogels collectively mineralised in a manner similar to that described in **Section 3.3.3**, there was no difference in hydrogel mineralisation and

density between the different preconditioning groups. A small but significant increase in volume was observed in hydrogels stimulated for 5 days/week compared with statically cultured hydrogels. Preconditioned hMSC/collagen hydrogels were then implanted into femur defects and cultured for 2 weeks, and maintained their viability during culture. Interestingly, μCT analysis after 2 weeks indicated that the mineralisation of the implants decreased during culture in the femur defects. No differences were observed between static and hydrostatically preconditioned implants, with an approximate 4 fold decrease in implant mineralisation in across the experimental groups after 2 weeks implanted in the femur constructs.

The final part of this chapter examined experimental results from hydrostatically preconditioned hydrogels using non optimised seeding conditions, and compared them with hydrostatically preconditioned hydrogels manufactured using the optimised seeding conditions described in **Section 3.3.3**. The 2 week preconditioning period showed that daily bioreactor stimulation enhanced the contraction of the hydrogels by encapsulated hMSCs, resulting in smaller volume hydrogels compared with static preconditioning. However, the overall mineralisation of the hydrogels was far lower than hydrogels cultured under the same conditions using the optimised seeding conditions. In contrast to the results described in **Section 4.3.9**, mineralisation of the hydrogels following implantation into the femur defects increased, with hydrogels receiving hydrostatic preconditioning prior to implantation being significantly more mineralised than statically preconditioned hydrogels after a two week culture period.

4.5.2. Cell migration

The organotypic model described in this chapter aimed to recapitulate the *in vivo* fracture repair process *in vitro.* If we look back to chapter 1 in which the stages of fracture repair are detailed, we can compare the stages of fracture repair with observations from this study, and assess to what extent we have successfully recapitulated an *in vivo* repair process. First it must be stated that this model differs considerable from an *in vivo* repair process due to the lack vascular and immune systems that would initiate inflammation and neovascularisation of the fracture site. Despite this, the invasion of fibroblastic periosteal chick cells into the defect region was extensive and occurred almost immediately after the defect was created. The invasion of chick cells occurred from both epiphyseal and distal femur ends and eventually formed a periosteum that encapsulated the defect site entirely. Histological sections of acellular implants showed chick cells to a lesser extent also migrating into central regions of the implant. For hMSC seeded implants the number of migrating chick cells into the implant would likely be less due to the increase in collagen density in cell seeded vs acellular hydrogels(Wu et al. 2014). The invasion of chick cells from both epiphyseal and distal ends to bridge the gap could indicate the presence of directional cues that guide migration across the long axis of the femur. Some reports have has indicated preferred directional growth from the epiphyseal end of the femur when using explanted proliferative zones developing femurs as implants (Smith et al. 2013). In this study, whilst a directional preference of migration was not observed from either distal or epiphyseal end of the femurs, the system still provides a useful model for future study of the migration patterns of native periosteal fibroblasts cells into a fracture site. Further to this, recent developments in transgenic chick embryos with fluorescent proteins could elucidate what signalling events are important in governing invasion of periosteal fibroblasts into a fracture site.

The migration of hMSCs into the medullary cavity, as well as into the chick bone collar was an interesting and unexpected observation. The *in vitro* migratory capacity of MSCs has been shown to increase toward the presence of a variety of chemokines and growthfactors (Ponte et al. 2007). Based on this, it's possible that signalling molecules from the femurs encouraged migration of the hMSCs from the hydrogels into the femur tissue. However, it is likely that these observations simply reflected random migration of MSCs from the defect site into the femur. In either case, this result presents interesting future opportunities to study how changes in the local cell envornment (i.e. from collagen hydrogels to a more physiological bone niche) determine changes in cell behaviour. For example, evidence indicates that Wnt signalling regulates the invasion capacity of hMSCs(Neth et al. 2006). It has been widely demonstrated that wnt signalling also plays an important role in embryonic chick development(Wilson et al. 2001)(Anakwe et al. 2003), and more specifically in developing chick limbs (Kawakami et al. 2001)(Hartmann & Tabin 2000). Hence a useful future study could be to investigate the changes in Wnt mediated signalling events such as β-catenin activity in MSCs as they migrate from the defect site into the medullary cavity of the femur.

4.5.3. Use of internal fixation

The presence of an intramedullary rod in the form of a borosilicate glass capillary tube represented a crucial aspect of success in the model. As mentioned previously the presence of the rod made fabricating the constructs relatively easy, allowed them to be handled in culture. Importantly the presence of the rod did not adversely interact with the either hMSCs or native chick tissue. The rod also appeared provided contact guidance for cells bridging the defect, (**Figure 9D iv**). In humans, IMN's are commonly used for treating femoral shaft non unions (Ricci et al. 2009). They have also proved successful in treating neglected femur shaft non unions (Tall et al. 2012). In terms of recapitulating the

fracture repair processes, the incidence of femur capping reported by Smith el at. (Smith et al. 2014a)(Smith et al. 2014b) might represent a scenario of neglected non-union due to inadequate fixation. The use of the IMN in the form of a boro-silicate capillary needle in this chapter thus overcame this issue, and demonstrates the usefulness of fixatives for improving the performance of organotypic fracture repair models. Further to this, it would be interesting to establish plate fixatives in this model, as well as studying the implant femur interface and its effect on biological tissue such as changes in localised fibrosis and/or mineralisation. One study suggests that increases pressure during physiological total hip replacement implants can exert fluid flow on cells at the implant bone interface (Alidousti et al. 2011). If this were present in our system we might expect to see changes in mineralisation in cells around the IMN due to changes in fluid flow in these regions

4.5.4. Effect of hydrostatic pressure on undifferentiated hMSC/collagen implant femur constructs

Daily hydrostatic pressure significantly increased bone formation in the defects whereas no evidence was found that the presence of hMSCs affected bone formation. This was qualitatively confirmed by comparing µCT sections profiling the density distribution and corresponding histological sections, demonstrating bone mineral deposits within these dense regions. The reduction in defect mineralisation in stimulated acellular defects supports my observations from the previous chapter which describe cell density dependant mineralisation of collagen hydrogels. Interestingly, stimulated hMSC/collagen implants showed a gradient of mineralisation in the implants from the periphery toward the centre. Since it was observed that chick cells formed a periosteum that encapsulated the defect, it could be that cell signalling from the chick cells to hMSCs in the defect enhanced hMSC differentiation and production of mineralised bone matrix. This could

explain why a gradient of mineralisation was observed from the peripheral regions of the defect toward the centre (**Section 4.3.5 Div).** In future experiments it would be useful to characterise if the increase in bone deposition in stimulated hMSC seeded defects was due to hMSCs, native chick cell migrating into the defect, or a combination of both. If the latter case were so it might be useful also to characterise the heterogeneity of the chick cell population around the defect to determine if cell-cell communication by specific bone cell phenotypes influences hMSC differentiation. This in turn could provide useful information on the benefits of different co-culture models to encouraging osteogenic differentiation of MSCs.

4.5.5. Trabecular architecture

The analysis by a two way ANOVA in **Section 4.3.6** indicates that hydrostatic loading of the femurs constructs was the primary stimulus for cell based remodelling of trabecular architecture in the defects. It is generally accepted that bone architecture is not preprogramed in genes and the ability of cells to produce a bone matrix that allows minimal weight with suitable strength is determined by external mechanical stimuli(Huiskes et al. 2000). The results in this chapter appear to be consistent with studies that have investigated dynamic loading, in which hydrostatic stimulation encourages the formation of thicker and more numerous trabecular architecture (Rubin et al. 2002). Interestingly, many of these studies have employed dynamic stimulation on the assumption that physical deformation of the microenvironment is conducive to bone formation. The hydrostatic bioreactor is assumed to apply static loading, where the force is mediated through increasing the external fluid pressure around cells. It appears then that regardless of the nature of force applied (static or dynamic), its effects on trabecular architecture are broadly similar. It may of course be the case that the microenvironment in the model is not static. Without further experimentation, we cannot rule out the

possibility of different pressure gradients existing between the surrounding culture media and the internal structure of the cultured femurs. Indeed different pressures are found to localise in different regions of femurs themselves(Gurkan & Akkus 2008). Computational modelling of bone organ cultures has also suggested that externally applied hydrostatic forces produce significant shear stress at the calcified/noncalcified interface and further concluded that hydrostatic compression resulted in local shear stresses in the ossifying bone centre(Wong & Carter 1990). There is also some experimental evidence confirming this computational hypothesis, in which anabolic responses in bone rudiments exposed to intermittent hydrostatic pressure undergo shear stresses at different tissue interfaces within the explant(Burger et al. 1992). However in a more recent finite element model of hdystatic pressure in explanted bone rudiements, the authors dispute this claim, suggesting that the increase in pressure on cells might instead result in a change in the chemical potential of water in cells themselves, resulting in an equilibration of ions across the cell membrane that lead to cell signalling events (Tanck et al. 1999).

4.5.6. Preconditioned implants

The premise behind using the bioreactor in a clinical setting was based on the hypothesis that it could be used to hydrostatically precondition cell seeded implants. By accelerating the rate at which the tissue matures *in vitro* before implanting it into the patient, I aimed to improve the outcome of healing at the injury site. Whilst in this thesis I was able to produce mineralised collagen hydrogels containing MSC's in static culture, when implanted into the chick femur model, a reduction in the value mineralisation was observed after 2 weeks. This could indicate a period of bone resorption in the implants during this time. The natural process of bone resorption involves the release of acid phosphatase by osteoclasts. As discussed in chapter 1, osteoclast progenitor cells are multi nucleated macrophages generally thought to derive from haematopoietic stem cells

(Boyle et al. 2003). It could be possible that an active population of chick osteoclasts reside in the femurs themselves and could have contributed to the decrease in implant mineralisation during culture. However, an early study on *in vitro* chick femur cultures by Roach showed virtually no bone resorption during culture due to a lack of mature osteoclasts at day 14 of development(Roach 1990). Since the model uses femurs extracted at an even early time point (day 11), and the femurs do not yet show any signs of vascularisation, it seems unlikely that a mature population of chick osteoclasts was present in sufficient numbers demineralise the implants. It is possible that cell secreted collagenases could have caused the reduction in mineralisation in the femurs. Significant remodelling of the defect sight was observed in **Section 4.3.6**, which could have been in part mediated by chick cells secreting collagenases in response to ascorbic acid (D'Angelo et al. 2000). If this were the case then, it's reasonable to suggest that collagenases secreted by native cells induced degradation of the preconditioned implants. Since hMSCs in the preconditioned implants had already undergone differentiation prior to implantation, their ability to lay down new bone matrix to mineralise the defects was likely far lower than the undifferentiated hMSCs used in the first part of this study.

As discussed in the introduction of this chapter, the reduction in mineralisation of preconditioned implants has been reported by a number of groups (Boyle et al. 2003, Lyons et al. 2010, Castano-Izquierdo et al. 2007). A study by Lutolf et al. showed that successful bone healing in rat cranial defects using collagen based implantss was dependant on cell invasion of the implants via integrin and matrix metalloproteinase dependant mechanisms(Lutolf et al. 2003). A summarised view of the results in this chapter appear to be in agree with the hypothesis that cell invasion of the implants is important for encouraging new bone formation. In undifferentiated hMSC and acellular collagen implants, chick periosteal cells were able to invade the implants and mediate

mineralisation in the defect site, possible influencing the differentiation of neighbouring hMSCs with soluble factors. This effect was also present in hydrostatically preconditioned implants using non optimised seeding parameters. Since the hydrogels did not mineralise and had a relatively low density after the 4 week preconditioning period, chick cells were able to invade and mineralise the defect. Supporting this hypothesis was the peripheral mineralisation similar to that observed in undifferentiated hMSC/collagen implants. The effect of 5days/week hydrostatic preconditioning in suboptimal seeding conditions, reduced the overall volume of the constructs by about half that of statically culture hydrogels. This lower surface area may have influenced the observed increase in defect mineralisation in preconditioned hydrogels, since chick cells would have taken less to proliferate and encapsulate the defect site before laying down new bone matrix.

4.6. Conclusion

In this chapter, I designed and constructed an organotypic model of fracture repair using isolated embryonic chick femurs. The model enabled the investigation of implanting hMSC/collagen hydrogels into femur defects to encourage bridging and repair of the fracture site. I tested the use of undifferentiated hMSCs/collagen hydrogels against hydrostatically preconditioned hMSC/collagen hydrogels on the premise that hydrostatic preconditioning of the hydrogels prior to implantation in the defects could enhance repair. I found that daily application of pressure over a 2 week period on entire constructs containing undifferentiated hMSC/collagen hydrogels enhanced the rate of repair. There were no differences in hydrogel mineralisation prior to implantation between statically cultured and hydrostatically preconditioned hydrogels. Further to this, the mineralisation of preconditioned hydrogels was nearly 4 times less than the same hydrogels analysed before implantation. By contrast, hydrostatically preconditioned hydrogels with non-

optimised seeding conditions were poorly mineralised prior to implantation, which allowed chick cells to begin mineralising the defects during the 2 week culture period.

In conclusion, the results from this chapter demonstrate the importance of a combination of hydrostatic pressure and cell invasion of the implant material in driving bone formation in an organotypic fracture repair model. This provides us an excellent platform for future studies in which we can elucidate the underlying biological mechanisms that control this process.

Chapter 5

General discussion and future work

5.1. Summary of hypotheses

The aim of this thesis was to develop and validate a hydrostatic force bioreactor for applications in bone tissue engineering. My approached to address this was to evaluate the bioreactor as a clinical translation platform to hydrostatically preconditioning mesenchymal stem cell seeded scaffolds. In doing so, I aimed to establish if such systems could one day be implemented to overcome limitations in orthopaedic practises which employ temporary fixatives and/or autografts. My hypothesis was that by providing a suitable growth environment for adult stem cells, I could generate tissue engineered bone grafts *in vitro* that would be suitable to treat non-union fractures. I aimed to prove a level of preclinical efficacy that would demonstrate the usefulness of these systems in translating bone tissue engineering from the lab to the clinic.

To evaluate preclinical efficacy, I first wanted validate that the bioreactor induced changes in cell behaviour, and that these changes were consistent with the current body of literature reporting cellular responses to hydrostatic loading. Second, I aimed to establish if the bioreactor was effective in accelerating the rate of bone formation in cell seeded scaffolds, which represents a viable route to generate tissue engineered bone grafts. In addressing the second aim of this thesis, I focused heavily on the environmental factors that influence stem cell behaviour in collagen type 1 scaffolds. The final part of this thesis aimed to establish an organotypic preclinical model that accurately recapitulates the process of fracture repair, whilst also overcoming the ethical concerns of using live animal models.

Ultimately, in exploring these facets of bone tissue engineering, I wanted to define a logical approach to determine the efficacy of hydrostatic force bioreactors as translational tools in the field of regenerative medicine.

5.2. Outcome of initial hypotheses

The outcome of my initial hypotheses is that whilst the bioreactor is very useful from a research point of view, the system in its current form may not be appropriate for preconditioning hMSC/collagen hydrogels to be used as bone implants. Despite changes in the contraction of hydrostatically preconditioned hydrogels in **Section 4.4**, I have drawn this conclusion based on two main experimental findings:

- Mature osteogenic phenotypes (late stage osteoblasts) and MSC precursors responded differently to hydrostatic loading in the bioreactor, with late stage osteoblasts responding in a way that is more consistent with the current literature describing mechanotransduction in cells.
- Committed osteoblast phenotypes (MG63s) responded to hydrostatic loading in monolayers and 3D collagen scaffolds by producing more bone matrix than static controls. Whilst I succeeded in generating mineralised bone matrix in MSC seeded collagen scaffolds after 4 weeks, the addition of daily hydrostatic loading did not increase the rate of bone formation.

5.3. Addressment of outcomes

There could a number of reasons why hydrostatic loading did not enhance mineralisation of the MSCs/collagen hydrogels, and it may be that with further experimentation we might find the bioreactor can indeed enhance osteogenic differentiation and bone formation by primary human stem cells. First we must consider that the experiments using MSCs were performed from a single donor. It has been known for a period of time now the osteogenic potential of MSCs from different donors is highly variable (Phinney et al. 1999). It may that screening of different donors in our bioreactor system could determine if the bioreactor can in fact enhance bone formation in MSCs. Coupled with this, bone marrow derived stem cells within a single donor contain a heterogeneous population of cells. This population can be isolated into homogeneous populations

that carry different levels of potency with respect to specific differentiation potentials (Boxall & Jones 2012). It might be that different populations of adult stem cell carry different levels of 'osteogenic potential' with respect to their response to hydrostatic loading. This could therefore warrant testing the response of MSCs characterised to and isolated to express particular surface markers such as Stro-1 or SSEA-4(Feng-Juan lv et al. 2014). Another potential argument could be that whilst collagen provided a suitable environment for MG63s to respond positively to pressure, it may not have been adequate for generating responses in hMSCs. Further studies in different material scaffolds might elucidate a bone forming response in hMSC due to bioreactor stimulation that was not observed using collagen scaffolds.

Aside from these considerations, it could be that MSCs are not as responsive to hydrostatic pressure as more differentiated phenotypes. This was a common theme throughout this thesis. In chapter 2, late stage OB MLOA5 cells were more responsive than MSCs to hydrostatic pressure. In chapter 3, pre-osteoblast MG63s encapsulated in collagen were more responsive to hydrostatic pressure than MSCs encapsulated in collagen, described in chapter 4. Coupled with this, in chapter 4 we also saw what appeared to be a gradient of mineralisation from the outside toward the centre of our stimulated femur defects containing what were initially undifferentiated MSCs. This implied that the response of chick cells to hydrostatic pressure (which has been demonstrated previously (Henstock et al. 2013)) influenced the differentiation of the implanted MSCs. Whilst there is an extensive body of literature documenting the interaction of OSs, OBs and MSCs in the context of stem cell differentiation, surprisingly little has been done to characterise changes in the functional responses of cells to hydrostatic loading as they undergo differentiation. That is to say, if we differentiate a mesenchymal stem cell into an OB and then into an osteocyte, what are the changes in its response to hydrostatic loading?

Current evidence describes changes in the cytoskeletal network and correspondingly resistance to cytoskeletal disruption in MSCs as they undergo differentiation toward a more osteoblastic phenotype (Rodríguez et al. 2004)(Yourek et al. 2007). Since in chapter 3 we saw

changes between MSCs and late stage osteoblasts (and also MG63 osteoblasts like cells in chapter 4) in their ability to undergo cytoskeletal modelling, it's not unreasonable to hypothesise that a potential mechanosensory mechanism could be underpinned by changes in the cytoskeletal as cells differentiate. It would not be difficult to test this hypothesis in future experiments. Recent advances in differentiation protocols of MSCs to osteocyte phenotypes (Thompson et al. 2015) could allow us to determine if changes in the cell cytoskeletal during osteogenic differentiation dictate their ability to respond to hydrostatic loading.

5.4. Drawing parallels in the results

Although as discussed above my initial hypothesis was not confirmed, throughout the body of this research there existing distinct commonalities in the results that yield some interesting discussion points. The first commonalty was the effect of substrate stiffness on ALP activity in **Section 2.3.2.6** and collagen concentration dependant changes in bone formation in **Section 3.3.3.3.** It has been shown that increases in concentration of acellular collagen hydrogels is proportional to changes in hydrogel stiffness via a power law relationship (Yang et al. 2009) with an exponent value ~ 0.67, the same relationship and also exponent value of that found in **Section 3.3.3.3c.** This implies that increases in collagen concentration in my hydrogel would see corresponding increases in hydrogel stiffness, thus increasing bone formation. We could expand this idea to incorporate changes in cell density and stiffness, since if MSCs are mineralising their surrounding matrix and they are closer together as a result of cell density, then the overall stiffness of the construct would increase, potentially creating a positive feedback mechanism. It's reasonable to postulate that had ALP staining of the hydrogels been done, we would have observed both concentration and cell density dependant increases in ALP staining due to an increase in ECM stiffness. Interestingly Yang et al cite earlier theoretical models which predict concentration dependant changes in the stiffness of semi flexible polymers solutions, a consequence of which is the formation of liquid crystal phases above certain critical concentrations (Morse 1998)(Khokhlov 1978) (see **Section 5.6 and Appendix Ch2).**

5.5. Pre-clinical research potential of the bioreactor

5.5.1 High throughput screening

Since the response of osteocytes to hydrostatic loading is thought to be one of the mechanisms that regulates bone homeostasis, it's reasonable to suggest that changes in their response to mechanical loading occur as they transition from a healthy to an osteoporotic phenotype. One study indicates an interaction between the Sost gene and Wnt signalling to be responsible for regulating osteocyte response to mechanical stimuli (Lin et al. 2009), which might suggest changes in this pathway in cells from healthy and osteoporotic donors. Others have pointed towards the shape of osteocyte in determining their mechanosensitivity, with rounded morphologies producing higher levels of NO than flat morphologies (Bacabac et al. 2008), implying the ECM environment of osteocyte lacuna may play a part in determining osteocyte mechanosenstivity. However, there is evidence challenging this hypothesis, whereby no significant differences were observed in osteocyte lacuna size and shape between healthy and osteoporotic bone tissue (McCreadie et al. 2004). Aside from the uncertainty in the literature regarding mechanosenstivity in osteocytes, we can infer that hydrostatic bioreactor described in this thesis could provide a screening platform to study changes in mechanosensitivity in cells isolated from different disease states. Since the bioreactor houses standard tissue culture plates (which are commercially available in sizes of 6-384 wells), it could allow rapid and high throughput study of changes in for example NO production between healthy and osteoporotic bone cells. Additionally, the system could also be used to identify drug compounds designed to restore function to diseased cell phenotypes, generating valuable preclinical data for the development of pharmacological strategies to treat osteoporosis.

5.5.2. Leaning from developmental systems

In chapter 4, whilst I did not delineate whether new bone in stimulated hMSC/collagen defects was produced by chick cells or MSCs (or both), it highlights the need for biomimetic niches *in vitro* that incorporate not just an appropriate cell matrix environment, but also mixed populations of cells that complement their behaviour in the context of enhancing tissue formation. This concept is already well established in the literature through the development of co-culture models, which is in some respects is what the organotypic model in chapter 4 represents. One potential advantage in considering the fracture repair model as a form of co-culture is the flexibility in the design of the model. This enables us to further study of how developmental cues from the embryonic femur determine the behaviour of adult human MSCs.

I discussed in chapter 1, there are inherent difficulties in translating animal models into humans due to interspecies differences. Since in our fracture repair model we are using human cells in an animal model, we can provide direct evidence of interspecies translation that could help us understand what factors are important in driving bone formation in mesenchymal stem cells. As an example, organotypic chick femurs can be isolated at a range of different developmental stages, each of which exhibit different expression levels of markers associated with skeletal development (collagen type I/II, Stro-1) (Kanczler et al. 2012). Based on this, using the organotypic fracture repair model, we could test changes in the differentiation potential of human MSCs due to cell signalling from chick skeletal cells at different stages of development. In addition, it has also been demonstrated that chick femurs produce more bone at later stages of development in response to hydrostatic pressure (Henstock et al. 2013). Firstly this observation supports our previous hypothesis that more mature osteogenic phenotypes more effectively translate hydrostatic pressure into bone forming responses. Second, by studying the changes in cell signalling from chick cells due to hydrostatic loading at different developmental stages, we could identify candidate signalling events that enhance hydrostatically induced osteogenic differentiation of human MSCs. Thus by combining organotypic developmental models with adult stem cells from humans, we may be able to overcome the translational problems associated

with interspecies differences, whilst also adhering to the three R's principle, generating more ethical robust preclinical evaluation of bone tissue engineering strategies.

5.6. The ECM environment

Another recurring theme in the experimental outcomes of this thesis was the importance of an ECM environment that more closely recapitulates the native bone niche. This was seen in chapter 2, whereby a stiff ECM was required to allowing MSCs to undergo osteogenic differentiation. In chapter 3, providing the appropriate ratio of ECM and cells allowed MSCs generate a densely mineralised matrix environment that was rich in proteins typically found in the native bone niche. Moreover, this process had a high rate of predictability, in which the physical amount of collagen present in the ECM determined the mineralisation and density of the hydrogel, and also the distribution of the encapsulated cells. What was particularly interesting about this process was first the linear dependence of bone formation on the cellular distribution, and secondly the end point collagen concentration of a low vs high initial concentration. Lower starting concentrations resulted in much higher final concentrations with a densely packed cell matrix structure, resulting in more mature bone tissue formation by MSCs over 4 weeks.

As mentioned previously, a common observation throughout this thesis was that small changes in the ECM environment had a large impact on the development of the resultant tissue. This would likely have impacted too on a cells ability to respond to hydrostatic pressure. Based on this, I believe that in order to elucidate a maximal output response from hydrostatic force bioreactors such as the one described in this thesis; we must ask, what are the environmental factors that most effectively allow stem cells to undergo osteogenic differentiation *in vitro?* Based on the evidence reported by the literature, coupled with the evidence presented in this thesis, I propose that an appropriate ECM environment to initiate differentiation and bone formation in MSCs should provide.

- The appropriate soluble factors and signalling molecules that induce differentiation of MSCs, of which the correct combination of factors should be based models studying developmental bone niches.
- Environments that accurately recapitulate the change in spatial, conformational and mechanical properties of the ECM as cells undergo the transition from MSC precursor to encapsulated osteocyte. Biphasic scaffolds being developed for osteochondral repair might represent a fulfilment of this requirement.
- Environments that accurately recapitulate the change in protein and mineral concentration of the ECM as cells undergo the transition from MSC precursor to encapsulated osteocyte.

If these goals can be achieved in the future, then applying hydrostatic pressure using bioreactors systems might provide the appropriate forms of stimuli as MSCs undergo osteogenic differentiation. For example in an ideal biphasic scaffold, we might picture higher levels of strain being exerted in one area of the scaffold, containing less committed bone cell phenotypes (the stem cell pool). Then by contrast, lower levels of strain and higher levels of hydrostatic pressure and/or fluid flow being exerted in areas of the scaffold containing more differentiated cell phenotypes such as osteoblasts and osteocytes. Due to the nature of biphasic scaffold systems, application of a single external force would result in multiply forms of mechanical stimuli to cells in different regions of the scaffold (**Figure 2A)**.

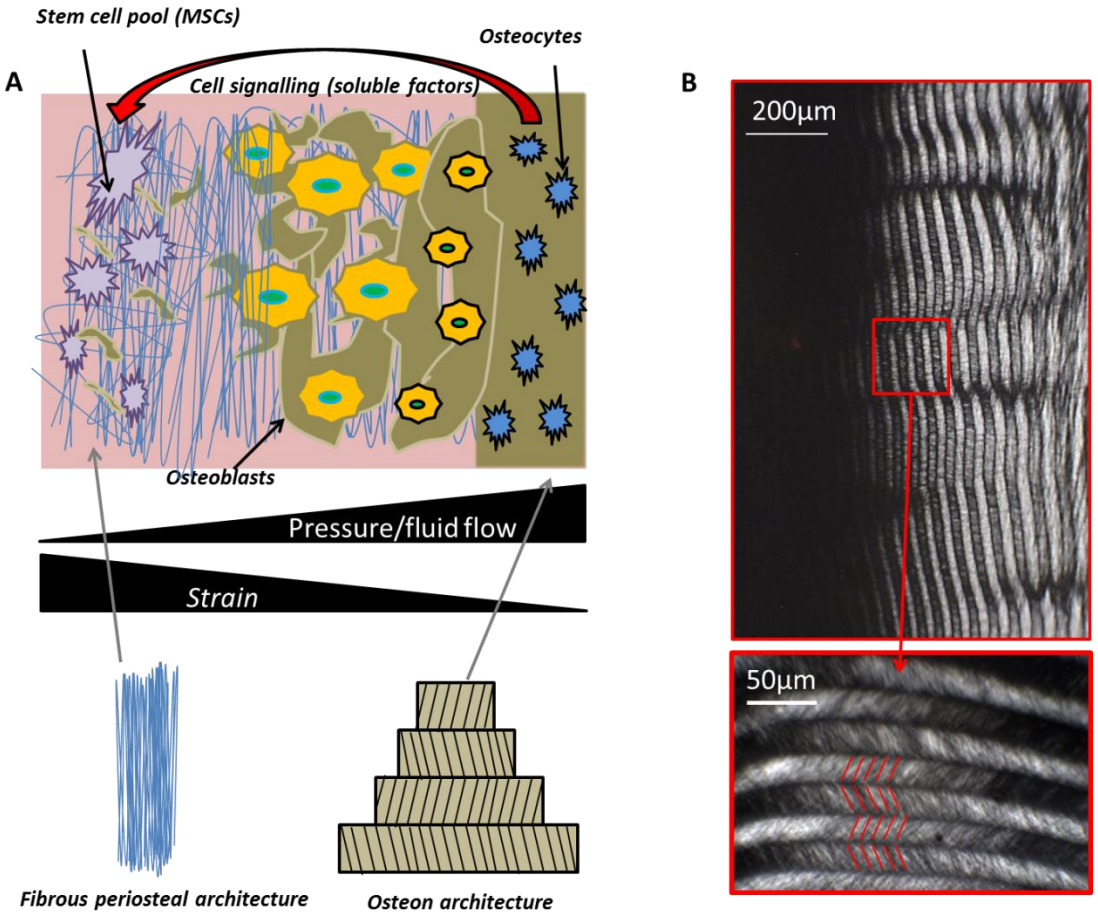

Figure 1. A) Cartoon representation of a biphasic scaffold concept. B) Production of lamellar arrangements of collagen type 1 that mimic osteon architecture.

The concept of biphasic scaffolds containing gradient niches might one day allow truly biomimetic tissue equivalents to be grown *in vitro*, enabling the researcher to elucidate how the cell-matrix environment influences mechanically induced turnover of bone.

Figure 2B represents one potential avenue for addressing the problem of generating hierarchical tissue structures. **Figure 2B,** whilst is not detailed in the main body of this thesis (**see appendix ch2**), was the result of attempting to address the standardisation issue encountered with collagen hydrogels discussed in **Section 4.4**. It became apparent that the behaviour of collagen type 1 at very high concentrations (>50mgs/ml) was

remarkable different to the behaviour at commercially available concentrations (3-11mg/ml). At these higher concentrations, the self-assembly process of collagen adopts liquid crystalline phase behaviour, resulting in architectures that mimic the hierarchical structure of bone. Consequently this may also imply that the lamellar structure of bone and indeed many other tissue structures are the result of a similar physiochemical process. To that end, one aspect of future work that will follow on from this thesis is to explore the underlying mechanisms that control this process. By attempting to more closely mimic the architecture of native bone, it is hoped a deeper understanding can be obtained of how the ECM environment governs a cells response to mechanical forces such as hydrostatic pressure.

References

- Adachi, T. et al., 2009. Calcium response in single osteocytes to locally applied mechanical stimulus: Differences in cell process and cell body. Journal of Biomechanics, 42(12), pp.1989–1995.
- Aerssens, J. et al., 1998. Interspecies differences in bone composition, density, and quality: Potential implications for in vivo bone research. Endocrinology, 139(2), pp.663–670.
- Afoke, N.Y., Byers, P.D. & Hutton, W.C., 1987. Contact pressures in the human hip joint. The Journal of bone and joint surgery. British volume, 69(4), pp.536–541.
- Ahlmann, E. et al., 2002. Comparison of anterior and posterior iliac crest bone grafts in terms of harvest-site morbidity and functional outcomes. The Journal of bone and joint surgery. American volume, 84-A(5), pp.716–20.
- Aishwarya, S., 2008. Collagen-coated polycaprolactone microparticles as a controlled drug delivery system. Journal of …, 25(5), pp.298–306.
- Albrektsson, T. & Johansson, C., 2001. Osteoinduction, osteoconduction and osseointegration. European Spine Journal, 10(SUPPL. 2), pp.96–101.
- Alidousti, H., Taylor, M. & Bressloff, N.W., 2011. Do capsular pressure and implant motion interact to cause high pressure in the periprosthetic bone in total hip replacement? Journal of biomechanical engineering, 133(12), p.121001.
- Amini, A.R., Laurencin, C.T. & Nukavarapu, S.P., 2012. Bone tissue engineering: recent advances and challenges. Critical reviews in biomedical engineering, 40(5), p.2.
- Anakwe, K. et al., 2003. Wnt signalling regulates myogenic differentiation in the developing avian wing. Development (Cambridge, England), 130(15), pp.3503–3514.
- Anderson, C.T. et al., 2008. Primary cilia: Cellular sensors for the skeleton. Anatomical Record, 291(9), pp.1074–1078.
- Angele, P. et al., 2003. Cyclic hydrostatic pressure enhances the chondrogenic phenotype of human mesenchymal progenitor cells differentiated in vitro. Journal of orthopaedic research : official publication of the Orthopaedic Research Society, 21, pp.451–457.
- Antebi, B. et al., 2013. Biomimetic collagen-hydroxyapatite composite fabricated via a novel perfusion-flow mineralization technique. Tissue engineering. Part C, Methods, 19(7), pp.487–96. Available at: http://www.pubmedcentral.nih.gov/articlerender.fcgi?artid=3662382&tool=pmcentrez&rendertype=abstract.
- Arnsdorf, E.J. et al., 2009. Mechanically induced osteogenic differentiation--the role of RhoA, ROCKII and cytoskeletal dynamics. Journal of cell science, 122(Pt 4), pp.546–53.

Available at: http://www.pubmedcentral.nih.gov/articlerender.fcgi?artid=2714434&tool=pmcentrez&rendertype=abstract [Accessed February 4, 2015].

- Aubin, J.E., 2001. Regulation of osteoblast function and formation. Reviews in Endocrine & Metabolic Disorders, 2(1), pp.81–94.
- Awad, H. a et al., 2000. In vitro characterization of mesenchymal stem cell-seeded collagen scaffolds for tendon repair: effects of initial seeding density on contraction kinetics. Journal of Biomedical Materials Research, 51(2), pp.233–240. Available at: http://www.ncbi.nlm.nih.gov/pubmed/10825223.
- Baas, E. et al., 2010. In vitro bone growth responds to local mechanical strain in three-dimensional polymer scaffolds. Journal of Biomechanics, 43(4), pp.733–739.
- Babensee, J.E. et al., 1998. Host response to tissue engineered devices. Advanced Drug Delivery Reviews, 33(1-2), pp.111–139. Available at: http://www.sciencedirect.com/science/article/pii/S0169409X98000234.
- Babis, G.C. & Soucacos, P.N., 2005. Bone scaffolds: the role of mechanical stability and instrumentation. Injury, 36 Suppl 4, pp.S38–44. Available at: http://www.ncbi.nlm.nih.gov/pubmed/16291322 [Accessed March 1, 2013].
- Bacabac, R.G. et al., 2008. Round versus flat: Bone cell morphology, elasticity, and mechanosensing. Journal of Biomechanics, 41(7), pp.1590–1598.
- Bain, G. et al., 2003. Activated β-catenin induces osteoblast differentiation of C3H10T1/2 cells and participates in BMP2 mediated signal transduction. Biochemical and Biophysical Research Communications, 301(1), pp.84–91. Available at: http://linkinghub.elsevier.com/retrieve/pii/S0006291X02029510 [Accessed August 14, 2013].
- Batra, N. et al., 2012. Mechanical stress-activated integrin α5β1 induces opening of connexin 43 hemichannels. Proceedings of the National Academy of Sciences of the United States of America, 109(9), pp.3359–64.
- Birmingham, E., Niebur, G. & McHugh, P., 2012. Osteogenic differentiation of mesenchymal stem cells is regulated by osteocyte and osteoblast cells in a simplified bone niche. European cells & materials, 23(353), pp.13–27.
- Bivi, N. et al., 2012. Cell autonomous requirement of connexin 43 for osteocyte survival: Consequences for endocortical resorption and periosteal bone formation. Journal of Bone and Mineral Research, 27(2), pp.374–389.
- Boden, S.D. et al., 1998. Laparoscopic anterior spinal arthrodesis with rhBMP-2 in a titanium interbody threaded cage. Journal of spinal disorders, 11(2), pp.95–101. Available at: http://www.ncbi.nlm.nih.gov/pubmed/9588464.

- Bolgen, N. et al., 2008. Three-dimensional ingrowth of bone cells within biodegradable cryogel scaffolds in bioreactors at different regimes. Tissue Eng Part A, 14(10), pp.1743–1750.
- Bonewald, L.F. et al., 2006. Mechanism by which MLO-A5 late osteoblasts/early osteocytes mineralize in culture: similarities with mineralization of lamellar bone. Calcified tissue …, 79(5), pp.340–353.
- Bonewald, L.F., 2007. Osteocytes as dynamic multifunctional cells. Annals of the New York Academy of Sciences, 1116, pp.281–290.
- Bonewald, L.F., 2011. The amazing osteocyte. Journal of bone and mineral research : the official journal of the American Society for Bone and Mineral Research, 26(2), pp.229–38.
- Bouet, G. et al., 2015. Validation of an in Vitro 3D Bone Culture Model With Perfused and Mechanically Stressed Ceramic Scaffold. European Cells and Materials, 29, pp.250–267.
- Boxall, S.A. & Jones, E., 2012. Markers for characterization of bone marrow multipotential stromal cells. Stem Cells International.
- Boyle, W.J., Simonet, W.S. & Lacey, D.L., 2003. Osteoclast differentiation and activation. Nature, 423(May), pp.337–342.
- Brenner, S.L. & Korn, E.D., 1980. The effects of cytochalasins on actin polymerization and actin ATPase provide insights into the mechanism of polymerization. Journal of Biological Chemistry, 255(3), pp.841–844.
- Brown, R.A., 2013. In the beginning there were soft collagen-cell gels: Towards better 3D connective tissue models? Experimental Cell Research, 319(16), pp.2460–2469.
- Brumback, R.J. et al., 1988. Intramedullary nailing of femoral shaft fractures. Part I: Decision-making errors with interlocking fixation. The Journal of bone and joint surgery. American volume, 70(10), pp.1441–52. Available at: http://www.ncbi.nlm.nih.gov/pubmed/3198668.
- Bueno, E.M. & Glowacki, J., 2009. Cell-free and cell-based approaches for bone regeneration. Nature reviews. Rheumatology, 5(12), pp.685–697. Available at: http://dx.doi.org/10.1038/nrrheum.2009.228.
- Burge, R. et al., 2008. THE COST OF OSTEOPOROTIC FRACTURES IN THE UNITED KINGDOM. Value in Health, 4(2), pp.66–67.
- Burger, E.H., Klein-Nulend, J. & Veldhuijzen, J.P., 1992. Mechanical stress and osteogenesis in vitro. Journal of bone and mineral research : the official journal of the American Society for Bone and Mineral Research, 7 Suppl 2, pp.S397–401. Available at: http://www.ncbi.nlm.nih.gov/pubmed/24036726.
- Burr, D.B. et al., 1996. In vivo measurement of human tibial strains during vigorous activity. Bone, 18(5), pp.405–410.

- Byers, B.A. et al., 2006. Effects of Runx2 genetic engineering and in vitro maturation of tissue-engineered constructs on the repair of critical size bone defects. Journal of Biomedical Materials Research - Part A, 76(3), pp.646–655.
- Cardó-Vila, M., Arap, W. & Pasqualini, R., 2003. αvβ5 integrin-dependent programmed cell death triggered by a peptide mimic of annexin V. Molecular Cell, 11, pp.1151–1162.
- Castano-Izquierdo, H. et al., 2007. Pre-culture period of mesenchymal stem cells in osteogenic media influences their in vivo bone forming potential. Journal of Biomedical Materials Research - Part A, 82(1), pp.129–138.
- Chan, M.E. et al., 2009. A Trabecular Bone Explant Model of Osteocyte-Osteoblast Co-Culture for Bone Mechanobiology. Cellular and molecular bioengineering, 2(3), pp.405–415. Available at: http://www.pubmedcentral.nih.gov/articlerender.fcgi?artid=2935082&tool=pmcentrez&rendertype=abstract.
- Chen, J.-H. et al., 2010. Boning up on Wolff's Law: mechanical regulation of the cells that make and maintain bone. Journal of biomechanics, 43(1), pp.108–18. Available at: http://www.ncbi.nlm.nih.gov/pubmed/19818443 [Accessed March 11, 2013].
- Chen, M., Sun, Y. & Zhao, C., 2007. Factors related to contraction and mechanical strength of collagen gels seeded with canine endotenon cells. … Research Part B: …, 82B(2), pp.519–525. Available at: http://onlinelibrary.wiley.com/doi/10.1002/jbm.b.30757/full [Accessed August 17, 2015].
- Chen, N.X. et al., 2000. Ca(2+) regulates fluid shear-induced cytoskeletal reorganization and gene expression in osteoblasts. American journal of physiology. Cell physiology, 278(5), pp.C989–C997.
- Cheng, A. et al., 2014. Additively manufactured 3D porous Ti-6Al-4V constructs mimic trabecular bone structure and regulate osteoblast proliferation, differentiation and local factor production in a porosity and surface roughness dependent manner. Biofabrication, 6(4), p.045007.
- Chenyu, H. & Rei, O., 2012. Effect of Hydrostatic Pressure on Bone Regeneration using human mesenchymal stem cells. TISSUE ENGINEERING: Part A, 18(20), pp.2106–2113.
- Chow, S.Y. et al., 1984. Electrophysiological Properties of Osteoblastlike Cells from the Cortical Endosteal Surface of Rabbit Long Bones Preparation o f Osteoblastlike Cells on Collagen Gel for Membrane Potential Measurements. Calcified Tissue International, pp.401–408.
- Christensen, S.T. et al., 2007. Sensory cilia and integration of signal transduction in human health and disease. Traffic (Copenhagen, Denmark), 8(2), pp.97–109. Available at: http://www.ncbi.nlm.nih.gov/pubmed/17241444 [Accessed February 28, 2013].

- Chung, P., Zhou, S. & Eslami, B., 2014. Effect of age on regulation of human osteoclast differentiation. Journal of cellular …, (February 2014), pp.1–27. Available at: http://www.ncbi.nlm.nih.gov/pubmed/24700654\nhttp://onlinelibrary.wiley.com/doi/10.1002/jcb.24792/abstract.
- Collin-Osdoby, P. et al., 2000. Decreased nitric oxide levels stimulate osteoclastogenesis and bone resorption both in vitro and in vivo on the chick chorioallantoic membrane in association with neoangiogenesis. Journal of bone and mineral research : the official journal of the American Society for Bone and Mineral Research, 15(3), pp.474–88. Available at: http://www.ncbi.nlm.nih.gov/pubmed/10750562.
- Cook, S.D. et al., 2002. Healing course of primate ulna segmental defects treated with osteogenic protein-1. Journal of Investigative Surgery, 15(2), pp.69–79.
- Cooper, C. et al., 2006. Review: developmental origins of osteoporotic fracture. Osteoporosis international : a journal established as result of cooperation between the European Foundation for Osteoporosis and the National Osteoporosis Foundation of the USA, 17(3), pp.337–47. Available at: http://www.ncbi.nlm.nih.gov/pubmed/16331359 [Accessed July 16, 2014].
- Correia, C. et al., 2012. Dynamic Culturing of Cartilage Tissue : The Significance of Hydrostatic Pressure. TISSUE ENGINEERING: Part A, 18, pp.1979–1990.
- Costa, D.O. et al., 2013. The differential regulation of osteoblast and osteoclast activity by surface topography of hydroxyapatite coatings. Biomaterials, 34(30), pp.7215–26. Available at: http://www.sciencedirect.com/science/article/pii/S014296121300700X.
- Cukierman, E. & Bassi, D., 2010. Physico-mechanical aspects of extracellular matrix influences on tumorigenic behaviors. Seminars in cancer biology, 20(3), pp.139–145. Available at: http://www.sciencedirect.com/science/article/pii/S1044579X10000258 [Accessed December 8, 2014].
- Czekanska, E. et al., 2012. In search of an osteoblast cell model for in vitro research. Eur Cell Mater, 24, pp.1–17. Available at: http://www.ecmjournal.org/journal/papers/vol024/pdf/v024a01.pdf [Accessed November 11, 2014].
- Czekanska, E.M. et al., 2014. A phenotypic comparison of osteoblast cell lines versus human primary osteoblasts for biomaterials testing. Journal of Biomedical Materials Research Part A, 102(8), pp.2636–2643. Available at: http://doi.wiley.com/10.1002/jbm.a.34937.
- Czekanska, E.M. et al., 2014. A phenotypic comparison of osteoblast cell lines versus human primary osteoblasts for biomaterials testing. Journal of Biomedical Materials Research Part A, 102(8), pp.2636–2643. Available at: http://doi.wiley.com/10.1002/jbm.a.34937.
- D'Angelo, M. et al., 2000. MMP-13 is induced during chondrocyte hypertrophy. Journal of Cellular Biochemistry, 77(4), pp.678–693.

- Dai, X. et al., 2013. Phosphorylation of angiomotin by Lats1/2 kinases inhibits F-actin binding, cell migration, and angiogenesis. Journal of Biological Chemistry, 288(47), pp.34041–34051.
- Davidson, R.M., Tatakis, D.W. & Auerbach, a L., 1990. Multiple forms of mechanosensitive ion channels in osteoblast-like cells. Pflügers Archiv : European journal of physiology, 416(6), pp.646–51. Available at: http://www.ncbi.nlm.nih.gov/pubmed/1701046.
- Dawson, J.I. et al., 2014. Concise review: bridging the gap: bone regeneration using skeletal stem cell-based strategies - where are we now? Stem cells (Dayton, Ohio), 32(1), pp.35–44. Available at: http://www.ncbi.nlm.nih.gov/pubmed/24115290.
- de Peppo, G.M. et al., 2013. Engineering bone tissue substitutes from human induced pluripotent stem cells. Proceedings of the National Academy of Sciences of the United States of America, 110(21), pp.8680–5. Available at: http://www.pubmedcentral.nih.gov/articlerender.fcgi?artid=3666730&tool=pmcentrez&rendertype=abstract.
- Delaine-Smith, R.M., Sittichokechaiwut, A. & Reilly, G.C., 2014. Primary cilia respond to fluid shear stress and mediate flow-induced calcium deposition in osteoblasts. The FASEB Journal, 28(1), pp.430–439. Available at: http://www.fasebj.org/cgi/doi/10.1096/fj.13-231894.
- Delling, M. et al., 2016. Primary cilia are not calcium-responsive mechanosensors. Nature, 531, pp.656–660.
- Delloye, C. et al., 1998. Simple bone cysts treated with aspiration and a single bone marrow injection. A preliminary report. International orthopaedics, 22(2), pp.134–8.
- Dhillon, M. & Dhatt, S., 2012. First aid and emergency mangament in bone injuries 1st editio. P. De Boer, ed., JP medical Ldt.
- DiResta, G.R. et al., 2005. Cell Proliferation of Cultured Human Cancer Cells are Affected by the Elevated Tumor Pressures that Exist In Vivo. Annals of Biomedical Engineering, 33(9), pp.1270–1280. Available at: http://link.springer.com/10.1007/s10439-005-5732-9 [Accessed March 16, 2015].
- Discher, D.E., Janmey, P. & Wang, Y.-L., 2005. Tissue cells feel and respond to the stiffness of their substrate. Science (New York, N.Y.), 310(5751), pp.1139–43. Available at: http://www.ncbi.nlm.nih.gov/pubmed/16293750.
- Dixon, J.E. et al., 2014. Combined hydrogels that switch human pluripotent stem cells from self-renewal to differentiation. Proceedings of the National Academy of Sciences of the United States of America, 111(15), pp.5580–5. Available at: http://www.pnas.org/content/111/15/5580.abstract.

- Dominici, M. et al., 2006. Minimal criteria for defining multipotent mesenchymal stromal cells. The International Society for Cellular Therapy position statement. Cytotherapy, 8(4), pp.315–7. Available at: http://www.ncbi.nlm.nih.gov/pubmed/16923606 [Accessed May 21, 2013].
- Dong, J. et al., 2007. Elucidation of a Universal Size-Control Mechanism in Drosophila and Mammals. Cell, 130(6), pp.1120–1133.
- Dragoo, J. et al., 2005. Tissue-engineered bone from BMP-2- transduced SCs derived from human fat. Plast Reconstr Surg, 115, p.1665.
- Driscoll, T.P. et al., 2015. Cytoskeletal to Nuclear Strain Transfer Regulates YAP Signaling in Mesenchymal Stem Cells. Biophysical Journal, 108(12), pp.2783–2793. Available at: http://www.sciencedirect.com/science/article/pii/S0006349515004956.
- Drukker, M., 2004. Immunogenicity of human embryonic stem cells: Can we achieve tolerance? Springer Seminars in Immunopathology, 26, pp.201–213.
- Dupont, S. et al., 2011. Role of YAP/TAZ in mechanotransduction. Nature, 474(7350), pp.179–183. Available at: http://dx.doi.org/10.1038/nature10137.
- el Haj, a J. et al., 1999. Mechanotransduction pathways in bone: calcium fluxes and the role of voltage-operated calcium channels. Medical & biological engineering & computing, 37(3), pp.403–409.
- El Haj, A.J. et al., 2012. An in vitro model of mesenchymal stem cell targeting using magnetic particle labelling. Journal of tissue engineering and regenerative medicine. Available at: http://www.ncbi.nlm.nih.gov/pubmed/23281176\nhttp://onlinelibrary.wiley.com/doi/10.1002/term.1636/full.
- Engler, A.J. et al., 2006. Matrix elasticity directs stem cell lineage specification. Cell, 126(4), pp.677–89. Available at: http://www.ncbi.nlm.nih.gov/pubmed/16923388 [Accessed July 9, 2014].
- F. M. Watt; T. S. Huck, 2013. Role of the extracellular matrix in regulating stem cell fate. Nature Reviews Molecular Cell Biology, 14, pp.467–474.
- Fan, X. et al., 2004. Nitric oxide regulates receptor activator of nuclear factor-kappaB ligand and osteoprotegerin expression in bone marrow stromal cells. Endocrinology, 145(2), pp.751–9. Available at: http://www.ncbi.nlm.nih.gov/pubmed/14563699 [Accessed September 30, 2015].
- Feichtinger, G. a et al., 2011. Enhanced reporter gene assay for the detection of osteogenic differentiation. Tissue engineering. Part C, Methods, 17(4), pp.401–410.
- Feldkamp, L. a et al., 1989. The direct examination of three-dimensional bone architecture in vitro by computed tomography. Journal of bone and mineral research, 4(1), pp.3–11.

- Feng-Juan lv et al., 2014. The surface markers and identity of human mesenchymal stem cells. Stem cells, pp.1–18. Available at: http://www.ncbi.nlm.nih.gov/pubmed/24578244.
- Ferguson, C. et al., 1999. Does adult fracture repair recapitulate embryonic skeletal formation? Mechanisms of Development, 87(1-2), pp.57–66.
- Fox, S.W., Chambers, T.J. & Chow, J.W., 1996. Nitric oxide is an early mediator of the increase in bone formation by mechanical stimulation. American Journal of Physiology - Endocrinology and Metabolism, 270, pp.E955–E960.
- Francis, C.S. et al., 2013. rhBMP-2 with a demineralized bone matrix scaffold versus autologous iliac crest bone graft for alveolar cleft reconstruction. Plastic and reconstructive surgery, 131, pp.1107–15. Available at: http://www.ncbi.nlm.nih.gov/pubmed/23385986.
- Friedenstein, a J., Piatetzky-Shapiro, I.I. & Petrakova, K. V, 1966. Osteogenesis in transplants of bone marrow cells. Journal of embryology and experimental morphology, 16(3), pp.381–390.
- Friedenstein, A.J., Chailakhjan, R.K. & Lalykina, K.S., 1970. The development of fibroblast colonies in monolayer cultures of guinea-pig bone marrow and spleen cells. Cell and tissue kinetics, 3(4), pp.393–403. Available at: http://onlinelibrary.wiley.com/doi/10.1111/j.1365-2184.1970.tb00347.x/abstract.
- García, J.R. & García, A.J., 2014. Cellular mechanotransduction: sensing rigidity. Nature materials, 13(6), pp.539–40. Available at: http://www.nature.com/nmat/journal/v13/n6/full/nmat3996.html#affil-auth.
- Garcia, M.L., 2004. Ion channels: gate expectations. Nature, 430(6996), pp.153–155.
- Gardinier, J. et al., 2009. Cyclic hydraulic pressure and fluid flow differentially modulate cytoskeleton re-organization in MC3T3 osteoblasts. Cellular and molecular …, 2(1), pp.133–143. Available at: http://link.springer.com/article/10.1007/s12195-008-0038-2 [Accessed September 30, 2015].
- Gardinier, J. et al., 2009. Cyclic hydraulic pressure and fluid flow differentially modulate cytoskeleton re-organization in MC3T3 osteoblasts. Cellular and molecular …, 2(1), pp.133–143. Available at: http://link.springer.com/article/10.1007/s12195-008-0038-2 [Accessed September 30, 2015].
- Geiger, M., 2003. Collagen sponges for bone regeneration with rhBMP-2. Advanced Drug Delivery Reviews, 55(12), pp.1613–1629. Available at: http://linkinghub.elsevier.com/retrieve/pii/S0169409X03001856 [Accessed April 16, 2015].
- Gellynck, K. et al., 2013. Small molecule stimulation enhances bone regeneration but not titanium implant osseointegration. Bone, 57(2), pp.405–12. Available at: http://www.ncbi.nlm.nih.gov/pubmed/24076022 [Accessed April 29, 2014].

- Geoghegan, E. & Byrnes, L., 2008. Mouse induced pluripotent stem cells. The International journal of developmental biology, 52(8), pp.1015–1022.
- Georgakopoulou, E.A. et al., 2013. Specific lipofuscin staining as a novel biomarker to detect replicative and stress-induced senescence. A method applicable in cryo-preserved and archival tissues. Aging, 5(1), pp.37–50.
- Georgakopoulou, E.A. et al., 2013. Specific lipofuscin staining as a novel biomarker to detect replicative and stress-induced senescence. A method applicable in cryo-preserved and archival tissues. Aging, 5(1), pp.37–50.
- Giraud Guille, M.M. et al., 2005. Bone matrix like assemblies of collagen: from liquid crystals to gels and biomimetic materials. Micron (Oxford, England : 1993), 36(7-8), pp.602–8. Available at: http://www.ncbi.nlm.nih.gov/pubmed/16169238 [Accessed August 22, 2015].
- Giraud-Guille, M.-M. et al., 2008. Liquid crystalline properties of type I collagen: Perspectives in tissue morphogenesis. Comptes Rendus Chimie, 11(3), pp.245–252. Available at: http://linkinghub.elsevier.com/retrieve/pii/S1631074807002032 [Accessed August 22, 2015].
- Giraud-Guille, M.-M., Besseau, L. & Martin, R., 2003. Liquid crystalline assemblies of collagen in bone and in vitro systems. J Biomech, 36(10), pp.1571–1579.
- Glueck, M. et al., 2015. Induction of Osteogenic Differentiation in Human Mesenchymal Stem Cells by Crosstalk with Osteoblasts. BioResearch open access, 4(1), pp.121–30. Available at: http://www.pubmedcentral.nih.gov/articlerender.fcgi?artid=4497645&tool=pmcentrez&rendertype=abstract.
- Golub, E.E. & Boesze-Battaglia, K., 2007. The role of alkaline phosphatase in mineralization. Current Opinion in Orthopaedics, 18, pp.444–448.
- Golub, E.E. & Boesze-Battaglia, K., 2007. The role of alkaline phosphatase in mineralization. Current Opin Orthop, 18, pp.444–448.
- Gomes, P.S. & Fernandes, M.H., 2011. Rodent models in bone-related research: the relevance of calvarial defects in the assessment of bone regeneration strategies. Laboratory Animals, 45(1), pp.14–24. Available at: http://lan.sagepub.com/lookup/doi/10.1258/la.2010.010085.
- Gori, F. et al., 1999. Differentiation of human marrow stromal precursor cells: bone morphogenetic protein-2 increases OSF2/CBFA1, enhances osteoblast commitment, and inhibits late adipocyte maturation. Journal of bone and mineral research, 14(9), pp.1522–1535.
- Gothard, D. & Smith, E., 2014. Tissue engineered bone using select growth factors: A comprehensive review of animal studies and clinical translation studies in man. European Cells & Materials, 28, pp.166–208.

- Gothard, D. et al., 2014. Tissue engineered bone using select growth factors: A comprehensive review of animal studies and clinical translation studies in man. Eur Cell Mater, 28, pp.166–168.
- Götherström, C. et al., 2014. Pre- and postnatal transplantation of fetal mesenchymal stem cells in osteogenesis imperfecta: a two-center experience. Stem cells translational medicine, 3(2), pp.255–64.
- Gough, J.E., Notingher, I. & Hench, L.L., 2004. Osteoblast attachment and mineralized nodule formation on rough and smooth 45S5 bioactive glass monoliths. Journal of biomedical materials research. Part A, 68(4), pp.640–50. Available at: http://www.ncbi.nlm.nih.gov/pubmed/14986319.
- Grant, W.T., Wang, G.J. & Balian, G., 1987. Type X collagen synthesis during endochondral ossification in fracture repair. The Journal of biological chemistry, 262(20), pp.9844–9. Available at: http://www.ncbi.nlm.nih.gov/pubmed/3597444.
- Grayson, W.L. et al., 2008. Effects of Initial Seeding Density and Fluid Perfusion Rate on Formation of Tissue-Engineered Bone. Tissue Engineering Part A, 14(11), pp.1809–1820. Available at: http://www.liebertonline.com/doi/abs/10.1089/ten.tea.2007.0255.
- Gregory, C. a et al., 2004. An Alizarin red-based assay of mineralization by adherent cells in culture: comparison with cetylpyridinium chloride extraction. Analytical biochemistry, 329(1), pp.77–84. Available at: http://www.ncbi.nlm.nih.gov/pubmed/15136169.
- Gu, Y. et al., 2001. Three types of K+ currents in murine osteocyte-like cells (MLO-Y4). Bone, 28(1), pp.29–37.
- Guo, J. et al., 2007. Anti-inflammation role for mesenchymal stem cells transplantation in myocardial infarction. Inflammation, 30(3-4), pp.97–104. Available at: http://www.ncbi.nlm.nih.gov/pubmed/17497204.
- Gurkan, U.A. & Akkus, O., 2008. The mechanical environment of bone marrow: a review. Annals of biomedical engineering, 36(12), pp.1978–91. Available at: http://www.ncbi.nlm.nih.gov/pubmed/18855142 [Accessed June 10, 2014].
- Hadjidakis, D.J. & Androulakis, I.I., 2006. Bone remodeling. Annals of the New York Academy of Sciences, 1092, pp.385–96. Available at: http://www.ncbi.nlm.nih.gov/pubmed/17308163 [Accessed October 7, 2014].
- Hall, J.E. & Guyton, A.C., 2006. Textbook of Medical Physiology, Available at: http://www.us.elsevierhealth.com/Medicine/Physiology/book/9781416045748/Guyton-and-Hall-Textbook-of-Medical-Physiology/.
- Harada, S. & Rodan, G. a, 2003. Control of osteoblast function and regulation of bone mass. Nature, 423(6937), pp.349–55. Available at: http://www.ncbi.nlm.nih.gov/pubmed/12748654.

- Harkness, R.D., 1961. Biological Functions of Collagen. Biological reviews, 36(4), pp.399–45.
- Harmey, D. et al., 2004. Concerted regulation of inorganic pyrophosphate and osteopontin by akp2, enpp1, and ank: an integrated model of the pathogenesis of mineralization disorders. The American journal of pathology, 164(4), pp.1199–1209.
- Hartmann, C. & Tabin, C.J., 2000. Dual roles of Wnt signaling during chondrogenesis in the chicken limb. Development (Cambridge, England), 127(14), pp.3141–3159.
- Haskin, C. & Athanasiou, K., 1993. A heat-shock-like response with cytoskeletal disruption occurs following hydrostatic pressure in MG-63 osteosarcoma cells. Biochemistry and cell …, 71, pp.361–371. Available at: http://www.nrcresearchpress.com/doi/abs/10.1139/o93-054 [Accessed January 28, 2015].

- Haskin, C. & Athanasiou, K., 1993. A heat-shock-like response with cytoskeletal disruption occurs following hydrostatic pressure in MG-63 osteosarcoma cells. Biochemistry and cell …, 71, pp.361–371. Available at: http://www.nrcresearchpress.com/doi/abs/10.1139/o93-054 [Accessed January 28, 2015].

- Henstock, J.R. et al., 2013. Cyclic hydrostatic pressure stimulates enhanced bone development in the foetal chick femur in vitro. Bone, 53(2), pp.468–477. Available at: http://www.ncbi.nlm.nih.gov/pubmed/23333177 [Accessed February 24, 2013].

- Henstock, J.R. et al., 2013. Cyclic hydrostatic pressure stimulates enhanced bone development in the foetal chick femur in vitro. Bone, 53(2), pp.468–477. Available at: http://www.ncbi.nlm.nih.gov/pubmed/23333177 [Accessed February 24, 2013].
- Henstock, J.R. et al., 2013. Cyclic hydrostatic pressure stimulates enhanced bone development in the foetal chick femur in vitro. Bone, 53(2), pp.468–477. Available at: http://www.ncbi.nlm.nih.gov/pubmed/23333177 [Accessed February 24, 2013].
- Henstock, J.R. et al., 2013. Cyclic hydrostatic pressure stimulates enhanced bone development in the foetal chick femur in vitro. Bone, 53(2), pp.468–477. Available at: http://www.ncbi.nlm.nih.gov/pubmed/23333177 [Accessed February 24, 2013].

- Henstock, J.R. et al., 2014. Remotely Activated Mechanotransduction via Magnetic Nanoparticles Promotes Mineralization Synergistically With Bone Morphogenetic Protein 2: Applications for Injectable Cell Therapy. Stem Cells Translational Medicine, 3(11), pp.1363–1374. Available at: http://www.pubmedcentral.nih.gov/articlerender.fcgi?artid=4214839&tool=pmcentrez&rendertype=abstract.
- Herberts, C. a, Kwa, M.S.G. & Hermsen, H.P.H., 2011. Risk factors in the development of stem cell therapy. Journal of translational medicine, 9(1), p.29. Available at: http://www.translational-medicine.com/content/9/1/29.

- Hille, B., 1984. Ion Channels of Excitable Membranes M. Sunderland, ed. , p.5.
- Hoang, Q. et al., 2003. Bone recognition mechanism of porcine osteocalcin from crystal structure. Nature, pp.977–980. Available at: http://www.nature.com/nature/journal/v425/n6961/abs/nature02079.html [Accessed February 10, 2015].
- Hoang, Q. et al., 2003. Bone recognition mechanism of porcine osteocalcin from crystal structure. Nature, pp.977–980. Available at: http://www.nature.com/nature/journal/v425/n6961/abs/nature02079.html [Accessed February 10, 2015].
- Hoemann, C.D., El-Gabalawy, H. & McKee, M.D., 2009. In vitro osteogenesis assays: Influence of the primary cell source on alkaline phosphatase activity and mineralization. Pathologie Biologie, 57(4), pp.318–323. Available at: http://linkinghub.elsevier.com/retrieve/pii/S0369811408001569.
- Hoffmann, W. et al., 2015. Novel Perfused Compression Bioreactor System as an in vitro Model to Investigate Fracture Healing. Frontiers in bioengineering and biotechnology, 3, p.10. Available at: http://www.pubmedcentral.nih.gov/articlerender.fcgi?artid=4313709&tool=pmcentrez&rendertype=abstract.
- Hollands, C., 1986. The Animals (scientific procedures) Act 1986. Lancet, 2(8497), pp.32–33.
- Holy, C.E., Shoichet, M.S. & Davies, J.E., 2000. Engineering three-dimensional bone tissue in vitro using biodegradable scaffolds: investigating initial cell-seeding density and culture period. Journal of biomedical materials research, 51(3), pp.376–82. Available at: http://www.ncbi.nlm.nih.gov/pubmed/10880079.
- Horwitz, E.M. et al., 2002. Isolated allogeneic bone marrow-derived mesenchymal cells engraft and stimulate growth in children with osteogenesis imperfecta: Implications for cell therapy of bone. Proceedings of the National Academy of Sciences of the United States of America, 99(13), pp.8932–7. Available at: http://www.pubmedcentral.nih.gov/articlerender.fcgi?artid=124401&tool=pmcentrez&rendertype=abstract.
- Huang, A.H. et al., 2010. Long-term dynamic loading improves the mechanical properties of chondrogenic mesenchymal stem cell-laden hydrogels. European Cells and Materials, 19(215), pp.72–85.
- Hui, T.Y. et al., 2008. In vitro chondrogenic differentiation of human mesenchymal stem cells in collagen microspheres: influence of cell seeding density and collagen concentration.

Biomaterials, 29(22), pp.3201–12. Available at: http://www.ncbi.nlm.nih.gov/pubmed/18462789 [Accessed February 14, 2013].

- Huiskes, R. et al., 2000. Effects of mechanical forces on maintenance and adaptation of form in trabecular bone. Nature, 405(6787), pp.704–6. Available at: http://www.ncbi.nlm.nih.gov/pubmed/10864330.

- Huiskes, R. et al., 2000. Effects of mechanical forces on maintenance and adaptation of form in trabecular bone. Nature, 405(6787), pp.704–6. Available at: http://www.ncbi.nlm.nih.gov/pubmed/10864330.

- Huo, B. et al., 2008. Fluid Flow Induced Calcium Response in Bone Cell Network. Cellular and Molecular Bioengineering, 1(1), pp.58–66. Available at: http://link.springer.com/10.1007/s12195-008-0011-0.
- Hutmacher, D.W., 2000. Scaffolds in tissue engineering bone and cartilage. Biomaterials, 21(24), pp.2529–2543.
- Ignarro, L. & Buga, G., 1987. Endothelium-derived relaxing factor produced and released from artery and vein is nitric oxide. Proceedings of the …, 84(December), pp.9265–9269. Available at: http://www.pnas.org/content/84/24/9265.short [Accessed October 7, 2015].
- Ignatius, a et al., 2005. Tissue engineering of bone: effects of mechanical strain on osteoblastic cells in type I collagen matrices. Biomaterials, 26(3), pp.311–8. Available at: http://www.ncbi.nlm.nih.gov/pubmed/15262473 [Accessed October 24, 2014].

- Ignatius, a et al., 2005. Tissue engineering of bone: effects of mechanical strain on osteoblastic cells in type I collagen matrices. Biomaterials, 26(3), pp.311–8. Available at: http://www.ncbi.nlm.nih.gov/pubmed/15262473 [Accessed October 24, 2014].

- Ingber, D.E. & Levin, M., 2007. What lies at the interface of regenerative medicine and developmental biology? Development (Cambridge, England), 134(14), pp.2541–7. Available at: http://www.ncbi.nlm.nih.gov/pubmed/17553905 [Accessed August 12, 2013].
- Jaiswal, N. et al., 1997. Osteogenic differentiation of purified, culture-expanded human mesenchymal stem cells in vitro. Journal of cellular biochemistry, 64(2), pp.295–312.
- Jeong, J.Y. et al., 2012. Effects of intermittent hydrostatic pressure magnitude on the chondrogenesis of MSCs without biochemical agents under 3D co-culture. Journal of materials science. Materials in medicine, 23(11), pp.2773–81. Available at: http://www.ncbi.nlm.nih.gov/pubmed/22802107 [Accessed February 24, 2013].
- Johnston, C.E. & Birch, J.G., 2008. A tale of two tibias: a review of treatment options for congenital pseudarthrosis of the tibia. Journal of children's orthopaedics, 2(2), pp.133–49.
- Jones, H.H. et al., 2007. Humeral hypertrophy in response to exercise in Response to Exercise *. The Journal of Bone and Joint Surgery, pp.204–208.

- Kaarniranta, K. et al., 2000. Protein synthesis is required for stabilization of hsp70 mRNA upon exposure to both hydrostatic pressurization and elevated temperature. FEBS Letters, 475, pp.283–286.
- Kadhim, M. et al., 2014. Treatment of unicameral bone cyst: systematic review and meta analysis. Journal of children's orthopaedics, 8(2), pp.171–91. Available at: http://www.pubmedcentral.nih.gov/articlerender.fcgi?artid=3965764&tool=pmcentrez&rendertype=abstract.
- Kalfas, I.H., 2001. Principles of bone healing. Neurosurgical focus, 10(4), p.E1.
- Kamioka, H., Honjo, T. & Takano-Yamamoto, T., 2001. -dimensional distribution of osteocyte processes revealed by the combination of confocal laser scanning microscopy and differential interference contrast microscopy. Bone, 28(2), pp.145–149. Available at: http://www.sciencedirect.com/science/article/pii/S875632820000421X [Accessed July 16, 2014].
- Kanczler, J.M. et al., 2012. A Novel Approach for Studying the Temporal Modulation of Embryonic Skeletal Development Using Organotypic. TISSUE ENGINEERING: Part A, 18(10).
- Kanczler, J.M. et al., 2012. A Novel Approach for Studying the Temporal Modulation of Embryonic Skeletal Development Using Organotypic. TISSUE ENGINEERING: Part A, 18(10).
- Kanczler, J.M. et al., 2012. A Novel Approach for Studying the Temporal Modulation of Embryonic Skeletal Development Using Organotypic. TISSUE ENGINEERING: Part A, 18(10).
- Kaneko, K. et al., 2014. Integrin αv in the mechanical response of osteoblast lineage cells. Biochemical and biophysical research communications, 447(2), pp.352–7. Available at: http://www.pubmedcentral.nih.gov/articlerender.fcgi?artid=4260650&tool=pmcentrez&rendertype=abstract [Accessed October 4, 2015].
- Kato, Y. et al., 2001. Establishment of an osteoid preosteocyte-like cell MLO-A5 that spontaneously mineralizes in culture. Journal of bone and mineral research : the official journal of the American Society for Bone and Mineral Research, 16(9), pp.1622–33. Available at: http://www.ncbi.nlm.nih.gov/pubmed/11547831.
- Katz, M.L. & Robison, W.G., 2002. What is lipofuscin? Defining characteristics and differentiation from other autofluorescent lysosomal storage bodies. In Archives of Gerontology and Geriatrics. pp. 169–184.
- Kawakami, Y. et al., 2001. WNT signals control FGF-dependent limb initiation and AER induction in the chick embryo. Cell, 104(6), pp.891–900.

- Khokhlov, A.R., 1978. Liquid-crystalline ordering in the solution of semiflexible macromolecules. Physics Letters A, 68(1), pp.135–136.
- Kim, S., Choi, Y. & Park, M., 2007. ERK 1/2 activation in enhanced osteogenesis of human mesenchymal stem cells in poly (lactic-glycolic acid) by cyclic hydrostatic pressure. Journal of BiomedicalMaterials Research Research Part A, 80(4), pp.826–36. Available at: http://onlinelibrary.wiley.com/doi/10.1002/jbm.a.30945/full [Accessed July 31, 2014].
- Klazen, C. a H. et al., 2010. Vertebroplasty versus conservative treatment in acute osteoporotic vertebral compression fractures (Vertos II): an open-label randomised trial. Lancet, 376(9746), pp.1085–92. Available at: http://www.ncbi.nlm.nih.gov/pubmed/20701962 [Accessed June 25, 2014].
- Klein-Nulend, J. & H, B., 1995. Sensitivity of osteocytes to biomechanical stress in vitro. The FASEB Journal, 4, pp.441–445.
- Klein-Nulend, J. et al., 1995. Pulsating fluid flow increases nitric oxide (NO) synthesis by osteocytes but not periosteal fibroblasts--correlation with prostaglandin upregulation. Biochemical and biophysical research communications, 217(2), pp.640–648.
- Klein-Nulend, J. et al., 2013. Mechanosensation and transduction in osteocytes. Bone, 54(2), pp.182–90. Available at: http://www.ncbi.nlm.nih.gov/pubmed/23085083 [Accessed April 29, 2014].
- Klyushnenkova, E. et al., 2005. T cell responses to allogeneic human mesenchymal stem cells: immunogenicity, tolerance, and suppression. Journal of biomedical science, 12(1), pp.47–57. Available at: http://www.ncbi.nlm.nih.gov/pubmed/15864738.
- Koike, M. et al., 2005. Effects of mechanical strain on proliferation and differentiation of bone marrow stromal cell line ST2. Journal of bone and mineral metabolism, 23(3), pp.219–25. Available at: http://www.ncbi.nlm.nih.gov/pubmed/15838624 [Accessed October 24, 2014].
- Komori, T. et al., 1997. Targeted disruption of Cbfa1 results in a complete lack of bone formation owing to maturational arrest of osteoblasts. Cell, 89(5), pp.755–64. Available at: http://www.ncbi.nlm.nih.gov/pubmed/9182763.
- Kraiwattanapong, C. et al., 2005. Comparison of Healos/bone marrow to INFUSE(rhBMP-2/ACS) with a collagen-ceramic sponge bulking agent as graft substitutes for lumbar spine fusion. Spine, 30(9), pp.1001–1007; discussion 1007.
- Kubo, T. et al., 1998. Interleukin 8 is produced by hydrostatic pressure in human osteoblast cell line, MG-63. Pathophysiology, 5, pp.199–204. Available at: http://www.sciencedirect.com/science/article/pii/S0928468098000212 [Accessed January 28, 2015].

- Kubo, T. et al., 1998. Interleukin 8 is produced by hydrostatic pressure in human osteoblast cell line, MG-63. Pathophysiology, 5, pp.199–204. Available at: http://www.sciencedirect.com/science/article/pii/S0928468098000212 [Accessed January 28, 2015].
- Kurd, M. et al., 2015. Fusion in degenerative spondylolisthesis: comparison of osteoconductive and osteoinductive bone graft substitutes. European spine journal : official publication of the European Spine Society, the European Spinal Deformity Society, and the European Section of the Cervical Spine Research Society, 24(5), pp.1066–73. Available at: http://www.ncbi.nlm.nih.gov/pubmed/25371089.
- Lawrence, B.J. & Madihally, S. V., 2008. Cell colonization in degradable 3D porous matrices. Cell adhesion & migration, 2(1), pp.9–16.
- Lawrence, R.C. et al., 2008. Estimates of the prevalence of arthritis and other rheumatic conditions in the United States. Part II. Arthritis and rheumatism, 58(1), pp.26–35. Available at: http://www.pubmedcentral.nih.gov/articlerender.fcgi?artid=3266664&tool=pmcentrez&rendertype=abstract [Accessed February 28, 2013].
- Le Blanc, K. et al., 2005. Fetal mesenchymal stem-cell engraftment in bone after in utero transplantation in a patient with severe osteogenesis imperfecta. Transplantation, 79(11), pp.1607–1614.
- Lee, D.-Y. et al., 2010. Oscillatory flow-induced proliferation of osteoblast-like cells is mediated by alphavbeta3 and beta1 integrins through synergistic interactions of focal adhesion kinase and Shc with phosphatidylinositol 3-kinase and the Akt/mTOR/p70S6K pathway. The Journal of biological chemistry, 285(1), pp.30–42. Available at: http://www.pubmedcentral.nih.gov/articlerender.fcgi?artid=2804177&tool=pmcentrez&rendertype=abstract [Accessed January 29, 2015].

- Lee, D.-Y. et al., 2010. Oscillatory flow-induced proliferation of osteoblast-like cells is mediated by alphavbeta3 and beta1 integrins through synergistic interactions of focal adhesion kinase and Shc with phosphatidylinositol 3-kinase and the Akt/mTOR/p70S6K pathway. The Journal of biological chemistry, 285(1), pp.30–42. Available at: http://www.pubmedcentral.nih.gov/articlerender.fcgi?artid=2804177&tool=pmcentrez&rendertype=abstract [Accessed January 29, 2015].

- Lee, K.L. et al., 2015. The primary cilium functions as a mechanical and calcium signaling nexus. Cilia, 4(1), pp.1–13. Available at: http://www.ciliajournal.com/content/4/1/7.
- Lee, K.L., Hoey, D. a. & Jacobs, C.R., 2010. Primary Cilia-Mediated Mechanotransduction in Bone. Clinical Reviews in Bone and Mineral Metabolism, 8(4), pp.201–212. Available at: http://link.springer.com/10.1007/s12018-010-9078-y [Accessed June 12, 2013].

- Lee, O.K. et al., 2004. Isolation of multipotent mesenchymal stem cells from umbilical cord blood. Blood, 103, pp.1669–1675.
- Lee, W.-C.C. et al., 2007. Effects of uniaxial cyclic strain on adipose-derived stem cell morphology, proliferation, and differentiation. Biomechanics and modeling in mechanobiology, 6(4), pp.265–273.
- Lerner, T. & Liljenqvist, U., 2013. Silicate-substituted calcium phosphate as a bone graft substitute in surgery for adolescent idiopathic scoliosis. European spine journal : official publication of the European Spine Society, the European Spinal Deformity Society, and the European Section of the Cervical Spine Research Society, 22 Suppl 2, pp.S185–94. Available at: http://www.ncbi.nlm.nih.gov/pubmed/22948551.
- Leucht, P. et al., 2013. Primary cilia act as mechanosensors during bone healing around an implant. Medical Engineering and Physics, 35(3), pp.392–402.
- Li, N., Sul, J.-Y. & Haydon, P.G., 2003. A calcium-induced calcium influx factor, nitric oxide, modulates the refilling of calcium stores in astrocytes. The Journal of neuroscience : the official journal of the Society for Neuroscience, 23(32), pp.10302–10310.
- Lichte, P. et al., 2011. Scaffolds for bone healing: concepts, materials and evidence. Injury, 42(6), pp.569–73. Available at: http://www.ncbi.nlm.nih.gov/pubmed/21489531 [Accessed March 22, 2013].
- Lidor, C. et al., 1987. LEVELS IN OF ACTIVE CALLUS OF VITAMIN REPAIR IN CHICKS THE. Journal of Bone and Joint Surgery, 69-B(1), pp.132–136.
- Lienemann, P.S., Lutolf, M.P. & Ehrbar, M., 2012. Biomimetic hydrogels for controlled biomolecule delivery to augment bone regeneration. Advanced Drug Delivery Reviews, 64(12), pp.1078–1089. Available at: http://dx.doi.org/10.1016/j.addr.2012.03.010.
- Lin, C. et al., 2009. Sclerostin mediates bone response to mechanical unloading through antagonizing Wnt/beta-catenin signaling. Journal of bone and mineral research : the official journal of the American Society for Bone and Mineral Research, 24(10), pp.1651–1661.
- Lin, C. et al., 2009. Sclerostin mediates bone response to mechanical unloading through antagonizing Wnt/beta-catenin signaling. Journal of bone and mineral research : the official journal of the American Society for Bone and Mineral Research, 24(10), pp.1651–1661.
- Ling, L., Nurcombe, V. & Cool, S.M., 2009. Wnt signaling controls the fate of mesenchymal stem cells. Gene, 433(1-2), pp.1–7. Available at: http://www.ncbi.nlm.nih.gov/pubmed/19135507.
- Lipello, L. et al., 1985. Metabolic Response of Articular-Cartilage Segments to Low-Levels of Hydrostatic-Pressure. Connect Tissue Res, 13(2), pp.99–107.

- Liu, B. & Neufeld, a H., 2001. Nitric oxide synthase-2 in human optic nerve head astrocytes induced by elevated pressure in vitro. Archives of ophthalmology, 119(2), pp.240–5. Available at: http://www.ncbi.nlm.nih.gov/pubmed/11176986.
- Liu, C. et al., 2010. Effects of cyclic hydraulic pressure on osteocytes. Bone, 46(5), pp.1449–56. Available at: http://www.pubmedcentral.nih.gov/articlerender.fcgi?artid=3417308&tool=pmcentrez&rendertype=abstract [Accessed September 30, 2015].
- Liu, C., Xia, Z. & Czernuszka, J.T., 2007. Design and Development of Three-Dimensional Scaffolds for Tissue Engineering. Chemical Engineering Research and Design, 85(7), pp.1051–1064. Available at: http://www.sciencedirect.com/science/article/pii/S0263876207731428.
- Liu, F., Malaval, L. & Aubin, J.E., 2003. Global amplification polymerase chain reaction reveals novel transitional stages during osteoprogenitor differentiation. Journal of cell science, 116(Pt 9), pp.1787–96. Available at: http://jcs.biologists.org/cgi/doi/10.1242/jcs.00376\nhttp://www.ncbi.nlm.nih.gov/pubmed/12665559.
- Liu, G. et al., 2016. Saos-2 Cell Mediated Mineralization on Collagen Gels : Effect of Densification and Bioglass Incorporation. Journal of biomedical materials research: Part A, (321), pp.1–42.
- Liu, W. et al., 2005. Mechanoregulation of intracellular Ca2+ concentration is attenuated in collecting duct of monocilium-impaired orpk mice. American journal of physiology. Renal physiology, 289(5), pp.F978–88. Available at: http://www.ncbi.nlm.nih.gov/pubmed/15972389 [Accessed April 11, 2013].
- Lode, A., Bernhardt, A. & Gelinsky, M., 2008. Cultivation of human bone marrow stromal cells on three-dimensional scaffolds of mineralized collagen: influence of seeding density on colonization, proliferation and. Journal of tissue engineering …, (August), pp.400–407. Available at: http://onlinelibrary.wiley.com/doi/10.1002/term.110/abstract [Accessed August 17, 2015].
- Lomas, A.J. et al., 2013. Poly (3-Hydroxybutyrate-co-3-Hydroxyhexanoate)/Collagen Hybrid Scaffolds for Tissue Engineering Applications. TISSUE ENGINEERING Part C, 19(8), pp.577–585.
- Long, F., 2011. Building strong bones: molecular regulation of the osteoblast lineage. Nature Reviews Molecular Cell Biology, 13(1), pp.27–38. Available at: http://dx.doi.org/10.1038/nrm3254.

- Long, F., 2011. Building strong bones: molecular regulation of the osteoblast lineage. Nature Reviews Molecular Cell Biology, 13(1), pp.27–38. Available at: http://dx.doi.org/10.1038/nrm3254.
- Lu, J. et al., 2015. The Lineage Specification of Mesenchymal Stem Cells Is Directed by the Rate of Fluid Shear Stress. Journal of Cellular Physiology, (April), p.n/a–n/a. Available at: http://doi.wiley.com/10.1002/jcp.25278.
- Lu, X.L. et al., 2012. Calcium response in osteocytic networks under steady and oscillatory fluid flow. Bone, 51(3), pp.466–473.
- Luangphakdy, V. et al., 2013. Evaluation of osteoconductive scaffolds in the canine femoral multi-defect model. Tissue engineering. Part A, 19(5-6), pp.634–48. Available at: http://www.ncbi.nlm.nih.gov/pubmed/23215980.
- Liu, Z.-J., Zhuge, Y. & Velazquez, O.C., 2009. Trafficking and differentiation of mesenchymal stem cells. *Journal of cellular biochemistry*, 106(6), pp.984–991.
- Luo, N. et al., 2014. Primary cilia signaling mediates intraocular pressure sensation. Proceedings of the National Academy of Sciences of the United States of America, 4(24), pp.1–6. Available at: http://www.ncbi.nlm.nih.gov/pubmed/25143588.
- Lutolf, M.P. et al., 2003. Repair of bone defects using synthetic mimetics of collagenous extracellular matrices. Nat Biotechnol, 21(5), pp.513–518. Available at: http://www.ncbi.nlm.nih.gov/pubmed/12704396\nhttp://www.nature.com/nbt/journal/v21/n5/pdf/nbt818.pdf.
- Lyons, F.G. et al., 2010. The healing of bony defects by cell-free collagen-based scaffolds compared to stem cell-seeded tissue engineered constructs. Biomaterials, 31(35), pp.9232–9243.
- Ma, P.X., 2004. Scaffolds for tissue fabrication. Materials Today, 7(5), pp.30–40.
- Mackie, E.J., Tatarczuch, L. & Mirams, M., 2011. The skeleton: a multi-functional complex organ: the growth plate chondrocyte and endochondral ossification. The Journal of endocrinology, 211(2), pp.109–21. Available at: http://www.ncbi.nlm.nih.gov/pubmed/21642379 [Accessed August 21, 2013].
- Majid, D.S. a. et al., 2001. Nitric Oxide Dependency of Arterial Pressure-Induced Changes in Renal Interstitial Hydrostatic Pressure in Dogs. Circulation Research, 88(3), pp.347–351. Available at: http://circres.ahajournals.org/cgi/doi/10.1161/01.RES.88.3.347.
- Malone, A.M.D. et al., 2007. Primary cilia mediate mechanosensing in bone cells by a calcium-independent mechanism. Proceedings of the National Academy of Sciences of the United States of America, 104(33), pp.13325–13330.

- Malone, A.M.D. et al., 2007. The role of actin cytoskeleton in oscillatory fluid flow-induced signaling in MC3T3-E1 osteoblasts. American journal of physiology. Cell physiology, 292(5), pp.C1830–C1836.
- Mana-Capelli, S. et al., 2014. Angiomotins link F-actin architecture to Hippo pathway signaling. Molecular Biology of the Cell, 25(10), pp.1676–1685. Available at: http://www.molbiolcell.org/cgi/doi/10.1091/mbc.E13-11-0701.
- Mancini, L. et al., 2000. The biphasic effects of nitric oxide in primary rat osteoblasts are cGMP dependent. Biochemical and biophysical research communications, 274(2), pp.477–481.
- Manolagas, S.C., 2000. Birth and death of bone cells: basic regulatory mechanisms and implications for the pathogenesis and treatment of osteoporosis. Endocrine reviews, 21(2), pp.115–137.
- Marcacci, M. et al., 2007. Stem cells associated with macroporous bioceramics for long bone repair: 6- to 7-year outcome of a pilot clinical study. Tissue engineering, 13(5), pp.947–55. Available at: http://www.ncbi.nlm.nih.gov/pubmed/17484701.
- Marolt, D. et al., 2012. Engineering bone tissue from human embryonic stem cells. Proceedings of the National Academy of Sciences, 109(22), pp.8705–8709. Available at: http://www.pnas.org/cgi/doi/10.1073/pnas.1201830109.
- Marsell, R. & Einhorn, T.A., 2011. The biology of fracture healing. Injury, 42(6), pp.551–555.
- Maxson, S. & Burg, K.J.L., 2012. Synergistic Effects of Conditioned Media and Hydrostatic Pressure on the Differentiation of Mesenchymal Stem Cells. Cellular and Molecular Bioengineering, 5(4), pp.414–426. Available at: http://www.springerlink.com/index/10.1007/s12195-012-0248-5 [Accessed March 7, 2013].
- McCreadie, B.R. et al., 2004. Osteocyte lacuna size and shape in women with and without osteoporotic fracture. Journal of Biomechanics, 37(4), pp.563–572.
- McGarry, J.G., Klein-Nulend, J. & Prendergast, P.J., 2005. The effect of cytoskeletal disruption on pulsatile fluid flow-induced nitric oxide and prostaglandin E2 release in osteocytes and osteoblasts. Biochemical and biophysical research communications, 330(1), pp.341–8. Available at: http://www.ncbi.nlm.nih.gov/pubmed/15781270.
- McGarry, J.G., Klein-Nulend, J. & Prendergast, P.J., 2005. The effect of cytoskeletal disruption on pulsatile fluid flow-induced nitric oxide and prostaglandin E2 release in osteocytes and osteoblasts. Biochemical and biophysical research communications, 330(1), pp.341–8. Available at: http://www.ncbi.nlm.nih.gov/pubmed/15781270.
- McNamara, I., Deshpande, S. & Porteous, M., 2010. Impaction grafting of the acetabulum with a mixture of frozen, ground irradiated bone graft and porous synthetic bone substitute

(Apapore 60). The Journal of bone and joint surgery. British volume, 92(5), pp.617–23. Available at: http://www.ncbi.nlm.nih.gov/pubmed/20435995.

- Meinel, L. et al., 2005. Silk implants for the healing of critical size bone defects. Bone, 37(5), pp.688–698.
- Metzger, T.A. et al., 2015. Pressure and shear stress in trabecular bone marrow during whole bone loading. Journal of Biomechanics, 48(12), pp.3035–3043.
- Meyer, E.G. et al., 2011. The effect of cyclic hydrostatic pressure on the functional development of cartilaginous tissues engineered using bone marrow derived mesenchymal stem cells. Journal of the mechanical behavior of biomedical materials, 4(7), pp.1257–65. Available at: http://www.ncbi.nlm.nih.gov/pubmed/21783134 [Accessed February 24, 2013].
- Michael Delaine-Smith, R. et al., 2015. Preclinical models for in vitro mechanical loading of bone-derived cells. BoneKEy Reports, 4(AUGUST), p.728. Available at: http://www.nature.com/doifinder/10.1038/bonekey.2015.97.
- Micol, L. a et al., 2011. High-density collagen gel tubes as a matrix for primary human bladder smooth muscle cells. Biomaterials, 32(6), pp.1543–8. Available at: http://www.ncbi.nlm.nih.gov/pubmed/21074843 [Accessed September 18, 2015].
- Miyanishi, K. et al., 2006. Effects of Hydrostatic Pressure and Transforming Growth Factor-β3 on Adult Human Mesenchymal Stem Cell Chondrogenesis. TISSUE ENGINEERING, 12(6).
- Mollace, V. et al., 2005. Modulation of prostaglandin biosynthesis by nitric oxide and nitric oxide donors. Pharmacological, 57(2), pp.217–252. Available at: http://pharmrev.aspetjournals.org/content/57/2/217.short.
- Morse, D.C., 1998. Viscoelasticity of Concentrated Isotropic Solutions of Semiflexible Polymers. 1. Model and Stress Tensor. Macromolecules, 31(20), pp.7030–7043. Available at: http://pubs.acs.org/doi/abs/10.1021/ma9803032\nhttp://dx.doi.org/10.1021/ma9803032.
- Mullender, M. et al., 2004. Mechanotransduction of bone cells in vitro: mechanobiology of bone tissue. Medical & biological engineering & computing, 42(1), pp.14–21. Available at: http://www.ncbi.nlm.nih.gov/pubmed/14977218.
- Mullender, M.G. et al., 2006. Release of Nitric Oxide, but not Prostaglandin E2,by Bone Cells Depends on Fluid Flow Frequency. Journal of orthopaedic research, 24(6), pp.1170–1177. Available at: http://www.ncbi.nlm.nih.gov/pubmed/16705700.
- Munrow, M. & Piekarski, K., 1977. Transport mechanism operating between blood supply and osteocytes in long bones. Nature, 269(80–82), pp.80–82.
- Muschler, G.F. et al., 2010. The Design and Use of Animal Models for Translational Research in Bone Tissue Engineering and Regenerative Medicine. TISSUE ENGINEERING: Part B, 16(1), pp.123–145.

- Nakamura, A. et al., 2009. Osteocalcin secretion as an early marker of in vitro osteogenic differentiation of rat mesenchymal stem cells. Tissue engineering. Part C, Methods, 15(2), pp.169–180.
- Nauta, A.J. et al., 2006. Donor-derived mesenchymal stem cells are immunogenic in an allogeneic host and stimulate donor graft rejection in a nonmyeloablative setting. Blood, 108(6), pp.2114–20. Available at: http://www.pubmedcentral.nih.gov/articlerender.fcgi?artid=1895546&tool=pmcentrez&rendertype=abstract.
- Neen, D. et al., 2006. Healos and bone marrow aspirate used for lumbar spine fusion: a case controlled study comparing healos with autograft. Spine, 31(18), pp.E636–E640.
- Neidel, J., Schulze, M. & Lindschau, J., 1995. Association between degree of bone-erosion and synovial fluid-levels of tumor necrosis factor alpha in the knee-joints of patients with rheumatoid arthritis. Inflammation research : official journal of the European Histamine Research Society ... [et al.], 44(5), pp.217–21. Available at: http://www.ncbi.nlm.nih.gov/pubmed/7655997.
- Nemir, S. & West, J.L., 2010. Synthetic Materials in the Study of Cell Response to Substrate Rigidity. Annals of Biomedical Engineering, 38(1), pp.2–20. Available at: http://link.springer.com/10.1007/s10439-009-9811-1.
- Neth, P. et al., 2006. Wnt signaling regulates the invasion capacity of human mesenchymal stem cells. Stem cells, 24, pp.1892–1903.
- Niemeyer, P. et al., 2007. Comparison of immunological properties of bone marrow stromal cells and adipose tissue-derived stem cells before and after osteogenic differentiation in vitro. Tissue engineering, 13(1), pp.111–21. Available at: http://www.ncbi.nlm.nih.gov/pubmed/17518585 [Accessed May 31, 2013].
- Niemeyer, P. et al., 2010. Comparison of mesenchymal stem cells from bone marrow and adipose tissue for bone regeneration in a critical size defect of the sheep tibia and the influence of platelet-rich plasma. Biomaterials, 31(13), pp.3572–9. Available at: http://www.ncbi.nlm.nih.gov/pubmed/20153047 [Accessed May 31, 2013].
- Nirmalanandhan, V.S. et al., 2006. Effects of Cell Seeding Density and Collagen Concentration Cell – Seeded Collagen Constructs. TISSUE ENGINEERING, 12(7), pp.1865–1871.
- Nishiyama, T. & Tominaga, N., 1988. Quantitative evaluation of the factors affecting the process of fibroblast-mediated collagen gel contraction by separating the process into three phases. Collagen and related …, 8(3), pp.259–273. Available at: http://www.sciencedirect.com/science/article/pii/S0174173X88800451 [Accessed August 17, 2015].

- Nussbaum, J. et al., 2007. Transplantation of undifferentiated murine embryonic stem cells in the heart: teratoma formation and immune response. The FASEB journal : official publication of the Federation of American Societies for Experimental Biology, 21(7), pp.1345–1357.
- O'Brien, F.J., 2011. Biomaterials & scaffolds for tissue engineering. Materials Today, 14(3), pp.88–95. Available at: http://dx.doi.org/10.1016/S1369-7021(11)70058-X.
- Oh, J.W. et al., 2014. Organotypic Skin Culture. J Invest Dermatol, 133(11).
- Olsen, S.M., Stover, J.D. & Nagatomi, J., 2011. Examining the role of mechanosensitive ion channels in pressure mechanotransduction in rat bladder urothelial cells. Annals of biomedical engineering, 39(2), pp.688–97. Available at: http://www.ncbi.nlm.nih.gov/pubmed/21104316 [Accessed April 24, 2013].
- Olszta, M.J. et al., 2007. Bone structure and formation: A new perspective. Materials Science and Engineering: R: Reports, 58(3-5), pp.77–116. Available at: http://linkinghub.elsevier.com/retrieve/pii/S0927796X07000642 [Accessed July 16, 2014].
- Orbay, H., Tobita, M. & Mizuno, H., 2012. Mesenchymal stem cells isolated from adipose and other tissues: basic biological properties and clinical applications. Stem cells international, 2012, p.461718. Available at: http://www.pubmedcentral.nih.gov/articlerender.fcgi?artid=3361347&tool=pmcentrez&rendertype=abstract [Accessed May 23, 2013].
- Oreffo, R.O.C. et al., 2005. Mesenchymal stem cells: lineage, plasticity, and skeletal therapeutic potential. Stem cell reviews, 1(2), pp.169–178.
- Orlando, B. et al., 2013. Leader genes in osteogenesis: A theoretical study. Archives of Oral Biology, 58(1), pp.42–49. Available at: http://dx.doi.org/10.1016/j.archoralbio.2012.07.010.
- Orr, D.E. & Burg, K.J.L., 2008. Design of a modular bioreactor to incorporate both perfusion flow and hydrostatic compression for tissue engineering applications. Annals of Biomedical Engineering, 36(7), pp.1228–1241.
- Oryan, A., Alidadi, S. & Moshiri, A., 2013. Current concerns regarding healing of bone defects. Hard Tissue, 2(2), pp.1–12.
- Packer, J.W. & Colditz, J.C., 1986. Bone injuries treatment and rehab. Hand rehabilitation, 2(1), pp.81–91.
- Park, H. et al., 2007. Nanofabrication and microfabrication of functional materials for tissue engineering. Tissue engineering, 13(8), pp.1867–77. Available at: http://www.ncbi.nlm.nih.gov/pubmed/17518744 [Accessed August 17, 2015].
- Parreno, J. & Hart, D. a, 2009. Molecular and mechano-biology of collagen gel contraction mediated by human MG-63 cells: involvement of specific intracellular signaling pathways and the cytoskeleton. Biochemistry and cell biology = Biochimie et biologie cellulaire, 87(6), pp.895–904.

- Parreno, J. et al., 2008. Osteoblastic MG-63 cell differentiation, contraction, and mRNA expression in stress-relaxed 3D collagen I gels. Molecular and cellular biochemistry, 317(1-2), pp.21–32. Available at: http://www.ncbi.nlm.nih.gov/pubmed/18566755.
- Patino, M.G. et al., 2002. Collagen : An Overview. Implant Dentistry, 11(3), pp.280–285.
- Pautke, C. et al., 2004. Characterization of osteosarcoma cell lines MG-63, Saos-2 and U-2 OS in comparison to human osteoblasts. Anticancer Research, 24(6), pp.3743–3748.
- Pautke, C. et al., 2004. Characterization of osteosarcoma cell lines MG-63, Saos-2 and U-2 OS in comparison to human osteoblasts. Anticancer Research, 24(6), pp.3743–3748.
- Phinney, D.G. et al., 1999. Donor variation in the growth properties and osteogenic potential of human marrow stromal cells. Journal of cellular biochemistry, 75(3), pp.424–36. Available at: http://www.ncbi.nlm.nih.gov/pubmed/10536366.
- PIETERNELLA, S. et al., 2003. Mesenchymal stem cells in human second-trimester bone marrow, liver, lung, and spleen exhibit a similar immunophenotype but a heterogeneous multilineage differentiation potential. Hematopoietic Stem Cells research, 88(8), pp.845–852.
- Pitt, C.G. et al., 1981. Aliphatic polyesters II. The degradation of poly (DL-lactide), poly (epsilon-caprolactone), and their copolymers in vivo. Biomaterials, 2(4), pp.215–220.
- Pittenger, M.F. et al., 1999. Multilineage potential of adult human mesenchymal stem cells. Science, 284(5411), pp.143–147.
- Plotkin, L.I. & Bellido, T., 2013. Beyond gap junctions: Connexin43 and bone cell signaling. Bone, 52(1), pp.157–66. Available at: http://www.pubmedcentral.nih.gov/articlerender.fcgi?artid=3513515&tool=pmcentrez&rendertype=abstract [Accessed July 31, 2015].
- Plotkin, L.I. et al., 2005. Mechanical stimulation prevents osteocyte apoptosis: requirement of integrins, Src kinases, and ERKs. American journal of physiology. Cell physiology, 289(3), pp.C633–43. Available at: http://www.ncbi.nlm.nih.gov/pubmed/15872009.
- Ploumis, A. et al., 2010. Healos graft carrier with bone marrow aspirate instead of allograft as adjunct to local autograft for posterolateral fusion in degenerative lumbar scoliosis: a minimum 2-year follow-up study. Journal of neurosurgery. Spine, 13(2), pp.211–5. Available at: http://www.ncbi.nlm.nih.gov/pubmed/20672956.
- Polacheck, W.J. et al., 2014. Mechanotransduction of fluid stresses governs 3D cell migration. Proceedings of the National Academy of Sciences of the United States of America, 111(7), pp.2447–52. Available at: http://www.ncbi.nlm.nih.gov/pubmed/24550267 [Accessed July 13, 2014].
- Ponte, A.L. et al., 2007. The In Vitro Migration Capacity of Human Bone Marrow Mesenchymal Stem Cells: Comparison of Chemokine and Growth Factor Chemotactic Activities. Stem Cells, 25(7), pp.1737–1745.

- Porta, G. Della et al., 2015. Synergistic effect of sustained release of growth factors and dynamic culture on osteoblastic differentiation of mesenchymal stem cells. Journal of Biomedical Materials Research Part A, 103(6), pp.2161–2171. Available at: http://doi.wiley.com/10.1002/jbm.a.35354.
- Qi, M. et al., 2009. Expression of bone-related genes in bone marrow MSCs after cyclic mechanical strain: implications for distraction osteogenesis. International journal of oral science, 1(3), pp.143–50. Available at: http://www.pubmedcentral.nih.gov/articlerender.fcgi?artid=3475587&tool=pmcentrez&rendertype=abstract.
- Quarles, L.D., Siddhanti, S.R. & Medda, S., 1997. Developmental regulation of osteocalcin expression in MC3T3-E1 osteoblasts: Minimal role of the proximal E-box cis-acting promoter elements. Journal of Cellular Biochemistry, 65(1), pp.11–24.
- Rahaman, M.N. et al., 2011. Bioactive glass in tissue engineering. Acta Biomaterialia, 7(6), pp.2355–2373. Available at: http://dx.doi.org/10.1016/j.actbio.2011.03.016.
- Rauch, F. & Glorieux, F.H., 2004. Osteogenesis imperfecta. Lancet, 363(9418), pp.1377–1385.
- Rawlinson, S.C.F., Pitsillides, a. a. & Lanyon, L.E., 1996. Involvement of different ion channels in osteoblasts' and osteocytes' early responses to mechanical strain. Bone, 19(6), pp.609–614.
- Reed, a a C. et al., 2003. Vascularity in a new model of atrophic nonunion. The Journal of bone and joint surgery. British volume, 85(4), pp.604–610.
- Reher, P. et al., 2002. Ultrasound stimulates nitric oxide and prostaglandin E 2 production by human osteoblasts. Bone, 31(1), pp.236–241. Available at: http://www.sciencedirect.com/science/article/pii/S8756328202007895 [Accessed September 30, 2015].
- Reinwald, Y. et al., 2015. Evaluation of the growth environment of a hydrostatic force bioreactor for preconditioning of tissue-engineered constructs. Tissue engineering. Part C, Methods, 21(1), pp.1–14. Available at: http://www.ncbi.nlm.nih.gov/pubmed/24967717 [Accessed January 30, 2015].
- Reubinoff, B.E. et al., 2000. Embryonic stem cell lines from human blastocysts: somatic differentiation in vitro. Nat. Biotechnol., 18, pp.399–404.
- Reynolds, A.R. et al., 2009. Stimulation of tumor growth and angiogenesis by low concentrations of RGD-mimetic integrin inhibitors. Nature medicine, 15(4), pp.392–400.
- Rhee, S., 2009. Fibroblasts in three dimensional matrices: cell migration and matrix remodeling. Experimental & molecular medicine, 41(12), pp.858–865.

- Ricci, W.M., Gallagher, B. & Haidukewych, G.J., 2009. Intramedullary nailing of femoral shaft fractures: current concepts. The Journal of the American Academy of Orthopaedic Surgeons, 17(5), pp.296–305.
- Richards, M. et al., 1998. Bone regeneration and fracture healing. Experience with distraction osteogenesis model. Clinical Orthopaedics and Related Research, (355 Suppl), pp.S191–204. Available at: http://www.ncbi.nlm.nih.gov/pubmed/9917639\nhttp://www.ncbi.nlm.nih.gov/pubmed/9917639?ordinalpos=1&itool=EntrezSystem2.PEntrez.Pubmed.Pubmed_ResultsPanel.Pubmed_DefaultReportPanel.Pubmed_RVDocSum.
- Roach, H.I., 1990. Long-term organ culture of embryonic chick femora: a system for investigating bone and cartilage formation at an intermediate level of organization. Journal of bone and mineral research : the official journal of the American Society for Bone and Mineral Research, 5(1), pp.85–100. Available at: http://www.ncbi.nlm.nih.gov/pubmed/2309583.
- Roberts, C.A. et al., 2012. Developmental Cues for Bone Formation from Parathyroid Hormone and Parathyroid Hormone-Related Protein in an Ex Vivo Organotypic Culture System of Embryonic Chick Femora. TISSUE ENGINEERING Part C, 18(12), pp.984–995.
- Rodríguez, J.P. et al., 2004. Cytoskeletal organization of human mesenchymal stem cells (MSC) changes during their osteogenic differentiation. Journal of Cellular Biochemistry, 93(4), pp.721–731.
- Rothstein, S.N., Federspiel, W.J. & Little, S.R., 2009. A unified mathematical model for the prediction of controlled release from surface and bulk eroding polymer matrices. Biomaterials, 30(8), pp.1657–1664. Available at: http://dx.doi.org/10.1016/j.biomaterials.2008.12.002.
- Rubin, C. et al., 2002. Mechanical strain, induced noninvasively in the high-frequency domain, is anabolic to cancellous bone, but not cortical bone. Bone, 30(3), pp.445–52. Available at: http://www.ncbi.nlm.nih.gov/pubmed/11882457.
- Rubin, C., Xu, G. & Judex, S., 2001. The anabolic activity of bone tissue, suppressed by disuse, is normalized by brief exposure to extremely low-magnitude mechanical stimuli. FASEB journal : official publication of the Federation of American Societies for Experimental Biology, 15(12), pp.2225–9. Available at: http://www.ncbi.nlm.nih.gov/pubmed/11641249.
- Rubin, J., Rubin, C. & Jacobs, C.R., 2006. Molecular pathways mediating mechanical signaling in bone. Gene, 367, pp.1–16. Available at: http://www.ncbi.nlm.nih.gov/pubmed/16361069 [Accessed March 18, 2013].
- Rucci, N., 2008. Molecular biology of bone remodelling. Clinical cases in mineral and bone metabolism : the official journal of the Italian Society of Osteoporosis, Mineral Metabolism,

and Skeletal Diseases, 5(1), pp.49–56. Available at: http://www.pubmedcentral.nih.gov/articlerender.fcgi?artid=2781193&tool=pmcentrez&rendertype=abstract.

- Rupani, A., Balint, R. & Cartmell, S.H., 2012. Osteoblasts and their applications in bone tissue engineering. Cell Health and Cytoskeleton, 4, pp.49–61.
- Sachs, F., 1985. MECHANOTRANSDUCER ION CHANNELS IN CHICK SKELETAL MUSCLE: THE EFFECTS OF EXTRACELLULAR pH. J.Physiol, 363, pp.119–134.
- Sackin, H., 1995. Stretch-activated ion channels. Kidney international, 48(4), pp.1134–47. Available at: http://www.ncbi.nlm.nih.gov/pubmed/8569075.
- Said, G.Z. et al., 2013. Non-Anatomical Surgical Solutions for Difficult Non-Unions : Case Series El-Sharkawi. Trauma Mon., 17(4), pp.10–14.
- Salingcarnboriboon, R. et al., 2003. Establishment of tendon-derived cell lines exhibiting pluripotent mesenchymal stem cell-like property. Experimental Cell Research, 287(2), pp.289–300.
- Salvemini, D. et al., 1993. Mechanism of Nitric Oxide–Induced Vasodilatation. Proceedings of the National Academy of Sciences of the United States of America, 90(15), pp.7240–7244.
- Schatzker, J. et al., 2005. The rationale of operative fracture care: Third edition,
- Schneider, R.K. et al., 2010. The osteogenic differentiation of adult bone marrow and perinatal umbilical mesenchymal stem cells and matrix remodelling in three-dimensional collagen scaffolds. Biomaterials, 31(3), pp.467–80. Available at: http://www.ncbi.nlm.nih.gov/pubmed/19815272 [Accessed August 9, 2013].
- Schwab, W. et al., 1999. Immunohistochemical localization of the differentiation marker E11 in dental development of rats. Acta histochemica, 101(4), pp.431–6. Available at: http://www.ncbi.nlm.nih.gov/pubmed/10611931.
- Schwartz, S.D. et al., 2015. Human embryonic stem cell-derived retinal pigment epithelium in patients with age-related macular degeneration and Stargardt's macular dystrophy: follow-up of two open-label phase 1/2 studies. The Lancet, 385(9967), pp.509–516. Available at: http://linkinghub.elsevier.com/retrieve/pii/S0140673614613763.
- Scott, A. et al., 2008. Mechanotransduction in human bone: in vitro cellular physiology that underpins bone changes with exercise. Sports medicine (Auckland, N.Z.), 38(2), pp.139–60. Available at: http://www.ncbi.nlm.nih.gov/pubmed/18201116.
- Secco, M. et al., 2008. Multipotent stem cells from umbilical cord: cord is richer than blood! Stem cells, 26(1), pp.146–150.
- Sen, B. et al., 2015. Intranuclear Actin Regulates Osteogenesis. Stem Cells, 33(10), pp.3065–3076.

- Sen, M.K. & Miclau, T., 2007. Autologous iliac crest bone graft: should it still be the gold standard for treating nonunions? Injury, 38 Suppl 1, pp.75–80. Available at: http://www.ncbi.nlm.nih.gov/pubmed/17383488 [Accessed June 13, 2014].
- Serpooshan, V. et al., 2010. Reduced hydraulic permeability of three-dimensional collagen scaffolds attenuates gel contraction and promotes the growth and differentiation of mesenchymal stem cells. Acta biomaterialia, 6(10), pp.3978–87. Available at: http://www.ncbi.nlm.nih.gov/pubmed/20451675 [Accessed August 21, 2013].
- Serra, M. et al., 2012. Process engineering of human pluripotent stem cells for clinical application. Trends in Biotechnology, 30(6), pp.350–359.
- Shao, Y. et al., 2012. Primary cilia modulate Ihh signal transduction in response to hydrostatic loading of growth plate chondrocytes. Bone, 50(1), pp.79–84. Available at: http://www.sciencedirect.com/science/article/pii/S8756328211012014 [Accessed October 4, 2015].
- Shi, S. & Gronthos, S., 2003. Perivascular niche of postnatal mesenchymal stem cells in human bone marrow and dental pulp. Journal of bone and mineral research : the official journal of the American Society for Bone and Mineral Research, 18(4), pp.696–704.
- Shrivats, A.R., McDermott, M.C. & Hollinger, J.O., 2014. Bone tissue engineering: State of the union. Drug Discovery Today, 19(6), pp.781–786. Available at: http://dx.doi.org/10.1016/j.drudis.2014.04.010.
- Siller-Jackson, A.J. et al., 2008. Adaptation of connexin 43-hemichannel prostaglandin release to mechanical loading. The Journal of biological chemistry, 283(39), pp.26374–82. Available at: http://www.pubmedcentral.nih.gov/articlerender.fcgi?artid=2546557&tool=pmcentrez&rendertype=abstract [Accessed January 30, 2015].
- Siller-Jackson, A.J. et al., 2008. Adaptation of connexin 43-hemichannel prostaglandin release to mechanical loading. The Journal of biological chemistry, 283(39), pp.26374–82. Available at: http://www.pubmedcentral.nih.gov/articlerender.fcgi?artid=2546557&tool=pmcentrez&rendertype=abstract [Accessed January 30, 2015].
- Sittichockechaiwut, A. et al., 2009. Use of rapidly mineralising osteoblasts and short periods of mechanical loading to accelerate matrix maturation in 3D scaffolds. Bone, 44(5), pp.822–9. Available at: http://www.ncbi.nlm.nih.gov/pubmed/19442630 [Accessed January 30, 2015].
- Sittichockechaiwut, A. et al., 2009. Use of rapidly mineralising osteoblasts and short periods of mechanical loading to accelerate matrix maturation in 3D scaffolds. Bone, 44(5), pp.822–9. Available at: http://www.ncbi.nlm.nih.gov/pubmed/19442630 [Accessed January 30, 2015].

- Sittichokechaiwut, A. et al., 2010. SHORT BOUTS OF MECHANICAL LOADING ARE AS EFFECTIVE AS DEXAMETHASONE AT INDUCING MATRIX PRODUCTION BY HUMAN BONE MARROW MESENCHYMAL STEM CELLS. European cells & materials, 20, pp.45–57.

- Sittichokechaiwut, A. et al., 2010. SHORT BOUTS OF MECHANICAL LOADING ARE AS EFFECTIVE AS DEXAMETHASONE AT INDUCING MATRIX PRODUCTION BY HUMAN BONE MARROW MESENCHYMAL STEM CELLS. European cells & materials, 20, pp.45–57.
- Sittichokechaiwut, A. et al., 2010. SHORT BOUTS OF MECHANICAL LOADING ARE AS EFFECTIVE AS DEXAMETHASONE AT INDUCING MATRIX PRODUCTION BY HUMAN BONE MARROW MESENCHYMAL STEM CELLS. European cells & materials, 20, pp.45–57.

- Sivakumar, M., Dhanadurai Suresh Kumar, K. & Rajeswari, S., 1995. Failures in stainless steel orthopaedic implant devices : A survey. JOURNAL OF MATERIALS SCIENCE LETTERS, 14, pp.351–354.
- Smith, E.L. et al., 2014a. Evaluation of skeletal tissue repair, Part 1: Assessment of novel growth-factor-releasing hydrogels in an ex vivo chick femur defect model. Acta Biomaterialia, 10(10), pp.4186–4196. Available at: http://linkinghub.elsevier.com/retrieve/pii/S174270611400258X.

- Smith, E.L. et al., 2014a. Evaluation of skeletal tissue repair, Part 1: Assessment of novel growth-factor-releasing hydrogels in an ex vivo chick femur defect model. Acta Biomaterialia, 10(10), pp.4186–4196. Available at: http://linkinghub.elsevier.com/retrieve/pii/S174270611400258X.

- Smith, E.L. et al., 2014b. Evaluation of skeletal tissue repair, Part 2: Enhancement of skeletal tissue repair through dual-growth-factor-releasing hydrogels within an ex vivo chick femur defect model. Acta Biomaterialia, 10(10), pp.4197–4205. Available at: http://linkinghub.elsevier.com/retrieve/pii/S1742706114002372.

- Smith, E.L. et al., 2014b. Evaluation of skeletal tissue repair, Part 2: Enhancement of skeletal tissue repair through dual-growth-factor-releasing hydrogels within an ex vivo chick femur defect model. Acta Biomaterialia, 10(10), pp.4197–4205. Available at: http://linkinghub.elsevier.com/retrieve/pii/S1742706114002372.

- Smith, E.L. et al., 2015. The Effects of 1α, 25-dihydroxyvitamin D3 and Transforming Growth Factor-β3 on Bone Development in an Ex Vivo Organotypic Culture System of Embryonic Chick Femora. PloS one, 10(4), p.e0121653. Available at: http://www.scopus.com/inward/record.url?eid=2-s2.0-84926661086&partnerID=tZOtx3y1.

- Smith, E.L., Kanczler, J.M. & Oreffo, R.O.C., 2013. A new take on an old story: chick limb organ culture for skeletal niche development and regenerative medicine evaluation. European cells & materials, 26, pp.91–106; discussion 106. Available at: http://www.ncbi.nlm.nih.gov/pubmed/24027022.

- Smith, E.L., Kanczler, J.M. & Oreffo, R.O.C., 2013. A new take on an old story: chick limb organ culture for skeletal niche development and regenerative medicine evaluation. European cells & materials, 26, pp.91–106; discussion 106. Available at: http://www.ncbi.nlm.nih.gov/pubmed/24027022.

- Smucker, J.D. & Fredericks, D.C., 2012. Assessment of Progenix(®) DBM putty bone substitute in a rabbit posterolateral fusion model. The Iowa orthopaedic journal, 32, pp.54–60. Available at: http://www.pubmedcentral.nih.gov/articlerender.fcgi?artid=3565415&tool=pmcentrez&rendertype=abstract.
- Song, G. et al., 2007. Mechanical stretch promotes proliferation of rat bone marrow mesenchymal stem cells. Colloids and surfaces. B, Biointerfaces, 58(2), pp.271–7. Available at: http://www.ncbi.nlm.nih.gov/pubmed/17499488.
- Sophia Fox, A.J., Bedi, A. & Rodeo, S.A., 2009. The basic science of articular cartilage: structure, composition, and function. Sports health, 1(6), pp.461–8. Available at: http://www.pubmedcentral.nih.gov/articlerender.fcgi?artid=3445147&tool=pmcentrez&rendertype=abstract.
- Stein, G.S. et al., 2004. Runx2 control of organization, assembly and activity of the regulatory machinery for skeletal gene expression. Oncogene, 23(24), pp.4315–4329.
- Stephens, L.E. et al., 1995. Deletion of ??1 integrins in mice results in inner cell mass failure and peri-implantation lethality. Genes and Development, 9(15), pp.1883–1895.
- Stevens, M.M. et al., 2005. In vivo engineering of organs: the bone bioreactor. Proceedings of the National Academy of Sciences of the United States of America, 102(32), pp.11450–5. Available at: http://www.pubmedcentral.nih.gov/articlerender.fcgi?artid=1183576&tool=pmcentrez&rendertype=abstract.
- Stevens, M.M., 2008. Biomaterials for bone tissue engineering. Materials Today, 11(5), pp.18–25. Available at: http://dx.doi.org/10.1016/S1369-7021(08)70086-5.
- Steward, a J. et al., 2012. Cell-matrix interactions regulate mesenchymal stem cell response to hydrostatic pressure. Acta biomaterialia, 8(6), pp.2153–9. Available at: http://www.ncbi.nlm.nih.gov/pubmed/22426136 [Accessed March 21, 2013].
- Steward, a J., Wagner, D.R. & Kelly, D.J., 2013. The pericellular environment regulates cytoskeletal development and the differentiation of mesenchymal stem cells and determines

their response to hydrostatic pressure. European cells & materials, 25, pp.167–78. Available at: http://www.ncbi.nlm.nih.gov/pubmed/23389751.

- Su, W.-T., Wang, Y.-T. & Chou, C.-M., 2014. Optimal fluid flow enhanced mineralization of MG-63 cells in porous chitosan scaffold. Journal of the Taiwan Institute of Chemical Engineers, 45(4), pp.1111–1118. Available at: http://www.sciencedirect.com/science/article/pii/S1876107013002927.
- Subramony, S.D. et al., 2013. The guidance of stem cell differentiation by substrate alignment and mechanical stimulation. Biomaterials, 34(8), pp.1942–1953. Available at: http://dx.doi.org/10.1016/j.biomaterials.2012.11.012.
- Sumanasinghe, R.D., Bernacki, S.H. & Loboa, E.G., 2006. Osteogenic Differentiation of Human Mesenchymal Stem Cells on Bone Morphogenetic Protein (BMP-2) mRNA Expression. Tissue engineering, 12(12).
- Takahashi, K. & Yamanaka, S., 2006. Induction of Pluripotent Stem Cells from Mouse Embryonic and Adult Fibroblast Cultures by Defined Factors. Cell, 126(4), pp.663–676.
- Takahashi, K. et al., 1991. Fracture healing of chick femurs in tissue culture. Acta orthopaedica Scandinavica, 62(4), pp.352–5. Available at: http://www.ncbi.nlm.nih.gov/pubmed/1882675.
- Tall, M. et al., 2012. Femur malunion treated with open osteotomy and intramedullary nailing in developing countries. Orthopaedics and Traumatology: Surgery and Research, 98(7), pp.784–787.
- Tall, M. et al., 2014. Treatment of nonunion in neglected long bone shaft fractures by osteoperiosteal decortication. Orthopaedics & traumatology, surgery & research : OTSR, 100(6 Suppl).
- Tan, J. et al., 2015. Decreased osteogenesis of adult mesenchymal stem cells by reactive oxygen species under cyclic stretch: a possible mechanism of age related osteoporosis. Bone Res., 3(February), p.15003. Available at: http://www.nature.com/articles/boneres20153.
- Tan, S.D. et al., 2007. Osteocytes subjected to fluid flow inhibit osteoclast formation and bone resorption. Bone, 41(5), pp.745–51. Available at: http://www.ncbi.nlm.nih.gov/pubmed/17855178.
- Tanck, E. et al., 1999. Why does intermittent hydrostatic pressure enhance the mineralization process in fetal cartilage? Journal of Biomechanics, 32(2), pp.153–161.
- Tang, Y. et al., 2013. MT1-MMP-Dependent Control of Skeletal Stem Cell Commitment via a β1-Integrin/YAP/TAZ Signaling Axis. Developmental Cell, 25(4), pp.402–416. Available at: http://dx.doi.org/10.1016/j.devcel.2013.04.011.
- Tasevski, V. & Sorbetti, J., 2005. Influence of mechanical and biological signals on gene expression in human MG-63 cells: evidence for a complex interplay between hydrostatic

compression and vitamin D3 or TGF-beta1 on MMP-1 and MMP-3 mRNA levels. … and cell biology, 83(6), pp.96–107. Available at: http://www.nrcresearchpress.com/doi/abs/10.1139/o04-124 [Accessed January 28, 2015].

- Tatsumi, S. et al., 2007. Targeted Ablation of Osteocytes Induces Osteoporosis with Defective Mechanotransduction. Cell Metabolism, 5(6), pp.464–475. Available at: http://www.sciencedirect.com/science/article/pii/S1550413107001283.
- Taubenberger, A. V et al., 2010. The effect of unlocking RGD-motifs in collagen I on pre-osteoblast adhesion and differentiation. Biomaterials, 31(10), pp.2827–35. Available at: http://www.ncbi.nlm.nih.gov/pubmed/20053443 [Accessed January 26, 2015].
- Tee, S.-Y. et al., 2011. Cell Shape and Substrate Rigidity Both Regulate Cell Stiffness. Biophysical Journal, 100(5), pp.L25–L27. Available at: http://linkinghub.elsevier.com/retrieve/pii/S0006349511001275.
- Teitelbaum, S.L., 2000. Bone resorption by osteoclasts. Science (New York, N.Y.), 289(5484), pp.1504–1508. Available at: http://www.sciencemag.org/content/289/5484/1504.full?sid=905b7269-cfd8-4725-ac93-3a99b2aca7fa\nhttp://www.sciencemag.org/cgi/doi/10.1126/science.289.5484.1504.
- Temiyasathit, S. et al., 2012. Mechanosensing by the primary cilium: deletion of Kif3A reduces bone formation due to loading. PloS one, 7(3), p.e33368. Available at: http://www.pubmedcentral.nih.gov/articlerender.fcgi?artid=3299788&tool=pmcentrez&rendertype=abstract [Accessed October 4, 2015].
- Thompson, W.R. et al., 2015. Osteocyte specific responses to soluble and mechanical stimuli in a stem cell derived culture model. Scientific reports, 5, p.11049. Available at: http://www.pubmedcentral.nih.gov/articlerender.fcgi?artid=4460727&tool=pmcentrez&rendertype=abstract.
- Tibbitt, M.W. & Anseth, K.S., 2009. Hydrogels as extracellular matrix mimics for 3D cell culture. Biotechnology and bioengineering, 103(4), pp.655–63. Available at: http://www.pubmedcentral.nih.gov/articlerender.fcgi?artid=2997742&tool=pmcentrez&rendertype=abstract [Accessed July 9, 2014].
- Tjabringa, G.S. et al., 2006. Polyamines modulate nitric oxide production and COX-2 gene expression in response to mechanical loading in human adipose tissue-derived mesenchymal stem cells. Stem cells (Dayton, Ohio), 24(10), pp.2262–9. Available at: http://www.ncbi.nlm.nih.gov/pubmed/16794268 [Accessed September 30, 2015].
- Tortelli, F. et al., 2010. The development of tissue-engineered bone of different origin through endochondral and intramembranous ossification following the implantation of mesenchymal stem cells and osteoblasts in a murine model. Biomaterials, 31(2), pp.242–9. Available at: http://www.ncbi.nlm.nih.gov/pubmed/19796807 [Accessed July 16, 2014].

- Tse, J.R. & Engler, A.J., 2010. Preparation of hydrogel substrates with tunable mechanical properties. Current protocols in cell biology / editorial board, Juan S. Bonifacino ... [et al.], Chapter 10(June), p.Unit 10.16. Available at: http://www.ncbi.nlm.nih.gov/pubmed/20521229 [Accessed April 29, 2015].
- Tsiridis, E., Upadhyay, N. & Giannoudis, P., 2007. Molecular aspects of fracture healing: which are the important molecules? Injury, 38 Suppl 1, pp.S11–25. Available at: http://www.ncbi.nlm.nih.gov/pubmed/17383481 [Accessed July 13, 2014].
- Ubl, J., Murer, H. & Kolb, H.A., 1988. Ion channels activated by osmotic and mechanical stress in membranes of opossum kidney cells. J. Membr. Biol., 104(3), pp.223–232.
- Udagawa, N. et al., 1990. Origin of osteoclasts: mature monocytes and macrophages are capable of differentiating into osteoclasts under a suitable microenvironment prepared by bone marrow-derived stromal cells. Proceedings of the National Academy of Sciences of the United States of America, 87(18), pp.7260–4. Available at: http://www.pubmedcentral.nih.gov/articlerender.fcgi?artid=54723&tool=pmcentrez&rendertype=abstract.
- Undale, A.H. et al., 2009. Mesenchymal Stem Cells for Bone Repair and Metabolic Bone Diseases. Mayo Clinic Proceedings, 84(10), pp.893–902.
- Väänänen, H.K. et al., 2000. The cell biology of osteoclast function. Journal of cell science, 113 (Pt 3, pp.377–81. Available at: http://www.ncbi.nlm.nih.gov/pubmed/10639325.
- van't Hof, R.J. & Ralston, S.H., 1997. Cytokine-induced nitric oxide inhibits bone resorption by inducing apoptosis of osteoclast progenitors and suppressing osteoclast activity. Journal of bone and mineral research : the official journal of the American Society for Bone and Mineral Research, 12(11), pp.1797–804. Available at: http://www.ncbi.nlm.nih.gov/pubmed/9383684.
- Visconti, L. a, Yen, E.H.K. & Johnson, R.B., 2004. Effect of strain on bone nodule formation by rat osteogenic cells in vitro. Archives of oral biology, 49(6), pp.485–92. Available at: http://www.ncbi.nlm.nih.gov/pubmed/15099806 [Accessed October 24, 2014].
- Wang, Y. et al., 2012. The predominant role of collagen in the nucleation, growth, structure and orientation of bone apatite. Nature Materials, 11(8), pp.724–733. Available at: http://dx.doi.org/10.1038/nmat3362.
- Want, A. & Nienow, A., 2012. Large-scale expansion and exploitation of pluripotent stem cells for regenerative medicine purposes: beyond the T flask. Regenerative …, 7(1), pp.71–84. Available at: http://www.futuremedicine.com/doi/abs/10.2217/rme.11.101 [Accessed August 20, 2015].
- Weightman, A. et al., 2014. Alignment of multiple glial cell populations in 3D nanofiber scaffolds: toward the development of multicellular implantable scaffolds for repair of neural

injury. Nanomedicine : nanotechnology, biology, and medicine, 10(2), pp.291–5. Available at: http://www.ncbi.nlm.nih.gov/pubmed/24090767 [Accessed July 7, 2015].

- Weightman, A.P. et al., 2014. An in vitro spinal cord injury model to screen neuroregenerative materials. Biomaterials, 35(12), pp.3756–65. Available at: http://www.ncbi.nlm.nih.gov/pubmed/24484676 [Accessed July 7, 2015].
- Weinman, J., Servaes, S. & Anupindi, S. a., 2013. Treated unicameral bone cysts. Clinical Radiology, 68(6), pp.636–642. Available at: http://www.ncbi.nlm.nih.gov/pubmed/23360874.
- Whitfield, J.F., 2008. The solitary (primary) cilium--a mechanosensory toggle switch in bone and cartilage cells. Cellular signalling, 20(6), pp.1019–24. Available at: http://www.ncbi.nlm.nih.gov/pubmed/18248958 [Accessed July 10, 2013].
- Wijenayaka, A.R. et al., 2011. Sclerostin stimulates osteocyte support of osteoclast activity by a RANKL-dependent pathway. PLoS ONE, 6(10).
- Williams, D. & Sebastine, I., 2005. Tissue engineering and regenerative medicine: manufacturing challenges. Nanobiotechnology, IEE …, 152(6), pp.207–210. Available at: http://ieeexplore.ieee.org/xpls/abs_all.jsp?arnumber=1563508 [Accessed August 20, 2015].
- Wills, M., 2004. Orthopedic complications of childhood obesity. Pediatric physical therapy : the official publication of the Section on Pediatrics of the American Physical Therapy Association, 16(4), pp.230–5. Available at: http://www.ncbi.nlm.nih.gov/pubmed/17057553 [Accessed February 24, 2013].
- Wilson, S.I. et al., 2001. The status of Wnt signalling regulates neural and epidermal fates in the chick embryo. Nature, 411(May), pp.325–330.
- Wimalawansa, S.J., 2010. Nitric oxide and bone. In Annals of the New York Academy of Sciences. pp. 391–403.
- Wong, D.A. et al., 2008. Neurologic impairment from ectopic bone in the lumbar canal: a potential complication of off-label PLIF/TLIF use of bone morphogenetic protein-2 (BMP-2). The spine journal : official journal of the North American Spine Society, 8(6), pp.1011–8. Available at: http://www.sciencedirect.com/science/article/pii/S1529943007002689.
- Wong, M. & Carter, D.., 1990. Theoretical stress analysis of organ culture osteogenesis. Bone, 11(2), pp.127–131.
- Woodruff, M. a. et al., 2012. Bone tissue engineering: from bench to bedside. Materials Today, 15(10), pp.430–435. Available at: http://linkinghub.elsevier.com/retrieve/pii/S1369702112701943 [Accessed July 19, 2015].
- Wu, P.-H. et al., 2014. Three-dimensional cell migration does not follow a random walk. Proceedings of the National Academy of Sciences, 111(11), pp.3949–3954. Available at: http://www.pnas.org/cgi/doi/10.1073/pnas.1318967111.

- Xiao, Z. et al., 2006. CILIA-LIKE STRUCTURES AND POLYCYSTIN-1 IN OSTEOBLASTS/OSTEOCYTES AND ASSOCIATED ABNORMALITIES IN SKELETOGENESIS AND RUNX2 EXPRESSION. J Biol Chem, 281(41), pp.30884–30895.
- Xiong, J. & O'Brien, C.A., 2012. Osteocyte RANKL: New insights into the control of bone remodeling. Journal of Bone and Mineral Research, 27(3), pp.499–505.
- Xu, Y. et al., 2015. Cyclic Tensile Strain Induces Tenogenic Differentiation of Tendon-Derived Stem Cells in Bioreactor Culture. BioMed research …, 2015. Available at: http://www.hindawi.com/journals/bmri/2015/790804/abs/ [Accessed September 30, 2015].
- Yahara, I. et al., 1982. Correlation between effects of 24 different cytochalasins on cellular structures and cellular events and those on actin in vitro. Journal of Cell Biology, 92(1), pp.69–78.
- Yan, Y. et al., 2012. Mechanical strain regulates osteoblast proliferation through integrin-mediated ERK activation. PloS one, 7(4), p.e35709. Available at: http://www.pubmedcentral.nih.gov/articlerender.fcgi?artid=3335094&tool=pmcentrez&rendertype=abstract [Accessed November 27, 2013].
- Yang, J.T., Rayburn, H. & Hynes, R.O., 1993. Embryonic mesodermal defects in alpha 5 integrin-deficient mice. Development, 119(4), pp.1093–1105. Available at: http://www.ncbi.nlm.nih.gov/entrez/query.fcgi?cmd=Retrieve&db=PubMed&dopt=Citation&list_uids=7508365.
- Yang, Y. et al., 2002. Development of a “mechano-active” scaffold for tissue engineering. Biomaterials, 23(10), pp.2119–2126.
- Yang, Y.L., Leone, L.M. & Kaufman, L.J., 2009. Elastic moduli of collagen gels can be predicted from two-dimensional confocal microscopy. Biophysical Journal, 97(7), pp.2051–2060. Available at: http://dx.doi.org/10.1016/j.bpj.2009.07.035.
- Yannas, I. V et al., 1989. Synthesis and characterization of a model extracellular matrix that induces partial regeneration of adult mammalian skin. Proceedings of the National Academy of Sciences of the United States of America, 86(3), pp.933–937.
- Yasuda, H. et al., 1998. Osteoclast differentiation factor is a ligand for osteoprotegerin/osteoclastogenesis-inhibitory factor and is identical to TRANCE/RANKL. Proceedings of the National Academy of Sciences of the United States of America, 95(7), pp.3597–602. Available at: http://www.pubmedcentral.nih.gov/articlerender.fcgi?artid=19881&tool=pmcentrez&rendertype=abstract.
- Yeung, T. et al., 2005. Effects of substrate stiffness on cell morphology, cytoskeletal structure, and adhesion. Cell Motility and the Cytoskeleton, 60(1), pp.24–34.

- Young, M.F., 2003. Bone matrix proteins: their function, regulation, and relationship to osteoporosis. Osteoporosis international : a journal established as result of cooperation between the European Foundation for Osteoporosis and the National Osteoporosis Foundation of the USA, 14 Suppl 3, pp.S35–42. Available at: http://www.ncbi.nlm.nih.gov/pubmed/12730768.
- Younger, E.M. & Chapman, M.W., 1989. Morbidity at bone graft donor sites. Journal of orthopaedic trauma, 3(3), pp.192–195.
- Yourek, G., Hussain, M. a & Mao, J.J., 2007. Cytoskeletal changes of mesenchymal stem cells during differentiation. ASAIO journal (American Society for Artificial Internal Organs : 1992), 53(2), pp.219–28. Available at: http://www.ncbi.nlm.nih.gov/pubmed/17413564.
- Yu, H.-C. et al., 2010. Mechanical stretching induces osteoprotegerin in differentiating C2C12 precursor cells through noncanonical Wnt pathways. Journal of bone and mineral research : the official journal of the American Society for Bone and Mineral Research, 25(5), pp.1128–37. Available at: http://www.ncbi.nlm.nih.gov/pubmed/20200998 [Accessed November 27, 2013].
- Zaidi, S.K. et al., 2004. Tyrosine phosphorylation controls Runx2-mediated subnuclear targeting of YAP to repress transcription. The EMBO journal, 23(4), pp.790–9. Available at: http://emboj.embopress.org/content/23/4/790.abstract.
- Zamzam, M.M. et al., 2009. Efficacy of aspiration and autogenous bone marrow injection in the treatment of simple bone cysts. International orthopaedics, 33(5), pp.1353–8. Available at: http://www.pubmedcentral.nih.gov/articlerender.fcgi?artid=2899137&tool=pmcentrez&rendertype=abstract.
- Zhang, D., Weinbaum, S. & Cowin, S., 1998. Estimates of the peak pressures in bone pore water. J Biomech Eng, 120, pp.697–703.
- Zhang, D., Weinbaum, S. & Cowin, S.C., 1998. Estimates of the Peak Pressures in Bone Pore Water. Journal of Biomechanical Engineering, 120(6), p.697. Available at: http://biomechanical.asmedigitalcollection.asme.org/article.aspx?articleid=1401628.
- Zhang, K. et al., 2006. E11/gp38 Selective Expression in Osteocytes: Regulation by Mechanical Strain and Role in Dendrite Elongation. Molecular and Cellular Biology, 26(12), pp.4539–4552. Available at: http://mcb.asm.org/cgi/doi/10.1128/MCB.02120-05.
- Zhang, W. et al., 2012. Effect of calcium citrate on bone integration in a rabbit femur defect model. Asian Pacific Journal Of Tropical Medicine, 5(4), pp.310–4. Available at: http://www.ncbi.nlm.nih.gov/pubmed/22449524.
- Zhao, B. et al., 2007. Inactivation of YAP oncoprotein by the Hippo pathway is involved in cell contact inhibition and tissue growth control. Genes & Development, 21(21), pp.2747–2761.

- Zhao, Y.-H. et al., 2015. Hydrostatic pressure promotes the proliferation and osteogenic/chondrogenic differentiation of mesenchymal stem cells: the roles of RhoA and Rac1. Stem Cell Research, 14(3), pp.283–296. Available at: http://www.sciencedirect.com/science/article/pii/S1873506115000331.
- Zhao, Y.-H. et al., 2015. Hydrostatic pressure promotes the proliferation and osteogenic/chondrogenic differentiation of mesenchymal stem cells: the roles of RhoA and Rac1. Stem Cell Research. Available at: http://linkinghub.elsevier.com/retrieve/pii/S1873506115000331 [Accessed March 16, 2015].
- Zhu, L. et al., 2006. Tissue-engineered bone repair of goat femur defects with osteogenically induced bone marrow stromal cells. Tissue Engineering, 12(3), pp.423–433.
- Zuk, P. a et al., 2001. Multilineage cells from human adipose tissue: implications for cell-based therapies. Tissue engineering, 7(2), pp.211–28. Available at: http://www.ncbi.nlm.nih.gov/pubmed/11304456.
- Zuk, P.A. et al., 2002. Human Adipose Tissue Is a Source of Multipotent Stem Cells. Molecular biology of the cell, 13(December), pp.4279–4295.
- Zwingenberger, S. et al., 2013. Establishment of a femoral critical-size bone defect model in immunodeficient mice. Journal of Surgical Research, 181(1), pp.1–8. Available at: http://dx.doi.org/10.1016/j.jss.2012.06.039.

Appendix

Chapter 1

hMSC characterisation

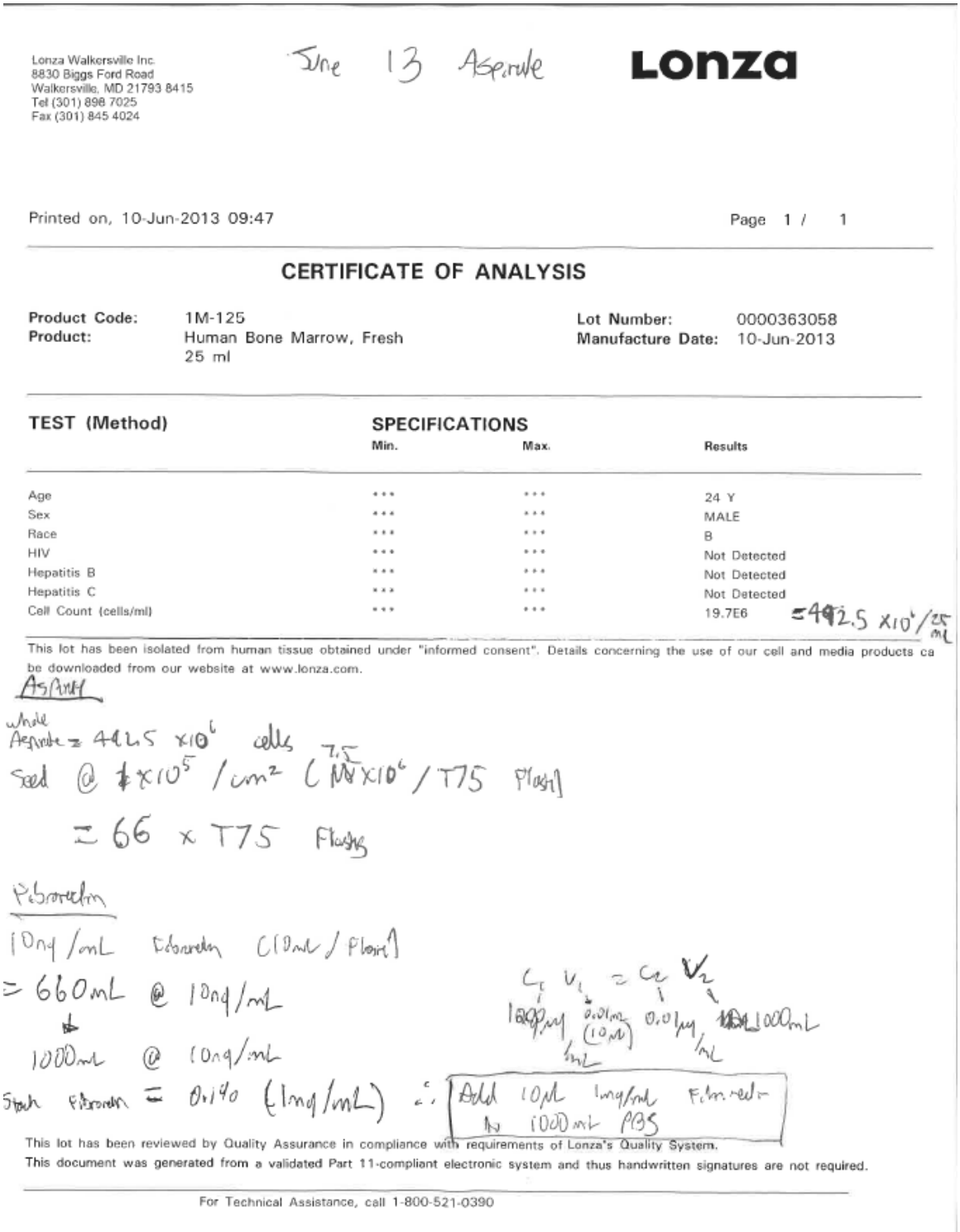

Lonza Walkersville Inc.
8830 Biggs Ford Road
Walkersville, MD 21793 8415
Tel (301) 898 7025
Fax (301) 845 4024

June 13 Aspirate

Lonza

Printed on, 10-Jun-2013 09:47 Page 1 / 1

CERTIFICATE OF ANALYSIS

Product Code: 1M-125
Product: Human Bone Marrow, Fresh 25 ml
Lot Number: 0000363058
Manufacture Date: 10-Jun-2013

TEST (Method)	SPECIFICATIONS Min.	Max.	Results
Age	***	***	24 Y
Sex	***	***	MALE
Race	***	***	B
HIV	***	***	Not Detected
Hepatitis B	***	***	Not Detected
Hepatitis C	***	***	Not Detected
Cell Count (cells/ml)	***	***	19.7E6 =492.5 x10⁶/25 mL

This lot has been isolated from human tissue obtained under "informed consent". Details concerning the use of our cell and media products ca be downloaded from our website at www.lonza.com.

Aspirate

Whole Aspirate = 492.5 x10⁶ cells

Seed @ 7.5 x10⁵ /cm² (7.5 x10⁶ / T75 Flask)

= 66 x T75 Flasks

Fibronectin

10ng/mL Fibronectin (10mL / Flask)

= 660mL @ 10ng/mL

+

1000mL @ 10ng/mL

Stock Fibronectin = 0.1% (1mg/mL) ∴ Add 10µL 1mg/mL Fibronectin to 1000mL PBS

$C_1 V_1 = C_2 V_2$

1mg/mL, 0.01mL (10µL), 0.01µg/mL, 1000mL

This lot has been reviewed by Quality Assurance in compliance with requirements of Lonza's Quality System.
This document was generated from a validated Part 11-compliant electronic system and thus handwritten signatures are not required.

For Technical Assistance, call 1-800-521-0390

Figure 1: Certificate of analysis for hMSC Donor

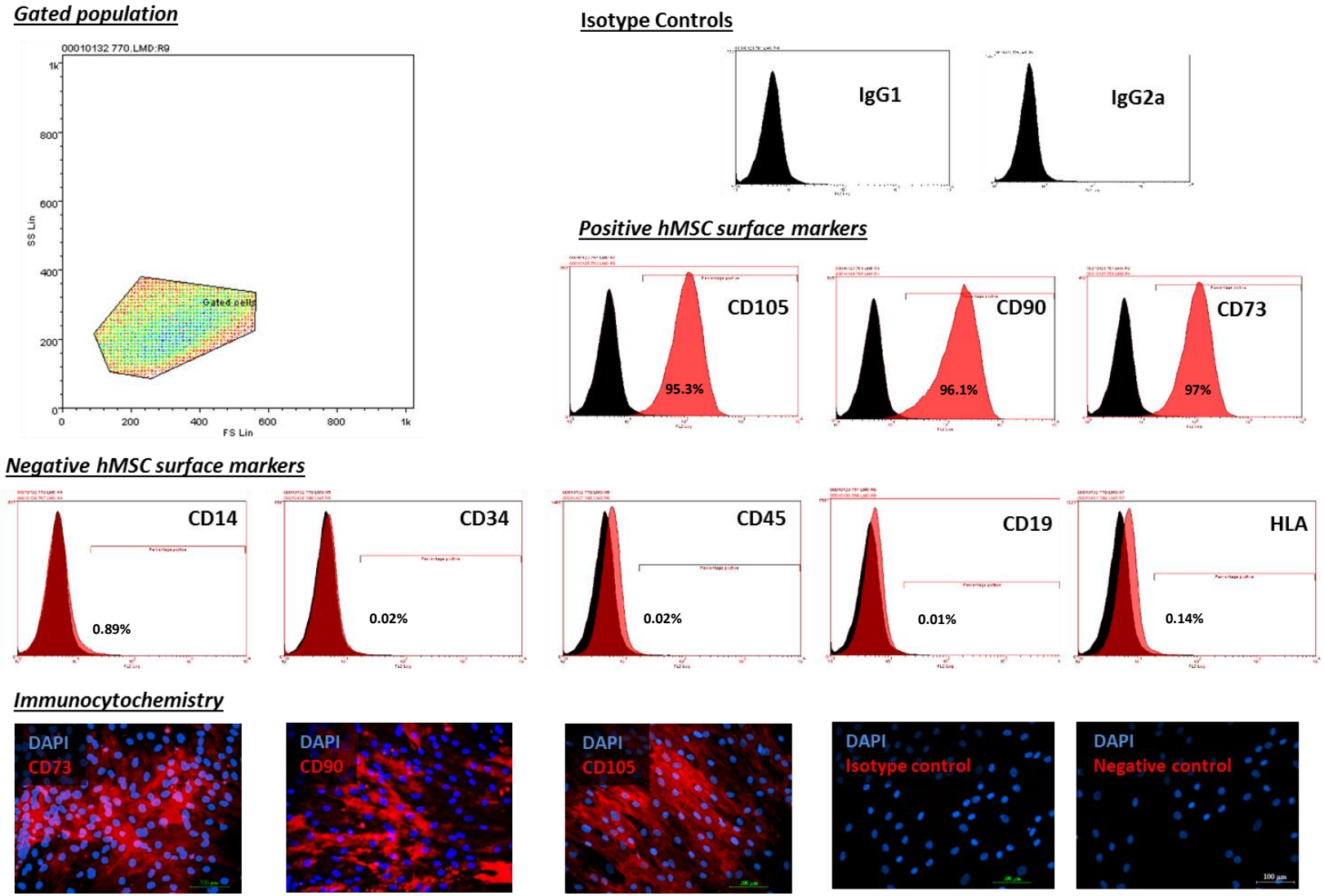

Figure 2: Characterisation of hMSC surface markers by flow cytometry and immunocytochemistry. *Immunofluorescent images courtesy of S.Moise. Negative control represents a cocktail antibody stain for negative surface markers CD14, CD34, CD45,CD19 and HLA.*

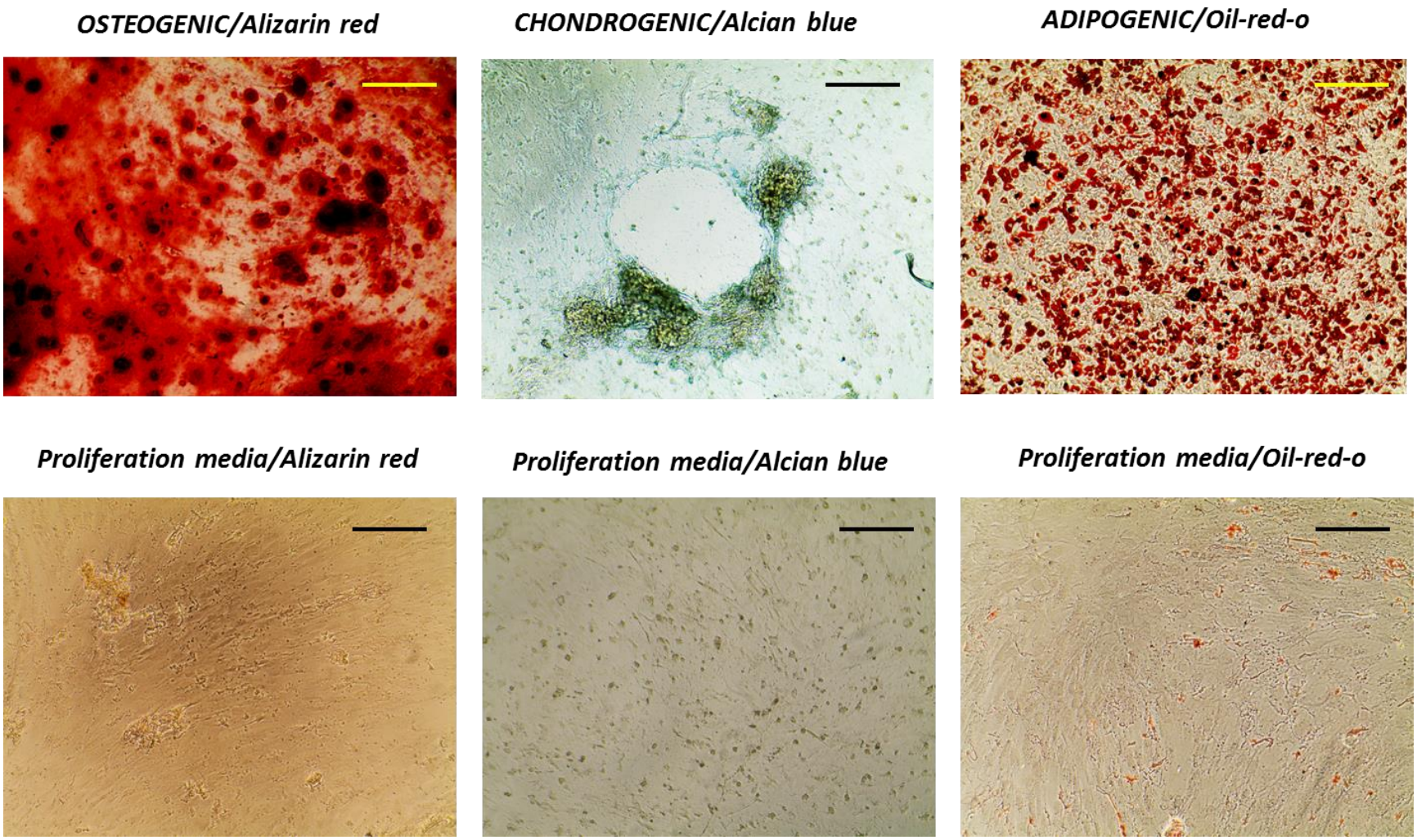

Figure 3. Trilineage differentiation of hMSCs after 28 days in vitro culture in different media compositions. *Scale bars = 200µm*

Appendix

Chapter 2

Self-assembling supramolecular collagen scaffolds for applications in tissue engineering

(The contents of this chapter have been accepted for publication in ACS Biomaterials Science and Engineering, March 2016)

Introduction

The ability to generate hierarchical tissue structures *in vitro* might one day allow researchers recreate truly biomimetic cell niches in a dish. This could enable detailed study of how topographical cues within the extracellular matrix influence cell behaviour. Understanding these mechanisms could greatly improve our ability to engineer functional tissue equivalents that can be used to treat a diverse range of acute and/or pathological abnormalities. Liquid crystallinity in biopolymers such as collagen has provided scientists with inference as to the formation of anisotropic structures in tissue such as bone[1], skin[2] and cornea[3]. Observations of liquid crystallinity in collagen are typically observed in concentrations higher than 50mg/ml, far in excess of commercially available concentrations and hence limiting the ability of the researcher to readily study these interesting properties. Previous reports have successfully utilised liquid crystal phase formation in collagen to generate ordered substrates to support cell growth[4,5]. However, current methods in the literature lack the benefit of simplicity and/or standardisation that is required to permit these materials to become common place in the lab. Furthermore, no one has yet shown distinct levels of liquid crystal phase formation from a single solution of collagen. In this report we describe three simple cost effective methods to produce aligned collagen substrates to serve broad range of tissue engineering applications. Each method is fully scalable and requires only the very basic lab equipment, allowing rapid fabrication of collagen substrates that mimic the hierarchical structure of native tissues.

Materials and methods

Substrate fabrication

2ml stock concentrations of rat tail derived collagen (9.31mg/ml, BD biosciences) were dialysed overnight against either 30% or 50% PEG-400(sigma) in 500mM acetic acid. The dialysis procedure was performed in 3ml capacity dialysis cassettes (thermos-fisher). The final concentration was estimated by volume at 50-60 mg/ml (30%PEG) and 80-90mg/ml for (50%PEG) (**Figure 1A&B**).

Method A

Method A (**Figure 1, method A)** used a 50% PEG dialysis buffer and required careful removal of the viscous collagen 'frame' from the dialysis cassette, which was then transferred to a petri dish. The petri dish was placed in an ammonia chamber (consisting of a square petri dish lines with paper towels soaked in concentrated ammonium chloride (Fisher scientific)) overnight to induce polymerisation in the substrate. The collagen frame was templated, with templates then transferred to phosphate buffered saline (PBS) in well plates and stored at 4^{o}C until ready for use.

Method B

Method B could be performed in both 30% and 50% PEG solution to dialyse the collagen. After removal of the collagen from the cassette, the frame was placed into an Eppendorf tube and heated to 50^{0}C to reduce the viscosity of the collagen. The solution was drawn into a hypodermic syringe needle (29G) and placed upright in the fridge for 30 minutes. The collagen was then extruded onto glass slides into long fibres of strongly bi-refringent collagen. The slides were placed in an ammonia chamber overnight (as before) and stored in PBS at 4^{o}C until ready for use.

Method C

Method C could be performed with either 30% or 50% PEG solution to dialyse the collagen. Solutions were heated to 50^{o}C (as before) to reduce viscosity and pipetted dropwise onto either glass coverslips or microscope slides. The solutions were covered and placed in the fridge for 30minutes before adding a neutralising buffer (equivalent 1M-HEPES) to immerse the collagen (**Figure1 method C)**. Samples were left overnight at room temperature to evaporate the immersing buffer. The samples were then placed in the ammonium chamber for a further 4 hours before washing briefly in distilled water and subjection to 15minute UV sterilisation prior to cell seeding.

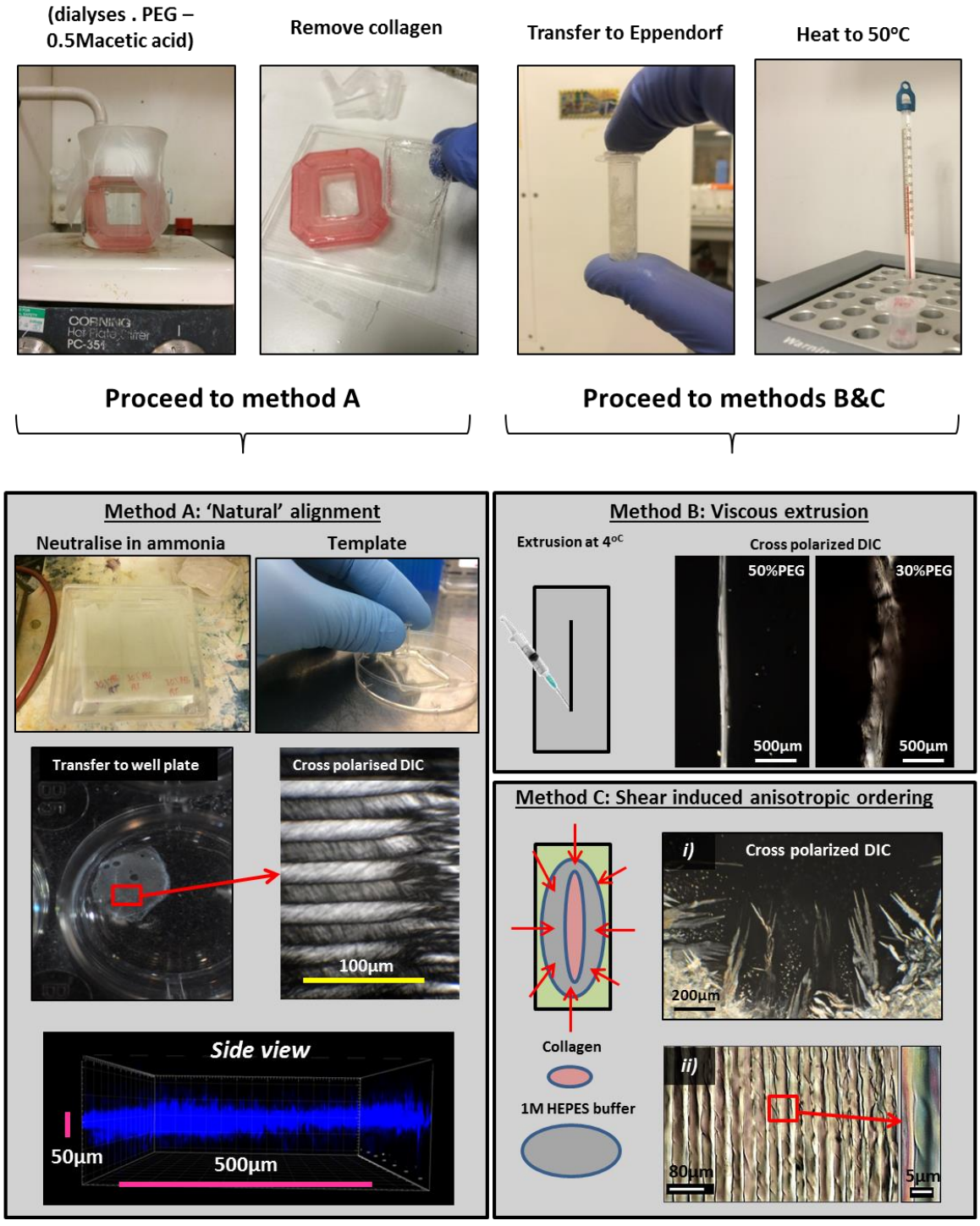

Figure 1: *Fabrication of anisotropic collagen substrates from a single solution of high concentration collagen.*

Cell culture

Mesenchymal stem cells were isolated via plastic adherence from a human bone marrow aspirate and maintained in cultured in proliferation media consisting of DMEM (1ng/ml glucose, w/o L-Glutamine (Lonza) containing 10% foetal calf serum (Biosera), 2% penicillin-streptomycin (Lonza), 1% Non-essential amino acids (Sigma) and 1% L-Glutamine (Lonza). Prior to seeding onto collagen substrates, cells were labelled with a PKH26 fluorescent tracker (Sigma) according to the manufacturer's instructions. For osteogenic differentiation of MSCs, cells were maintained in proliferation media supplemented with 150µg/ml ascorbic acid (Sigma), 10^{-8}M dexamethasone (Sigma) and 2mM sodium β-glycerophosphate (Sigma). Experiments were terminated by fixing samples in 10% neutrally buffered formalin (Fisher) for 15 minutes at room temperature.

Histology

After fixation, cell nuclei were stained using Harris haematoxylin solution (Sigma) for 30 seconds followed by 30 secs emersion in Scots tap water. Cell cytoplasm was stained using Eosin, immersing samples for 30 seconds followed by brief washes in DH_2O. The Von kossa method was employed to detect bone formation using 5% silver nitrate (sigma) in DH_2O. Samples were washed thoroughly in DH_2O before immersion in silver nitrate solution for 30 minutes, followed again by thorough washes in DH_2O. Samples were then exposed to 90mjoule UV irradiation for 15 minutes in a Bio rad GenX UV chamber.

Immunocytochemistry

Immunocytochemistry was performed by blocking non-specific binding using 1%BSA (Agilent) in PBS for 1 hr at room temperature. Primary antibody staining was performed overnight at 4^{o}C using human Osteocalcin monoclonal antibody (R&D systems) diluted to 2µg/ml in 0.1% BSA in PBS-0.1% -tween. Samples were then incubated in Alexafluora 488 or (2µg/ml, 0.1% BSA, 0.1% Tween-20 in PBS) (Abcam) for 1hr at room temperature in the dark. Nuclear staining was performed with 4', 6-diamidino-2-phenylindole (DAPI) for 15 minutes at room temperature in the dark.

Tissue sample preparation

Dissected pig cornea and chicken tendon were fixed in neutrally buffered formalin before paraffin embedding using an automated vacuum tissue processor (Kedee). 10µm sections were cut using a microtome, with sections transferred to microscope slides. Sections were then deparaffinised in xylene and rehydrated in serial ethanol dilutions in dH_2O. Sections were mounted onto slides with coverslips using DPX mounting medium (Sigma) prior to imaging.

Imaging

Confocal imaging of the samples was performed using an Olympus U-TBI 90 confocal microscope, employing either reflectance mode, or using standard fluorescence mode. Polarised light microscopy was performed using a Brunel SP300 polarising microscope. Samples were places between cross polarisers and images were captured using an inverted digital camera (Nikon). Whole mount fluorescence imaging was

performed using a Leica Mz10F dissection microscope. Histologically stained samples were imaged using an EVOS® FL Colour Imaging System.

Raman spectroscopy

Raman spectra for collagen substrates fabricated using 'Method A' were taken on a DXR Raman microscope (Thermo scientific) using a 532nm laser. Raman spectral mapping was performed using an Olympus TH4-200 10x objective through a 50μm pinhole aperture. Spectra from a total of 252 points were obtained over an area of 2.6x0.8mm with a summed average of 10 spectra/point. Spectral analysis was performed using an Omnic Specta software platform.

Results

Method A

Alignment of the substrate using Method A was heterogeneous within the films. The central region of films (**Figure 1, method A)** was around 50μm thick and possessed anisotropic fibre arrangements. By contrast, the much thicker frame around the collagen films did not possess obvious anisotropic fibres, suggesting surface boundary conditions play an important role in guiding alignment. Further supporting this hypothesis was the presence of more pronounced anisotropy in regions localised to boundary conditions introduced by the formation of air bubbles **(Figure 2C&D)**. The induction of collagen alignment by stress cues was supported by observations made under polarised light in viscous solutions prior to polymerisation of the substrate in ammonia vapours. By applying a local stress cues using tweezers (**Figure2 Bi**) we observed through cross polarisers strongly birefringent patterns representing the local alignment of collagen. After the stress cue was removed, the solution returned to its original state (**Figure 2Bii)**. The substrate morphology and the comprising cells labelled with PKH26 could be monitored live in culture using confocal microscopy (**Figure 2E)**. hMSCs cultured on the substrates underwent osteogenic differentiation after 14 days culture in osteogenic media This was demonstrated by Von Kossa staining, showing the formation bone nodules on the substrate (**Figure 2F, black granules)** and by immunocytochemistry at day 14, which showed differentiating hMSCs secreting osteocalcin into the surrounding ECM (**Figure 2F inset).**

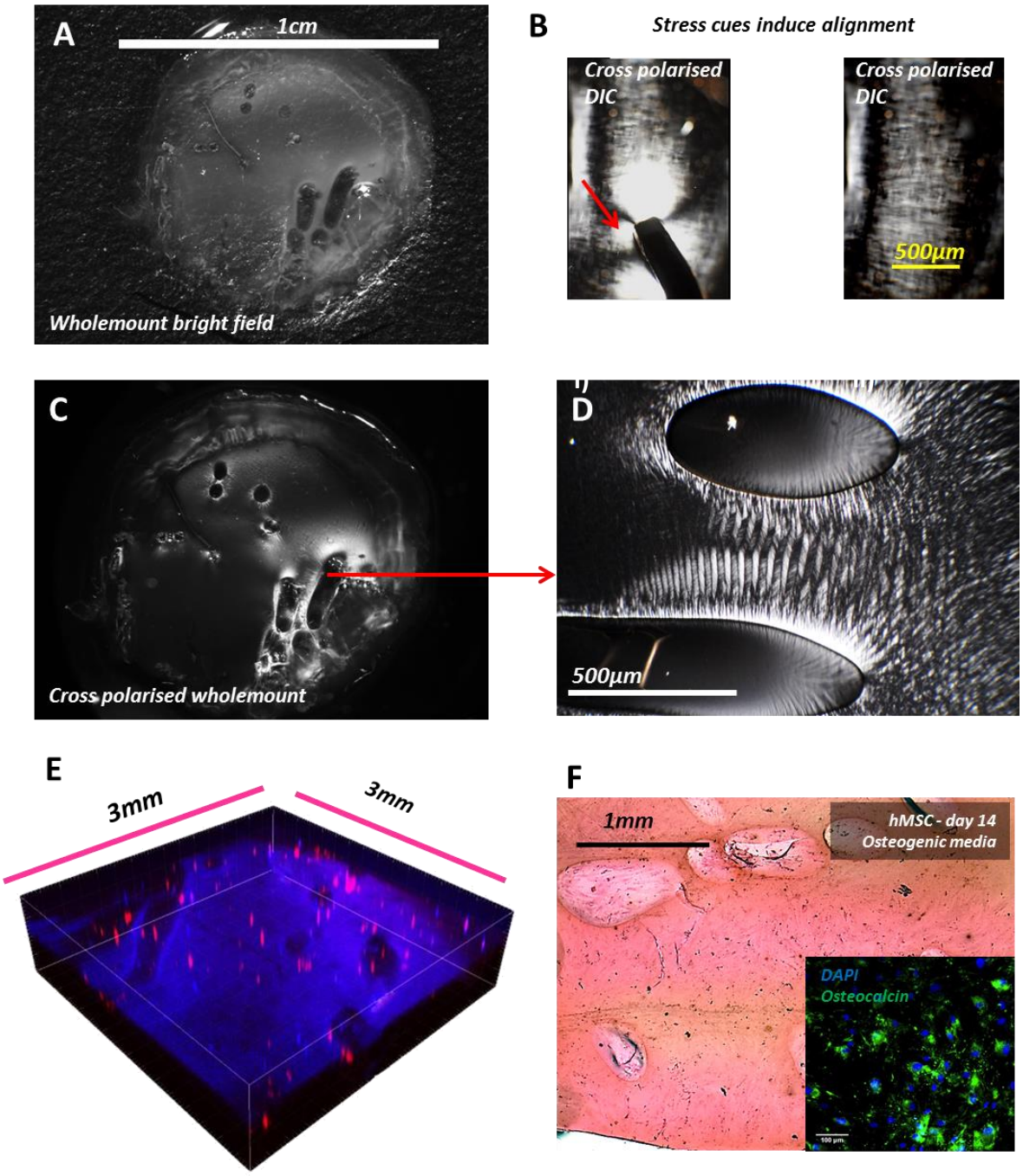

Figure 2: Macroscale collagen films possessing anisotropic fibre arrangements support the growth and differentiation of hMSCs. A) *Multiple templated films of collagen could be obtained from a single dialysis cassette; in this case the template yielded circular films with a 1cm diameter.* ***C****) Cross polarised imaging of high collagen concentrations in solution show typical birefringence patterns, which when subjected to stress cues* ***(Bi)*** *induces local alignment of collagen (arrow inset),Which was diminished after removal of the stress cue****(Bii)****.* ***D)*** *Birefringence in the templated films represented areas of anisotropic ordering between surface boundaries created by bubble formation during dialysis.* ***E****) Both substrate morphology (blue) and the comprising cells (red) could be monitored in live culture, and underwent osteogenic differentiation after 14 days (****F****). Black granules represent bone nodule formation and inset shows production of osteocalcin by hMSCs.*

Method B

The production of aligned collagen fibres using method B required high a collagen concentration (obtained in 50%PEG) yielding more homogeneous, birefringent fibres when compared with fibres produced using 30% PEG (**Figure 1, Method B**). After overnight exposure to ammonia vapours, hMSCs seeded onto the substrate aligned parallel to the fibre direction, which was confirmed using confocal microscopy (**Figure 3A**). Interestingly, reflectance microscopy performed 1 day after cell seeding, indicated changes in density of collagen within individual fibres. A column of dense, aligned collagen was present around the periphery of the fibres, with a reduction in density toward the centre of the fibre (**Figure 3B**). hMSCs remained adhered to the fibres across a culture period of 7 days and retained an aligned morphology parallel to the fibre direction (**Figure 3C-E**).

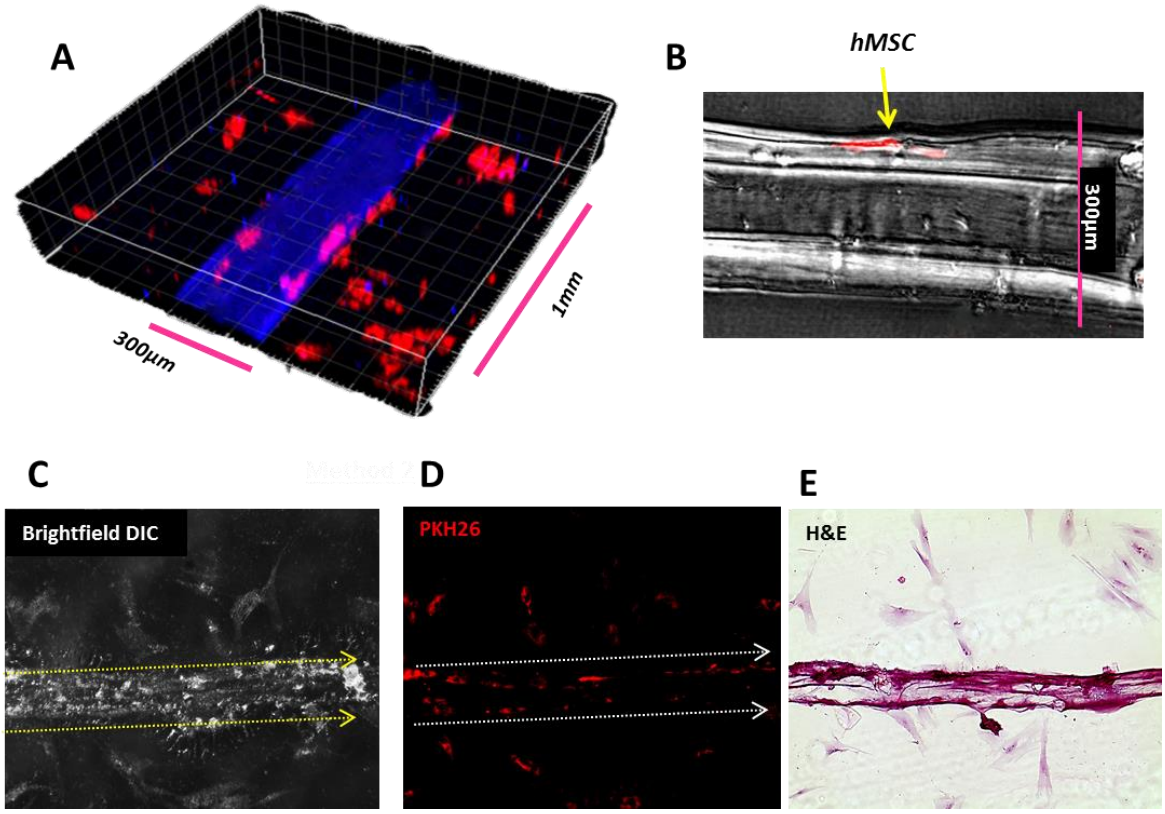

Figure 3: Production of aligned collagen fibres using viscous extrusion to support oriented growth of hMSCs. A) *Confocal imaging of the fibers day 1 after cell seeding showed adhered hMSC (red) aligned parallel to fiber direction (blue).* ***B)*** *Merged Z-stack reflectance microscopy indicated a change in fiber density between the fiber boundary and central regions of the fiber. After 7 days in culture, adhered MSCs s remained aligned in the direction of the fibers(inset arrows)* ***C,D&E)****.*

Method C

Method C describes a novel application using HEPES evaporation to template the collagen through crystallization (**Figure 1. Method C)**. Cross polarised imaging of the substrates after evaporation was complete, revealed a range of different orders, including regions of nested arcs (**Figure4A)** similar to that seen in lamellar bone[6], as well as areas of distinct anisotropic banding **(Figure4C)**. Temporal formation of different crystalline structures could be observed through cross polarisers, and showed rapid crystal growth across the substrate (**see supplementary video 1).** High magnification cross polarized images showed chiral nematic textures with helical pitch running orthogonal to the fibril orientation (**Figure 1, method 3, i&ii)**. During washing with distilled water, the crystalline HEPES structure rapidly dissolved (**see supplementary video 2)**, leaving behind the templated collagen underneath. Eosin staining of the substrates after fixation **(Figure4B)** showed the broad range of templated textures in the collagen due to HEPES evaporation. Higher magnification images (**Figure4D&E)** identify regions that were imaged using confocal microscopy during live culture. This enabled us to correlate the presence of oriented cells within the HEPES templated textures. hMSCs seeded onto substrates oriented themselves in the direction of banding **(Figure4F&G)** and showed no noticeable changes in viability after three days in culture.

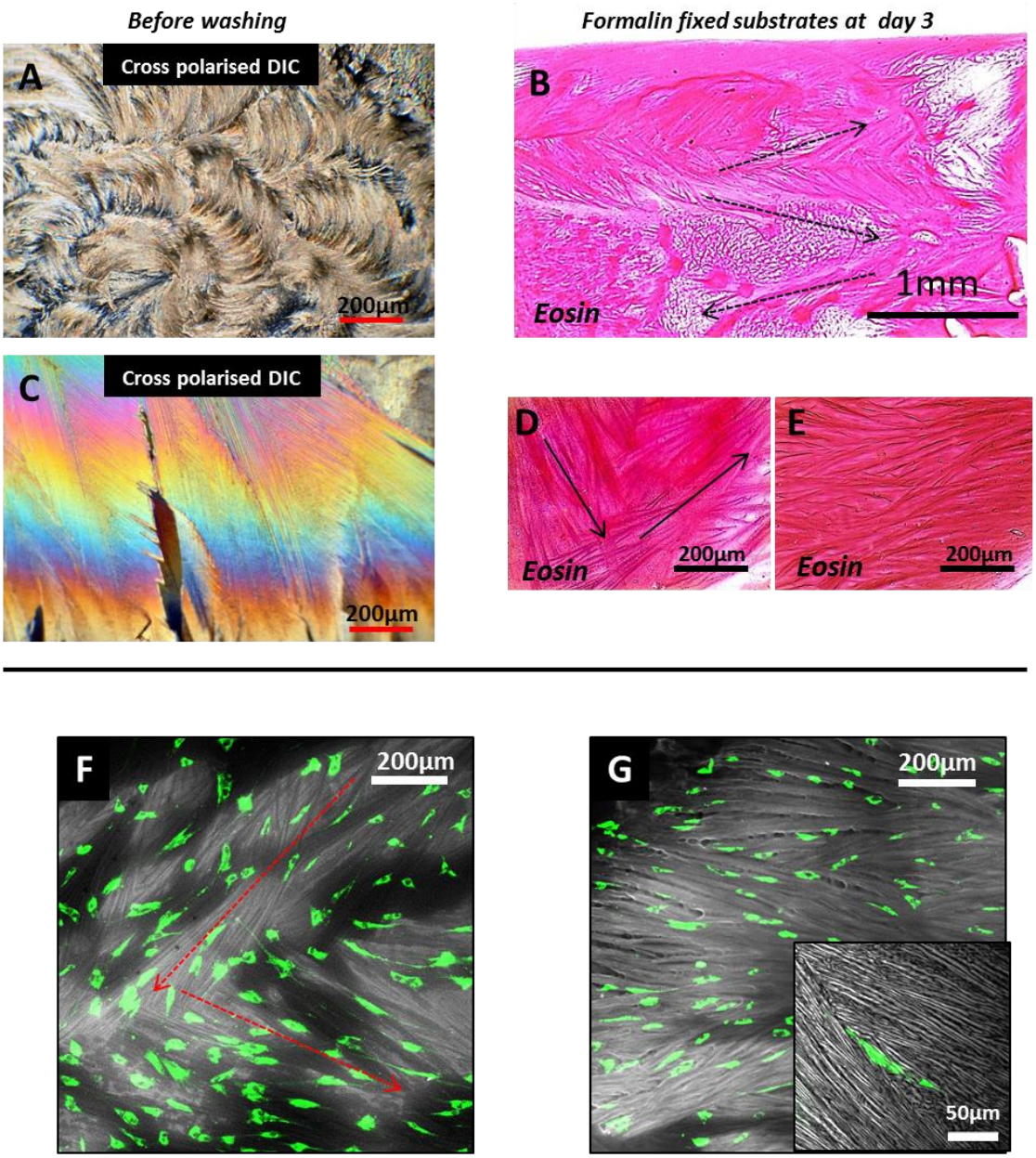

Figure 4: Evaporation of 1M HEPES buffer induces unique crystalline templates in highly concentrated collagen. (A&C) *The evaporation of 1M HEPES buffer over the substrates formed nested arc patterns as well anisotropic crystalline structures. During washing the HEPES structure rapidly dissolved (see supplementary video 2), leaving behind the templated collagen structure (**B**). Higher magnification imaging of the fixed substrates **(D&E)** identified regions that were monitored during live culture using confocal microscopy (**F&G**).*

Raman spectroscopy of naturally aligning films

Areas with prominent anisotropy in substrates produced using method A were analysed using Raman spectroscopy to assess the changes in substrate composition between regions assumed to be isotropic (random order and low birefringence) and areas containing strongly bi-refringent finger print textures (FT), assumed to be cholesteric phases of liquid crystal collagen. Spectral mapping of the 2800-3000cm^{-1} C-H stretching regions (non-specific to proteins and lipids) indicated an increase in the local concentration of collagen between isotropic and FT regions of the substrate (**Figure 5A-C)**. The resulting textures in the naturally aligning films also changed according to the composition of the dialysis buffer. 50% PEG400 in 0.5Macetic acid produced workable films with distinct banded structures, yielding Raman spectra typical of signature region of collagen type 1[7].

By changing the buffer to 50% PEG35000(300mg/ml in DH_2O)[8] 0.5Macetic acid, we first observed a dramatic increase in concentration. The collagen contained within the dialysis membrane in this instance was very difficult to work with, and was removed in small quantities of film fragment. Under the polarised microscope, the films fragments exhibited a changes in texture compared with the PEG400 dialysis method, and in certain areas selectively diffracted blue light (**Figure 5D, inset pictures**) the materials associated Raman spectra also changed relative to collagen dialysed against PEG-400 (**Figure 5D, inset red boxes)**. The shoulders in the 1400-1500cm^{-1} C-H region showed a shift in the peak centre of gravity between PEG 35000 and PEG 400 dialysed substrates. In the 1440-1490 Amide III region, there were slight peak shifts, as well as changes in the peak centre of gravity. A marked peak shift was observed in the 1000-1150cm^{-1} CH_2 deformation region, with the peak centre of gravity shifting from 1135cm^{-1} and 1059cm^{-1}, to 1096 and 1031cm^{-1} respectively between PEG400 and PEG35000. Additionally, the

hydroxyproline peak centre of gravity shifted from 886cm^{-1} in PEG 400 dialysed substrates to 876cm-^{1} in PEG 35000 dialysed substrates.

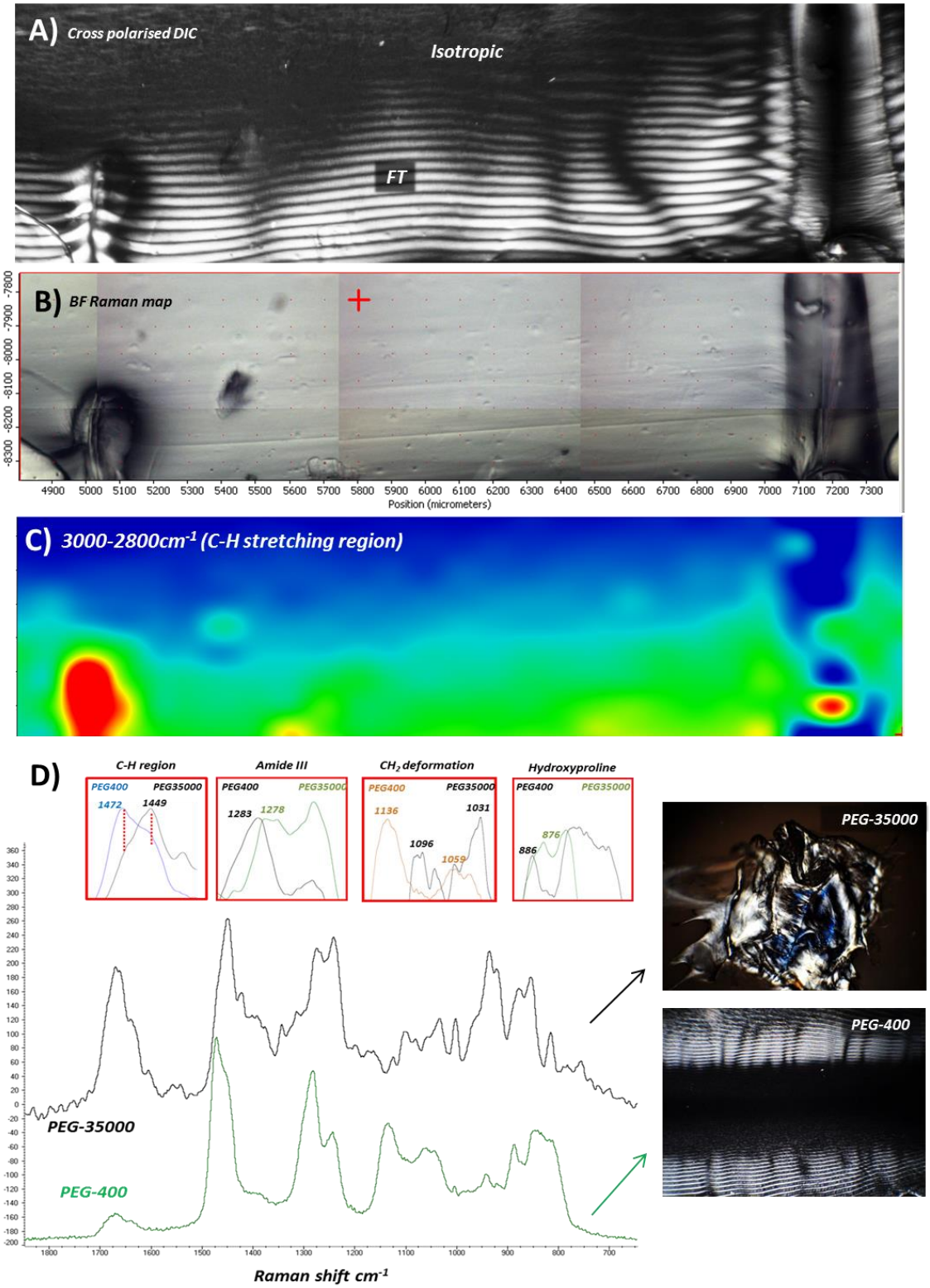

Figure 5: Raman spectroscopy of naturally aligned type 1 collagen films. A) *Cross polarised DIC of Raman mapping area showing the transition from isotropic to fingerprint textured (FT) collagen.* ***B)*** *Bright field Raman mapping area.* ***C)*** *Raman map of 3000-2800cm^{-1} C-H stretching region showing an increase in the local concentration of collagen in FT regions.* ***D)*** *Raman spectra of collagen films showing signature region for collagen type 1. Changes in Raman spectra due to dialysis against PEG35000 (top) and PEG400 (bottom) in different regions are shown in red boxes. Inset images show changes in texture under polarised light according to the corresponding Raman spectra.*

Discussion

The results described using the natural alignment method (Method A) show that the presence of topographical defects in the substrates during polymerisation produces stably aligned collagen fibres. Coupled with analysis by Raman spectroscopy, it appears that the presence of topographical defects influences the local concentration of collagen during dialysis, resulting in heterogeneously ordered films. The change in molecular orientation due to increasing concentration likely represents a lyotropic liquid crystal phase transition. Supporting this hypothesis are changes in the resultant textures of the material in different dialysis buffers, a result similarly observed by Peixoto et al. who studied in detail the changes in molecular orientation of collagen in different solvents as they undergo liquid crystal phase transitions[9].

The shifts in the Raman peaks, and also the change in the peak intensities between PEG400 and PEG35000 dialysed substrates further indicate significant structural changes in collagen assembly as the concentration is increased. The peak shifts observed in the hydroxyproline region could represent alterations in collagen triple helix stability due to a change in the bond energy of hydroxyproline residues [10]. Likewise, the prominent peak shift in the 1000-1150cm^{-1} could indicate the occurrence of a separate liquid crystal phase transition, whereby changes occur in the interaction of paraffinic side chains due to reduced water content in PEG35000 versus PEG400 substrates[11]. This hypothesis could be also supported by changes in the peak centre of gravity in the 1400-1500cm^{-1} region, indicative of paraffinic chains[12]. Deconvolution algorithms could further provide useful information on the underlying spectra which define the shoulder regions of these peaks. Collectively, the peaks shifts between the two substrates might explain the change in substrate texture under the microscope. It is reasonable to suggest that the lower concentration PEG400 system comprises of large scale anisotropic amphiphilic

aggregates linked by paraffinic side chains[13], and that the more concentrated PEG35000 system, having undergone a higher order phase transition, experienced significant changes in protein conformation. The dark blue appearance of PEG35000 substrates under the microscope could indicate the presence pre-cholesteric liquid crystal blue phases. Blue phases occur in an intermediate transition of chiral liquid crystals and are characterised by their cuboidal packing structure, and ability to selectively diffract light in the visible spectrum[14]. However, critical concentrations for blue phase liquid crystals have been reported to lie in between the isotropic and cholesteric phases[14], and thus it is unclear that if this were the case, why lower concentration PEG400 substrates exhibit such prominent cholesteric banding. Despite this, our results demonstrate how useful a tool Raman spectroscopy can be when probing changes in molecular chemistry of collagen solutions as they undergo supramolecular self-assembly.

Importantly from a tissue engineering perspective, the fabrication process did not adversely affect cell behaviour in the context of osteogenic differentiation of hMSCs. Collagen type 1 constitutes the majority of proteins found in human body, and comprises about 90% of the organic phase of bone tissue[15]. The ordered lamellar structure in bone is believed to be influenced by the formation of cholesteric phases in collagen[16]. Based on this, our results could well reflect the physiochemical process of hierarchical tissue formation under cell free *in vitro* conditions. It is unsurprising that we can differentiate hMSCs toward an osteoblastic lineage, since collagen is extensively reported to be an excellent growth substrate to promote bone formation[17,18,19]. The ability to control the orientation of collagen at the nanoscale and maintain this architecture during the culture and differentiation of stem cells might realise an important step forward in the production of biomimetic tissue equivalents. Further to this, whilst this has paper focused on the production of bone, the orientation in our naturally aligned collagen films is remarkable

similar to that seen in cornea and tendon (**Figure 6)**. Further work to explore the behaviour of different cell types such as corneal stromal fibroblasts or tenocytes, could provide evidence for a range of tissue engineering applications for the collagen substrates described in this report.

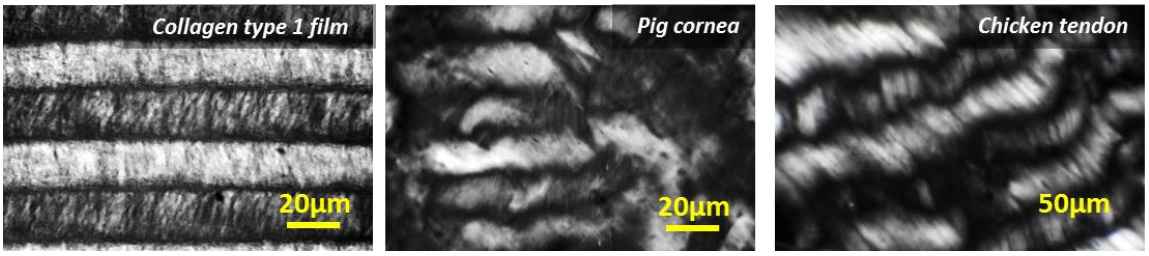

Figure 6: Cross polarised images comparing collagen orientation in type 1 collagen films, pig cornea and chicken tendon.

The results obtained using method 2 represent a simplified adaptation of methods described by Kirkwood and Fuller [4], in which a tri axial robotic arm was used to extrude 20mg/ml solutions of collagen onto slides, after which ambient desiccation further increased concentration and induced fibrillogensis. This automated fabrication method has also been further adapted to manufacture bilayer transparent films for use as corneal substitutes[20]. Our results suggest that by using a higher starting concentration of collagen we can significantly reduce the complexity of the system, making the production of these aligned fibres far more available to researchers. However it should not be understated that the use of automation presents a system with a higher rate of reproducibility, and also reflects more accurately a process controlled manufacturing platform. (**Figure 3B**) reports a novel finding, whereby alignment using narrow channel extrusion might represent electrostatic interactions between the collagen and stainless steel surface of the needle. It is reasonable to suggest the increased alignment of the collagen molecules on the fibre periphery was due to interactions with the adsorbing steel surface during

dynamic flow. Li and colleagues describe a similar phenomenon in molecular configurations of DNA in torsional flow cells, reporting changes in molecular deformation of DNA closer to an adsorbing glass surface[21]. Approaches to modelling polymer dynamics in shear flow have been reported by a number of different groups[22,23], suggesting our liquid crystalline fibre production method could provide a useful experimental platform to validate these models.

The formation of cholesteric order in HEPES/collagen substrates in method C, infers liquid crystal phase formation driven by shear force during HEPES evaporation. Chung et al reported a similar phenomenon in genetically engineered viruses using an oscillating dip coat method [24].They concluded that shear force was responsible for driving aligned fibril formation with chiral nematic helical axis aligned orthogonal to the fibril direction. Our results might reflect a system where shear stress, induced by crystalline HEPES, orients the collagen molecules; however at this stage we do not have precise control of the collagen/HEPES system. It is reasonable to postulate that liquid crystal director growth in our collagen system could be controlled through specific environmental factors such as temperature, humidity or pressure. Further to this, it would be interesting to test the effects of different buffers on the resultant properties of the substrate, such as for example stiffness or optical transparency.

The use of dialysis membranes to induce LC behaviour in collagen is widely established in the literature. Similar to our system, Saidi et al. used dialysis membranes to concentrate collagen solutions above the critical concentration required for liquid crystal self assembly[25]. They then neutralised the solution using PEG titration and spatially confined the solutions between coverslips to induce aligned fibre formation during fibrillogenesis [25]. Interestingly whilst this study was able to produce aligned collagen substrates, they did not report higher order chiral structures running orthogonal to the axis

of anisotropy. Furthermore, we could argue that similar to the comparison of method made with Kirkwood and Fuller, that our procedure represents a simpler and more widely available technique. Coupled with this, since the alignment procedure described in Method A is performed in the dialysis cassettes and not using coverslips, it is easily scalable due to the dialysis cassettes being commercially available in a range of different sizes. Interestingly, the formation of a chiral axis in the substrates in method A was highly sensitive to the initial volume of collagen in the dialysis cassette, indicating that the alignment process is dependent on the degree of confinement during self-assembly.

Alignment of collagen using dialysis has also been achieved via incorporation of nanocrystalline cellulose into concentrated collagen solutions [26] and in high concentration collagen type III using a using a carbodiimide based chemistry technique [27]. Whilst alignment of collagen type IV using similar procedures has not to our knowledge been investigated, it is not unreasonable to suggest that alignment is achievable using these methods, particularly if we take into account early reports of liquid crystalline phases in collagen type IV extracted from bovine anterior lens capsules[28]. Based on existing evidence, together with recent theoretical models indicating that liquid crystalline behaviour can accurately describe experimental assemble patterns of collagen[29], it is surprising that these methods has not yet become routine in the field of tissue engineering. This may be in part due to the diverse and often complex set of protocols that are described to manufacture workable collagen substrates containing hierarchical assemblies. Utilising the available literature on collagen alignment to develop simple, rapid and cost effective protocols could make the use of self-assembled hierarchically ordered substrates far more available to tissue engineers. Further to this, the field of vibrational spectroscopy will no doubt benefit from low cost, reliable experimental

systems, which can accurately relate nanoscale alterations in protein conformation to changes in material properties.

Conclusion

In conclusion, by applying a broad range of basic laboratory techniques, we demonstrate remarkable versatility in this commonly used and widely available biomaterial. Using Raman spectroscopy we have also observed nanoscale conformational changes in protein structure that may represent distinct liquid crystal phase transitions in collagen. The need for simple and cost effective fabrication of biomimetic materials will be important in realising clinically relevant regenerative medicine therapies. As well as this, a deeper understanding of the physical processes that govern anisotropic ordering in biopolymers could greatly improve our ability to engineer materials that mimic the hierarchical structure of native tissues.

References

(1) Giraud Guille, M. M.; Mosser, G.; Helary, C.; Eglin, D. Bone Matrix like Assemblies of Collagen: From Liquid Crystals to Gels and Biomimetic Materials. *Micron* **2005**, *36*, 602–608.

(2) Giraud-Guille, M. M.; Besseau, L.; Chopin, C.; Durand, P.; Herbage, D. Structural Aspects of Fish Skin Collagen Which Forms Ordered Arrays via Liquid Crystalline States. *Biomaterials* **2000**, *21*, 899–906.

(3) De Sa Peixoto, P.; Deniset-Besseau, A.; Schmutz, M.; Anglo, A.; Illoul, C.; Schanne-Klein, M.-C.; Mosser, G. Achievement of Cornea-like Organizations in Dense Collagen I Solutions: Clues to the Physico-Chemistry of Cornea Morphogenesis. *Soft Matter* **2013**, *9*, 11241.

(4) Kirkwood, J.; Fuller, G. Liquid Crystalline Collagen: A Self-Assembled Morphology for the Orientation of Mammalian Cells. *Langmuir* **2009**, *25*, 3200–3206.

(5) Tang, M.; Ding, S.; Min, X.; Jiao, Y.; Li, L.; Li, H.; Zhou, C. Collagen Films with Stabilized Liquid Crystalline Phases and Concerns on Osteoblast Behaviors. *Mater. Sci. Eng. C* **2016**, *58*, 977–985.

(6) Sanchez, C.; Arribart, H.; Guille, M. M. G. Biomimetism and Bioinspiration as Tools for the Design of Innovative Materials and Systems. *Nat. Mater.* **2005**, *4*, 277–288.

(7) Júnior, Z. S. S.; Botta, S. B.; Ana, P. A.; França, C. M.; Fernandes, K. P. S.; Mesquita-Ferrari, R. A.; Deana, A.; Bussadori, S. K. Effect of Papain-Based Gel on Type I Collagen - Spectroscopy Applied for Microstructural Analysis. *Sci. Rep.* **2015**, *5*, 11448.

(8) Nudelman, F.; Pieterse, K.; George, A.; Bomans, P. H. H.; Friedrich, H.; Brylka, L. J.; Hilbers, P. a J.; de With, G.; Sommerdijk, N. a J. M. The Role of Collagen in Bone Apatite Formation in the Presence of Hydroxyapatite Nucleation Inhibitors. *Nat. Mater.* **2010**, *9*, 1004–1009.

(9) De Sa Peixoto, P.; Deniset-Besseau, A.; Schanne-Klein, M.-C.; Mosser, G. Quantitative Assessment of Collagen I Liquid Crystal Organizations: Role of Ionic Force and Acidic Solvent, and Evidence of New Phases. *Soft Matter* **2011**, *7*, 11203.

(10) Kotch, F. W.; Guzei, I. A.; Raines, R. T. Stabilization of the Collagen Triple Helix by O-Methylation of Hydroxyproline Residues. *J. Am. Chem. Soc.* **2008**, *130*, 2952–2953.

(11) Lippert, J. L.; Peticolas, W. L. Laser Raman Investigation of the Effect of Cholesterol on Conformational Changes in Dipalmitoyl Lecithin Multilayers. *Proc. Natl. Acad. Sci. U. S. A.* **1971**, *68*, 1572–1576.

(12) Talari, A. C. S.; Movasaghi, Z.; Rehman, S.; Rehman, I. ur. Raman Spectroscopy of Biological Tissues. *Appl. Spectrosc. Rev.* **2015**, *50*, 46–111.

(13) Neto, A. M. F.; Salinas, S. R. a. The Physics of Lyotropic Liquid Crystals: Phase Transitions and Structural Properties. In *The Physics of Lyotropic Liquid Crystals: phase transitions and structural properties*; Oxford University Press, 2005; p. 5.

(14) Seideman, T. The Liquid-Crystalline Blue Phases. *Reports Prog. Phys.* **1999**, *53*, 659–706.

(15) Hadjidakis, D. J.; Androulakis, I. I. Bone Remodeling. *Ann. N. Y. Acad. Sci.* **2006**, *1092*, 385–396.

(16) Giraud-Guille, M.-M.; Besseau, L.; Martin, R. Liquid Crystalline Assemblies of Collagen in Bone and in Vitro Systems. *J Biomech* **2003**, *36*, 1571–1579.

(17) Ignatius, a; Blessing, H.; Liedert, a; Schmidt, C.; Neidlinger-Wilke, C.; Kaspar, D.; Friemert, B.; Claes, L. Tissue Engineering of Bone: Effects of Mechanical Strain on Osteoblastic Cells in Type I Collagen Matrices. *Biomaterials* **2005**, *26*, 311–318.

(18) Parreno, J.; Buckley-Herd, G.; De-Hemptinne, I.; Hart, D. a. Osteoblastic MG-63 Cell Differentiation, Contraction, and mRNA Expression in Stress-Relaxed 3D Collagen I Gels. *Mol. Cell. Biochem.* **2008**, *317*, 21–32.

(19) Serpooshan, V.; Julien, M.; Nguyen, O.; Wang, H.; Li, A.; Muja, N.; Henderson, J. E.; Nazhat, S. N. Reduced Hydraulic Permeability of Three-Dimensional Collagen Scaffolds Attenuates Gel Contraction and Promotes the Growth and Differentiation of Mesenchymal Stem Cells. *Acta Biomater.* **2010**, *6*, 3978–3987.

(20) Muthusubramaniam, L.; Peng, L.; Zaitseva, T.; Paukshto, M.; Martin, G. R.; Desai, T. A. Collagen Fibril Diameter and Alignment Promote the Quiescent Keratocyte Phenotype. *J. Biomed. Mater. Res. - Part A* **2012**, *100 A*, 613–621.

(21) Li, L.; Hu, H.; Larson, R. G. DNA Molecular Configurations in Flows near Adsorbing and Nonadsorbing Surfaces. *Rheol. Acta* **2004**, *44*, 38–46.

(22) Smith, D. E.; Babcock, H. P.; Chu, S. Single-Polymer Dynamics in Steady Shear Flow. *Science* **1999**, *283*, 1724–1727.

(23) Claire, K.; Pecora, R.; V, S. U. Translational and Rotational Dynamics of Collagen in Dilute Solution. *J.of Phys. Chem. B* **1997**, *5647*, 746–753.

(24) Chung, W.-J.; Oh, J.-W.; Kwak, K.; Lee, B. Y.; Meyer, J.; Wang, E.; Hexemer, A.; Lee, S.-W. Biomimetic Self-Templating Supramolecular Structures. *Nature* **2011**, *478*, 364–368.

(25) Saeidi, N.; Karmelek, K. P.; Paten, J. A.; Zareian, R.; DiMasi, E.; Ruberti, J. W. Molecular Crowding of Collagen: A Pathway to Produce Highly-Organized Collagenous Structures. *Biomaterials* **2012**, *33*, 7366–7374.

(26) Rudisill, S. G.; DiVito, M. D.; Hubel, A.; Stein, A. In Vitro Collagen Fibril Alignment via Incorporation of Nanocrystalline Cellulose. *Acta Biomater.* **2015**, *12*, 122–128.

(27) Hayes, S.; Lewis, P.; Islam, M. M.; Doutch, J.; Sorensen, T.; White, T.; Griffith, M.; Meek, K. M. The Structural and Optical Properties of Type III Human Collagen Biosynthetic Corneal Substitutes. *Acta Biomater.* **2015**, *25*, 121–130.

(28) Gathercole, L. J.; Barnard, K.; Atkins, E. D. T. Molecular Organization of Type IV Collagen: Polymer Liquid Crystal-like Aspects. *Int. J. Biol. Macromol.* **1989**, *11*, 335–338.

(29) Brown, A. I.; Kreplak, L.; Rutenberg, A. D. An Equilibrium Double-Twist Model for the Radial Structure of Collagen Fibrils. *Soft Matter* **2014**, *10*, 8500–8511.